2018

RATIONAL DESIGN OF ALLOSTERIC MODULATORS OF HEMOGLOBIN AS DUAL ACTING ANTISICKLING AGENTS

Piyusha P. Pagare
Virginia Commonwealth University

RATIONAL DESIGN OF ALLOSTERIC MODULATORS OF HEMOGLOBIN AS DUAL

ACTING ANTISICKLING AGENTS

A dissertation submitted in partial fulfillment of the requirements for the degree of Doctor of
Philosophy in Medicinal Chemistry at Virginia Commonwealth University.

By

PIYUSHA P. PAGARE,

B. Sc., Chemistry, Ramnarain Ruia College, Mumbai University, 2009

M. Sc. Organic Chemistry, Ramnarain Ruia College, Mumbai University, 2012

DIRECTOR: DR. YAN ZHANG,

PROFESSOR, MEDICINAL CHEMISTRY

Virginia Commonwealth University
Richmond, Virginia
May 2018

ACKNOWLEDGEMENT

I am deeply indebted to my advisor Dr. Yan Zhang for being an excellent mentor. I would like to thank him for his overwhelming enthusiasm, constructive criticism, perpetual encouragement, timely advice & meticulous attention. His wide knowledge and logical way of thinking has been of great value to me. His caring and supportive nature along with systematic planning and perseverance has shaped me as both a scientist and an individual. I would like to thank my secondary advisor Dr. Martin Safo for his constant guidance and support at every stage of my research. Thank you Dr. Safo for personally training me and sparking in me an interest and drive for structural biology. I will always be grateful to both of them for giving me the opportunity to work in their lab, and for their constructive inputs and support. Thank you, Drs. Zhang and Safo for molding me both professionally and personally.

I would like to thank Dr. Jürgen Venitz, Dr. Umesh Desai and Dr. Xiang-Yang Wang for being a part of my graduate advisory committee. Many thanks to Dr. Desai for his advice, guidance and encouragement. A sincere thanks to Dr. Jürgen Venitz to allow me to work in his lab for the binding studies. In addition, thanks to Dr. Abdulmalik for performing functional studies on our compounds and for the discussions that helped me better understand the research.

I would like to thank Dr. Mohini Ghatge and Dr. Guoyan Xu (Grace) for their invaluable help and support. I would like to express my gratitude to Mohini for all the help during my assays and providing me the best of her advice, research and otherwise. Thank you Dr. Faik Musayev for the help with x-ray crystallography instrument. I am wholeheartedly thankful to my lab mates Dr. Samuel Obeng, Dr. Dwight Williams, Bethany, Dr. Saheem Zaidi, Dr. Yi Zheng, Dr. Huiqun Wang (Wendy), Dr. Hongguang Ma (Brian) and Dr. Boshi Huang for helping me in crucial times. It was they who made this lab a wonderful place for me throughout my working period. Special thanks to Dwight for not only being my lab mate but a brother then and even after leaving the lab. A big shout out to Brie and Samuel for being my best friends in the department.

I am grateful to the Department of Medicinal Chemistry, Institute of Structural Biology Drug Discovery and Development and School of Pharmacy at the Virginia Commonwealth

TABLE OF CONTENTS

LIST OF TABLES

LIST OF FIGURES

xvii

LIST OF SCHEMES

LIST OF ABBREVIATIONS

°C	Degree celsius
^{13}C-NMR	^{13}C- Nuclear magnetic resonance
^{1}H-NMR	Proton nuclear magnetic resonance
2,3-DPG	2,3- Diphosphoglycerate
5HMF	5-Hydroxymethyl-2-furfural
Å	Angstrom
AEH	Allosteric effectors of hemoglobin
ALDH	Aldehyde dehydrogenase
Arg	Arginine
ArH	Aromatic hydrogen
Asn	Asparagine
Asp	Aspartate
Ca^{2+}	Calcium ions
$CDCl_3$	Deuterated chloroform
CH_2Cl_2	Dichloromethane
CH_3CN	Acetonitrile
CHOP	Children's Hospital of Philadelphia
Cl^-	Chloride ions
CO	Carbon monoxide
CO_2	Carbon dioxide
Cys	Cysteine
dd	Doublet of doublet
Deoxy	Deoxygenated
DMF	Dimethylformamide
DMSO	Dimethyl sulfoxide
DNA	Deoxyribose nucleotide
ESI	Electron spray ionization
EtOAc	Ethyl acetate
EtOH	Ethanol
Fc	Calculated structure factor
FDA	Food and Drug Administration
Fe	Iron
Fo	Observed structure factor
g	Grams
Gln	Glutamine

Glu	Glutamic acid
H	Hydrogen
h	Hours
H^+	Proton
H_2O	Water
H_2SO_4	Sulfuric acid
Hb	Hemoglobin
Hb A	Normal adult hemoglobin
Hb F	Fetal hemoglobin
Hb S	Sickle hemoglobin
HCl	Hydrochloric acid
H_{ct}	Hematocrit
His	Histidine
HPLC	High performance liquid chromatography
Hz	Hertz
I	Intensity
IR	Infrared
IRB	Institutional review board
J	Coupling constant
K	Kelvin
K^+	Potassium ions
K_2CO_3	Potassium carbonate
Leu	Leucine
Lit	Literature
Lys	Lysine
m	Multiplet
m/z	Mass/charge ratio
mA	Milliampere
Met	Methionine
Mg	Milligrams
$MgSO_4$	Magnesium sulphate
Min	Minutes
mL	Milliliters
mmol	Millimoles
mM	Millimolar
mp	Melting point
MS	Mass spectrometry
N	Hill's coefficient
Na^+	Sodium ions
Na_2CO_3	Sodium carbonate
Na_2SO_4	Sodium sulphate
NaCl	Sodium chloride
$NaBH_4$	Sodium borohydride
$NaCNBH_3$	Sodium cyanoborohydride
$NaHCO_3$	Sodium bicarbonate
NDA	New Drug Application

NH_4Cl	Ammonium chloride
Pd/C	Palladium on carbon
nm	Nanometer
NO	Nitric oxide
O_2	Oxygen
OCH_3	Methoxy
OD	Optical density
OEC	Oxygen equilibrium curve
Oxy	Oxygenated
P_{50}	Partial pressure of oxygen at 50% hemoglobin saturation
PBS	Phosphate buffer saline
pCO_2	Partial pressure of carbon dioxide
PD	Pharmacodynamics
PDB	Protein Data Bank
PEG	Polyethylene glycol
Phe	Phenylalanine
pO_2	Partial pressure of oxygen
ppm	Parts per million
Pro	Proline
RBC	Red blood cells
Rpms	Revolutions per minute
R-state	Relaxed-state
s	Singlet
SCA	Sickle cell anemia
SCD	Sickle cell disease
Ser	Serine
sO_2	Percent oxygen saturation
t	Triplet
TFAA	Trifluoroacetic anhydride
tHb	Total hemoglobin
Thr	Threonine
TLC	Thin layer chromatography
TMS	Tetramethylsilane
TOF	Time of flight
T-state	Tense-state
Tyr	Tyrosine
UPLC-MS	Ultra-performance liquid chromatography-Mass spectrometry
UV-Vis	Ultraviolet-Visible
Val	Valine
μM	Micromolar

ABSTRACT

RATIONAL DESIGN OF ALLOSTERIC MODULATORS OF HEMOGLOBIN AS DUAL

ACTING ANTISICKLING AGENTS

Piyusha P. Pagare, Doctor of Philosophy in Medicinal Chemistry

A dissertation submitted in partial fulfillment of the requirements for the degree of Doctor of
Philosophy in Medicinal Chemistry at Virginia Commonwealth University.

Virginia Commonwealth University, 2018.

Director: Dr. Yan Zhang
Professor, Department of Medicinal Chemistry

Intracellular polymerization of deoxygenated sickle hemoglobin (Hb S) remains the principal cause of the pathophysiology associated with sickle cell disease (SCD). Naturally occurring and synthetic allosteric effectors of hemoglobin (AEH) have been investigated as potential therapeutic agents for the treatment of SCD. Several aromatic aldehydes, including vanillin have been studied previously as AEHs for their antisickling activities. Specifically, these compounds form Schiff-base adduct with Hb to stabilize the oxygenated (R) state, increase Hb affinity for O_2 and concomitantly prevent the hypoxia-induced primary pathophysiology of Hb S polymerization and RBC sickling in turn ameliorating several of the cascading secondary adverse effects. These compounds however, undergo significant metabolism leading to suboptimal pharmacokinetic properties, e.g. short duration of pharmacologic action and low bioavailability. These drawbacks have severely hampered the use of aromatic aldehydes as AEHs to treat SCD.

To counter these challenges, we designed and synthesized 14 novel compounds (PP-compounds) based on previously studied pyridyl derivative of vanillin. These modifications were expected to increase binding interactions with the protein and thus stabilize the Schiff-base adduct, as well as lead to perturbation of the surface-located F-helix that would stereospecifically destabilize polymer contacts. We investigated the in vitro pharmacokinetic/pharmacodynamic properties of these newly synthesized compounds to ascertain sustained binding and modification of normal human Hb. Subsequently, we conducted in vitro screening assays to test for inhibition of sickling, modification of Hb to the high-affinity form, as well as for a direct left-shift in oxygen equilibrium curves (OEC). Three selected compounds, PP6, PP10 and PP14, that demonstrated not only high antisickling activity but also showed sustained pharmacologic action were chosen for preliminary in vivo studies.

Our results showed maximal levels of Hb modification, which were sustained for the entire 24 h experimental period. In contrast, TD-7 after reaching maximum effect at 1 h gradually decreased in potency and at 24 h has lost 45% of its activity, consistent with the low bioavailability of this compound. These findings suggested that our modifications appeared to successfully limit drug metabolism in red blood cells. Most of these compounds showed almost complete inhibition of sickling at 2 mM concentration; with significant modification of Hb to a higher affinity Hb as well as increase in O_2 affinity of Hb.

Interestingly, while TD-7 demonstrated a clear linear correlation between its ability to increase Hb-O_2 affinity and antisickling activity, PP2, PP3, PP6, PP9, PP10 and PP14, showed weak correlation between these parameters. In fact, these compounds demonstrated high antisickling effect despite only marginally increasing Hb affinity for O_2. This observation indicated that these compounds possibly exhibit dual mechanism of antisickling activity. We hypothesize that their secondary mechanism of action is due to interactions with the surface located αF-helix that would lead to direct or stereospecific inhibition of polymer formation.

To establish the mode of interaction with Hb, we further conducted x-ray crystallography studies and co-crystalized PP2, PP6, PP9 and PP11 with CO-liganded Hb. Our studies showed that these compounds bind in symmetry-related fashion at the α-cleft of Hb to form Schiff-base adducts with the N-terminal Val1 and showed direct interactions with the F-helix which overall enhanced interactions with Hb.

PP6, PP10 and PP14 demonstrated significant in vivo modification of intracellular Hb in mice after IP administration, with increasing levels from 1 h to the 6 h experimental period. They also showed corresponding changes in O_2 affinity observed at 3 h and 6 h, compared to 0 h pre-treatment samples in vivo.

Thus, our results establish these compounds as novel, promising group of potent anti-sickling agents, demonstrate their proposed mechanism of action, and provide proof-of-concept justifications for our structure-based approach to developing potent therapeutics for SCD.

CHAPTER 1

1. INTRODUCTION

1.1. Structure and function of hemoglobin

Hemoglobin (Hb) is an allosteric protein with a molecular weight of about 64,500 and is formed by symmetric pairing of a dimer of polypeptide chains, α- and β-globins, into a tetrameric functional unit $\alpha 2\beta 2$ ($\alpha_1\beta_1$-$\alpha_2\beta_2$).[13–63] The major physiological role of Hb is to transport oxygen (O_2) from the lungs to the tissues by equilibrating between unliganded or deoxygenated Hb possessing low oxygen affinity, and the liganded or oxygenated Hb, which has a high oxygen affinity.[3,43–6] The two $\alpha\beta$- dimer are arranged around a two-fold axis of symmetry, resulting in a large central water cavity in the deoxy-Hb and a narrower one in the liganded-Hb.[7–9] The α- and β- clefts define the two entry points into this central water cavity. The two α-subunits ($\alpha 1$ and $\alpha 2$) contain 141 amino acid residues each forming 7 helices while the two β-subunits (and $\beta 1$ and $\beta 2$) contain 146 amino acid residues each forming 8 helices. These helices (A-H) are joined by non-helical segments referred to as corners (Figure **1**).[1,2,8,10–12]

Max Perutz and co-workers were the first to solve the crystal structures of both deoxygenated Hb (deoxy Hb) and its liganded form, oxygenated Hb (oxy Hb) or methemoglobin (met Hb).[12–15] The structure of liganded Hb in the form of carbonmonoxy Hb (COHb) has also been reported.

1

Since the structures of O_2-Hb and CO-Hb complexes are very similar, most of the liganded Hb structures are of the CO-Hb complex because it is comparatively more stable and thus easier to work with and crystalize than the O_2-Hb complex. Each of the subunit of this tetramer contains a heme, an iron-porphyrin IX, prosthetic group. The iron atoms in the heme group exist as ferrous (FeII) chemical valence state and are coordinated to four pyrrole nitrogen atoms in one plane (equatorial) and to an imidazole nitrogen atom of the histidine amino acid at position 8 of the F-helix viz., αHis87 at the α-subunit and βHis92 at the β-subunit respectively. The distal end of the heme is characterized by a pocket where gas atoms, e.g. oxygen, CO, NO etc., bind to the heme iron.[1,8,10,11,16,17] These gas atoms form the orthosteric ligands of hemoglobin and their reversible binding to the four ferrous atoms in the tetramer allows Hb to transport and/or deliver them.[1,18] When there is a ligand bound, the iron moves into the porphyrin plane towards the histidine residue whereas with no ligand bound (five coordinated) the iron moves out of the plane of the porphyrin ring.[8] The dissociation of ligand from the ferrous atom changes the normal quaternary oxy form to the quaternary deoxy form. This change results in tension at the heme group which lengthens the bond distances between the iron atoms and its six neighbors while in the quaternary oxy form, the heme structure is relaxed.
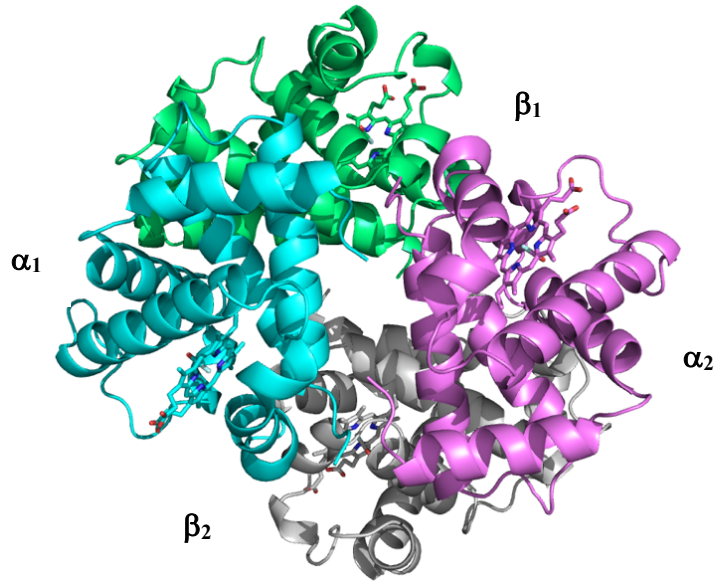
Figure 1. Structure of human hemoglobin with Hb subunits shown as ribbons (α1-cyan, α2-magenta, β1-grey and β2-green), heme groups shown as sticks.

Perutz named this quaternary oxy form which has high affinity for oxygen as the relaxed (R) state and the quaternary deoxy form which has low affinity for oxygen as the tense (T) respectively, thus providing the foundation to unravel the function of this protein.[8] The T and the R states have different structures which vary in the conformation of the $\alpha_1\beta_1$ relative to the $\alpha_2\beta_2$ subunits.[10,11,14,19] This allosteric transition for the R state to the T state with the release of oxygen results in the translation and rotation of the α1β1 subunits by 14° and 1Å relative to the α2β2 dimer which in turn results in formation of a larger central water cavity in the T-state as compared to the R state. The T and R state structures were used to define the two-state Monod-Wyman-Changeux (MWC) model that explains the mechanism of allosteric proteins.[20] This model assumes that ligand binding leads to switch from T→R states without any intermediate states. An alternative mechanism was also proposed as the Koshland-Nemethy-Filmer (KNF) model[21] which was later

refined by Perutz.[10,11] This KNF/Perutz model assumes that upon ligand binding each subunit of the Hb tetramer goes through conformational change which is transmitted to another subunit sending a signal leading to sequential changes in the affinity for ligand.[10,11,21] Following, other models that are variations of these two earlier models have been proposed.[22–28] All these models however, assume that Hb exists in two end states, defined by the classical T and R structure, without any intermediate states. Several recent studies now show that the T→R state transition is mediated by multi relaxed states that exhibit variable oxygen affinities.[29–34] X-ray crystal structures of several such relaxed states with different conformations, e.g. R2, RR2, RR3 and R3 have been reported, and have provided evidence of this multistate theory (Figure **2**).[7,8,35–39] The different relaxed (R) states show significant differences in their α- and β- clefts, central water cavities as well as interdimer interfaces.[39,40] Unless noted, R-state is used to denote the ensemble of relaxed states.
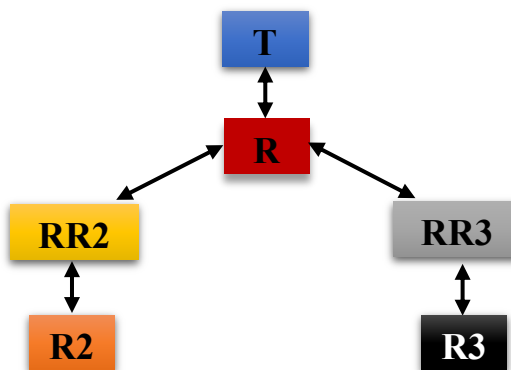
Figure 2. Schematic representation of the proposed allosteric pathway between different Hb states.[8]

1.2. Mechanism of oxygen transport by hemoglobin

Oxygen transport in the body occurs via a series of reversible loading and unloading of hemoglobin with oxygen. The primary factor determining whether oxygen is loaded or unloaded onto hemoglobin is the surrounding partial pressure of oxygen (pO_2). Oxygen is transported in the blood from the lungs, where the partial pressure of oxygen is relatively high, to the tissues where the partial pressure oxygen is much lower. The quantitative relationship between the oxygen partial pressure and the percentage of Hb molecules bound to oxygen is given by the Oxygen Equilibrium Curve (OEC) or the Oxygen Dissociation Curve (ODC).[1,41,42]

1.2.1. Oxygen Equilibrium Curve (OEC):
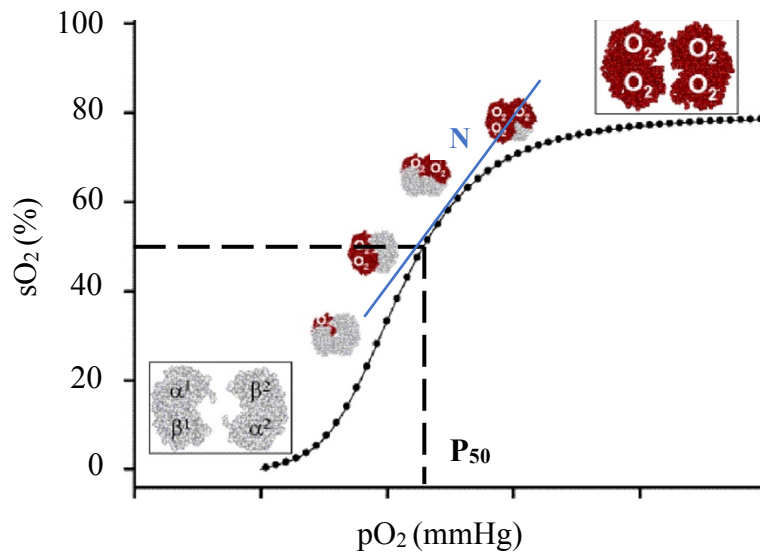
Figure 3. Oxygen equilibrium curve of hemoglobin binding[43]

The oxygen equilibrium curve (OEC) for Hb is the plot of the percent saturation of Hb (sO_2) against the partial pressure of O_2 (pO_2) (Figure **3**). It assumes a sigmoidal (S-shape) shape due to the cooperative nature of hemoglobin. In other words, this indicates that the binding of one molecule of O_2 to one subunit of Hb makes it easier for the subsequent molecules of O_2 to bind to the other subunits. This sequential increase in the ligand affinity at other heme sites shifts the allosteric equilibrium towards the R-state, which is observed by a left shift of the OEC.[10,23,43] Due to this, a high affinity Hb is obtained that readily binds to and holds O_2. The converse is true for shifting the equilibrium to the T-state, which is observed by a right shift of the OEC. This in turn results in a lower affinity Hb that more easily offloads O_2. The oxygen affinity of Hb is reported as P_{50}, the partial pressure of oxygen in mmHg at which 50% Hb saturation is obtained and n is the Hill's coefficient that measures the cooperativity of binding.[41,43,44] A right-shift of the OEC or decrease in Hb affinity for oxygen leads to increase in P50, while the converse is true.

1.2.2. Factors affecting the modulation of OEC:

Several allosteric effectors help in maintaining the Hb function of oxygen transport and delivery effectively. These include 2,3- diphosphoglycerate (2,3-DPG), hydrogen ions (H^+), chloride ions (Cl^-) and carbon dioxide (CO_2).[41,43,44] The following describes briefly the role of each factor in modulating the OEC (Figure **4**).

1) 2,3- Diphosphoglycerate (2,3-DPG): 2,3- DPG is an endogenous allosteric effector of Hb that preferentially binds to the β-cleft of deoxyHb. It ties the two subunits together through several

hydrogen bonding/ salt bridge interactions and stabilizes the T-state. This leads to a right shift of the OEC and decreasing the affinity of Hb for O_2 (Figure **4**).[45–48]
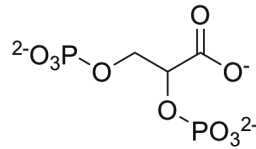
2,3-DPG

2) pH: In 1904, Christian Bohr observed that increase in the CO_2 or decrease in the blood pH result in decrease in the affinity of Hb for oxygen. This results in a right shift in the OEC increasing the O_2 offload.[49] At an acidic pH, e.g. in respiring tissues, the β-chain C-terminus amino acid $β_1$His146 ($β_2$His146) becomes protonated, forming a salt bridge interaction with the carboxyl group of $β_1$Asp94 ($β_2$Asp94) and hydrogen bonding interaction with the amine of $α_2$Lys40 ($α_1$Lys40). These interactions lead to stabilization of the T-state, facilitating release of oxygen to the tissues. At higher pH values, e.g. in the lungs, these interactions are broken to shift the allosteric equilibrium to the R-state and increasing the affinity of the protein for oxygen.[11,50,51]

3) Temperature: Increase in the temperature of blood results in reduced Hb-O_2 affinity thus showing a right shift in the OEC. In other words, increase in temperature stabilizes the T-state increasing the offloading of O_2 by hemoglobin (Figure **4**).[42,50,52]

4) Carbon monoxide (CO): CO has higher affinity for Hb than O_2. Thus, presence of CO results in decline in the O_2- carrying capacity of Hb. However, due to the cooperative nature of

oxygen binding, partial saturation of a Hb molecule with CO in turn increases the affinity for O_2. This shifts the OEC towards the left (Figure **4**).[42,51]
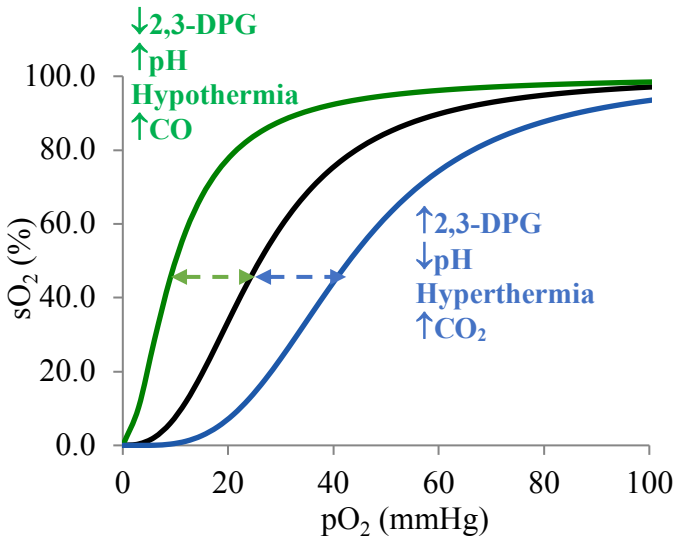
Figure 4. Shift in the OEC with varying 2,3-DPG, pH, Temperature, CO_2 and CO. Black curve indicates the normal OEC for Hb whereas curves in green and blue show the shift in the OEC due to various factors.

1.3. Hemoglobinopathies

There are seven types of normal hemoglobin molecules throughout a human's life. These include:

1) Embryonic Hemoglobin: The most common and in highest proportion in an embryo is Hemoglobin Gower I ($\zeta_2\varepsilon_2$). The other three forms of embryonic hemoglobin are present at much

lower levels and include Hemoglobin Gower II ($\alpha_2\varepsilon_2$), Hemoglobin Portland I ($\zeta_2\gamma_2$), and Hemoglobin Portland II ($\zeta_2\beta_2$).[53]

2) Fetal Hemoglobin: Once the embryo develops into a fetus the four embryonic hemoglobins are replaced by Hemoglobin F ($\alpha_2\gamma_2$). Hb F has higher affinity for oxygen than adult Hb and hence helps the growing fetus utilize the oxygen from its mother's bloodstream.[53]

3) Adult Hemoglobin: The two types of adult hemoglobin include Hemoglobin A ($\alpha_2\beta_2$) and Hemoglobin A$_2$ ($\alpha_2\delta_2$) with Hb A being the most prevalent as it takes up about 97% of the adult hemoglobin.[53]

The term 'hemoglobinopathy' includes all genetic hemoglobin disorders. These can be classified into two main groups: 1) thalassemia syndromes and 2) structural Hb variants or abnormal hemoglobins. Figure **5** shows the geographical distribution of major hemoglobinopathies.[54]

When gene defects cause disorder in Hb synthesis, it gives rise to thalassemia. Hemoglobin structure in this case is normal. In thalassemia, the reduced production of one of the globin chains upsets the balance of α- to β- chains and causes abnormal hemoglobin. α-thalassemia is caused due to partial or total deletion of one or more α-globin genes while β-thalassemia is a result of insufficient or no production of β-globin chains.[55,56]

Several hundred abnormal forms of Hb have been identified. Some are silent and cause no signs and symptoms, while others affect the functionality and stability of the Hb molecule. The most common and clinically significant Hb variants include:

1) Hemoglobin S (Hb S): This is the predominant hemoglobin in people with sickle cell disease. Hb S is a variant of normal adult hemoglobin (Hb A) caused by an amino acid substitution at position 6 of the β- chain (βGlu6→ βVal6) giving rise to α2βs2.[55–57]

2) Hemoglobin C (Hb C): Hb C is another structural variant of Hb A caused by an amino acid substitution occurring at the same position as HbS (βGlu6→ βLys6) giving rise to α2βc2.[55–57]

3) Hemoglobin E (Hb E): Hb E is one of the most common beta chain hemoglobin variant in the world. It is a structural variant of Hb A (βGlu26→ βLys26) affecting the production rate of Hb A.[55–57]

There are many other uncommon variants of Hb including Hemoglobin D, Hemoglobin G, Hemoglobin J, Hemoglobin H, Hemoglobin M, Hemoglobin Barts and Hemoglobin Constant Spring that are of lesser clinical significance.[55,56]

A.

B.
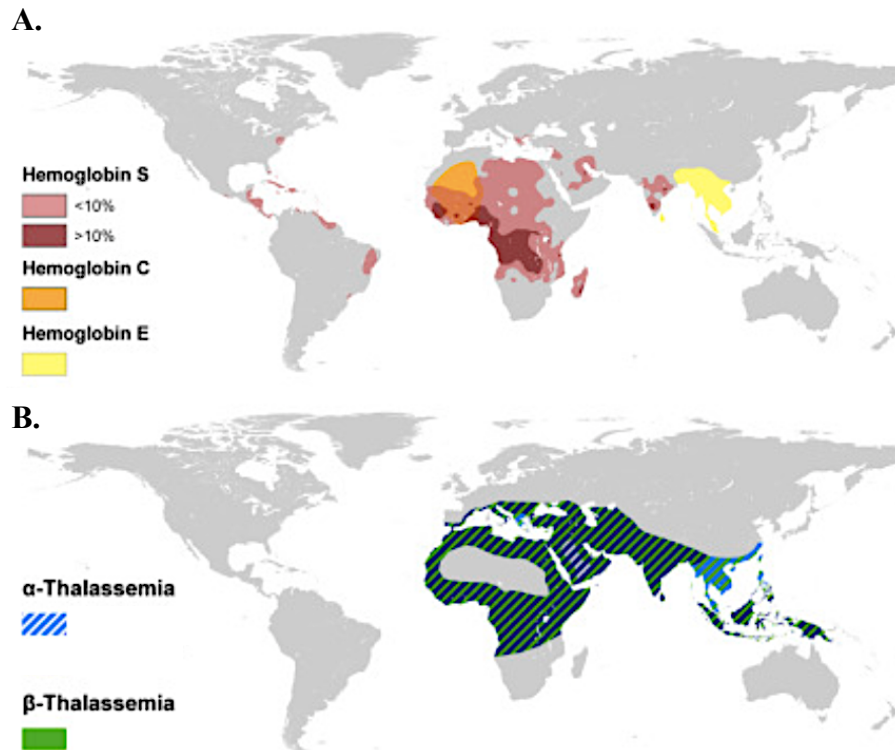
Figure 5. Map showing geographical distribution of hemoglobinopathies.[54]

1.4. Sickle cell disease

1.4.1. History

Sickle cell disease is an inherent genetic disorder characterized by sickle shaped RBCs. James Herrick, in 1910, first described elongated RBCs in a patient suffering from severe anemia which he later termed as 'sickle shaped'.[58] In 1945, Linus Pauling proposed that SCD might originate from an abnormality in the hemoglobin molecule. He demonstrated, by electrophoresis, the differential migration of sickle versus normal hemoglobin to validate his hypothesis.[59,60] He coined

the term 'molecular disease' for SCD.[61] Later, John Haldane hypothesized that SCD carriers might reflect a selective advantage in protection against Plasmodium falciparum malaria and proposed what we call today the 'malaria hypothesis' of SCD.[62] One of the major contributions was by Ingram et al., wherein they demonstrated that the mutant sickle hemoglobin (Hb S) differs from the normal hemoglobin (Hb A) by a single amino acid.[63,64]

1.4.2. Molecular and genetic basis of SCD
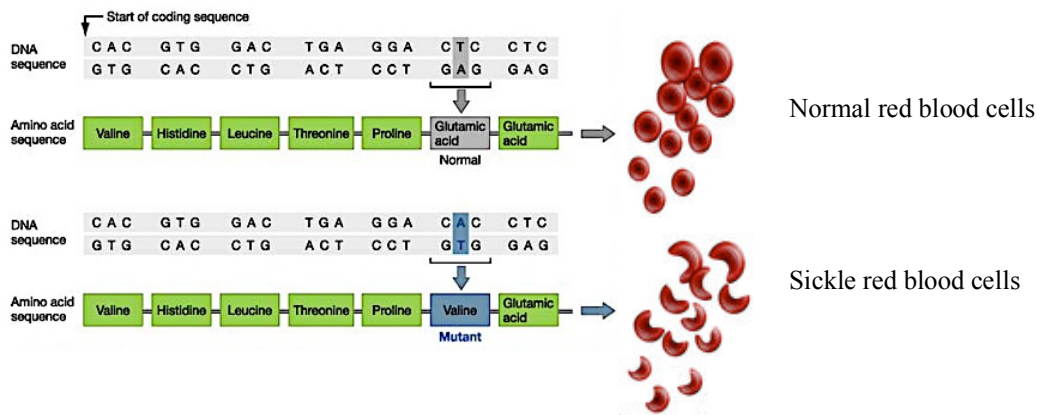
Figure 6. Representation of genetic mutation of Hb causing sickling of RBCs

In 1957, Ingram found a mutation in at the 6th position of the β- subunit of Hb.[63,64] This mutation is caused by the substitution of the polar glutamic acid (βGlu6) for the hydrophobic valine (βVal6). It occurs due to the mutation of the β-globin gene called the HBB gene (from A to T) Figure **6**).[63,65] The positions of Ala70, Phe85 and Leu88 residues, that make up the hydrophobic pocket, in the β-subunit of Hb S are positioned differently in the deoxy and oxy Hb S. This results in inefficient alignment between the βVal6 of one and βPhe85 of another Hb S molecule in case

of oxy (R) Hb S whereas in the deoxy (T) state the mutated Val6 of one Hb S molecule interacts with the hydrophobic pocket formed by Ala70, Phe85 and Leu88 residues of the β-subunit of another Hb S molecule.[66] resulting in the formation of 14-stranded fibers which have a tendency to aggregate and disrupt the cell membrane of RBCs.[65]
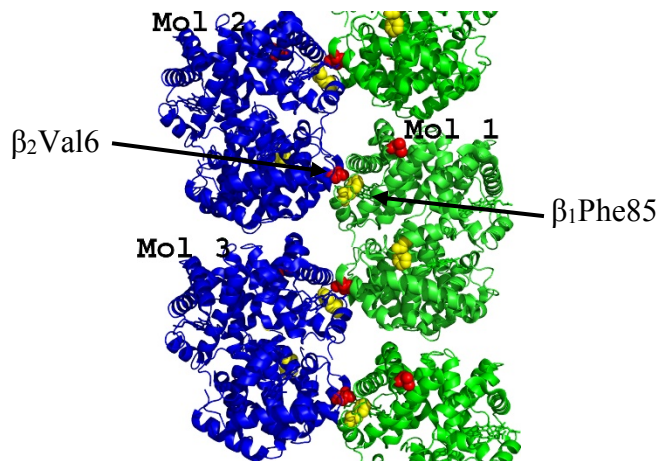
Figure 7. Structure of DeoxyHb S Polymer **(PDB code 2HBS).** Ribbon figure of the crystal packing of deoxyHb S where β2Val6 (red sphere) in one strand 12(blue) interacts with a hydrophobic pocket formed by β1Ala70, β1Phe85, and β1Leu88 (yellow sphere) from the β1 subunit of a hetero-tetramer positioned in the adjacent polymeric strand (green).[66]

This hydrophobic interaction does not occur in the oxy (R) state and therefore oxy Hb S does not polymerize. The primary interaction between Val6 and the hydrophobic pocket is stabilized by an adjacent hydrogen bonding interaction between βThr4 of one Hb S molecule and βAsp73 of the other Hb S molecule contributing to polymer stabilization. A significant shift in the position of βThr4 from deoxy to oxy Hb S results in weakening of this hydrogen bonding interaction explaining partly why oxy Hb S does not polymerize but deoxy Hb S does.[66–69] The polymer is

also stabilized by various secondary interactions.[57] A large number of naturally occurring mutations have been observed that reduce polymer formation by weakening the polymer-stabilizing contacts and of particular importance is the Hb variant Stanelyville (αAsn78 → αLys78).[57,70–72] The T→R transition results in a 14° rotation of the α1β1 dimer while the T→R2 transition results in a 22° rotation of the α1β1 dimer relative to the α2β2 dimer, due to which these secondary polymer contacts tat stabilize the polymer in deoxy- Hb S do not occur in oxy- Hb S.[66]

This mutation is mostly inherited in an autosomal recessive fashion. If one normal beta gene and one mutated beta gene are inherited, the person is heterozygous for the mutation and is called a 'carrier'. The mutation in this case does not cause any significant health concerns but can be passed on to the next generation. However, if two mutated beta genes of the same type are inherited, the person is homozygous meaning the person will show the symptoms and complications associated with SCD (Figure **8**).[73,74]
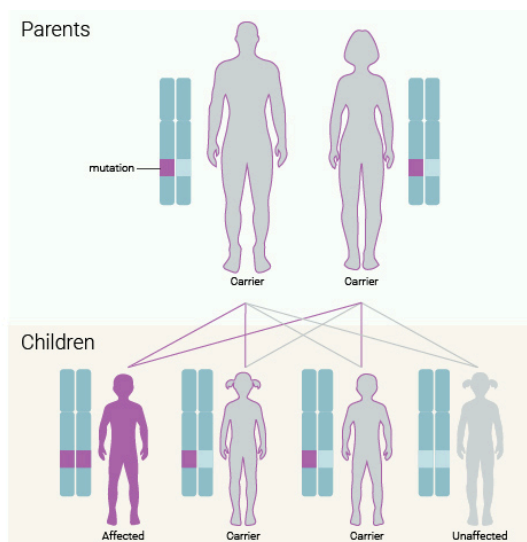
Figure 8. Inheritance of sickle cell trait[75]

1.4.3. Epidemiology

The World Health Organization (WHO) and the United Nations (UN) have declared SCD as a public burden as there are over 300,000 affected births every year.[73,76,77] The prevalence of sickle cell trait varies greatly globally but is seen most across sub-Saharan Africa, eastern Saudi Arabia, and central India as well as in the Caribbean, Central America, South America and Mediterranean countries (Figure **5**).[78,79] The Center for Disease Control and Prevention (CDC) estimated that in the US, SCD affects approximately 100,000 Americans; occurs among 1 out of every 365 African-American births and 1 out of every 16,300 Hispanic-American births. About 1 in 13 African-American babies are born with the sickle cell trait.[79] In the 1970s, SCD had a high mortality rate with majority of children born with SCD not surviving past 3 years.[76,80] In the US however, there has been a remarkable improvement in the survival of children with SCD with over 95% reaching adulthood. Unfortunately, the survival rates of adults with SCD has not improved that dramatically and their projected life expectancy still remains 20-30 years shorter than the general population (average person with SCD reaching the age of 45 years).[74,76,81]

SCD is also associated with high treatment costs. The total lifetime health care costs are estimated to be nearly $1 million, with annual costs ranging from over $10,000 for children to over $30,000 for adults.[73]

1.4.4. Pathophysiology

SCD patients are severely anemic due to the lack of oxygen reaching their tissues. To compensate for this, sickled RBCs contain high amounts of 2,3-DPG than normal RBCs.[82] As mentioned above, 2,3-DPG decreases the oxygen affinity for Hb resulting in increasing concentration of deoxy Hb[45,46,48] which polymerize, leading to sickling of RBCs.[57] Sickled RBCs have a shorter life span (16-20 days) as compared to normal RBCs (120 days).[73,83]

This leads to a downstream cascade of hypoxia, vaso-occlusion and the release of cytokines and infarction. Subsequent reperfusion of the ischemic tissue generates free radicals and reactive oxygen species (ROS) which scavenge nitric oxide (NO). Due to the rigid and brittle nature of the sickle RBCs they show high rates of hemolysis.[77,84] Hemolysis of RBCs releases the free Hb in the plasma which also contributes in scavenging NO. NO deficiency thus can lead to platelet activation, increased vascular resistance all contributing to the development of vasculopathy.[59,76,77] Pulmonary hypertension, gallstones, leg ulcers, osteonecrosis, acute chest syndrome, priapism and cerebrovascular diseases are some of the reported pathophysiology associated with SCD.[85] The ongoing vasculopathy and inflammation results in damage to various organs and transforms SCD into a chronic multisystem disorder. Approximately by their fifth decade, one half of the surviving patients develop some form of irreversible damage the lungs, kidneys, brain, retina or bones as well as other co-morbidities like diabetes and systemic hypertension which further affect their quality of life.[61,74]
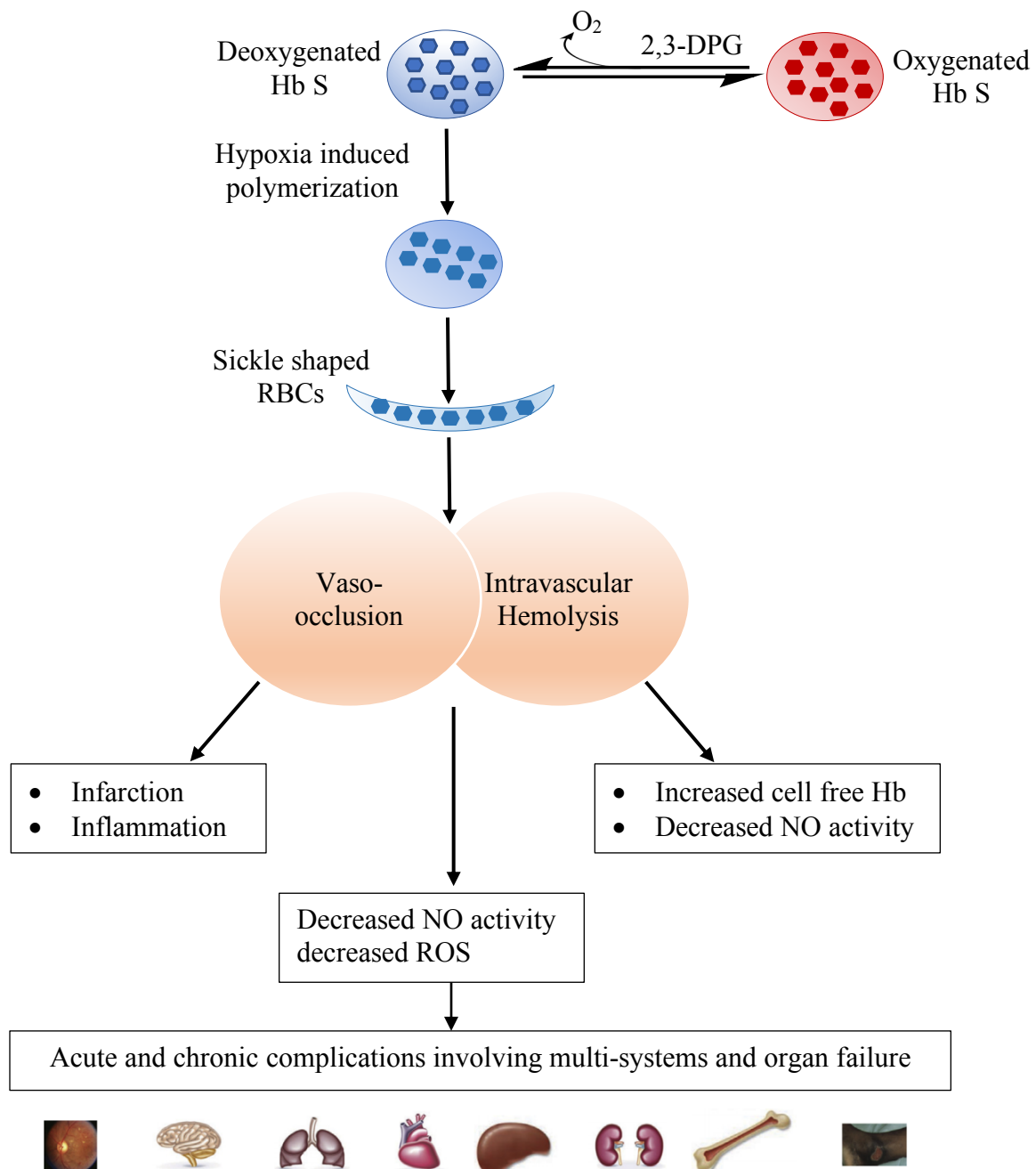
Figure 9. Pathophysiology of sickle cell disease[73]

1.4.5. Current treatment

In developed countries like the United States, the average life expectancy of a SCD patient is about 40-60 years. In the early 70s, this average life span was only 14 years. Advances in the diagnosis and care of SCD patients have made this improvement possible. These statistics are far worse for SCD patients in the third world countries. Additionally, SCD patients suffer from poor quality of life and burden of high medical costs.[86] At present, hematopoietic stem cell transplantation (HSCT) is the only cure for SCD.[86–89]

Although the molecular basis of SCD has been very well established, the development of novel targets therapies to treat SCD has been a challenge. Treatment generally focuses on pain management, treating the complications and acute care during sickling crisis. Hydroxyurea (Siklos) was the first drug approved by the U.S. Food and Drug Administration (FDA) to treat SCD in 1998.[90,91] Hydroxyurea induces the production of Hb F however the resulting side effects including myelosuppression prohibits its use in some patients.[92–94] However, research shows that many people in the developing countries do not have access to these drugs and/or is not taken consistently by individuals with SCD.[92] Recently, in 2017, L-glutamine oral powder (Endari) was approved by the U.S. FDA to treat the acute complications of SCD. It is the first pediatric treatment for SCD and the second only treatment for adults with SCD. L-glutamine in conjunction with nicotine adenine dinucleotide (NAD) increases the amount of free glutamine in the blood which is used to generate anti-oxidant molecules as a product of glutamine degradation. These anti-oxidant molecules help neutralize the oxidative stress in sickle red blood cells and help them regain their flexibility.[91,95]

1.5. Therapeutic strategies for SCD

Several naturals products have been reported to have antisickling effect and are still being used in Nigeria and other western African countries.[96–98] A number of agents have now been developed that interfere with one or more mechanisms and/or the kinetics of the sickling process. Some of the strategies to inhibit Hb S polymerization and sickling include:

1.5.1. Inducing Hb F synthesis:

It has been observed that increased levels of fetal hemoglobin (Hb F) can ameliorate the severity of sickle cell disease. Based on this observation, in the last few decades a lot of effort has been taken towards developing therapeutics for inducing Hb F. [99–101] This group of antisickling agents include drugs like the anticancer agents 5-azacytidine[102,103], cytosine arabinoside[104,105], Gemcitabine[105], the DNA methylating agent 5-aza-2`-deocycytidine (decitabine)[106], Tetrahydrouridine[107], butyrate[107,108], 2,2-dimethylbutyrate[107,109], Pomalidomide[110], erythropiotein[111], vinblastine[112] and hydroxyurea[92,94,113]. These agents are thought to act by reactivating the genetic switch to Hb F production. However, they show limited clinical use due to the possible toxicity as well as non-specific modification of genes other than the globin family.[99]
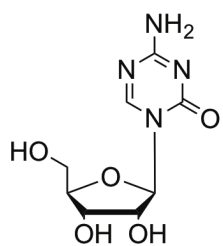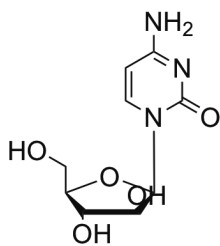
5-Azacytidine　　Cytosine arabinoside　　Gemcitabine　　Decitabine　　Tetrahydrouridine
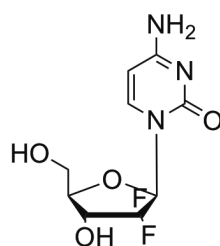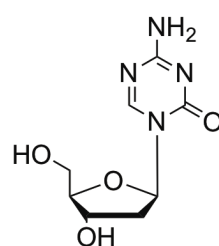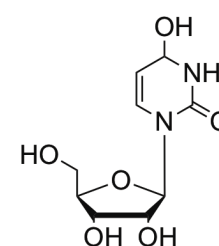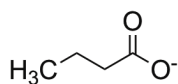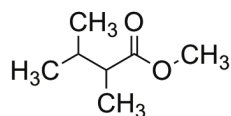
Butyrate　　2,2-Dimethylbutyrate　　Pomalidomide　　Hydroxyurea
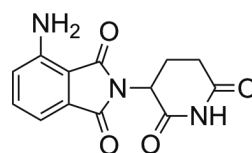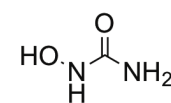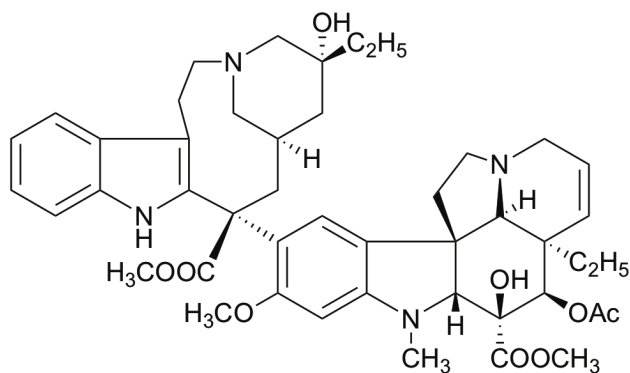
Vinblastine

1.5.2. Gene therapy:

Bone marrow transplant[114–116] or hematopoietic stem cell transplant[87–89] have been used as total gene replacement therapies for Hb S. Although beneficial, these methods show several drawbacks including bone marrow rejection, high cost of treatment and high mortality rates.[88]

1.5.3. Reducing intracellular Hb S concentration:

Sickle cell polymerization is highly dependent on the intracellular concentration of sickle hemoglobin.[117] Sickle cells have increased concentration of intracellular Ca^{+2} which leads to the loss of K^+, Cl^- and water from them causing dehydration. These dehydrated sickle RBCs have an increased tendency to polymerize. Two ion transport pathways, the K-Cl co-transport and the Ca-activated K channel play an important role in the dehydration of sickle RBCs and potential therapeutic approaches involve the use of drugs that block these mechanisms.[118,119] Some of these agents include peripheral vasodilators cetiedel[118,120] and beperdil[121,122], K^+ channel (Gardos channel) inhibitor Clotrimazole[119,123,124], pentoxifylline[125,126], the antibiotic monensin[127], tellurite[128], N-acetylcysteine[129,130], L-arginine[131]. Oral magnesium and zinc cations that inhibit the K^+, Cl^- co-transporter channel also show the same effect.[124,132,133] Many of these compounds are however toxic and hence not used regularly to treat SCD.
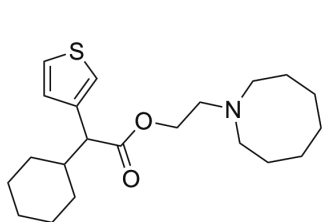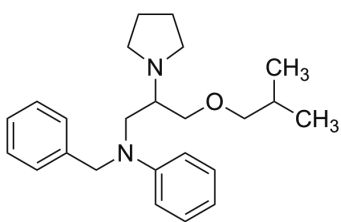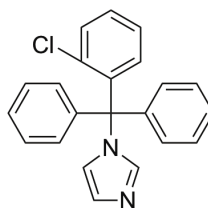
| Cetiedel | Beperdil | Clotrimazole | N-acetylcysteine |
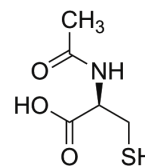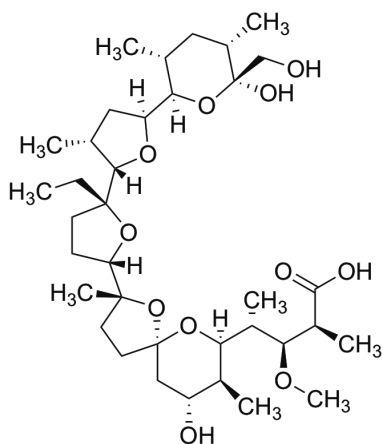
Monensin
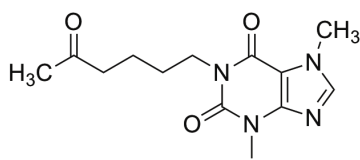
Pentoxifylline
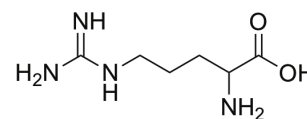
L-Arginine

1.5.4. Reducing the concentration of 2,3-DPG:

2,3-DPG is a major endogenous allosteric effector of hemoglobin that binds in the cleft between the β subunits and helps stabilize the T-state.[46,47,134] Binding of 2,3-DPG decreases Hb-O_2 affinity. Hence, lowering 2,3-DPG concentration could be a possible therapeutic strategy towards increasing the fraction of Hb S in the oxygenated or R-state.[48] A number of anions like phosphoglycolate and glycolate that increase the phosphatase activity of DPG synthase have been reported but have not been extensively studied for their potential use in SCD.[135,136]
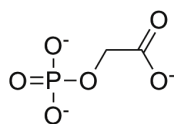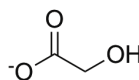
Phosphoglycolate   Glycolate

1.5.5. Blocking intermolecular polymer contacts:

The major milestones towards targeting hemoglobin for the treatment of sickle cell disease are the availability of the x-ray crystal structures of oxy and deoxy native (Hb A) and sickle (Hb S) hemoglobin[12,14,16,37,66,137,138] and the determination of residues that participate in intermolecular polymer contacts.[70,139] There are a number of compounds that are proposed to bind non covalently to the surface of the protein to destabilize polymer formation.[99] These chemicals include urea[83,140] and alkyl urea[141], dichloromethane[142], fluorinated compounds[143], amino acids like phenylalanine and arylalanines[144,145], ethanol and aromatic alcohols[145–147], tryptophan and analogs[148], oligopeptides[145], carbohydrate derivatives[99], substituted aromatic carboxylic acids[149,150] and cromolyn sodium[151,152]. Owing to the high amounts of protein in the body, these agents are also required in very large amounts. The major concern however is that the surface of the protein does not have any residues involved in an intermolecular contact or any deep clefts or crevices that would be required for tight noncovalent binding.[153]

| Urea | Phenylalanine | Tryptophan | Cromolyn sodium |
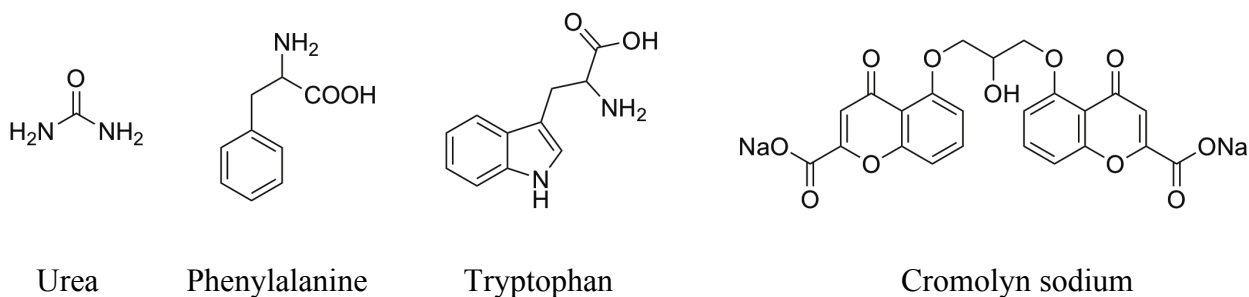
1.5.6. Increasing oxygen affinity of Hb:

A number of agents are known to bind covalently to Hb that stabilize the R-state and/or destabilize the T-state and increase the hemoglobin affinity to oxygen. They are called the allosteric effectors of hemoglobin (AEHs). This is advantageous because the deoxygenated (T) state of Hb S polymerizes while the oxygenated (R) state does not. These agents bind to specific sites on the protein molecule for e.g. N-terminal amino group of the α-chain, βCys93 and histidine residues like β2, β97, β143 and/or β146.[99,154] Examples of these reagents include cyanates[155], cystamine[156,157], nitrogen mustards[158], aspirin and its derivatives[159–161], acetyl phosphates[159], ethacrynic acid and its derivatives[66,149,162], Bis-(3,5-dibromosalicyl) fumarate was studied for its ability to cross link the β subunits of the tetramer and increase oxygen affinity.[163–165] A number of aromatic aldehydes including derivatives of pyridoxal, salicylaldehyde, phenoxypentanoic acid derivatives (BW12C)[166–168], 5-HMF and vanillin form an important class of agents that modulate the Hb-O_2 affinity by interacting with the N-terminal nitrogen of αVal1 residue and show antisickling properties.[169–176] These agents are quite promising but can lack specificity meaning they could react covalently with other non-specific enzymes and lead to toxicity.
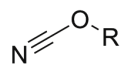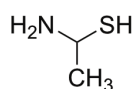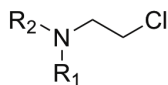
Cyanate   Cystamine   Nitrogen mustard   Aspirin   Acetyl phosphate
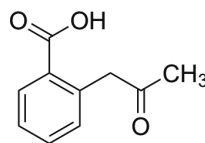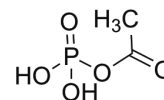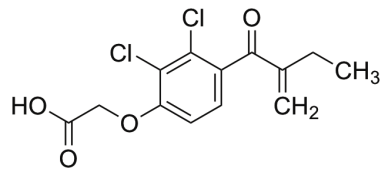
Ethacrynic acid
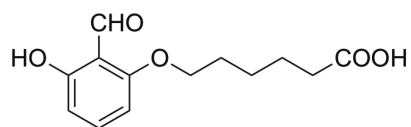
BW12C
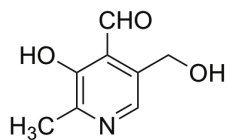
Pyridoxal
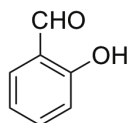
Salicylaldehyde
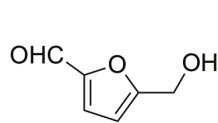
5-HMF
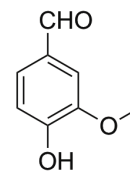
Vanillin

CHAPTER 2

2. DEVELOPMENT OF AROMATIC ALDEHYDES AS ANTISICKLING AGENTS

Several synthetic allosteric effectors have been studied as potential antisickling drug candidates based on the early observations of modification of hemoglobin by glucose in the blood.[177,178] Zaugg and coworkers reported several benzaldehyde containing compounds that form Schiff base adducts with the N-terminus amino group of the α-chain of Hb S to increase its oxygen affinity. These compounds form a transient covalent bond since the Schiff base exists in an equilibrium between the bound and the free aldehyde.[169]
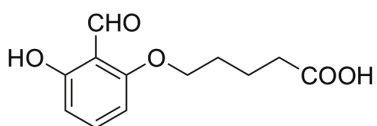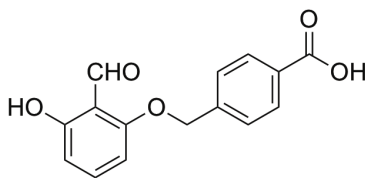
Valeresol   Tucaresol   Thiazo-vanillin
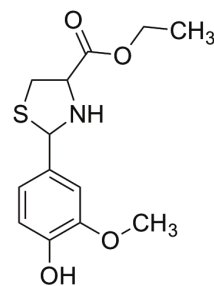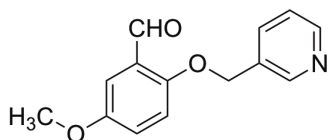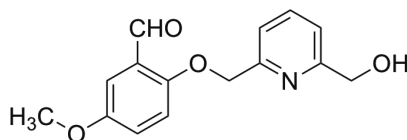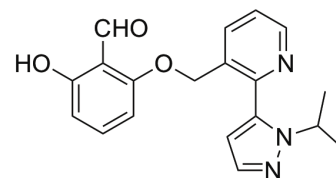
INN-312   TD-7   GBT-440

Peter Goodford and coworkers were the first to design left-shifting aromatic aldehyde-acid containing effectors of hemoglobin. They postulated that one molecule formed a cross-link between the two symmetry-related α-subunits via a Schiff base interaction with the N-terminus αVal1 of one α-subunit and a hydrogen-bond interaction with the opposite αVal1 of the second α-subunit in order to stabilize the R-state relative to the T-state.[166,167] However, the structural basis for these aldehydes was first elucidated by Abraham et al. with the help of the structure of deoxygenated Hb in complex with valeresol (12C79).[179] They observed that a pair of symmetry related molecules of valeresol (not 1 as proposed by Goodford) formed a Schiff-base interaction with the two αVal1 N-terminal amino groups. This binding however did not lead to any additional inter subunit interactions but led to the disruption of a water-mediated interaction between the αVal1 and αArg141 of the opposite α-subunits resulting in the destabilization of the T-state relative to the R-state.[179] Valeresol underwent human testing but was not orally bioavailable. It was potent but had a short duration of action of only 3 to 4 hours following intravenous administration.[180,181] Another synthetic allosteric effector of hemoglobin, tucaresol, has also been extensively studied. Tucaresol was orally bioavailable with more favorable in vivo human pharmacokinetics than valeresol but caused immune-mediated toxicity in phase-II studies.[44,168,182]

These studies led to a realization about the high dose requirements and the potential toxicity issues with covalent AEHs. Thus, Abraham et al. revisited the nontoxic food additive vanillin, which was previously shown by Zaugg and coworkers to show antisickling activity. Although non-toxic, vanillin too was not orally bioavailable resulting in the termination of its phase-I clinical study.[170] One of the reasons for the non-oral bioavailability of vanillin and tucaresol was thought

to be the susceptibility of the aldehyde group to aldehyde dehydrogenase (ALDH) mediated oxidative metabolism in the human RBCs. A prodrug of vanillin, thiazo-vanillin (MX1520), in which the aldehyde group was protected by L-cysteine to form a thiazolidine complex was studied. MX1520 showed significantly improved oral pharmacokinetic and pharmacodynamics properties compared to the free vanillin, shedding light on the viable strategy to improve oral bioavailability as well efficacy of such type of aldehyde containing antisickling compounds.[172] While none of the above studies resulted in a clinically useful candidate for sickle cell disease, they established the foundation for the use of aromatic aldehydes as potential SCD therapeutics as well as provided insights into the challenges that hamper this approach.

In a collaborative effort, Don Abraham, Martin Safo, Osheiza Abdulmalik and Toshio Asakura identified 5-hydroxymethyl-2-furfural (5HMF), a naturally occurring five membered aromatic aldehyde found in a variety of foods, as a promising new antisickling agent.[171,174] Unlike vanillin, 5HMF is highly bioavailable and in the phase I, double blind, placebo controlled normal volunteers single doses of 5-HMF were well tolerated and rapidly absorbed while in adult patients with SCD it was safely tolerated without severe complications.[183] However, it undergoes extensive oxidative metabolism and has a short half-life (~1 h) which reduces its pharmacologic effect.[154,171,184–186] This resulted in high dose requirements of 5HMF likely contributing to the termination of its phase II clinical trials. X-ray crystallographic analysis of 5HMF[171] (Figure **10**) and it analogs[173] in complex with the R2 as well as T state Hb showed that these compounds form Schiff base adducts with the αVal1 nitrogen atom in a symmetry related fashion. Binding to liganded Hb led to the stabilization of the R2 state via intricate direct and water-mediated interactions between the

compounds and Hb. Binding to unliganded Hb leads to additional destabilization of the T state thus shifting the allosteric equilibrium to the R state and increasing the oxygen affinity of Hb.[171]
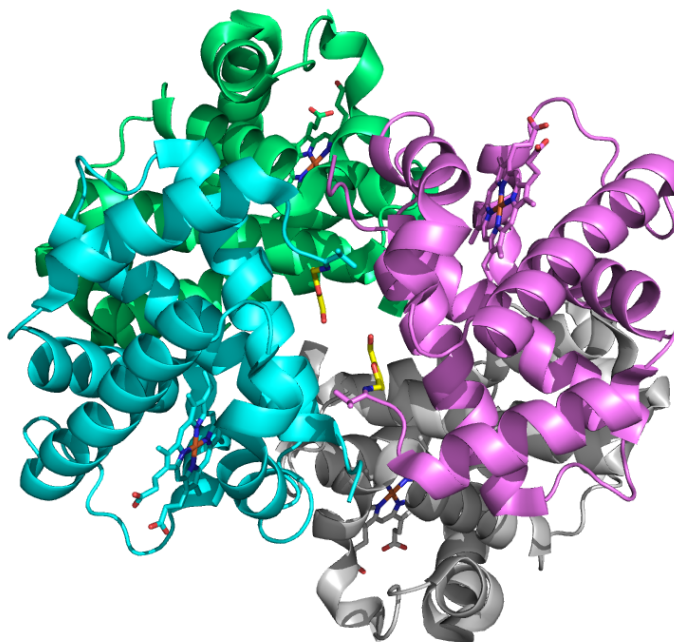
Figure 10. Crystal structure of Hb in R2 state in complex with a pair of 5-HMF molecules (yellow sticks) (PDB ID 1QXE) with Hb subunits shown as ribbons (α1-cyan, α2-magenta, β1-grey and β2-green), heme groups shown as sticks.

Recently, the Safo group based on 5HMF binding interactions with Hb, derivatized this compound to increase its interactions with the protein expecting to improve its potency and metabolic profiles. Although some of these derivatives showed up to a fourfold increase in potency, it was not enough to translate into an effective therapeutic dose.[173] Based on the atomic interactions between Hb and vanillin, several pyridyl derivatives of vanillin were also designed and synthesized by Abraham and Safo group. These compounds (designated as Name- INN) also

bind to the αVal1 to form Schiff base adducts with its backbone nitrogen atom and tie the two α-subunits together via a series of intricate direct and water mediated interactions thus stabilizing the R2 state of Hb (Figure **11**). Some of the INN compounds show as much as 90-fold and 2.5-fold more potency than vanillin and 5HMF.[187,188] Binding of one of the INN compounds, INN-312, also resulted in stereospecifically inhibiting polymer formation by placing the methoxypyridine substituent towards the surface of the Hb tetramer. This mode of binding resulted in additional contacts with the residues of the surface located αF-helix.[188] The αF-helix, in particular αAsn78 residue, has been shown to be critical in polymer stabilization, as shown by the Hb variant Stanleyville (αAsn78 → αLys78), which inhibits Hb S gelation.[57]
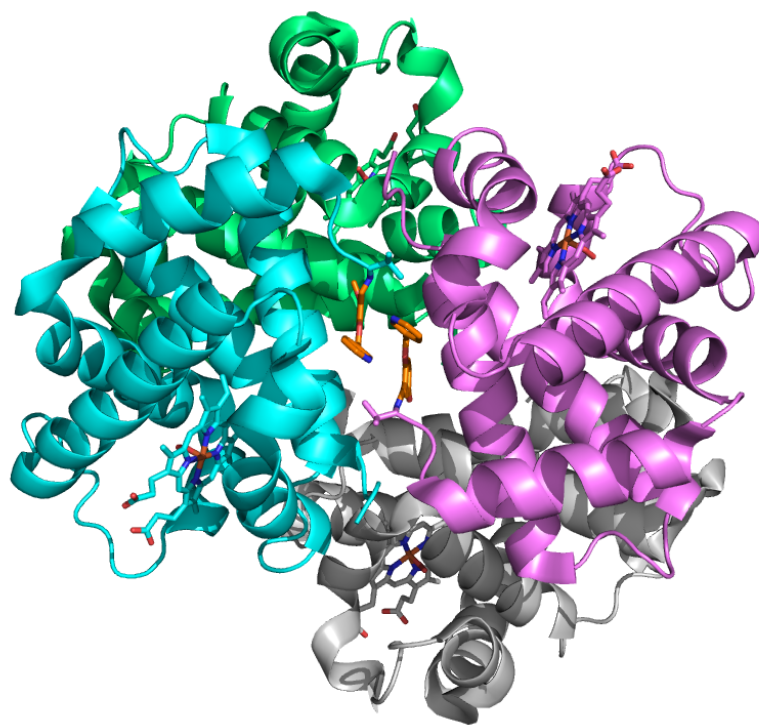
Figure 11. Crystal structure of Hb in R2 state in complex with a pair of INN-312 molecules (orange sticks) (PDB ID 3R5I) with Hb subunits shown as ribbons (α1-cyan, α2-magenta, β1-grey and β2-green), heme groups shown as sticks2.

The promising INN-series of compounds led to the design and study of the third generation of pyridyl substituted aromatic aldehyde containing antisickling agents called the TD-compounds by the Safo group. These showed remarkably superior pharmacological properties than the INN-compounds in vitro and enhanced anti-polymerization properties at significantly lower doses.[175]

Most recently, GBT-440 (Global Blood Therapeutics), another pyridyl derivative of aromatic aldehyde has been shown to increase both, the oxygen affinity of Hb S and counter polymerization with enhanced potency and improved pharmacokinetic properties.[189–192] GBT-440 is currently undergoing a phase III clinical trials for the treatment of SCD.[193]

CHAPTER 3

3. RATIONALE, GOAL AND SPECIFIC AIMS

3.1. Rationale

There are several challenges facing the use of aromatic aldehyde type covalent modifiers of Hb as antisickling agents. These include non-specific binding to plasma proteins, and rapid metabolism of the aldehyde in vivo due to the presence of aldehyde dehydrogenases (ALDH) in blood as well as in the RBCs. Oxidative metabolism compromises the effectiveness of these compounds dramatically. Another major challenge is the difficulty in designing pharmaceutically useful agents that are capable of sustained modification of the large amounts of intracellular Hb (~ 5mmol). Although this seems challenging, Sunshine and colleagues were the first to suggest that increasing the O_2 affinity of Hb S by only 4mm Hg could lead to therapeutically significant inhibition of intracellular polymerization.[117] Early clinical studies with tucaresol showed that therapeutic efficacy can be achieved by modification of 10% to 24% of Hb S and this magnitude maybe achievable in vivo.[168]

Structure based modifications from vanillin to INN and TD compounds increased the antisickling potency significantly. The INN compounds are pyridyl derivatives of vanillin,[187,188] while the TD compounds represent further modifications of the INN compounds (with a methoxy

group on the pyridine ring) rationalized to stereospecifically inhibit deoxy-Hb S polymer formation and increase the fraction of soluble oxy-Hb S in regions of low O_2 tensions. These compounds undergo significant metabolism leading to sub-optimal pharmacokinetic properties like short duration of action and low bioavailability. These compounds, therefore, are undesirable to treat SCD, preventing the development of one of the most potent compound, TD-7. Nonetheless, the development of antisickling agents like vanillin and 5HMF suggested that these allosteric modulators of Hb have little toxicity at high doses and also established aromatic aldehydes as a scaffold to design additional non-toxic agents as potential therapeutics for SCD.

Keeping in mind the challenges associated with aldehyde metabolism we hypothesized that derivatizing the INN/TD- compounds to novel derivatives with improved pharmacologic properties. We also aim to achieve stronger interactions with the surface located αF- helix which is known to be involved in polymer stabilization. Thus, we hypothesize, these compounds not only will increase Hb affinity for oxygen but also would lead to direct stereospecific inhibition of polymer formation.

3.2. Goal

The goal of the project is to design and synthesize small molecule allosteric modulators of hemoglobin that would:

1) Increase Hb affinity for oxygen and inhibit sickling of red blood cells (RBCs)

2) Make closer contacts with the surface αF- helix and destabilize polymer contacts

3) Decrease oxidative metabolism of the aldehyde pharmacophore

3.3. Specific Aims

3.3.1. Specific Aim 1:

RATIONAL DESIGN, SYNTHESIS AND INVESTIGATION OF PP-COMPOUNDS

3.3.1.1. Specific Aim 1A:

Synthesis of PP- compounds as allosteric modulators of Hb.

3.3.1.2. Specific Aim 1B:

Investigation of the functional and antisickling properties of PP-compounds in vitro and in vivo.

3.3.1.3. Specific Aim 1C:

Studying the atomic interactions of PP-compounds with liganded Hb to elucidate their mechanism of action.

3.3.2. Specific Aim 2:

ELUCIDATION OF THE ATOMIC INTERACTIONS BETWEEN LIGANDED HB AND A 5HMF DERIVATIVE (VZHE004), AND SEVERAL VANILLIN DERIVATIVES (INN-310, TD-7, VZHE039)

CHAPTER 4

4. SPECIFIC AIM 1:

RATIONAL DESIGN, SYNTHESIS AND INVESTIGATION OF PP-COMPOUNDS

4.1. Approach
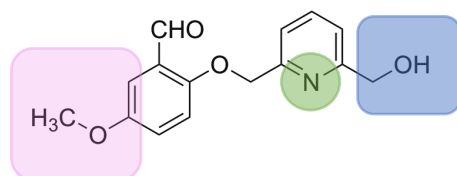
Figure 12. Structure of TD-7 and points of modifications for the synthesis of PP-compounds

Figure **12** shows the structure of TD-7, the most potent of the previous generation (TD) compounds. As mentioned above, we decided to further modify the TD-7 structure for further improvement in the biological activities and metabolic profile of the compounds. The modifications include:

1) Replacing the hydroxymethyl group on the pyridine ring with methyl ester group as well as varying its position on the pyridine ring which we hypothesized would increase the polymer

destabilization by making closer interactions with the αF- helix. Introduction of the bulkier, methyl ester group, we expect, would increase interactions with Hb that would lead to increased antisickling activity.

2) The pharmacophore- aldehyde group is the most susceptible to metabolism. Hence, we decided to introduce a hydroxyl group, ortho with respect to the aldehyde, on the benzaldehyde ring. This, we believe will help protect the aldehyde group from metabolism by aldehyde dehydrogenases (ALDH) by engaging in an intramolecular hydrogen bonding interaction in turn increasing the pharmacokinetic properties of these compounds.

3) Lastly, we varied the position of the pyridine nitrogen in an attempt to understand its role in the binding of these compounds to the protein.

From all the possible combinations of modifications listed above, synthesis of 20 compounds, on a whole, was plausible (Table **1**).

Table 1. Structures of proposed PP-compounds

| PP1 | PP5 |

PP2

PP6

PP3

PP10

PP4

PP7

PP8

PP11

PP9

PP14

PP12

PP13

PP15

PP16

PP17

PP18

PP19

PP20
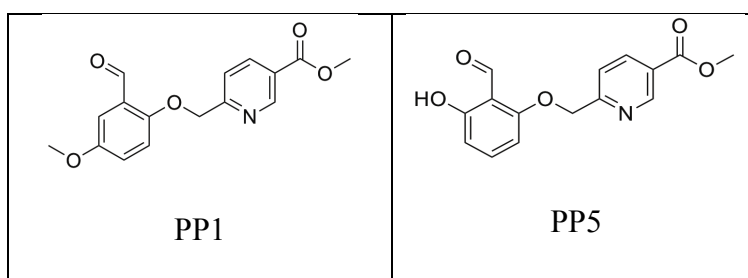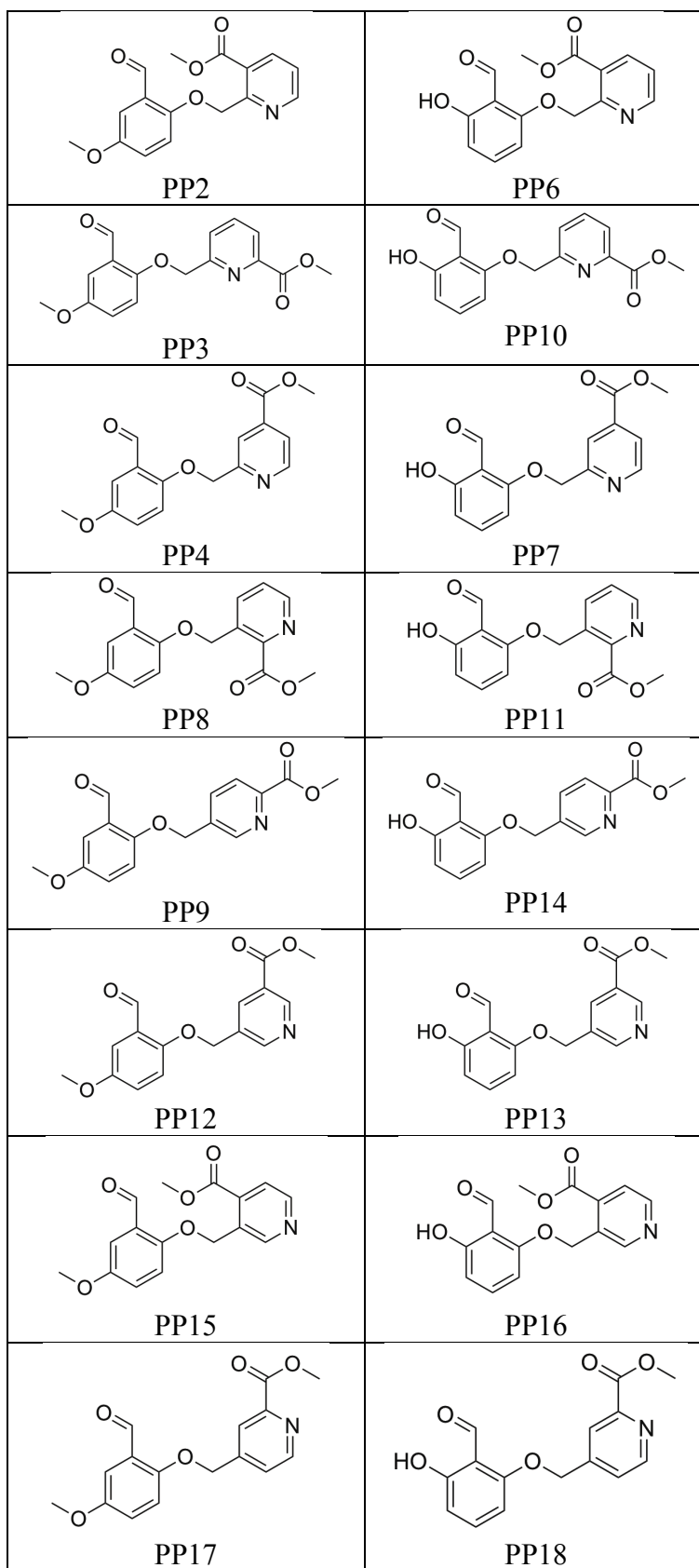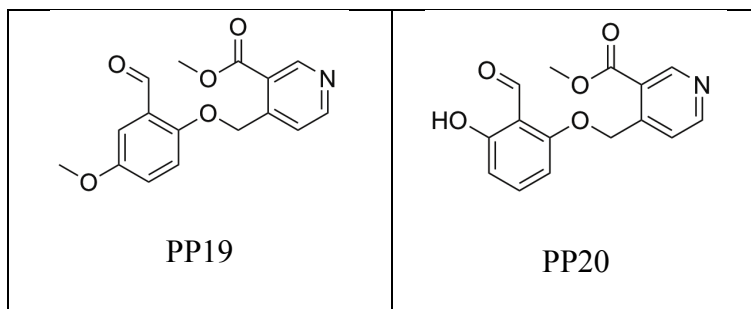
4.2. Specific Aim 1A: Synthesis of PP- compounds as allosteric modulators of Hb

4.2.1. Results

The synthesis of PP1, PP2, PP3, PP5, PP6, PP9, PP10 and PP14 was carried out in two steps. The first step was a radical catalyzed Wohl-Ziegler bromination reaction of a methyl substituted pyridylmethylester (Scheme **1**) to give bromomethyl substituted pyridylmethylester. The starting materials used for these reactions were methyl substituted methyl esters of nicotinic acid and picolinic acid. *N*-bromosuccinimide (NBS) was used as the brominating agent while 2,2`-azobis(2-methylpropionitrile) (AIBN) was used as the radical initiator. The reaction was carried out in carbon tetrachloride (CCl₄) as the solvent with the temperature ranging from 40-75°C depending on the reactivity of the starting materials.

SCHEME 1: Bromination of methyl substituted pyridylmethylesters

Reagents and conditions: (i) NBS (1 eq), AIBN (10%), anhydrous CCl$_4$, 40-75°C, 5-8h.

Due to the non-availability of the corresponding methyl ester starting material for the synthesis of PP4 and PP7, 2-methylisonicotnic acid was esterified to obtain methyl-2-methylisonicotinate (Scheme **2**). Fischer esterification was carried out using concentrated sulfuric acid as the catalyst. Methanol was used in excess to shift the equilibrium towards the product and the reaction was carried out at 68°C for 48h to yield the corresponding product. Methyl-2-methylisonicotinate was then brominated as shown in Scheme **1.**

SCHEME 2: Synthesis of methyl-2-methylisonicotinate
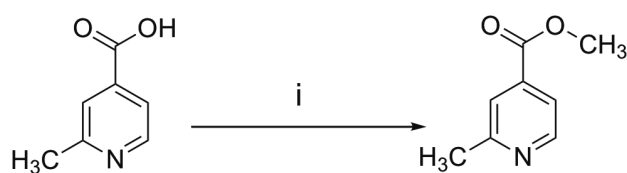
Reagents and conditions: (i) Concentrated H$_2$SO$_4$, CH$_3$OH, reflux, 48h.

The bromomethyl pyridine intermediates obtained were used to form an ether linkage between the phenolic oxygen of either 2-hydroxyl-5-methoxybenzaldehyde or 2,6- dihydroxybenzaldehyde via Williamson's synthesis to obtain the two series of PP-compounds, without and with the o-hydroxyl group respectively (Scheme **3**). Anhydrous K$_2$CO$_3$ was used as the base to facilitate the generation of the phenoxide ion. The reaction was carried out at room temperature with *N,N*-Dimethylformamide (DMF) as the solvent.

SCHEME 3: Synthesis of PP1-PP14
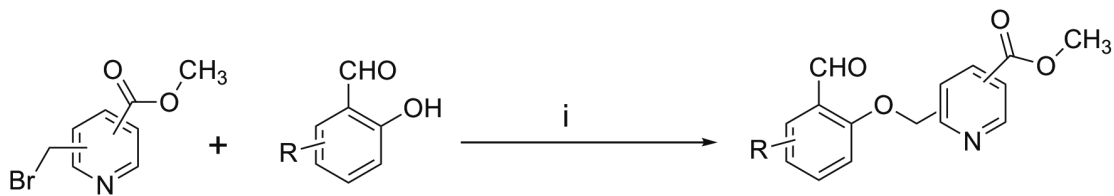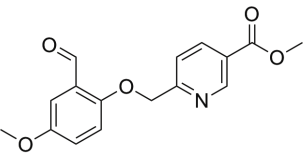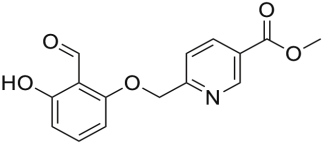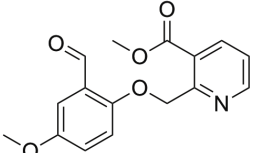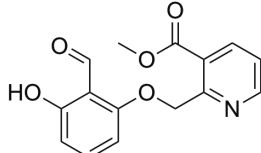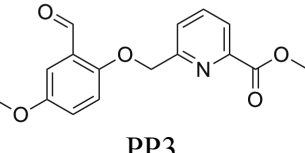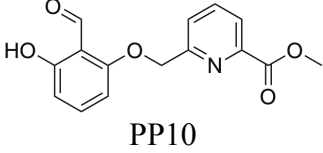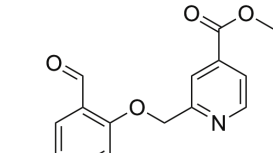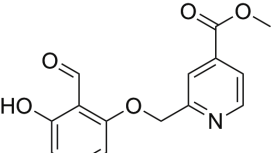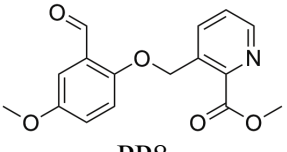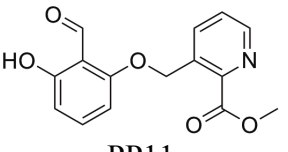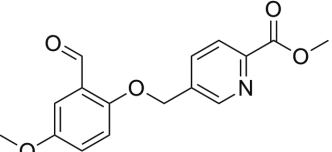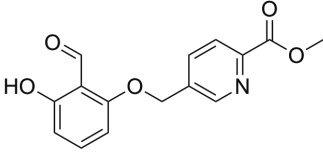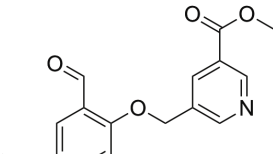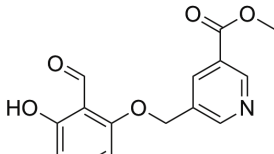
Reagents and conditions: (i) Anhydrous K_2CO_3, DMF, R.T., 5h. [R= o-OH or m-OCH$_3$]

Bromomethyl substituted pyridylmethylester derivatives were commercially available and used for the synthesis of PP8, PP11, PP12 and PP13 as per Scheme **3**.

For the synthesis of proposed compounds PP15 and PP16, methyl-3-methylisonicotinate was used as the starting material to carry out the bromination according to Scheme **1**. However, this reaction failed. Several manipulations of the reaction conditions were carried out to optimize the scheme but the monobromo intermediate could not be isolated. Similar results were obtained in the case of PP17-PP18 and PP19-PP20 where the bromination of methyl-4-methylpicolinate and methyl-4-methylnicotinate yielded the dibromo side products respectively.

Thus overall, 14 final compounds (PP1-PP14) were synthesized. The percentage yield obtained for each final compound is shown in **Table 2**. The final compounds were characterized by ^{1}HNMR, ^{13}CNMR, HRMS and IR and their purity was determined by HPLC.

Table 2. Percentage yield obtained for PP-compounds

Compound	Yield (%)	Compound	Yield (%)
PP1	89	PP5	82
PP2	84	PP6	82
PP3	90	PP10	82
PP4	86	PP7	85
PP8	78	PP11	68
PP9	81	PP14	78
PP12	79	PP13	71

4.2.2. Discussion

Wohl-Ziegler bromination is one of the most common methods to carry out selective bromination of the benzylic carbon in aromatic compounds without causing halogenation on the ring. The mechanism of this reaction involves bromine radicals wherein a radical initiator is needed for the hemolytic cleavage of Br_2 to generate free bromine radical which then abstracts a hydrogen atom from the benzylic carbon. AIBN was used as the radical initiator in place of the classically used dibenzoyl peroxide since it is a milder reagent.

One of the challenges of this reaction is controlling the formation of the dibromo side product. Monobromination of the methyl group causes the C-H bond to become more polar and highly reactive so that dibromination takes place very rapidly. The key to the success of this reaction is to maintain a low concentration of Br_2 to avoid this. NBS was used as the brominating agent since it is more stable than molecular Br_2. It always contains Br_2 in small quantities and thus provides a means to keep the concentration of Br_2 low to prevent side reactions. CCl_4 was used as the solvent of choice because the resulting succinimide after the reaction is insoluble and thus floats at the surface. This is a good indicator that the reaction is finished. External energy, either in the form of light or heat, is required for shifting the reaction equilibrium towards the product end. Temperature plays an important role in controlling the formation of the desired mono-bromo vs the di-bromo side product.
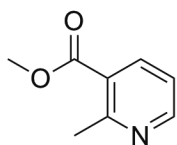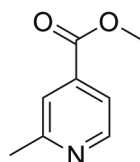
Methyl-2-methylnicotinate   Methyl-2-methylisonicotinate   Methyl-6-methylnicotinate
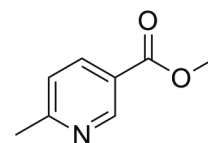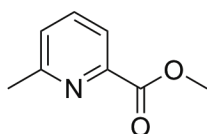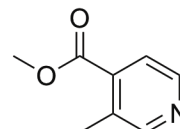
Methyl-6-methylpicolinate   Methyl-3-methylisonicotinate
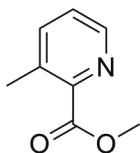
Methyl-3-methylpicolinate   Methyl-5-methylnicotinate   Methyl-5-methylpicolinate
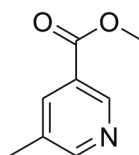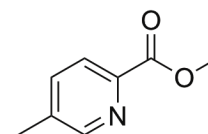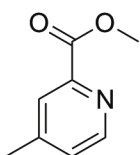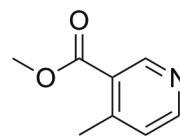
Methyl-4-methylpicolinate   Methyl-4-methylnicotinate

Due to the difference in the reactivity at the ortho, meta and para positions of the pyridine ring and the negative inductive effect (-I) of the ring nitrogen, different temperatures were required to carry out this reaction. The attacking bromine radical prefers positions of high electron density and abstracts hydrogens from carbon atoms which are farthest from the electron withdrawing substituents.[194] Specifically, higher temperature, i.e. reflux (75°C), was required for the

bromination of *ortho*-benzylic carbon while temperature of about 48°C afforded the monobromo product at the *meta*-benzylic carbon. Monobromo intermediate was not obtained in the case of methyl-4-methylpicolinate and methyl-4-methylnicotinate. This might be because, although this position is deactivated, it is farthest from the electron withdrawing nitrogen and hence, monobromination immediately results in dibromination of this transient intermediate which could not be therefore isolated. Bromination of methyl-3-methylisonicotinate resulted in what appeared to be an unstable monobromo intermediate which could not be isolated using column chromatography.

Presence of electron withdrawing methyl ester group also effects the reactivity of Wohl-Ziegler bromination. Ring deactivation due to the methyl ester group resulted in lower yields in case of bromination of methyl-6-methylnicotinate, methyl-2-methylnicotinate and methyl-5-methylpicolinate as compared to methyl-6-methylpicolinate and methyl-2-methylisonicotinate.

Following bromination, Williamsons etherification was carried out using either 2-hydroxy-5-methoxybenzaldehyde or 2,6-dihydroxybenzaldehyde. The electron withdrawing carbonyl group increases the acidity of the phenolic oxygen making it more susceptible to attack by the electrophile. In case of 2-hydroxy-5-methoxybenzaldehyde although the methoxy group is at the para position with respect to the phenol, its effect is not as pronounced as that of the carbonyl group. In case of 2,6-dihydroxybenzaldehyde, the second phenolic group is located at the meta position with respect to the first, hence its effect is also not that pronounced on the stabilization or destabilization of the phenoxide ion. In general, the desired products were obtained with reasonably higher yields with no side products as monitored by thin layer chromatography (TLC).
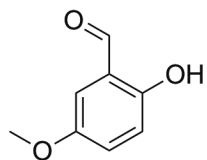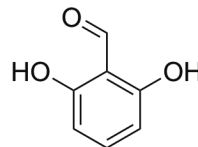
2-hydroxy-5-methoxybenzaldehyde   2,6-dihyrdoxybenzaldehyde

4.3. Specific Aim 1B: Investigation of the functional and antisickling properties of PP-compounds in vitro and in vivo

4.3.1 Results

The synthesized compounds were studied for their effect on Hb oxygen binding property, followed by their ability to prevent RBC sickling and modify Hb S.

4.3.1.1. Oxygen Equilibrium Curve (OEC) studies with whole blood

The primary mechanism of action by which aromatic aldehydes prevent hypoxia-induced polymerization of Hb S is by increasing Hb affinity for oxygen. Hence OEC studies were performed on all synthesized PP-compounds using 250mM stock solution in DMSO and normal whole blood to determine their effect on Hb oxygen binding property.

1) Concentration-dependent OEC studies:

Concentration-dependent OEC studies were carried out using 0.5mM, 1.0mM and 2.0mM concentrations of the compounds to 2ml of whole blood (Hematocrit adjusted to 30%). The solutions were incubated for 1.5h at 37°C, equilibrated in a tonometer with O_2 tensions of 6%, 20% and 40% for 7min each, followed by measuring the pO_2 and sO_2 values using *ABL700 series* table top automated blood gas analyzer. These values were used to calculate P_{50} using the software *Scientist*. TD-7 which was used as the positive control is known to exhibit its optimal activity between 1-2h. Similar observations have also been made for 5-HMF and hence 1.5h incubation time was used for these studies.[174] The results of concentration-dependent OEC studies are summarized in Figure **13** where the degree of shift in the P_{50} values, in percentage, as compared to the P_{50} of control (DMSO) is shown.
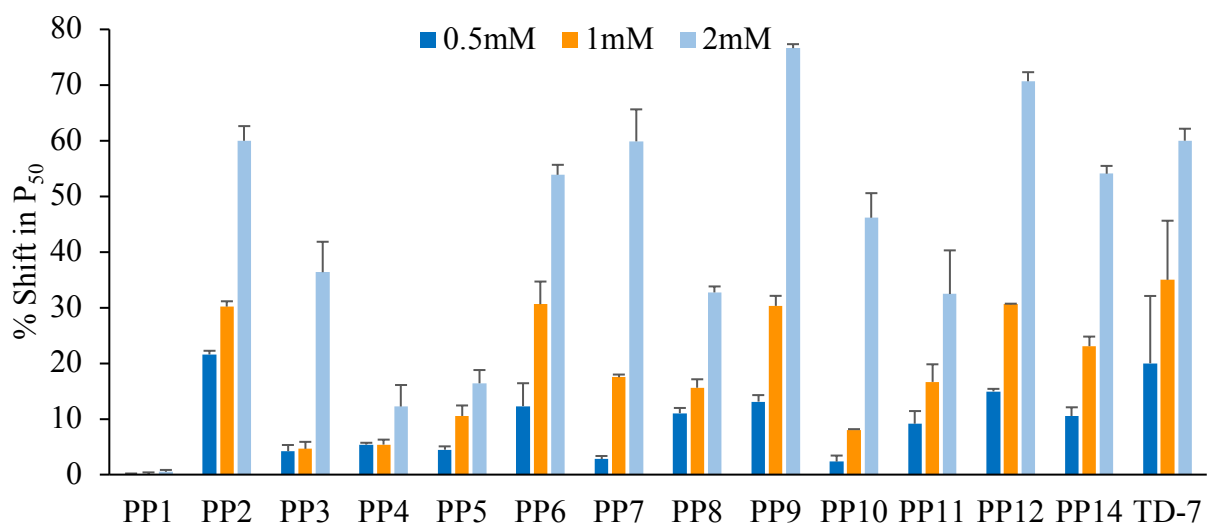
Figure 13. Concentration-dependent shift in the Hb-O_2 affinity (P_{50}) of PP-compounds in normal whole blood after 1.5 h incubation

The results show a dose-dependent effect for most PP-compounds. Compounds PP2, PP6, PP7, PP9, PP12 and PP14 showed the most significant shifts in their P_{50} values. PP1 and PP5 showed least potency due to solubility issue while PP4 appeared to show low potency because it had a slow onset of action (shown below). Vanillin, at 2mM concentration, shows only up to 21% shift in the P_{50}[171] whereas TD-7 showed relatively similar potency as most of the best PP-compounds. These observations confirmed that the structural modifications in PP-compounds conserved the potent in vitro activity previously seen in TD-7.

2) Time-dependent OEC studies:

Aromatic aldehydes are highly susceptible to oxidative metabolism resulting in most of these compounds having poor oral bioavailability, which has stymied their development for the treatment of SCD. Therefore, one of the major objective of this work was to obtain compounds that are less susceptible to the oxidative metabolism of the aldehyde pharmacophore. Keeping this in mind, time-dependent OEC studies were conducted in order to test the degree of P_{50} shifts with time. 2mM concentrations of PP-compounds were incubated with normal human blood (Hematocrit adjusted to 30%) at 37°C for 24h. TD-7 was used as the positive control. At defined time points (1, 4, 8, 12 and 24h) aliquot samples were drawn and subjected to OEC studies as mentioned above and the results are shown in Figure **14** and Figure **15**. Figure **14** shows the shift in P_{50} values of the PP-compounds containing the m-methoxy group on the benzaldehyde (PP2, PP3, PP4, PP8, PP9, PP12) while Figure **15** shows the shift in P_{50} of the PP-compounds containing the *ortho*-hydroxyl group on the benzaldehyde (PP6, PP7, PP10, PP11, PP13, PP14). PP2 showed optimal activity between 1-4h which then gradually decreased to half by 8h. Similarly, PP3 and

PP8 showed maximum potency at 8h followed by a gradual decrease over the course of 24h. PP12 followed a similar trend. PP4, on the other hand, showed a slow onset of action with an increase in the potency even at 24h. PP9 appeared to show sustained effect during the 24 h experiment duration.
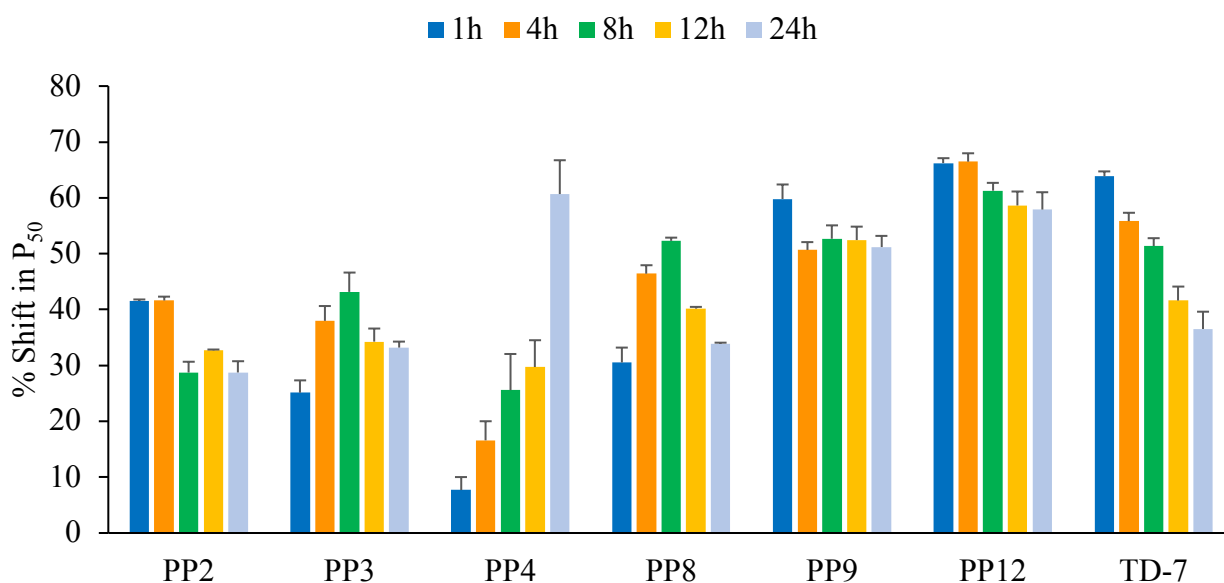
Figure 14. Time-dependent shift in the Hb-O$_2$ affinity (P$_{50}$) of *m*-methoxy substituted PP-compounds in normal whole blood at concentration of 2mM

In the case of the *ortho*-hydroxyl substituted PP-compounds, PP6, showed a slight decrease in potency after 8h which then was sustained during the 24h duration. All other derivatives, i.e. PP7, PP10, PP11, PP14 and PP13, showed sustained action over the duration of the experiment suggesting decreased metabolism of these compounds in whole blood. In contrast, TD-7, after reaching a maximal effect at 1h gradually decreased in potency and at 24h showed a loss of almost 45% of its activity.
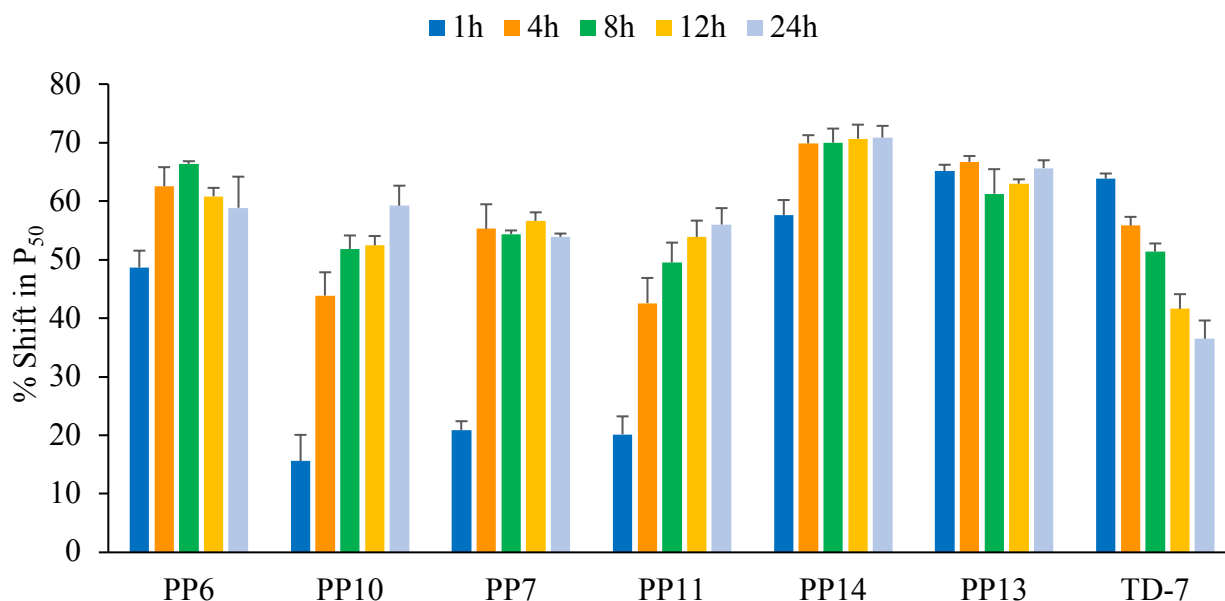
Figure 15. Time-dependent shift in the Hb-O$_2$ affinity (P$_{50}$) of *o*-hydroxyl substituted PP-compounds in normal whole blood at concentration of 2 mM

4.3.1.2. In vitro antisickling studies with sickle RBCs

The antisickling activities of aromatic aldehydes are primarily due to their ability to form a Schiff base adduct with sickle Hb to increase the protein affinity for oxygen thus preventing hypoxia induced Hb S polymerization. We thus investigated the compounds ability to modify sickle Hb, increase sickle Hb oxygen affinity, and prevent RBC sickling using homozygous sickle RBCs. These studies were conducted by our collaborator Dr. Osheiza Abdulmalik at the Children's Hospital of Philadelphia (CHOP).

The antisickling effects of PP-compounds were studied by incubating suspensions of SS cells in the absence or presence of the test compounds at 0.5, 1.0 and 2.0 mM concentrations in the presence of air for 1h followed by incubation under 4% O_2 at 37°C for 2h to induce hypoxia (Figure **16**).
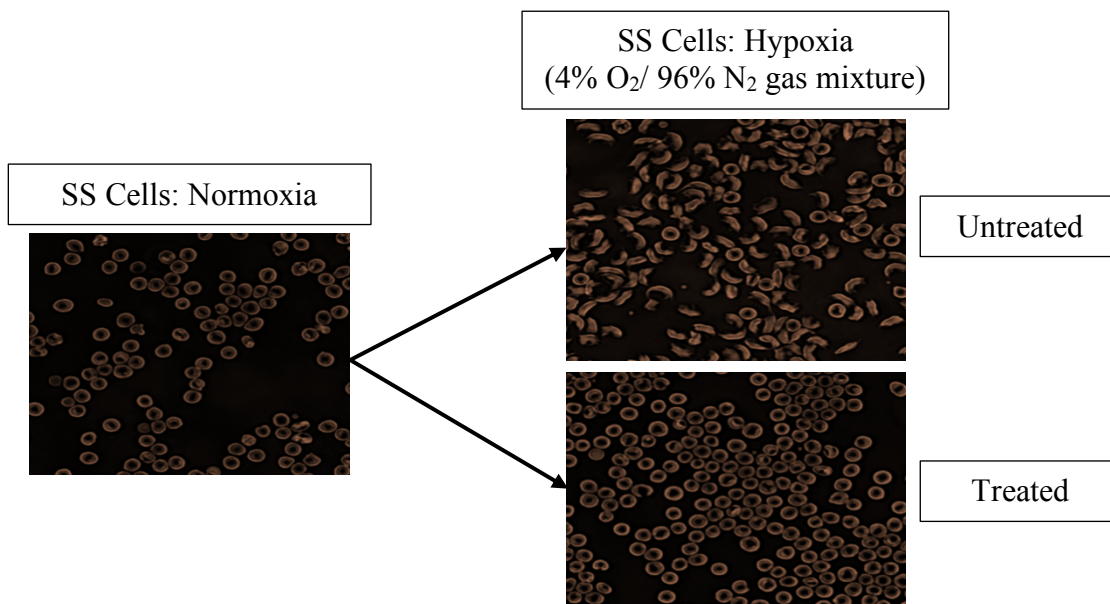
Figure 16. Schematic for antisickling assay

Concentration-dependent antisickling was observed for most PP-compounds (Figure **17**). As expected, due to their solubility issue, PP1 and PP5 did not show significant antisickling effect. Although PP11 and PP13 showed dose-dependent sickling inhibition, they did not show as much antisickling potency as other compounds. At 2.0 mM concentration of the compound, all other PP-compounds showed more than 90% sickling inhibition. At lower concentration of 0.5 mM, PP2, PP6, PP8 and PP14 showed more than 35% sickling inhibition as compared to only 26% by TD-

7. At 1.0 mM concentration, PP8 and PP9 showed almost 100% sickling inhibition while PP2, PP6 and PP14 showed more than 70% inhibition as compared to 47% by TD-7.
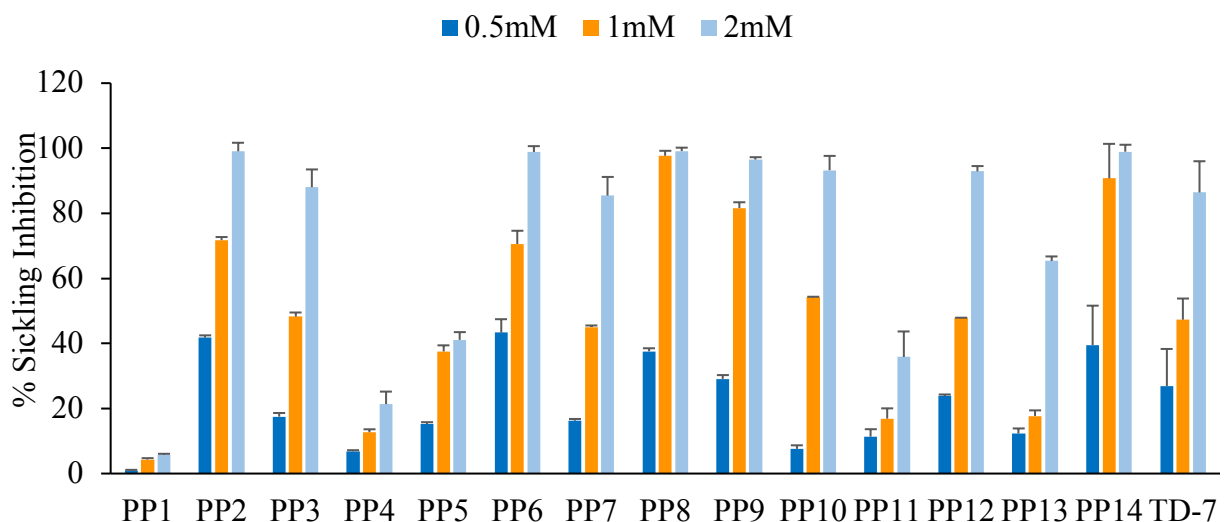
Figure 17. Inhibition of sickling by PP-compounds in SS RBCs

4.3.1.3. Hb- modification (adduct formation) studies with sickle RBCs

Aliquots from the antisickling study were hemolyzed and utilized for dose-dependent Hb modification study by cation exchange HPLC analyses. All compounds modified Hb S in a dose-dependent manner (Figure **18**) which was in correlation with the antisickling results (Figure **17**). PP1 and PP4 as expected from their solubility issue showed low Hb S modification. All other compounds showed very high Hb S modification with PP6, PP7, PP10, PP12, PP13, PP14 showing almost complete modification of Hb S at 2.0 mM concentration. At 1.0 mM concentration, PP6, PP8, PP9, PP12 and PP13 modified Hb S more than 60% which was similar to that seen for TD-7

(~60%). Compounds PP7, PP10 and PP14 showed more than 80% Hb S modification at 1.0 mM concentration. PP5 showed unusually high Hb S modification when compared to its low antisickling effect, which we considered to be an anomaly likely due to variable solubility of this compound.
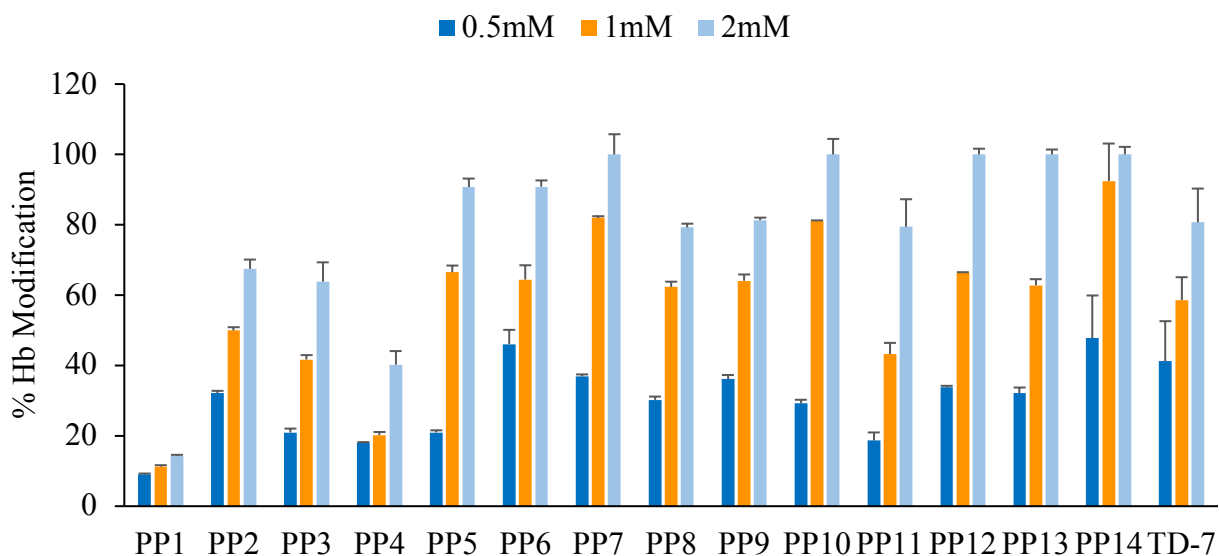
Figure 18. Concentration-dependent Hb modification (adduct formation) by PP-compounds in SS RBCs

4.3.1.4. OEC studies with sickle RBC lysates

In order to correlate the antisickling activity of PP-compounds and their primary mechanism of action of increasing the Hb affinity for O_2, aliquots from the Hb S-complex lysates from the antisickling studies were subjected to OEC studies. As observed with normal whole blood, the compounds showed a dose-dependent effect on increasing the Hb S affinity for O_2 (Figure **19**). As expected, PP1 and PP4 did not show much shift in the P_{50} values, however, PP5 again showed

anomalous behavior which could be attributed to its varying solubility. Compounds PP7, PP10, PP12, PP13 and PP14 appeared to show maximum increase in the Hb S affinity for O_2 which was comparable to that shown by TD-7 at 2.0 mM indicating that the structural modifications maintained the potency of these new class of compounds. This shift in the P_{50} correlated very well with the extent of Hb- modification however, poor correlation was observed with the antisickling properties for a number of compounds.
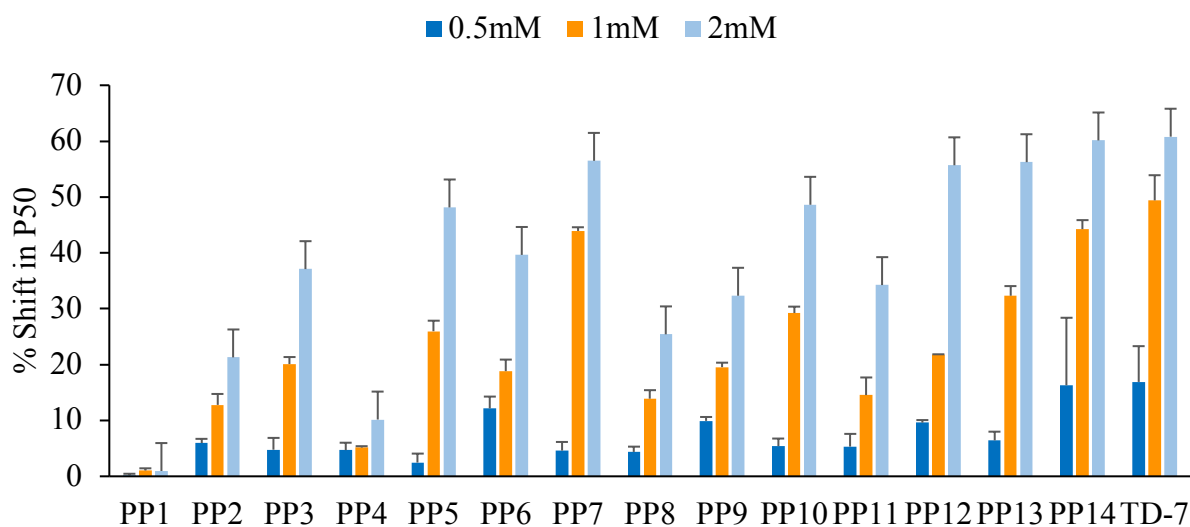
Figure 19. Concentration-dependent shift in the Hb-O_2 affinity (P_{50}) of PP-compounds in SS RBCs

4.3.1.5. RBC partitioning

Investigations of the RBC partitioning of organic small molecules have shown that lipophilicity and molecular size play an important role. Lipophilic compounds penetrate the RBCs via partitioning through the lipid bilayer membrane.[195,196] Knowledge of RBC partitioning of

compounds would thus enable us to determine the distribution of drug in the plasms vs RBCs. It also gives an idea about plasma protein binding of drugs and predicts drug distribution in vivo.

Studies to determine the partitioning of select PP compounds through the RBCs membrane were carried out using the antisickling assay mentioned above. Briefly, SS blood (volume 3x) was incubated with 2.0 mM concentration of the test compounds. Aliquot (volume 1x) was drawn and subjected to antisickling studies while the remaining 2x volume of blood was centrifuged to remove the plasma. The intention of removing the plasma was to remove any compound that remains in the plasma i.e. is not partitioned in the RBCs. This was repeated to obtain three separate aliquots which were subjected to antisickling studies in the expectation that if the compounds partition well into RBCs then all three aliquots would show more or less similar sickling inhibition.

The results are summarized in Figure **20**. PP8, PP10, PP12 and PP14 showed no significant decrease in their sickling inhibition in all three aliquots indicating that they partition well in the RBCs. Other PP compounds, including TD-7, showed a slight decrease in their antisickling activity. However, this decrease was not very significant and could not necessarily be attributed to the ability of the compounds to permeate the cell membrane. Though not conclusive, these results give a general idea about the ability of the compounds to enter the RBCs in order to bind to Hb and form Schiff base adducts.
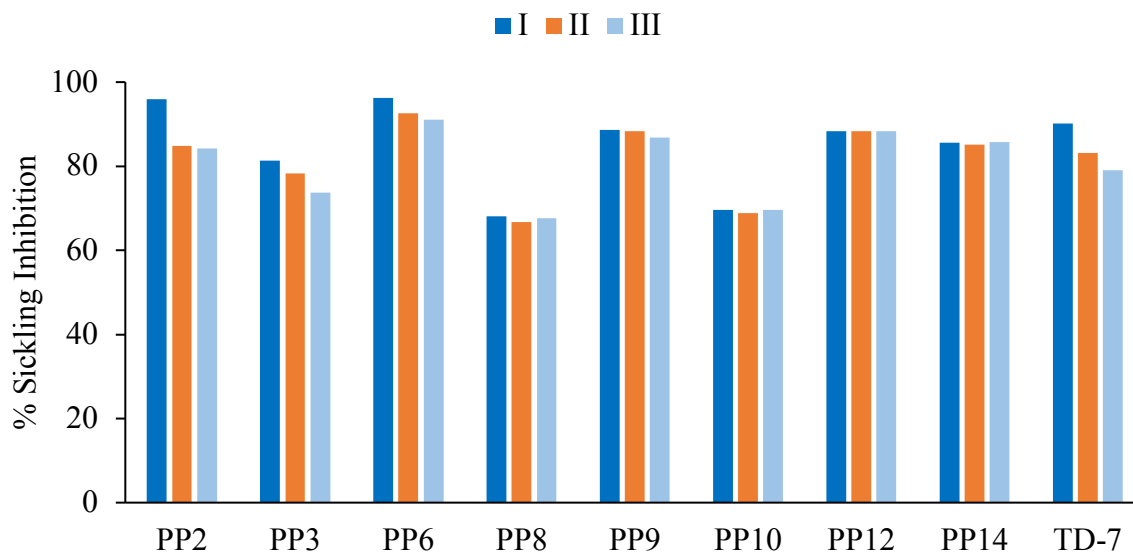
Figure 20. Sickling inhibition of aliquots (I, II and III) from partitioning buffer replacement assay of selected PP compounds

4.3.1.6. Investigation of the functional properties of PP compounds in vivo

Through extensive SAR studies, we have successfully developed several compounds that show significant antisickling activities. Some of these compounds, especially those with *ortho*- hydroxyl substitution relative to the aldehyde also showed sustained activity. We therefore selected three of these compounds, PP6, PP10 and PP14, for further in vivo PK/PD studies using wild-type mice. The wild type mice (C57BL/6)- two per group- received single I.P. doses of 150mg/kg (a total of 6 mice). Blood samples were obtained prior to treatment (0), and 1, 3 and 6h post treatment, via submandibular bleeding, and subjected to hemolysis using standard methods. Clarified lysates free of cell debris and red blood cell ghosts were analyzed by cation-exchange HPLC to determine the

levels of drug-modified Hb (adducts); and to conduct OEC studies to determine the degree of shift in P_{50} values.

All compounds showed significant in vivo modification of intracellular Hb with increasing levels from 1h to the 6h experimental period (Figure **21**). Mice treated with PP14 demonstrated the highest levels of modified Hb (19.1 ± 0.6 % at 6h), compared to 16.9 ± 1.4 % and 9.6 ± 1.9 % for PP6 treated and PP10 mice, respectively. Only 1.5 ± 0.3 % modified Hb was observed in mice treated with TD-7. Corresponding changes were observed in oxygen affinity at the measured time points of 3h and 6h, compared to 0h pre-treatment samples (Figure **22**). In case of their P_{50} shifts however, mice treated with PP6 showed highest levels of shifts (14.5% at 6h), compared to 5.5% and 11.5% for PP10 and PP14 treated mice respectively. Only approximately 1% shift in the P_{50} was observed in mice treated with TD-7.
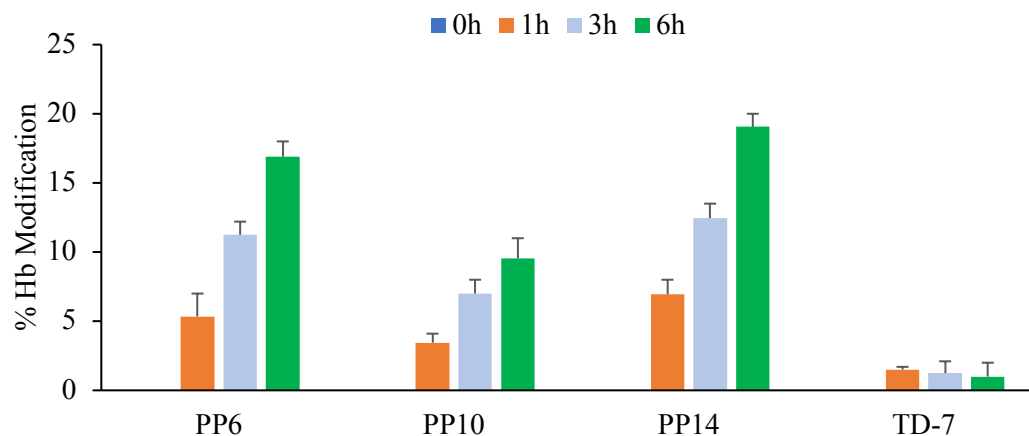
Figure 21. Time-dependent modification of Hb lysates in wild type mice (n=2) after 150mg/kg IP administration of test compounds
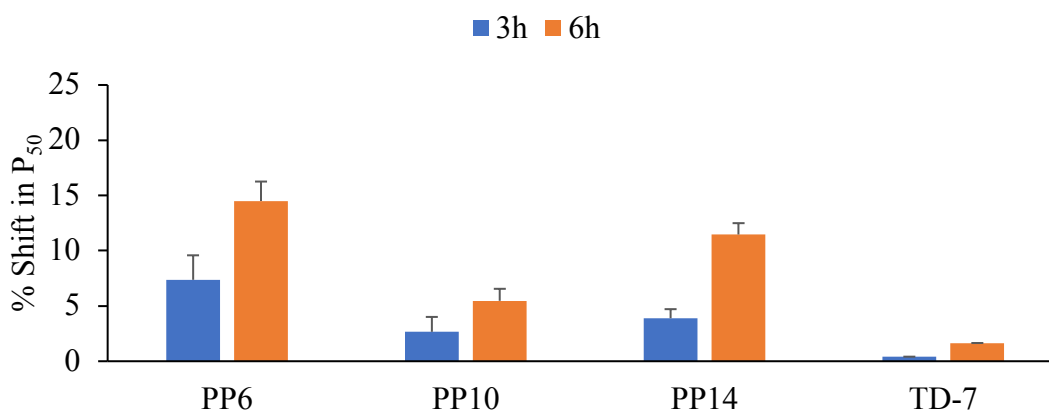
Figure 22. Time-dependent Hb O_2 affinity shifts in wild type mice (n=2) after 150mg/kg IP administration of test compounds

4.3.2. Discussion

Aromatic aldehydes form an important class of AEHs and have potential as therapeutics to treat SCD. They bind to Hb and modify it to a higher affinity Hb thus increasing the P_{50} shifts. Two major factors that determine the concentrations of AEH at the site of action are the kinetics of the transient covalent binding to Hb and the oxidative metabolism by ALDH in the RBCs as well as blood. Increasing the Hb affinity for O_2 forms the primary mechanism by which these compounds are expected to elicit their antisickling effects. Thus, OEC studies were conducted to determine the potency of the synthesized PP compounds. Dose-dependent studies were carried out using 0.5 mM, 1.0 M and 2.0 mM of compounds. The concentration of Hb in blood(~5.0 mM) warrants the use of such high concentrations of the test compounds. A narrow concentration range was used because most PP compounds and also TD-7 show maximal effects at 2.0 mM while

concentrations below 0.5 mM might be stoichiometrically not sufficient to saturate protein binding and likely below therapeutic range.

Whole blood, and not purified Hb, was used to study the effect of PP compounds on Hb affinity for O_2. This is because the presence of plasma proteins, serum enzymes and RBC cell membrane play an interfering role on the activity of the compounds. In the absence of these interfering components of whole blood these compounds are expected to show higher potencies than what is observed with whole blood. However, to obtain results more representative of the native system whole blood was used in place of purified Hb. PP compounds increased Hb affinity for O_2 in normal whole blood to varying degrees (Figure **13**). The inactivity shown by PP1 and PP5 was likely due to the fact that these two compounds were not soluble even in DMSO which was used for the assay. The most potent compounds are PP2, PP6, PP7, PP9, PP12 and PP14. The low biological activity of PP3, PP8, PP10 and PP11 could be due to the low intrinsic affinity for Hb or due to plasma protein binding and/or difficulty in RBC membrane permeation. It could also be due to significant metabolism by oxidases and ALDH in blood, liver and RBCs that are known to play a significant role in the bioavailability and potency of antisickling aromatic aldehydes.

Time-dependent OEC studies with PP compounds showed that most *ortho*-hydroxyl substituted exhibited extended pharmacologic effect in vitro when compared to analogous compounds without the *ortho*-hydroxyl moiety (Figure **15**). This suggests decreased metabolism of the compounds, likely due to the formation of intramolecular hydrogen bonding between the aldehyde carbonyl group and the *ortho*-hydroxyl group that protects the aldehyde from oxidative metabolism. Moreover, the *ortho*-hydroxyl has been shown to stabilize the Schiff-base interaction

between the compound and the N-terminal nitrogen of Hb that should slow down the dissociation of the aldehyde from the protein and prevent its metabolism in the RBCs. Interestingly, PP9, which had no *ortho*-hydroxyl group also showed sustainability. As will be discussed later, this observation is likely due to increased interactions with the protein that stabilize the bound compound, resulting in slow dissociation of the Schiff-base, and thus slowing down metabolism. These findings suggest a clear improvement in the metabolic profile of PP compounds over TD-7 in vitro which translated into improved pharmacokinetic properties in vivo. It is interesting that PP4, showed significant potency however because of a slow onset of action (Figure **14**) and the fact that it does not have a protective *ortho*-hydroxyl moiety this is not an ideal therapeutic candidate since it will be metabolized by the enzymes in blood and/or RBCs.

Furthermore, as seen with 5-HMF[174], INN-compounds[187] and TD-7; PP compounds had a major effect of Hb cooperativity as the shape of the OEC changed from sigmoidal to hyperbolic with addition of the compound (Figure **23**). This is a result of the stabilization of R-state Hb and restraining the cross-talk between the Hb subunits what is important for R→T transition.
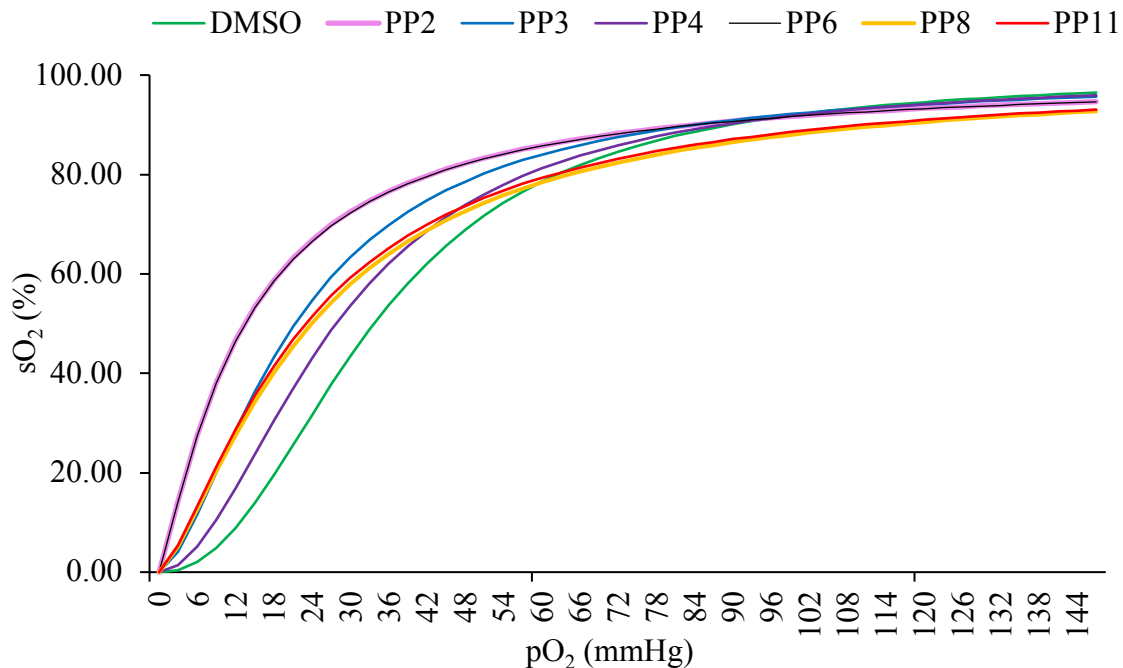
Figure 23. Representative figure showing the OEC shift of selected PP compounds at 2 mM concentration incubated for 1.5 h. The figure shows shift of the OEC curve from sigmoidal (DMSO) to hyperbolic (PP2, PP6).

The promising oxygen affinity results led to characterization of PP compounds for their antisickling properties in SS RBCs. The pathophysiology of SCD is driven by the hypoxia-induced polymerization of deoxy Hb S. We therefore tested the antisickling activities of the compounds in vitro by incubating 0.5, 1.0 and 2.0 mM concentrations with blood from subjects with homozygous SS (hematocrit 20%), under hypoxic conditions (4% O_2/ 96% N_2) at 37°C for 2h and assessed sickling by microscopy. Successively we conducted cation-exchange HPLC analyses to measure the degree of Hb modification, and OEC to assess P_{50} shifts using aliquots from the sickling studies. In the absence of test compounds, deoxygenation of SS RBCs resulted in sickling of RBCs (Figure **16**). When SS RBCs were incubated with PP compounds prior to exposure to hypoxia, we

observed significant reduction in the percentage of sickling in a dose-dependent manner (Figure **17**). The compounds PP2, PP6, PP8, PP9 and PP14 showed very high antisickling activity even at 1.0 mM concentration with a plateau effect observed for PP8 and PP14 resulting in 100% sickling inhibition at 2.0 mM. As noted above, this remarkable increase in the antisickling activity led us to investigate whether the improvement in the antisickling property is a result of the ability of the compounds to bind to Hb and modify it to a higher O_2 affinity. Hence, aliquots from the same experiment were subjected to OEC analysis as well as cation exchange HPLC analysis to determine P_{50} shifts and Hb-modification respectively. As observed with the normal whole blood, PP compounds potently increased Hb affinity for oxygen, Hb modification and inhibition of RBC sickling in dose-dependent fashions, and for some compounds we observed linear correlation between the three parameters. Interestingly, several of the PP compounds did not show such linearity; significantly inhibiting sickling but at remarkably low P_{50} shifts.

As seen from Figures **24** and **25** and Table **3**, % Hb-modification and % shift in the P_{50} values correlated very well with each other for the PP compounds. However, the antisickling properties and shift in P_{50} values showed poor linear correlation coefficient values (R^2) for the compounds PP2, PP3, PP6, PP8, PP9, PP10 and PP14. In fact, these compounds demonstrated the most potent antisickling effect despite only marginally increasing Hb affinity for oxygen (Table **4**). This may suggest a secondary, additional mechanism of antisickling action. We speculate that this secondary mechanism of antisickling action is due to perturbation of the surface located αF-helix a result of increased interactions between the compounds and the αF-helix and contributing to the antisickling effects of these compounds. The F-helix is very important in providing secondary interactions to stabilize the polymer.[67,72]
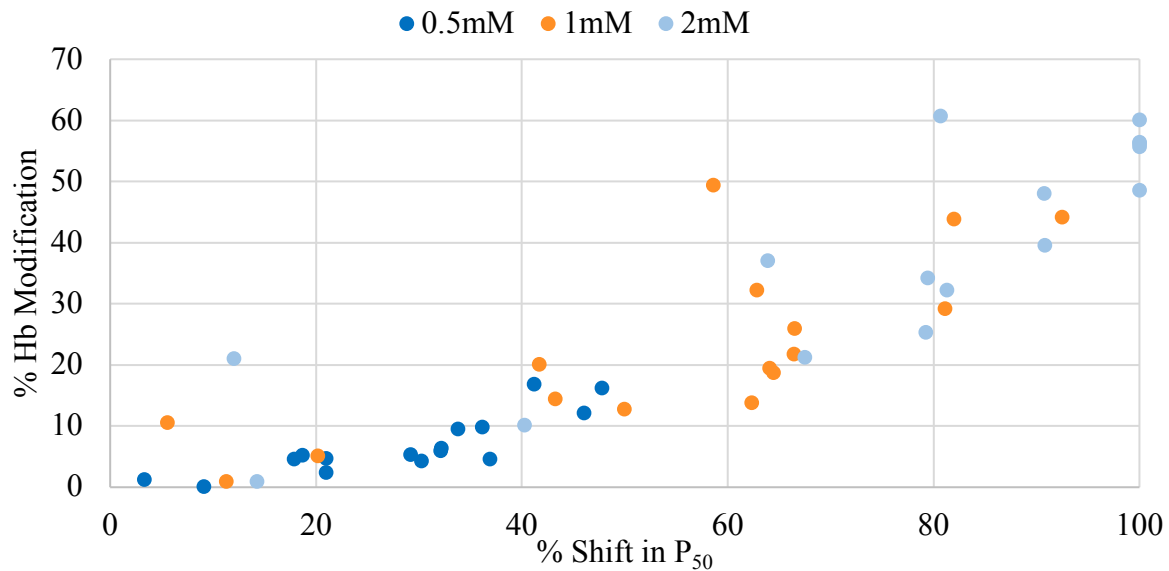
Figure 24. Correlation between % Hb-modification vs % Shift in P_{50} values for PP-compounds at 0.5 mM, 1.0 mM and 2.0 mM concentrations
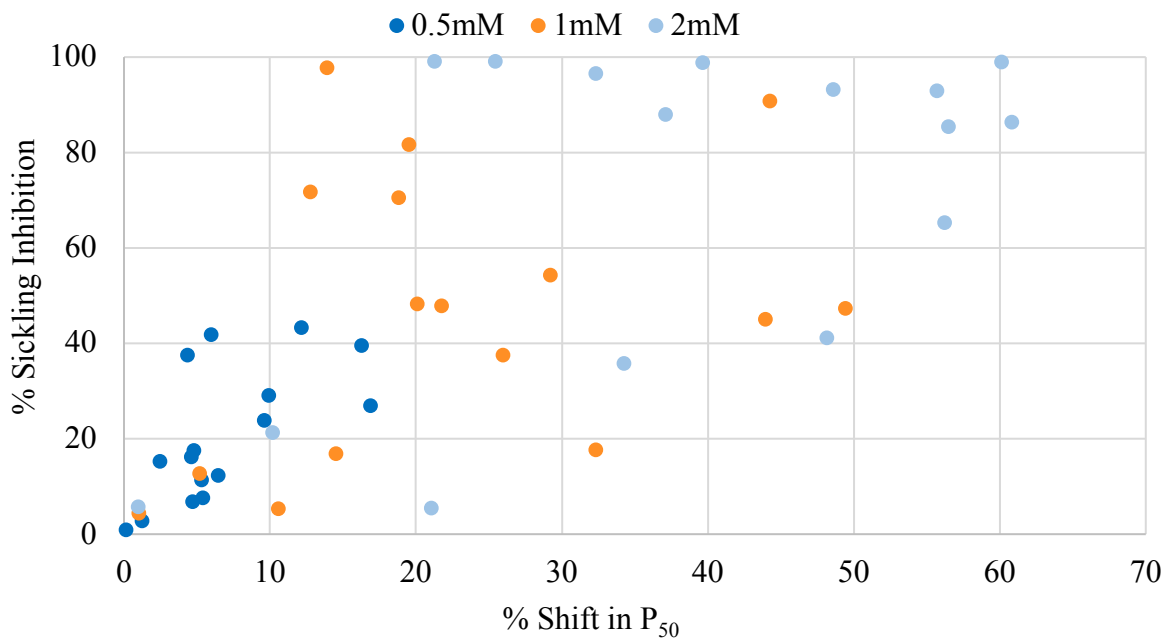
Figure 25. Correlation between % sickling inhibition vs % Shift in P_{50} values for PP-compounds at 0.5 mM, 1.0 mM and 2.0 mM concentrations

Table 3. Linear correlation coefficients obtained between the three functional parameters for PP compounds at 0.5 mM, 1.0 mM and 2.0 mM concentrations

Correlation Coefficient (R^2)			
Concentration	**0.5 mM**	**1.0 mM**	**2.0 mM**
% Hb-modification vs % Shift in P_{50}	0.86	0.88	0.93
% Sickling inhibition vs % Shift in P_{50}	0.6	0.31	0.5

Table 4. Oxygen equilibrium (P_{50}), Hb modification (adduct formation), and antisickling studies using SS RBCs with the seven outlier compounds

	% Shift in P_{50}			% Hb modification			% Sickling inhibition		
	0.5 mM	**1.0 mM**	**2.0 mM**	**0.5 mM**	**1.0 mM**	**2.0 mM**	**0.5 mM**	**1.0 mM**	**2.0 mM**
PP2	5.9±0.7	12.8±1.9	21.3±2.1	32.1±0.5	49.9±1.6	67.5±2.2	41.8±0.7	71.7±0.9	99±2.6
PP3	4.8±2.1	20.1±1.3	37.1±2.5	20.9±1.5	41.7±1.8	63.8±3.2	17.5±1.1	48.2±1.2	88±5.5
PP6	12.2±2.1	18.8±2.1	39.6±1.3	46±3.2	64.4±2.7	90.8±1.2	43.3±4.1	70.6±4.1	98.8±1.8
PP8	4.4±0.9	13.9±1.5	25.4±1.1	30.2±0.5	62.3±1.9	79.2±0.6	37.6±0.9	97.7±1.5	99.1±1.1
PP9	9.9±0.7	19.5±0.8	32.3±0.7	36.1±1.1	64±1.3	81.3±1.4	29.1±1.2	81.6±1.8	96.5±0.7
PP10	5.4±1.4	29.2±1.1	48.6±0.4	29.2±1.6	81.1±0.6	100±0.7	7.6±1.1	54.2±0.1	93.2±4.4
PP14	16.3±12	44.2±1.6	60.1±2.1	47.8±4.6	92.5±5	100±1.1	39.5±12	90.7±11	98.9±2.1

Amongst these outliers, PP6, PP10 and PP14 contain the *ortho*-hydroxyl group on the benzaldehyde ring. These compounds also showed extended pharmacologic effect. Thus, PP6, PP10 and PP14 were selected for preliminary in vivo studies. As seen in the in vitro studies, the three PP compounds showed significantly enhanced activity in vivo, when compared to previously studied precursor TD-7. which would be valuable for a regularly administered agent to treat SCD- as it is a chronic condition. The study clearly demonstrates the proposed mechanism of action of the PP compounds in vivo and suggests favorable PK properties compared to previously studied antisickling aromatic aldehydes e.g. TD-7.

4.4. Specific Aim 1C: Studying the atomic interactions of PP-compounds with liganded Hb to elucidate their mechanism of action

X-ray crystallography has played an important role in the structure-based drug design of derivatizing vanillin and its analogs to obtained more potent antisickling compounds. Based on the crystal structure of INN compounds and TD-7 (described in chapter 5), structural modifications were made to obtain PP compounds. It was hypothesized that these modifications would lead to increased interactions with the protein as well as make closer contacts with the αF-helix. To confirm our hypothesis, several PP compounds were co-crystallized with liganded Hb. The structures of O_2-Hb and CO-Hb complexes are very similar. However, the CO-Hb complex is comparatively more stable and thus easier to work with and crystalize than the O_2-Hb complex. Hence, CO-liganded Hb was used to study the binding interactions of these compounds with Hb.

We also used normal Hb for the structural studies since the quaternary structures of oxygenated sickle (Hb S) and normal (Hb A) are very similar, and the latter is easy to purify.[66]

Co-crystallization experiments were carried out under high salt (3.2-3.6 M sulfate/phosphate precipitant, pH 6.5) as well as low salt (10-20% PEG6000, 100 mM HEPES buffer, pH 7.4) precipitant conditions. Under low salt conditions, cherry red needle crystals were formed for most of PP compounds in 1-3 days and were used to collect x-ray diffraction data. Crystals obtained for PP7, PP10, PP12, PP13 and PP14 were very small and thin making crystal manipulation difficult for data collection. Crystals for PP1, PP2, PP3, PP4, PP5, PP6, PP8, PP9 and PP11 grew much larger to a size suitable for x-ray diffraction. The crystal structures of the COHb complexes with PP1, PP2, PP3, PP4, PP5, PP6, PP8, PP9 and PP11 were determined by molecular replacement method with Phenix[197] program using the native R2-state crystal structure (PDB ID 1BBB) as a search model. Structure refinement was carried out using both Phenix and CNS and correction was carried out using COOT.[198,199] As will be discussed later, only the complexes with PP2, PP6, PP9 and PP11 showed well-defined compound binding density to allow for refinement.

4.4.1. Results

4.4.1.1. Structural analysis of COHb-PP2 complex

The crystal structure of COHb-PP2 complex was solved using molecular replacement with the native R2 state structure (PDB ID 1BBB) and refined to 2.0Å. The overall tetrameric structure was

indistinguishable from 1BBB (RMSD ~0.4Å) detailed crystallographic data is summarized in Table **5**.

Table 5. Crystallographic data and refinement statistics for COHb-PP2 complex

Data collection statistics	
Space group	$P2_12_12_1$
Unit-cell *a, b, c* (Å)	62.84, 83.69, 105.06
Resolution (Å)	29.99- 1.85 (1.92- 1.85)
Unique reflections	46904
Redundancy	4.37 (4.14)
Completeness (%)	98.2 (96.0)
Average $I/\sigma(I)$	18.8 (3.4)
R_{merge} (%)[a]	3.7 (33.9)
Refinement Statistics	
Resolution (Å)	30.00- 2.00 (2.13- 2.00)
No. of reflections	37580 (5756)
R_{work} (%)	19.58 (25.4)
R_{free} (%)[b]	25.66 (33.1)
R.m.s.d. bonds (Å)	0.007
R.m.s.d. angles (°)	1.6
Dihedral angles	
Most favored (%)	95.76

Allowed (%)	3.71
Average B (Å^2)/atoms	
All atoms	30.59
Protein	28.02
Hemes	25.53
PP2	34.32
Water	42.93

$^a R_{\mathrm{merge}} = \Sigma_{hkl}\Sigma_i|I_i(hkl) - <I(hkl)>|/\Sigma_{hkl}\Sigma_i I_i(hkl)$. $^b R_{\mathrm{free}}$ was calculated from 5% randomly selected reflection for cross-validation. All other measured reflections were used during refinement.

As expected most aromatic aldehydes, two molecules of PP2 bound in a symmetry related fashion at the α-cleft of Hb (Figure **26**). The aldehyde group of PP2 formed a Schiff base interaction with the αVal1 nitrogen (1.5Å), directing the *ortho*-substituted pyridinylmethoxy methylester substituent upwards towards the surface of the α-cleft and close to the αF-helix. Since both molecules bound in a symmetrical fashion, detailed interactions of Hb will be focused on α2Val1 binding PP2. The benzaldehyde ring makes both intra and inter subunit hydrophobic interactions with α2Ala130, α2Ser131 and α1Thr134. Additionally, the two pyridine rings from the two PP2 molecules make face-to-face π-π stacking interactions (> 3.7 Å) with each other (Figure **27**). The ortho located pyridine nitrogen atom forms an inter-subunit water mediated hydrogen bonding interaction with hydroxyl group of α1Ser131.
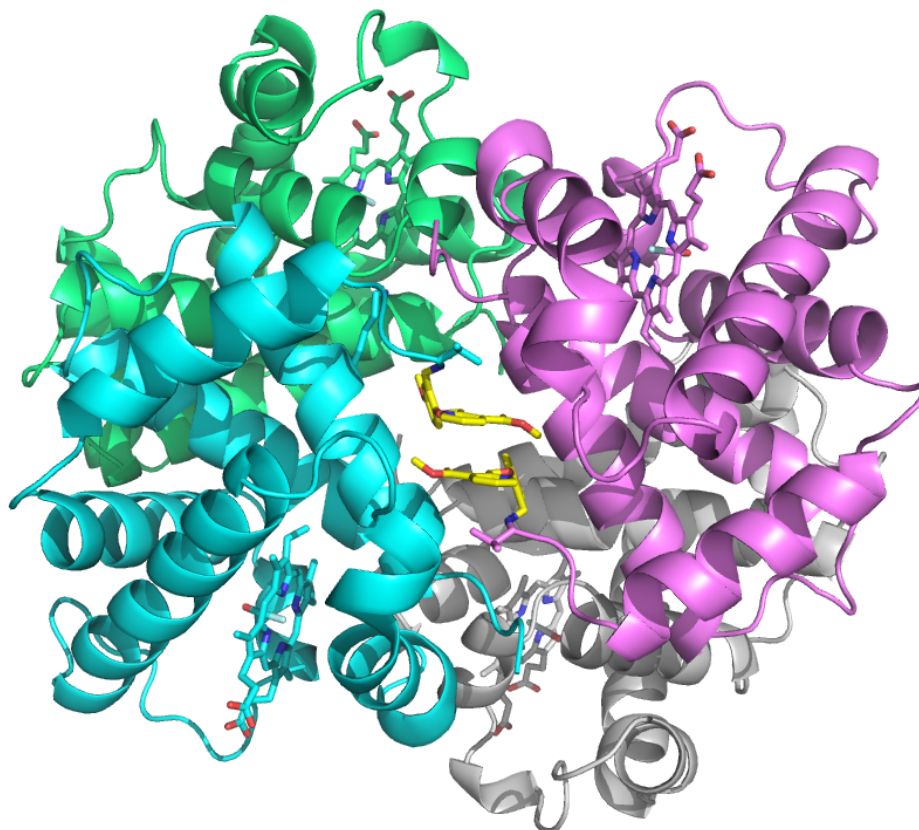
Figure 26. Crystal structure of Hb in R2 state in complex with a pair PP2 molecules (yellow sticks) at the α-cleft of Hb with the α (α$_1$- cyan; α$_2$- magenta) and β (β$_1$- grey; β$_2$- green) ribbons, heme groups are shown as sticks while CO molecules are shown as light blue sticks.
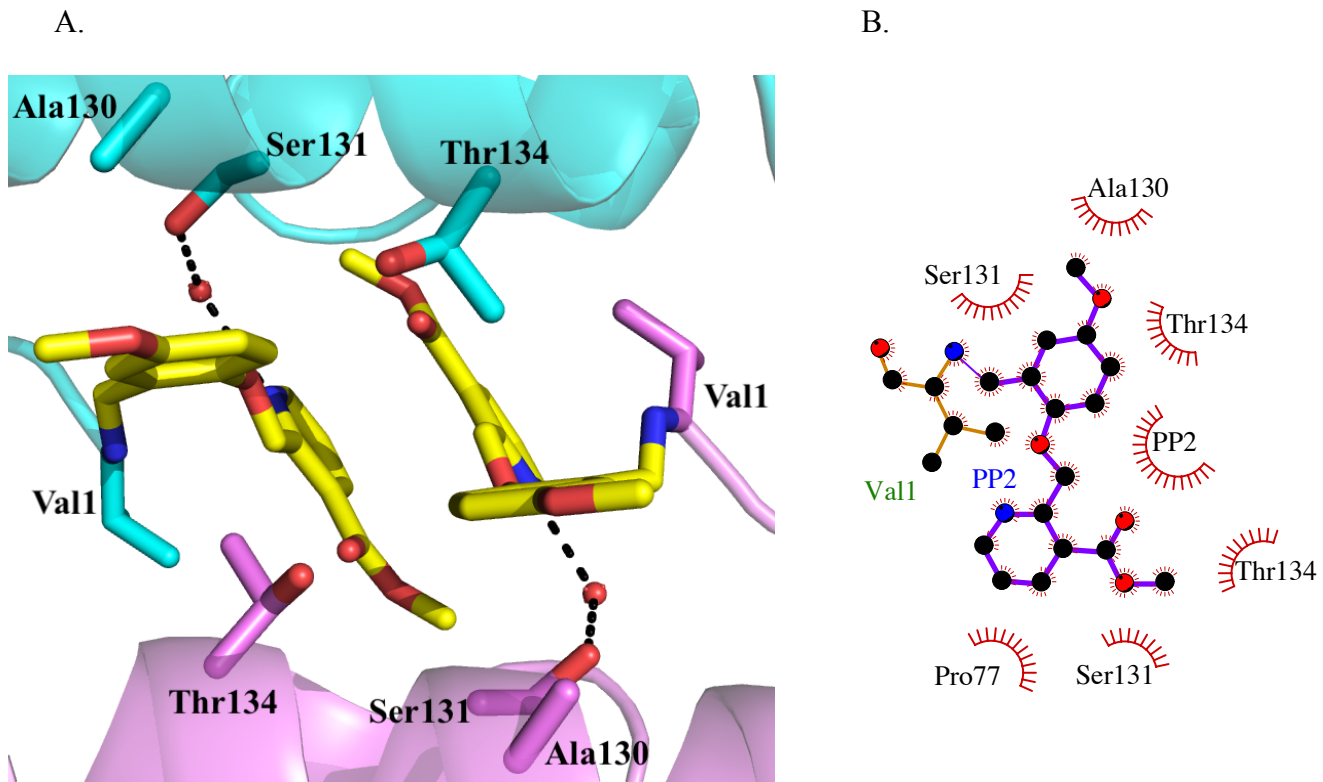
Figure 27. (A) Close up view of the binding pocket of PP2 (yellow sticks) in the central water cavity of Hb shown as ribbons (α_1- cyan; α_2- magenta) and water molecules shown as red spheres (B) Two dimensional contacts between one PP2 molecule, protein and second PP2 molecule.
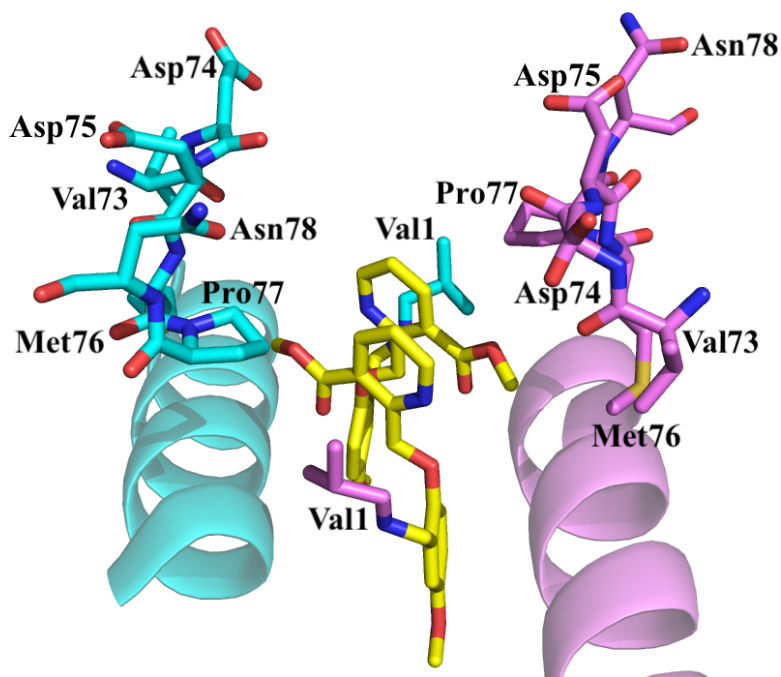
Figure 28. Binding pose of the two PP2 molecules (yellow sticks) showing interactions with the αF-helix of Hb with the α (α_1- cyan; α_2- magenta). Amino acid residues of the protein are shown as sticks.

The *ortho*-substituted pyridinylmethoxy-methylester made a 3.6 Å inter-subunit hydrophobic interaction with α1Pro77 of the surface located αF-helix (Figure **28**). We expect this hydrophobic interaction to perturb the polymer. Nonetheless, our design has predicted that this molecule will make even closer interactions to the F-helix. In summary, PP2 binds in a symmetry-related fashion making several intra- and inter-subunit interactions that should lead to stabilization of the R-state Hb, increase the protein affinity for oxygen, and concomitantly reduce the hypoxia-induced polymerization. Interaction with the F-helix, although not as strong as expected should also lead

to structural perturbation of the F-helix and contribute to the antisickling effect by destabilizing polymer formation.

4.4.1.2. Structural analysis of COHb-PP6 complex

The crystal structure of COHb-PP6 complex was solved using molecular replacement with the native R2 state structure (PDB ID 1BBB) and refined to 2.0Å. The overall tetrameric structure was indistinguishable from 1BBB (RMSD 0.3Å) detailed crystallographic data is summarized in Table **6**.

Table 6. Crystallographic data and refinement statistics for COHb-PP6 complex

Data collection statistics	
Space group	$P2_12_12_1$
Unit-cell *a, b, c* (Å)	62.64, 82.76, 104.77
Resolution (Å)	29.29- 2.00 (2.07- 2.00)
Unique reflections	150041
Redundancy	4.04
Completeness (%)	98.9 (99.7)
Average I/σ(I)	8.5 (2.3)
R_{merge} (%)[a]	7.9 (42.8)
Refinement Statistics	
Resolution (Å)	30.00- 2.00

No. of reflections	37580
R_{work} (%)	19.58
R_{free} (%)[b]	25.66
R.m.s.d. bonds (Å)	0.009
R.m.s.d. angles (°)	1.2
Dihedral angles	
Most favored (%)	95.94
Allowed (%)	3.71
Average B (Å^2)/atoms	
All atoms	34.02
Protein	33.75
Hemes	31.07
PP6	50.41
Water	36.97

[a]$R_{merge} = \Sigma_{hkl}\Sigma_i|I_i(hkl) - <I(hkl)>|/\Sigma_{hkl}\Sigma_iI_i(hkl)$. [b]$R_{free}$ was calculated from 5% randomly selected reflection for cross-validation. All other measured reflections were used during refinement.

As expected, and also observed in the PP2 structure, two molecules of PP6 bound in a symmetry related fashion at the α-cleft of Hb (Figure **29**). The aldehyde group of PP6 formed a Schiff base interaction with the αVal1 nitrogen, resulting in the *ortho*- substituted pyridinylmethoxy methylester substituent being directed upwards towards the surface of the α-cleft and close to the αF-helix. Unlike PP2 where the compound density was well defined, that of

PP6 was weak but good enough to fit the two molecules with some confidence. Specific bond distances will not be provided

Similar to PP2, it was observed that the pyridine rings make intra and inter subunit hydrophobic interactions with α2Ala130, α2Ser131, α2Thr134 and α1Thr134. The two pyridine rings from the two PP6 molecules make face-to-face π-π stacking interactions with each other (Figure **29** and **30**). Interestingly, the *ortho-* hydroxyl group is involved in both direct and water mediated hydrogen bonding interactions with the αVal1 nitrogen. This interaction, could help strengthen the transient covalent bond (Schiff base adduct) formed between PP6 and the nitrogen of αVal1 and lead to slow dissociation of the compound from its binding site. Consistently, this compound should show long sustained effect.
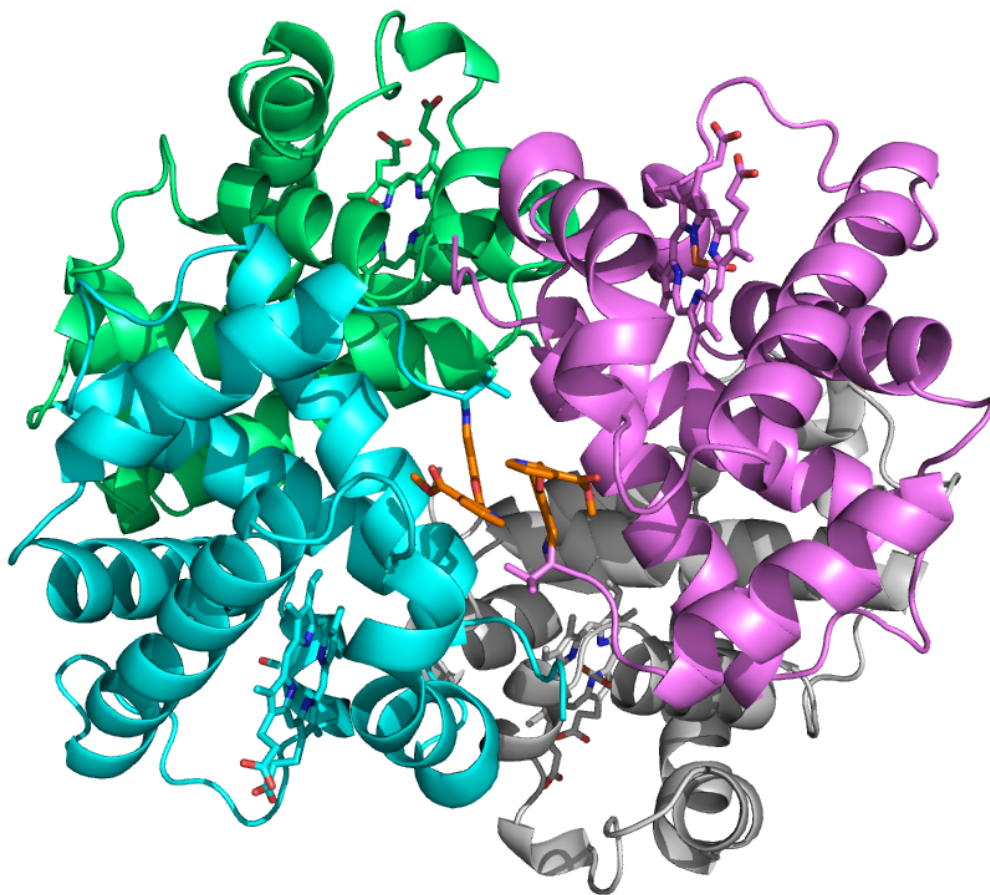
Figure 29. Crystal structure of Hb in R2 state in complex with a pair PP6 molecules (orange sticks) at the α-cleft of Hb with the α (α$_1$- cyan; α$_2$- magenta) and β (β$_1$- grey; β$_2$- green) ribbons, heme groups are shown as sticks while CO molecules are shown as light blue sticks.
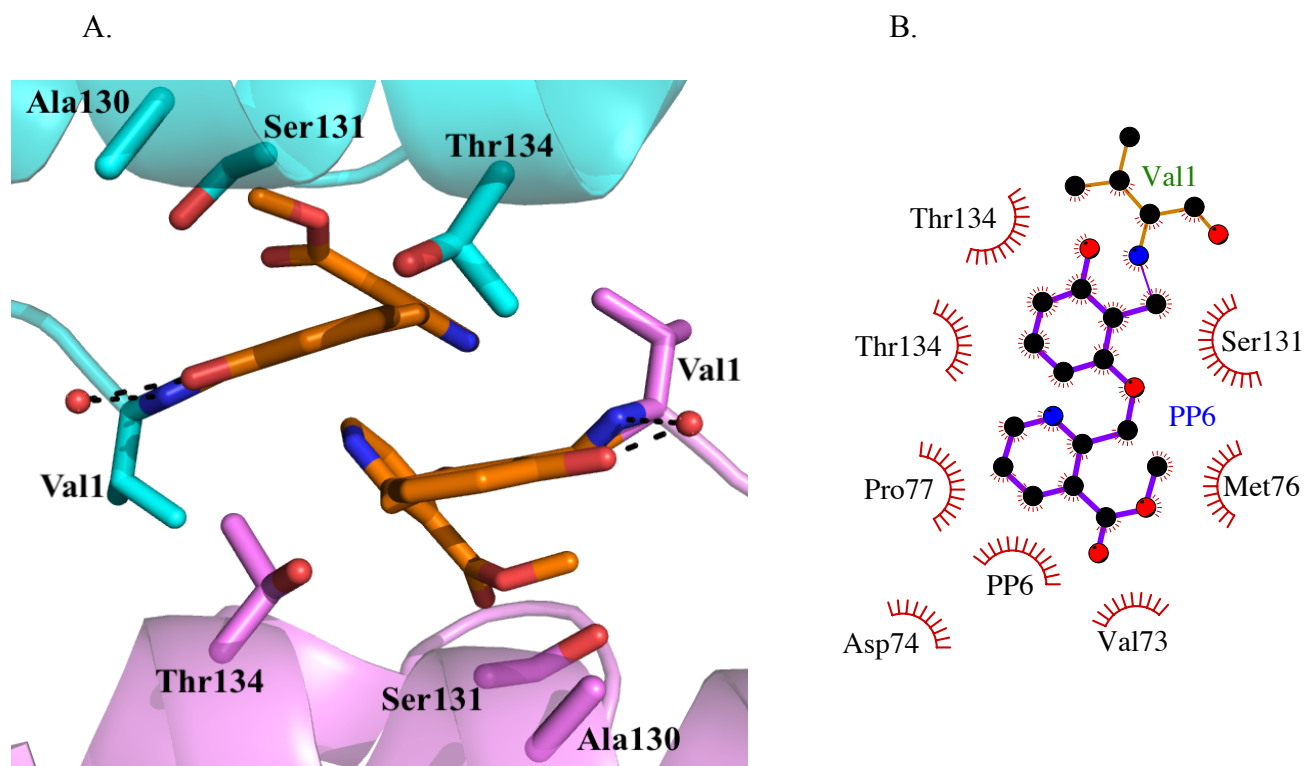
Figure 30. (A) Close up view of the binding pocket of PP6 (orange sticks) in the central water cavity of Hb shown as ribbons (α_1- cyan; α_2- magenta) and water molecules shown as red spheres (B) Two dimensional contacts between one PP6 molecule, protein and the second PP6 molecule.
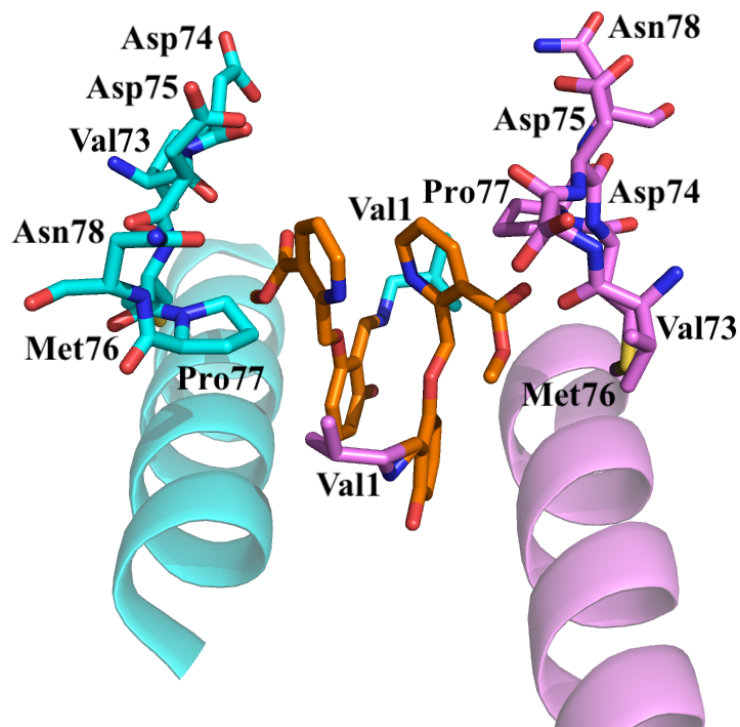
Figure 31. Binding pose of the two PP6 molecules (orange sticks) showing interactions with the αF-helix of Hb with the α (α₁- cyan; α₂- magenta). Amino acid residues of the protein are shown as sticks.

The Schiff base interaction between PP6 and Hb directed the pyridinylmethoxy-methylester group towards the surface of the α-cleft, with the pyridine ring making intra subunit hydrophobic interactions with the α2Pro77 of the αF-helix (Figure **31**). The ester oxygen also appears to make hydrogen bonding interactions with the backbone atoms of α2Val73 and α2Asp74 which are a part of the αF-helix. This we believe should lead to perturbation of the αF-helix and in turn destabilize polymer contacts.

4.4.1.3. Structural analysis of COHb-PP9 complex

The crystal structure of COHb-PP9 complex was solved using molecular replacement with the native R2 state structure (PDB ID 1BBB) and refined to 1.9Å. The structure showed very strong and well-defined electron density at the α-clefts and two molecules of PP9 modelled at the 2 αVal1.
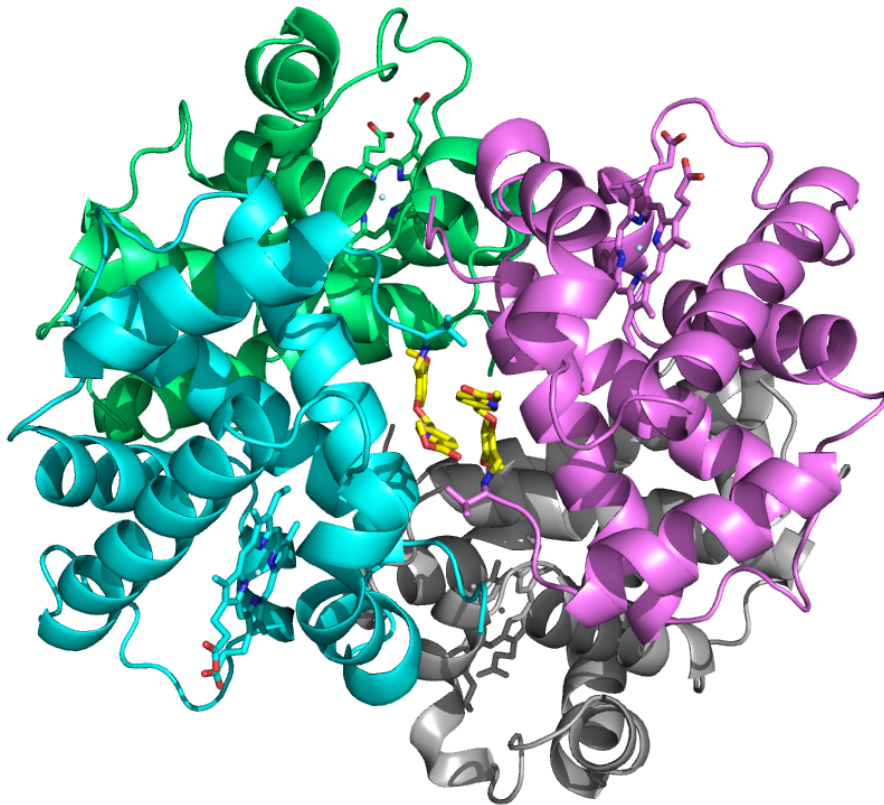
Figure 32. Crystal structure of Hb in R2 state in complex with a pair PP9 molecules (yellow sticks) at the α-cleft of Hb with the α (α$_1$- cyan; α$_2$- magenta) and β (β$_1$- light grey; β$_2$- green) ribbons, heme groups are shown as sticks.

As described above for PP2 structure, two molecules of PP9 bound in a symmetry related fashion, forming Schiff base interaction with the αVal1 nitrogen (1.5Å) at the α-cleft of Hb with the *ortho*-substituted pyridinylmethoxy-methylester also directed upwards towards the surface of the α-cleft and close to the αF-helix (Figure **32**). Since both molecules bound in a symmetrical fashion, detailed interactions of Hb will be focused on α2Val1 binding PP9. The benzaldehyde ring makes both intra- and inter-subunit hydrophobic interactions with α2Ala130, α2Ser131, α2Thr134 and α1Thr134. The two pyridine rings from the two PP9 molecules make face-to-face π-π stacking interactions (3.5 Å and greater) with each other (Figure **32** and **33**).
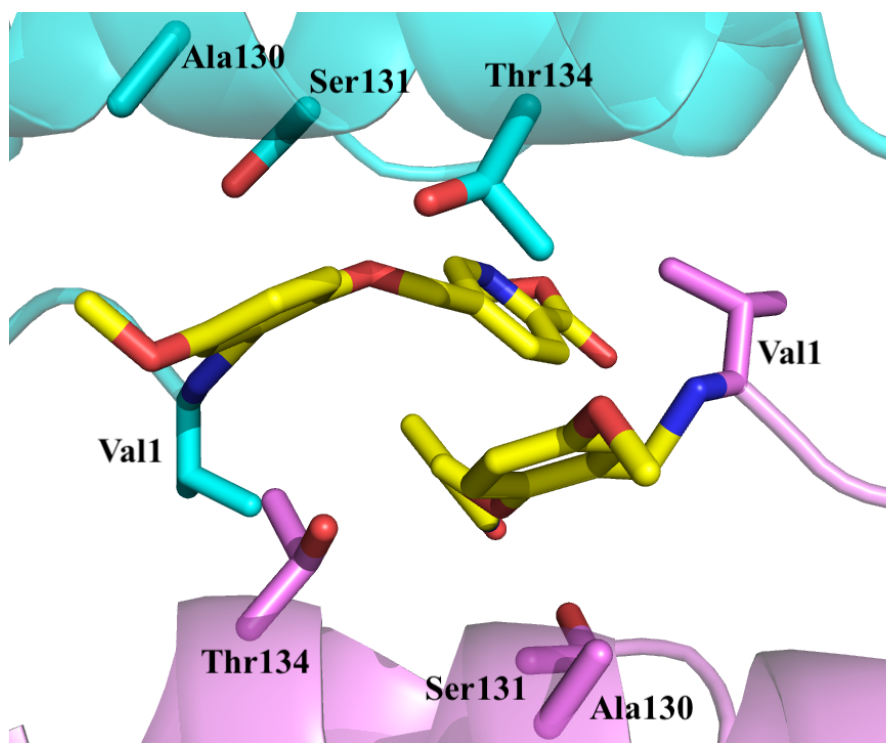
Figure 33. Close up view of the binding pocket of PP9 (yellow sticks) in the central water cavity of Hb shown as ribbons (α$_1$- cyan; α$_2$- magenta)
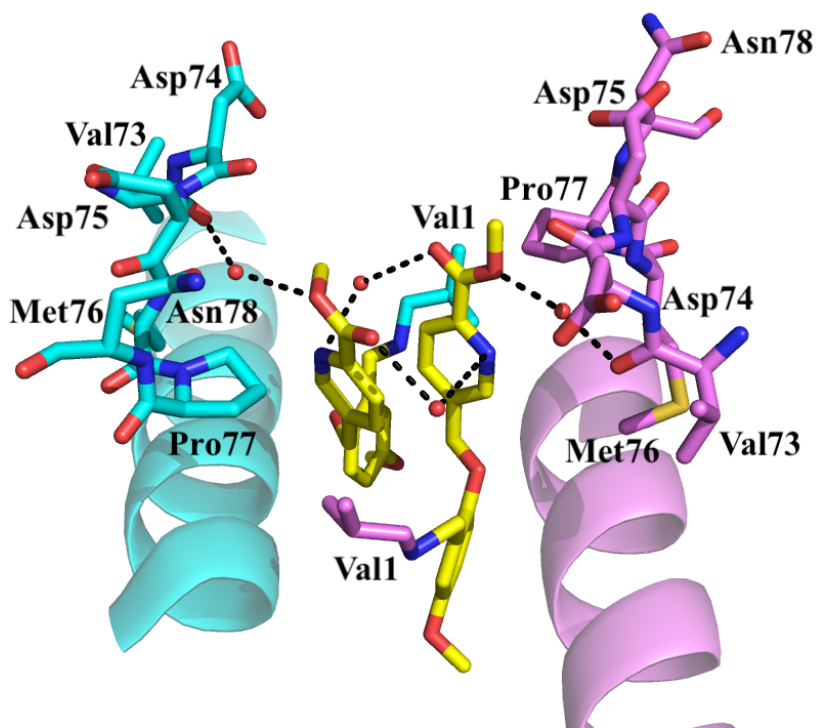
Figure 34. Binding pose of two PP9 molecules (yellow sticks) showing interactions with the αF-helix of Hb with the α (α$_1$- cyan; α$_2$- magenta). Amino acid residues of the protein are shown as sticks, water molecules are shown as red spheres.

Interestingly, the pyridinylmethoxy-methylester group has oriented toward the opposite αF-helix when compared to that of PP6. In fact, the pyridinylmethoxy-methylester makes intra-subunit hydrophobic interactions with α2Pro77 of the αF-helix (3. 1 Å and greater) instead of inter-subunit contact with α1Pro77 as observed for PP2. In addition, the hydrophobic contacts are stronger in PP9 than in PP2. The meta-located pyridine nitrogen and the oxygen of the ester also make intra-

subunit water-mediated interactions with the backbone atoms of α2Val73, α2Asp75 and α2Met76 of the αF-helix. In summary, PP9 binds in a symmetry-related fashion making several intra- and inter-subunit interactions that should lead to stabilization of the R-state Hb, increase the protein affinity for oxygen, and concomitantly reduce the hypoxia-induced polymerization. Importantly, the close interactions with the αF-helix should translate into significant perturbation of the helix and result in polymer destabilization, consistent with our design studies.

4.4.1.4. Structural analysis of COHb-PP11 complex

The crystal structure of COHb-PP11 complex was solved using molecular replacement with the native R2 state structure (PDB ID 1BBB) and refined to 1.9Å. Refinement is not completed and still ongoing. Detailed crystallographic data is summarized in Table **7**.

Table 7. Crystallographic data and refinement statistics for COHb-PP11 complex

Data collection statistics	
Space group	$P2_12_12_1$
Unit-cell *a, b, c* (Å)	62.71, 83.08, 104.95
Resolution (Å)	29.34- 1.90 (1.97- 1.90)
Unique reflections	43326
Redundancy	4.18
Completeness (%)	98.6 (99.4)
Average I/σ(I)	10.0 (2.3)

R_{merge} (%)[a]	6.1 (40.8)

Refinement Statistics

Resolution (Å)	29.34- 1.90 (1.97- 1.90)
No. of reflections	42414
R_{work} (%)	26.04 (36.52)
R_{free} (%)[b]	30.97 (42.17)
R.m.s.d. bonds (Å)	0.008
R.m.s.d. angles (°)	1.1
Dihedral angles	
Most favored (%)	95.58
Allowed (%)	3.89
Average B (Å^2)/atoms	
All atoms	29.32
Protein	30.80
Hemes	28.96
PP11	30.00
Water	--

[a]$R_{merge} = \Sigma_{hkl}\Sigma_i|I_i(hkl) - <I(hkl)>|/\Sigma_{hkl}\Sigma_iI_i(hkl)$. [b]$R_{free}$ was calculated from 5% randomly selected reflection for cross-validation. All other measured reflections were used during refinement.

As expected, two molecules of PP11 bound in a symmetry related fashion at the α-cleft of Hb, similar to the other discussed PP compounds (Figure **35**). The compound density was very strong and well defined than that observed for PP6 and could be fit with confidence. The aldehyde group

of PP11 formed a Schiff base interaction with the αVal1 nitrogen (1.3Å) at each α-cleft directing the directing the *ortho*-substituted pyridinylmethoxy-methylester substituent upwards towards the surface of the α-cleft and close to the αF-helix. Similar to what was observed in PP6, the *ortho*-hydroxyl moiety on the benzaldehyde ring (relative to the aldehyde) makes a very strong interaction with the αVal1 nitrogen that is involved in the Schiff-base interaction. This interaction is expected to stabilize the Schiff-base adduct and thus reduce the backward dissociation reaction. This is expected to reduce oxidative metabolism of PP11, consistent with the observation that PP11 exhibits significantly reduced metabolism. Since both molecules bound in a symmetrical fashion, other detailed interactions between PP11 and of Hb will be focused on α1Val1 binding since it showed better density than α2Val1 binding. The benzaldehyde ring made intra and inter subunit hydrophobic interactions with α1Ala130, α1Ser131, α1Thr134 and α2Thr134. The two pyridine rings form extensive face-to-face π-π stacking interactions (3.45Å) with each other (Figure **36** and **37**).
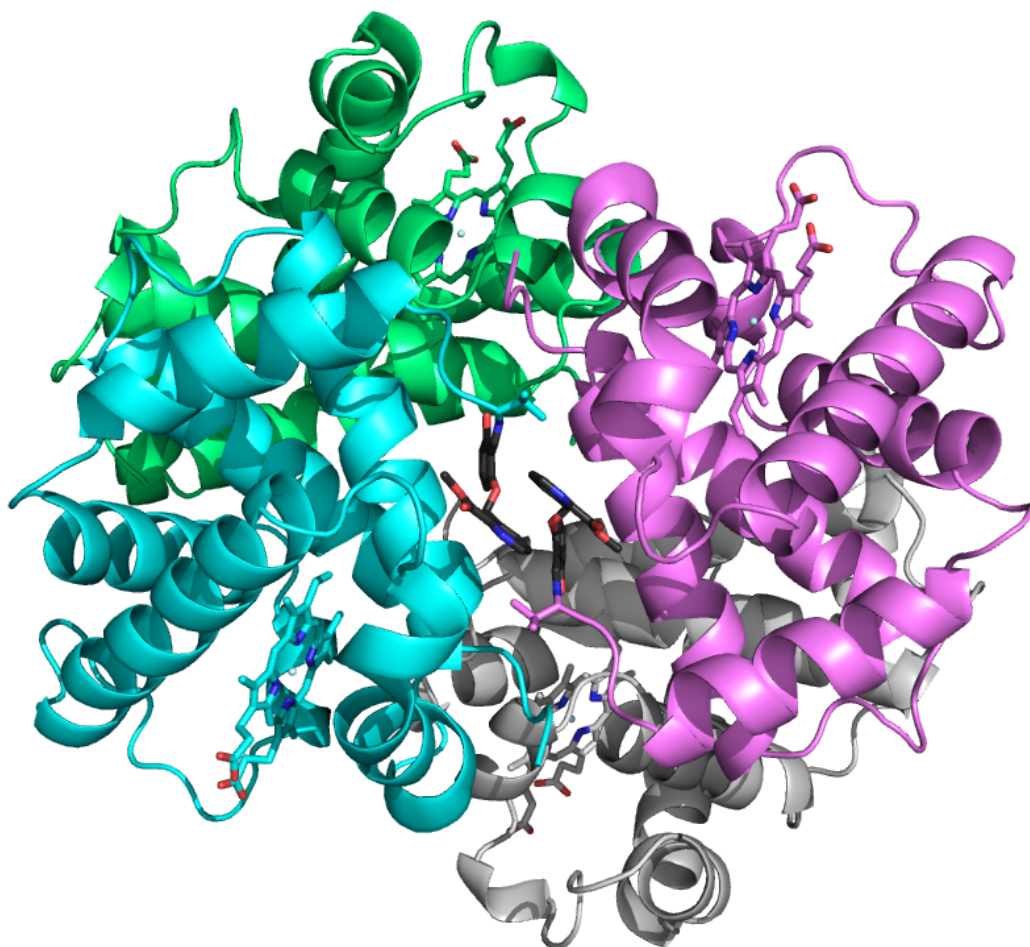
Figure 35. Crystal structure of Hb in R2 state in complex with a pair PP11 molecules (dark grey sticks) at the α-cleft of Hb with the α (α$_1$- cyan; α$_2$- magenta) and β (β$_1$- light grey; β$_2$- green) ribbons, heme groups are shown as sticks.

A.

B.
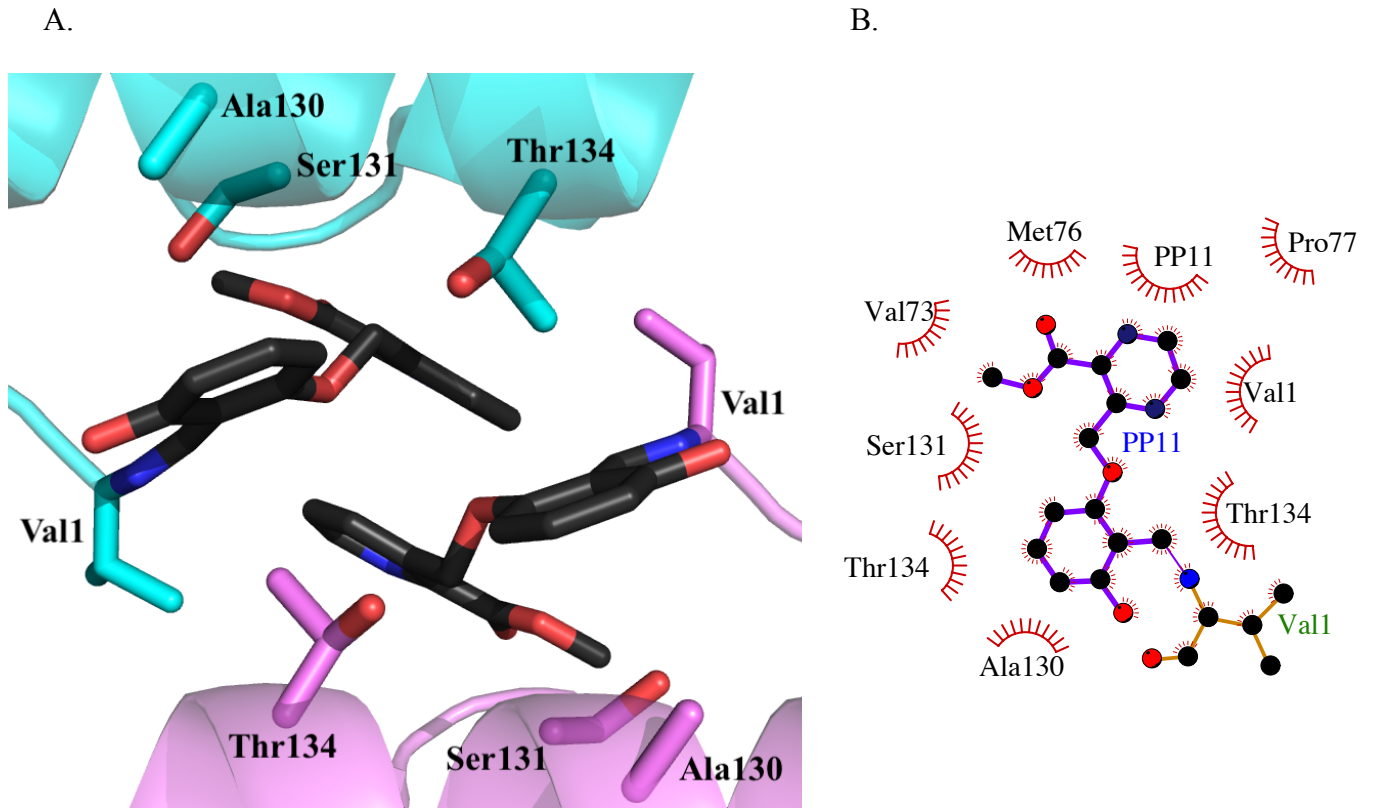
Figure 36. (A) Close up view of the binding pocket of PP11 (dark grey sticks) in the central water cavity of Hb shown as ribbons (α₁- cyan; α₂- magenta) (B) Two dimensional contacts between one PP6 molecule, protein and the second PP11 molecule.
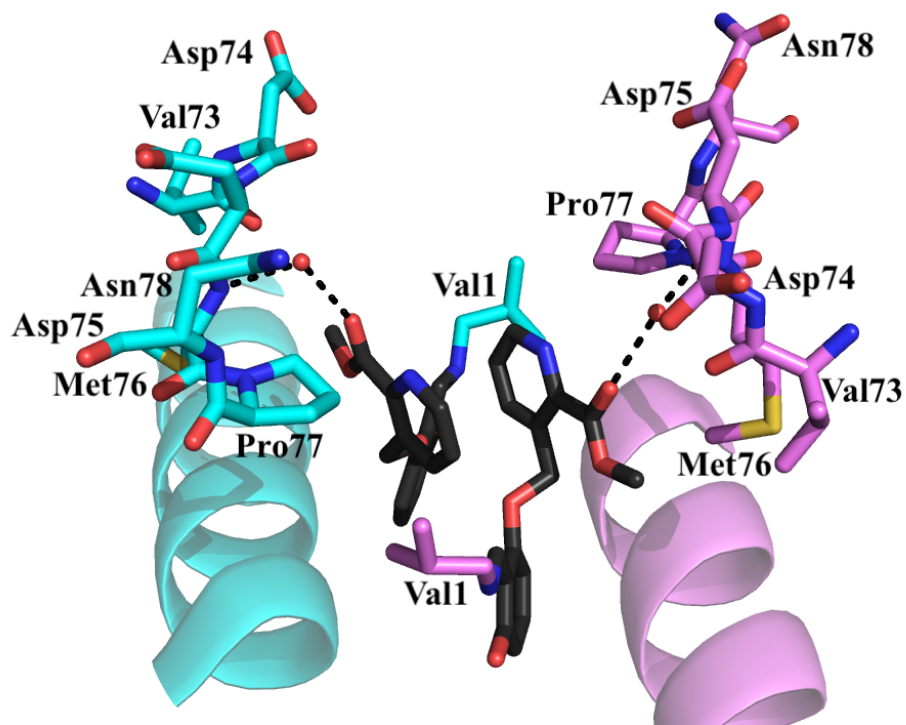
Figure 37. Binding pose of two PP11 molecules (dark grey sticks) showing interactions with the αF-helix of Hb with the α (α1- cyan; α2- magenta). Amino acid residues of the protein are shown as sticks, water molecules are shown as red spheres.

The pyridinylmethoxy-methylester group which is directed towards the surface of the protein makes intra subunit hydrophobic interactions with α1Pro77 of the αF-helix (3.5Å). This is similar to what was observed in PP6 but different from PP2, which made rather inter subunit hydrophobic interactions with the opposite α2 subunit, clearly showing some significant structural differences in the binding of these molecules. The carbonyl oxygen of the ester group also made intra subunit water mediated interactions with the backbone atoms of Val73, Asp75 and Met76 of the αF-helix (Figure **37**). Again, these water-mediated interactions are missing from the PP2 binding. These interactions with the αF-helix, we believe, should lead to perturbation of the αF-helix and in turn destabilize polymer contacts.

4.4.2. Discussion

X-ray crystal structures of several PP compounds were studied to elucidate the structural basis of their allosteric and antisickling properties. For structural studies, freshly made solution of PP compounds was added to deoxygenated Hb (30mg/mL protein) at Hb tetramer- complex ration of 1:10. The complex mixture was saturated with CO and allowed to incubate for 2h to form the COHb-compound complex. $NaBH_3CN$ was added to this mixture in order to reduce the Schiff-base adduct formed between the aldehyde of the compound and the N-terminal nitrogen of the protein to the corresponding irreversible alkylamine covalent bond. High salt conditions were used initially to carry out crystallization experiments with PP compounds (3.2- 3.6 M sulfate/ phosphate precipitant, pH 6.5). These conditions yielded trigonal bipyramidal shaped reddish crystals after 3 months. These crystals correspond to the classical R-state Hb. However, we did not observe bound compound, which is expected, as classical R-state structure has been shown not to bind these aromatic aldehydes due to sterically crowded α-cleft.

Crystallization was also carried out under deoxy conditions in an attempt to obtain T-state crystals. The electron density maps obtained for the deoxyHb-compound complexes showed sparse density at the N-terminal of α-cleft suggesting very weak compound binding. This could be due to the large binding pocket in case of deoxyHb which prevents tight binding of these compounds while making it difficult to form any inter sub-unit interactions with the protein. Similar observations have been reported for other aromatic aldehydes suggesting that these

molecules instead of stabilizing the T-state, rather, destabilize it, shifting the allosteric equilibrium to the R-state.[171]

In contrast to the classical R state, aromatic aldehydes are known to strongly bind to the R2 state structure of Hb and stabilize it.[171] Thus, using low salt conditions (10-20% PEG6000, 100 mM HEPES buffer, pH 7.4 cherry red needle crystals were obtained for several PP compounds that were isomorphous to previous aromatic aldehyde Hb R2 complex crystals. The R2 state crystals are very difficult to manipulate for data collection because of their thin needle morphology and fragility. Crystals were obtained for PP7, PP10, PP12, PP13 and PP14, however they were very small and thin making crystal manipulation difficult for data collection at present. Crystals for PP1, PP2, PP3, PP4, PP5, PP6, PP8, PP9 and PP11 grew much larger to a size suitable for x-ray diffraction data collection.

Table 8. PP compounds for which diffraction data was collected for their R2 state crystals

Compound	Resolution (Å)	R/R_{free}	Space group/ Cell dimensions
PP1	2.0	25.3/31.0	$P2_12_12_1$/ 62.56, 83.20, 104.97, 90, 90, 90
PP2	2.0	19.6/25.7	$P2_12_12_1$/ 62.84, 83.69, 105.06, 90, 90, 90
PP3	2.0	22.3/26.5	$P2_12_12_1$/ 62.84, 83.70, 105.06, 90, 90, 90
PP4	2.1	23.9/27.9	$P2_12_12_1$/ 62.66, 83.49, 105.01, 90, 90, 90
PP5	2.75	23.0/31.2	$P2_12_12_1$/ 62.68, 83.47, 104.87, 90, 90, 90

PP6	2.0	20.4/25.9	P2$_1$2$_1$2$_1$/ 62.64, 82.76, 104.77, 90, 90, 90
PP8	1.85	25.7/30.2	P2$_1$2$_1$2$_1$/ 62.71, 83.36, 105.09, 90, 90, 90
PP9	1.9	25.3/29.9	P2$_1$2$_1$2$_1$/ 63.68, 82.98, 105.03, 90, 90, 90
PP11	1.9	26.0/30.9	P2$_1$2$_1$2$_1$/ 62.71, 83.08, 104.95, 90, 90, 90

Diffraction data obtained for PP compounds in Table **8** was processed using the Phenix software to obtain the initial electron density maps. Analysis of the structure showed very weak and undefined electron density at the α-cleft binding site for some of the compounds including PP1, PP3, PP4, PP5 and PP8. The weak and broken density, even after repeated refinement cycles did not improve, and the refinements terminated without modeling of the compounds into the electron density. Compounds, PP2, PP6, PP9 and PP11, on the other hand, showed very strong electron density for the entire molecule at both α-clefts and thus were refined and studied in detail.

As predicted, all four compounds bound at the α-cleft of Hb in a symmetry related manner, making Schiff-base interactions with the αVal nitrogen. Nonetheless, PP9 showed a unique binding orientation from the other three compounds. Although the *ortho-* substituted pyridinylmethoxy-methylester of all four compounds (which is directed towards the surface of the protein) makes contacts with the α-helix, in PP2 this interaction is inter subunit rather than intra subunit as observed in the other three compounds. It appeared as though substitution on the aldehyde ring (*o*-OH vs *m*-OCH$_3$) might influence the conformation in which these compounds bind. For example, PP2 and PP6 differ in their chemical structure only by substitution at the benzaldehyde ring (*m*-OCH$_3$ vs *o*-OH) and still show two different binding conformations (Figure

38). Nonetheless, PP9 with *m*-OCH$_3$ still behaved different from PP2. It is quite possible that the differences in the binding orientation are due to the cumulative differences in the positions of the pyridine nitrogen, ester and *m*-OCH$_3$ vs *o*-OH. Interestingly, this almost 90° flip in the binding mode of PP2 vs the other PP compounds resulted in differences in the interactions with the surface located αF-helix residues (Figures **28, 31, 34** and **37**). PP6, PP9 and PP14 that are involved in intra subunit contact between the pyridinylmethoxy-methylester and the F-helix make significantly closer interactions, while the opposite is true for PP2. As noted above, PP9 makes both strong hydrophobic and water mediated interactions with the F-helix; PP6 makes strong hydrophobic but no water mediated interactions; while PP11 makes weak hydrophobic but strong water mediated interactions. These interactions in PP6, PP9 and PP14 should serve to perturb the F-helix in these structures than in PP2 and lead to greater polymer destabilization, contributing significantly to the antisickling effect of these compounds. Interaction with the F-helix is also consistent with the proposed dual antisickling mechanism of these compounds. There is an ongoing study by our collaborator, Dr. Abdulmalik to determine the contribution of direct polymer destabilization to the antisickling effects by these compounds.

The benzaldehyde portion of all molecules superimposed closely, making both intra- and inter-subunit hydrophobic interactions with α1Ala130, α1Ser131,α1Thr134, and α2Thr134 from both α-subunits. Irrespective of the orientation of the pyridinylmethoxy-methylester, the two pyridine rings form extensive face-to-face π-π stacking interactions in all four compounds (Figure **27, 30, 33** and **36**). These interactions should serve to stabilize the R-state and increase the oxygen affinity of Hb.

The difference in the atomic interactions can be related to the differences in the biological and functional activities of these compounds. Although, PP2 and PP6 show similar sickling inhibition (Figure **17**), PP6 shows an extended pharmacologic effect due to the *ortho*-hydroxyl group that not only protect the aldehyde through intermolecular hydrogen bonding but also stabilizes the Schiff-base formation (Figures **14** and **15**). PP6 also shows higher Hb S modification and P_{50} shifts (Figures **18** and **19**). Although, PP9 does not have the *ortho*-hydroxyl moiety, its significant interactions with the protein should lead to a stable Schiff-base adduct and may explain why this compound shows extended sustained effect, as well as significant antisickling activity. We note however that among the four compounds, PP11 showed weaker antisickling effect, which appeared to be due to its weak allosteric activity since it only modestly increased Hb affinity for oxygen when compared to the others. This observation cannot be explained by the crystal structure, but we speculate that the low biological effect may be due to cellular effect.
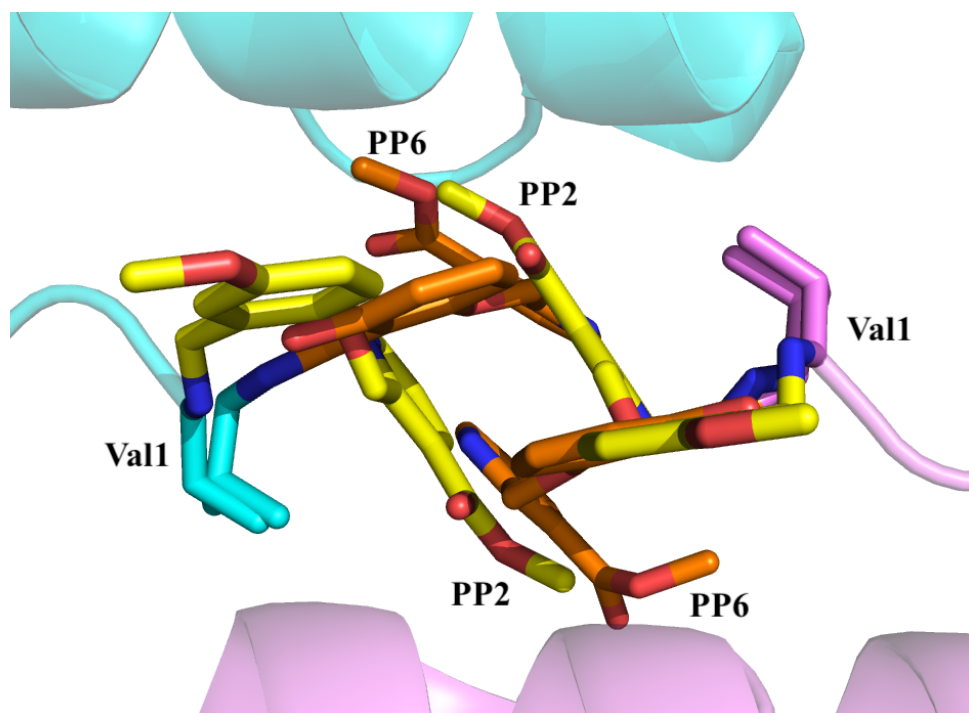
Figure 38. Overlap of PP2 (yellow sticks) and PP6 (orange sticks) bound to α-cleft Hb with the α (α$_1$- cyan; α$_2$- magenta).

Lastly, to study the effect of the pyridine ring nitrogen on Hb-compound interactions, we compared the structures PP6 and PP11 which differ only in the position of their ring nitrogen. Overlap of these two structures indicated that, as seen previously, PP6 and PP11 adopted very similar conformation with the methyl ester groups occupying similar position in the binding pocket (Figure **39**). There were no additional direct or water mediated interactions seen between the ring nitrogen atom and the protein in either of the molecules. These observations again led us to contemplate whether or not the nitrogen atom is critical for binding and/or the biological and functional activity of these compounds. The structure of COHb-PP11 complex however is yet to be completely refined and it might be too early to derive any conclusions about the contribution of various aspects of this compound to its binding.
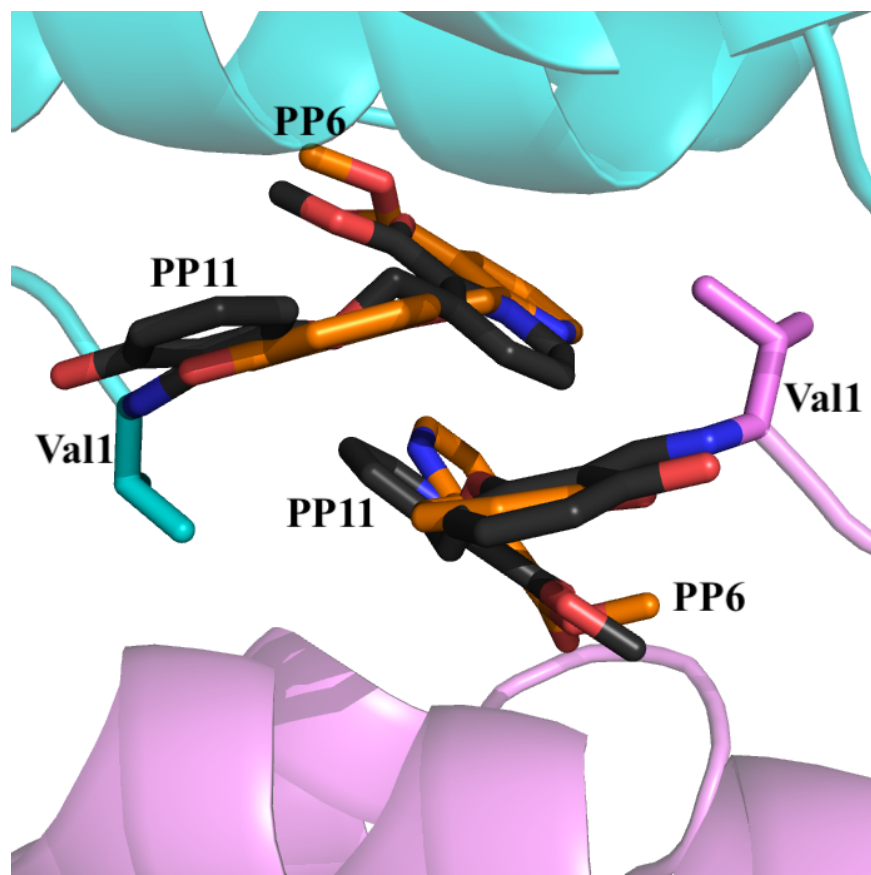
Figure 39. Overlap of PP6 (orange sticks) and PP11 (dark grey sticks) bound to α-cleft Hb with the α (α$_1$- cyan; α$_2$- magenta)

CHAPTER 5

5. SPECIFIC AIM 2:

ELUCIDATION OF THE ATOMIC INTERACTIONS BETWEEN LIGANDED HB AND 5-HMF DERIVATIVES AND PYRIDYL SUBSTITUTED AROMATIC ALDEHYDES (INN- AND TD- DERIVATIVES)

5.1. Structural studies of 5-HMF derivatives

5-hydroxymethyl-2-furfural (5-HMF) has been extensively studied in the clinic for the treatment of SCD. In an effort to develop analogs of 5-HMF with improved pharmacologic properties, 5-HMF was structurally modified into twelve ether and ester derivatives. One representative compound, VZHE004 was studied for its atomic interactions with Hb using x-ray crystallography.[173]
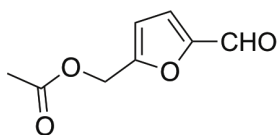
VZHE004

5.1.1. Structural analysis of COHb-VZHE004 complex

The crystal structure of COHb-VZHE004 complex was solved using molecular replacement with the native R2 state structure (PDB ID 1BBB) and refined to 1.85Å. The overall tetrameric structure is indistinguishable (RMSD ~0.4Å) from 1BBB or the R2 structure in complex with 5-HMF (PDB code 1QXE).[171] Detailed crystallographic data is summarized in Table **9**, and the structure deposited in the protein data bank (PDB) with the code 5URC.[173]

Table 9. Crystallographic data and refinement statistics for COHb-VZHE004 complex.[173]

Data collection statistics	
Space group	$P2_12_12_1$
Unit-cell *a, b, c* (Å)	62.64, 83.32, 104.95
Resolution (Å)	29.32- 1.85 (1.92- 1.85)
Unique reflections	47163
Redundancy	4.28 (3.71)
Completeness (%)	99.1 (96.5)
Average $I/\sigma(I)$	21.5 (6.5)
R_{merge} (%)[a]	3.8 (17.3)
Refinement Statistics	
Resolution (Å)	29.32- 1.85 (1.97- 1.85)
No. of reflections	47094 (7239)
R_{work} (%)	17.90 (28.80)

R$_{free}$ (%)[b]	22.3 (36.00)
R.m.s.d. bonds (Å)	0.007
R.m.s.d. angles (°)	1.7
Dihedral angles	
Most favored (%)	96.64
Allowed (%)	3.00
Average B (Å^2)/atoms	
All atoms	28.40
Protein	24.20
Hemes	21.60
VZHE004	37.10
Water	--
PDB ID	5URC

[a]$R_{merge} = \Sigma_{hkl}\Sigma_i|I_i(hkl) - <I(hkl)>|/\Sigma_{hkl}\Sigma_iI_i(hkl)$. [b]R$_{free}$ was calculated from 5% randomly selected reflection for cross-validation. All other measured reflections were used during refinement.

As seen in case of most aromatic aldehydes, including 5-HMF, a pair of VZHE004 molecules covalently bound in a symmetry related fashion at the α-cleft of Hb (Figure **40**). The electron density of VZHE004 was relatively weak especially at the methyl acetate position. Hence, the compound was refined as 5-HMF at the α2Val1 site, while the full VZHE004 was modelled at the α1Val1 binding site. Weak electron density for the methyl acetate group at the α1Val1 indicated possible conformational flexibility of the methyl acetate group. Hence, the methyl acetate was refined in two alternate conformations. The methyl acetate moiety appears to make hydrophobic

interactions with α2Ala130, α2Ser131, and α2Thr134, however the apparent disorder suggests these interactions to be weak.[173]

A.
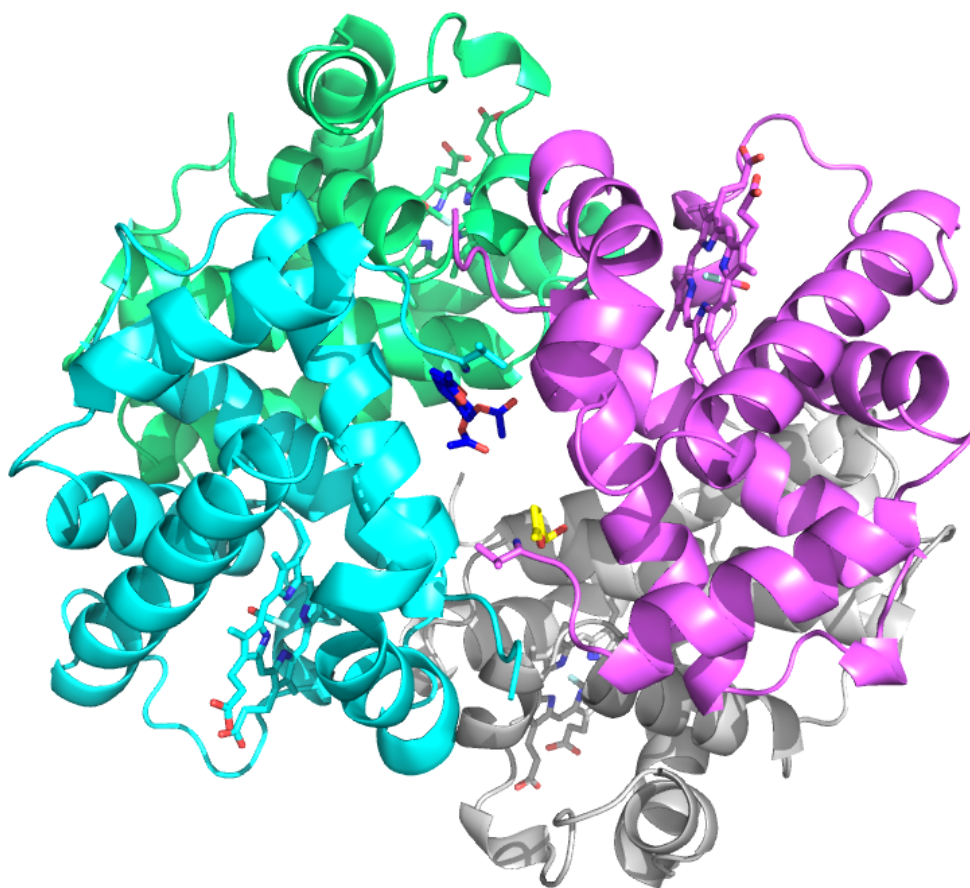
B.
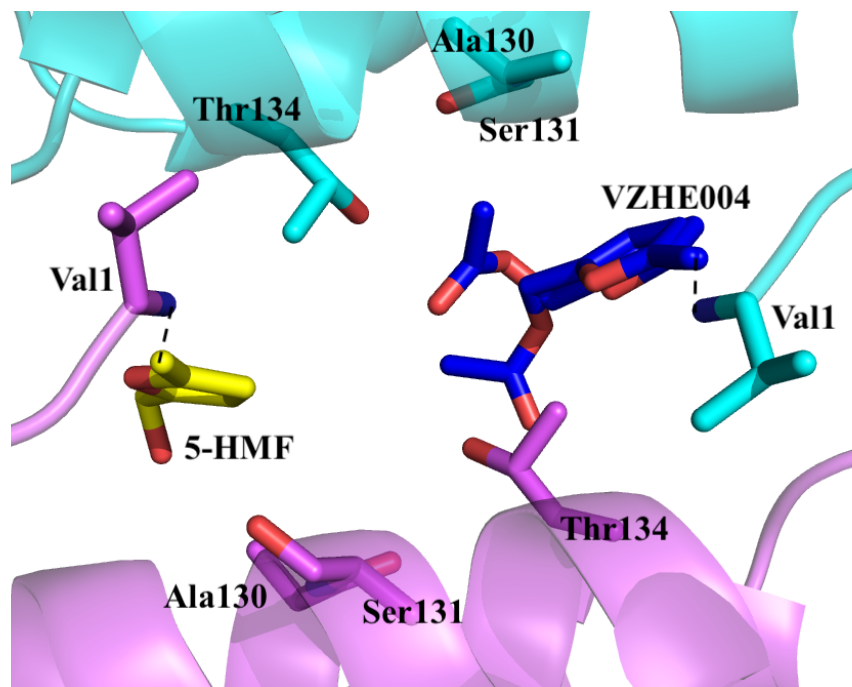
Figure 40. Crystal structure of Hb in R2 state in complex with VZHE004 (blue sticks) at the α-cleft of Hb with the α (α_1- cyan; α_2- magenta) and β (β_1- grey; β_2- green) ribbons, heme groups are shown as sticks while CO molecules are shown as light blue sticks (A) Overall view of the Hb-tetramer (B) Close up view of the binding pocket of VZHE004 (blue sticks) in the central water cavity of Hb. Note that the compound was refined as 5-HMF at the α2Val1 site while full VZHE004 was modelled at α1Val1 with the methyl acetate in two alternate conformations.[173]

5.1.2. Discussion

5-HMF is a pharmacophore of choice since it shows not only attractive Hb modifying and antisickling properties, but also has well known safety profiles and non-toxic major metabolites. Based on the binding mode of 5-HMF to liganded Hb, this compound was structurally modified to several ester and ether analogs with the prospect of increasing further interactions with Hb. To

confirm this hypothesis, x-ray crystal structure of VZHE004 in complex with COHb in the R2 state conformation was obtained and refined to 1.85Å (PDB ID 5URC). A lot of disorder was seen at the α-cleft of Hb which was thought might be due to partial hydrolytic cleavage of the ester group in VZHE004. However, UPLC-MS analysis of Hb-VZHE004 complex later confirmed that the observed electron density was likely due to disorder caused by the conformational flexibility of the methyl acetate group.

Overlap of VZHE004 and 5-HMF revealed that both molecules make similar interactions with the protein through direct and/or water mediated hydrogen bonding interactions with the hydroxyl group of αThr134 and αSer131 (Figure **41**). Other derivatives of 5-HMF are expected to bind similarly since the binding pocket is big enough to accommodate even bulkier substituents. We also expect similar disorder at the alcohol substitution, however derivatives with bulkier substituents should forge stronger interactions and show decreased disorder.

98
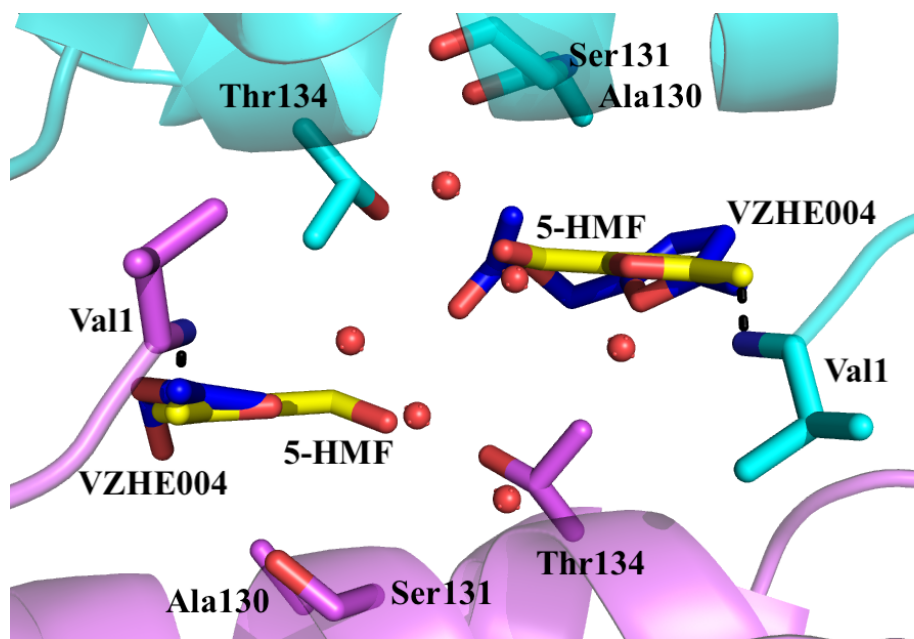
Figure 41. Crystal structures of COHb in complex with VZHE004 (PDB ID 5URC) and 5-HMF (PDB ID 1QXE) superimposed on each other showing similar binding modes to α-cleft Hb with the α (α$_1$- cyan; α$_2$- magenta)

Detailed biological and functional data as well as design and synthesis of the ester and ether analogs of 5-HMF can be reviewed at Xu, G. G.; Pagare, P. P.; Safo, R. P.; Gazi, A.; Chen, Q.; David, T.; Alabbas, A. B.; Musayev, F. N.; Venitz, J.; et al. Design, Synthesis, and Biological Evaluation of Ester and Ether Derivatives of Antisickling Agent 5-HMF for the Treatment of Sickle Cell Disease. *Mol. Pharm.* **2017**, *14*, 3499-3511.

5.2. Structural studies of pyridyl substituted aromatic aldehydes
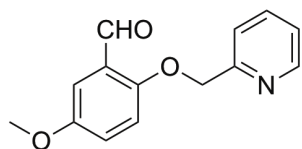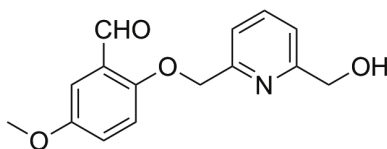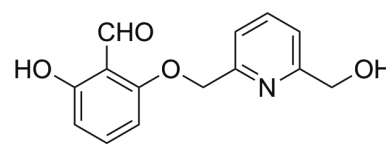
INN-310/SAJ-310   TD-7   VZHE039

5.2.1. Structural analysis of COHb-INN-310/SAJ-310 complex

The crystal structure of COHb-SAJ-310 complex was solved using molecular replacement with the native R2 state structure (PDB ID 1BBB) and refined to 1.95Å. The overall tetrameric structure is indistinguishable (RMSD ~0.4Å) from 1BBB or the R2 structure in complex with INN-312

(PDB code 3R5I).[188] Detailed crystallographic data is summarized in Table **10**, and the structure deposited in the protein data bank (PDB) with the code 6BNR.[200]

Table 10. Crystallographic data and refinement statistics for COHb-INN-310/SAJ-310 complex.[200]

Data collection statistics	
Space group	$P2_12_12_1$
Unit-cell *a, b, c* (Å)	62.82, 83.55, 104.91
Resolution (Å)	29.40- 1.95 (2.02- 1.95)
Unique reflections	40595
Redundancy	3.97 (3.76)
Completeness (%)	99.1 (99.3)
Average $I/\sigma(I)$	11.8 (2.3)
R_{merge} (%)[a]	5.8 (46.7)
Refinement Statistics	
Resolution (Å)	29.40- 1.95 (2.07- 1.95)
No. of reflections	40456 (6308)
R_{work} (%)	20.6 (32.30)
R_{free} (%)[b]	26.4 (35.40)
R.m.s.d. bonds (Å)	0.007
R.m.s.d. angles (°)	1.6
Dihedral angles	

Most favored (%)	95.76
Allowed (%)	4.24
Average B (Å^2)/atoms	
All atoms	38.85
Protein	37.50
Hemes	33.61
INN-310	43.61
Water	48.55
PDB ID	6BNR

$^a R_{\mathrm{merge}} = \Sigma_{hkl}\Sigma_{\mathrm{i}}|I_{\mathrm{i}}(hkl) - <I(hkl)>|/\Sigma_{hkl}\Sigma_{\mathrm{i}}I_{\mathrm{i}}(hkl)$. $^b R_{\mathrm{free}}$ was calculated from 5% randomly selected reflection for cross-validation. All other measured reflections were used during refinement.

Two molecules of INN-310/SAJ-310 bound in a symmetry related fashion at the α-cleft of Hb (Figure **42**) with their binding mode very similar to the binding of INN-312 (PDB ID 3R5I). The aldehyde group of the compounds formed a Schiff base interaction with the αVal1 nitrogen (1.5Å) at each α-cleft. Since both molecules bound in a symmetrical fashion, detailed interactions of Hb will be focused on α2Val1 binding SAJ-310. The benzaldehyde ring makes intra- and inter-hydrophobic interactions with α2Ser131 and α1Thr134, respectively, while the pyridinylmethoxy oxygen atom appears to make intra subunit hydrogen bonding interaction with the hydroxyl group of α2Ser131. Additionally, the pyridine rings from the two bound SAJ-310 molecules make extensive 3.7-4.0Å face-to-face π-π stacking interactions with each other (Figures **42** and **43**).
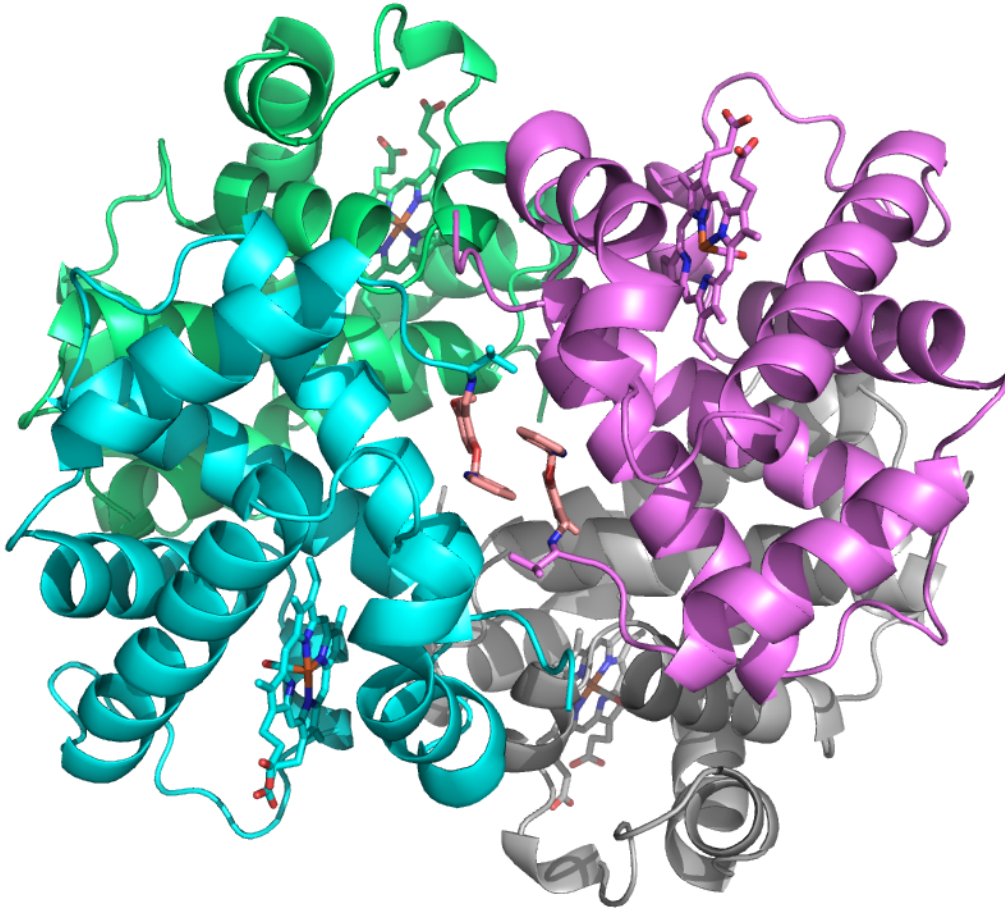
Figure 42. Crystal structure of Hb in R2 state in complex with a pair INN-310/SAJ-310 molecules (pink sticks) at the α-cleft of Hb with the α (α$_1$- cyan; α$_2$- magenta) and β (β$_1$- light grey; β$_2$- green) ribbons, heme groups are shown as sticks.

Figure 43. (A) Close up view of the binding pocket of INN-310/SAJ-310 (pink sticks) in the central water cavity of Hb shown as ribbons (α_1- cyan; α_2- magenta) (B) Two dimensional contacts between one INN-310/SAJ-310 molecule, protein and the second INN-310/SAJ-310 molecule.
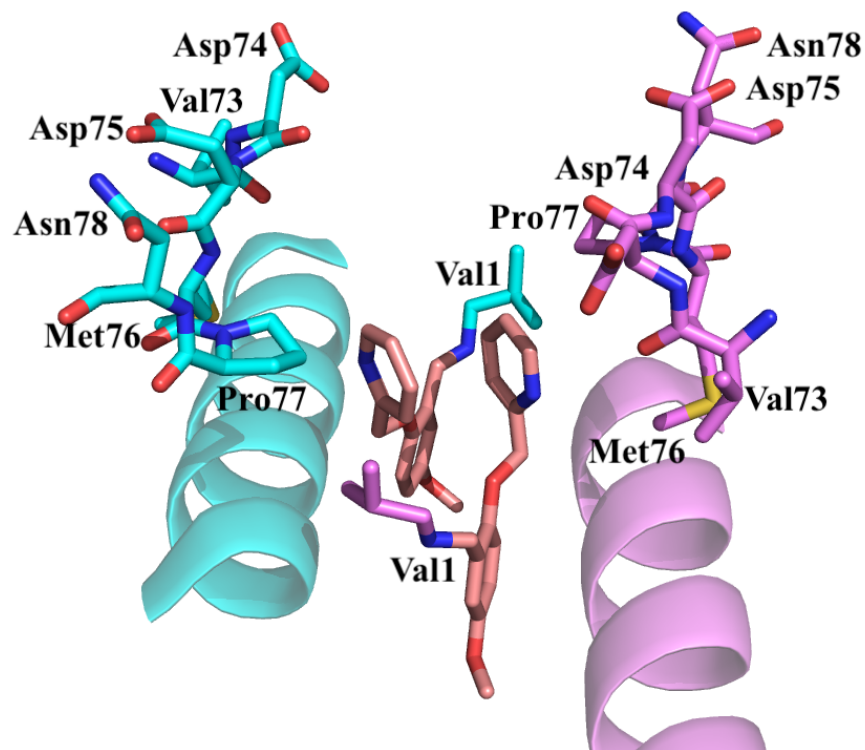
Figure 44. Binding pose of two INN-310/SAJ-310 molecules (pink sticks) showing interactions with the αF-helix of Hb with the α ($α_1$- cyan; $α_2$- magenta). Amino acid residues of the protein are shown as sticks.

It was observed that due the Schiff-base interaction between SAJ-310 and Hb, the pyridinylmethoxy group of the molecules was directed towards the surface of the protein. This resulted in weak intra subunit hydrophobic interactions (3.5-4.5Å) with αPro77 amino acid residue of the surface located F-helix (Figure **44**). We expect these hydrophobic interactions to perturb the polymer contacts although weakly as previously noted for INN-312.[200]

Detailed biological and functional data as well as design and synthesis of the SAJ- compounds can be reviewed at Pagare, P. P.; Ghatge, M. S.; Musayev, F. N.; Deshpande, T. M.; Chen, Q.;

Braxton, C.; Kim, S.; Venitz, J.; Zhang, Y.; Abdulmalik, O.; Safo, M. K. Rational design of pyridyl derivatives of vanillin for the treatment of sickle cell disease. *Bioorg. Med. Chem.* [Online] **2018** https://www.sciencedirect.com/science/article/pii/S0968089618303699 (accessed April 10, 2018).

5.2.2. Structural analysis of COHb-TD-7 complex

The crystal structure of COHb-TD-7 complex was solved using molecular replacement with the native R2 state structure (PDB ID 1BBB) and refined to 1.90Å. The overall tetrameric structure is indistinguishable (RMSD ~0.4Å) from 1BBB or the R2 structure in complex with INN-310 (PDB code 6BNR).[200] Detailed crystallographic data is summarized in Table **11.**

Table 11. Crystallographic data and refinement statistics for COHb-TD-7 complex.

Data collection statistics	
Space group	$P2_12_12_1$
Unit-cell *a, b, c* (Å)	62.69, 83.40, 104.93
Resolution (Å)	29.34- 1.90 (1.97- 1.90)
Unique reflections	43079
Redundancy	4.13 (3.68)
Completeness (%)	97.8 (95.00)
Average $I/\sigma(I)$	15.7 (3.8)
R_{merge} (%)[a]	4.7 (33.6)

Refinement Statistics

Resolution (Å)	29.34- 1.90 (2.02- 1.90)
No. of reflections	42867 (6491)
R_{work} (%)	19.76 (32.4)
R_{free} (%)[b]	24.87 (37.5)
R.m.s.d. bonds (Å)	0.006
R.m.s.d. angles (°)	1.7
Dihedral angles	
Most favored (%)	96.11
Allowed (%)	3.53
Average B (Å^2)/atoms	
All atoms	33.00
Protein	29.55
Hemes	29.55
TD-7	44.87
Water	43.79

[a]$R_{merge} = \Sigma_{hkl}\Sigma_i|I_i(hkl) - <I(hkl)>|/\Sigma_{hkl}\Sigma_iI_i(hkl)$. [b]$R_{free}$ was calculated from 5% randomly selected reflection for cross-validation. All other measured reflections were used during refinement.

Figure 45. Crystal structure of Hb in R2 state in complex with pair TD-7 molecules (orange sticks) at the α-cleft of Hb with the α (α₁- cyan; α₂- magenta) and β (β₁- light grey; β₂- green) ribbons, heme groups are shown as sticks.

As previously reported for INN-312 and INN-310/SAJ-310 binding, two molecules of TD-7 bind in a symmetrical fashion at the α-cleft of the tetramer, with the aldehydes making Schiff-base interactions with the two N-terminal amines of the αVal1 amino acids (Figure **45**). The pyridinylmethoxy group of TD-7 that is located *ortho* to the aldehyde group directs out of the central water cavity toward the protein surface. Detailed compound-Hb interactions will be focused on the α2Val1 binding effector, noting that the α1Val1 binding effector makes similar

symmetry-related interactions. The Schiff-base interaction between the aromatic aldehyde of TD-7 and the α2Val1 nitrogen leads to sandwiching of the benzaldehyde rings between and making intra subunit hydrophobic interactions with the side-chain of α2Ser130 and α2Thr134, as well as intersubunit hydrophobic interactions, with the side-chain of α1Thr134 from the opposite α1-subunit (Figure **46**). The methoxybenzaldehyde oxygen forms weak inter subunit hydrogen bonding interactions with the hydroxyl group of α1Thr134. The two pyridine rings from the two symmetry-related bound TD-7 molecules also make extensive face-to-face π-π interactions.
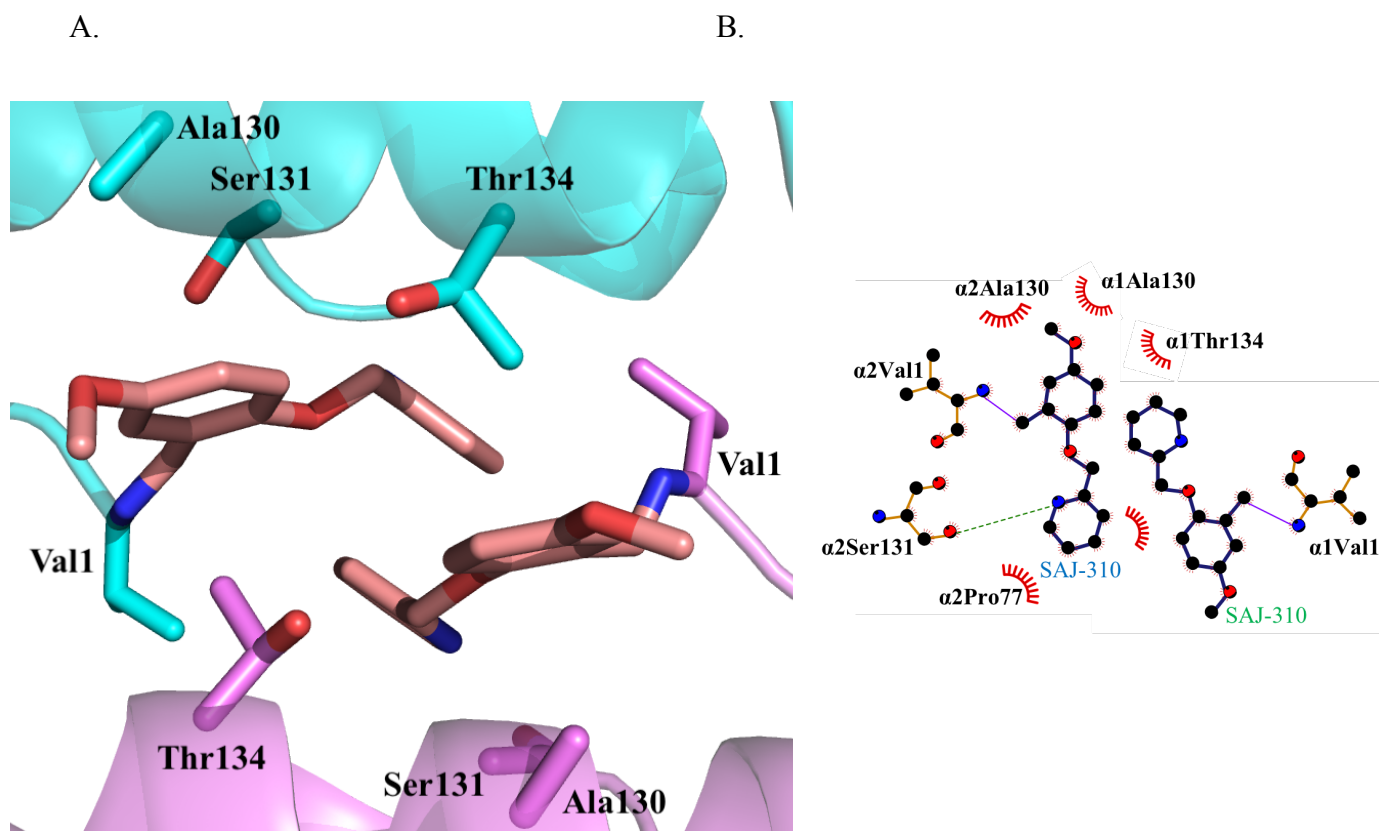
A.

B.
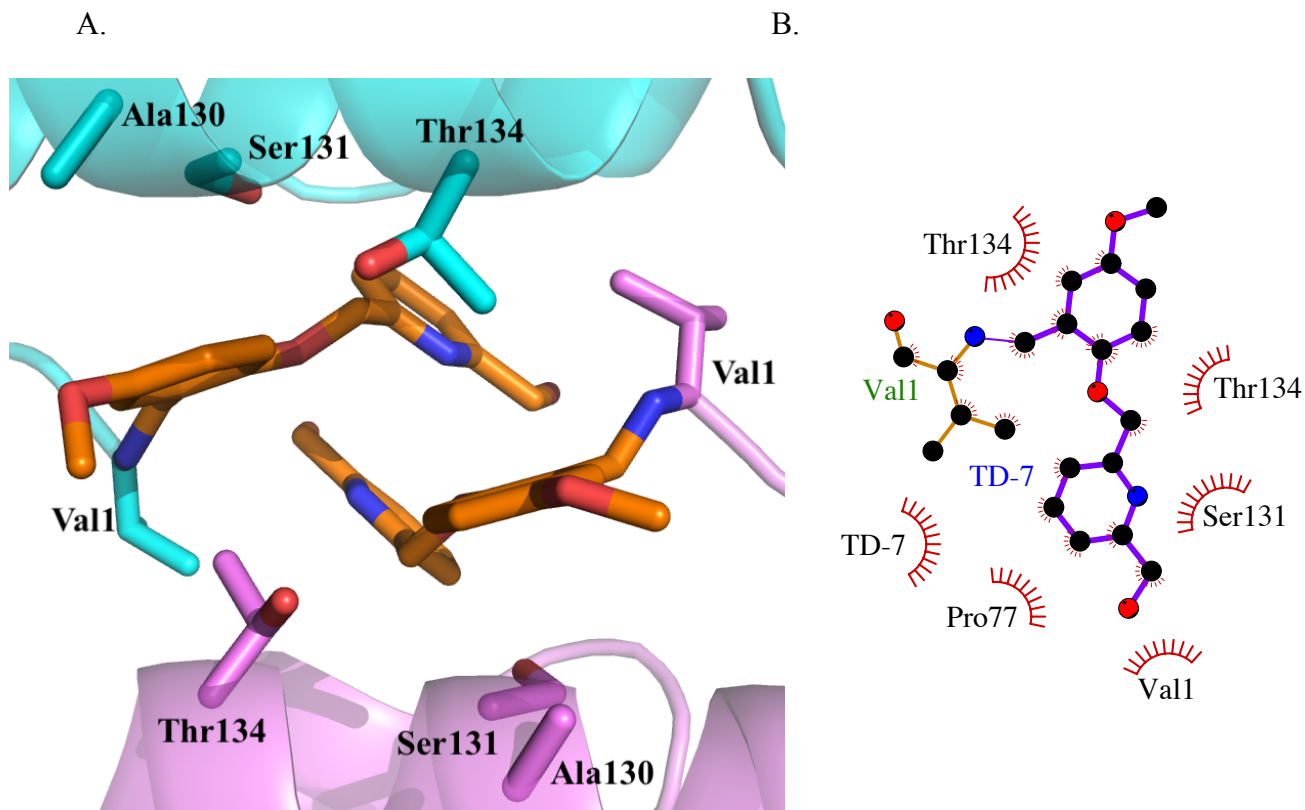
Figure 46. (A) Close up view of the binding pocket of TD-7 (orange sticks) in the central water cavity of Hb shown as ribbons (α_1- cyan; α_2- magenta) (B) Two dimensional contacts between one TD-7 molecule, protein and the second TD-7 molecule.

Figure 47. Binding pose of two TD-7 molecules (orange sticks) showing interactions with the αF-helix of Hb with the α (α_1- cyan; α_2- magenta). Amino acid residues of the protein are shown as sticks.

Additionally, the pyridine rings from TD-7 make very similar inter subunit hydrophobic interactions (3.5 – 4 Å) with the α2Pro77 and α2Met76 residues of the F-helix as seen in the case of other compounds (Figure **47**).

Unexpectedly, the pyridine hydroxymethyl moiety in TD 7 which was proposed and anticipated to make hydrogen bonding interaction with the backbone atoms of the F-helix and/or closer hydrophobic interaction with the F-helix did not make any such interaction with the protein.

5.2.3. Structural analysis of COHb-VZHE039 complex

The crystal structure of COHb-VZHE039 complex was solved using molecular replacement with the native R2 state structure (PDB ID 1BBB) and refined to 2.1Å. The structure showed very strong and well-defined electron density at the α-clefts and two molecules of VZHE039 modelled at the two αVal1. The crystallographic data is summarized in Table **12**.

Table 12. Crystallographic data and refinement statistics for COHb-VZHE039 complex.

Data collection statistics	
Space group	$P2_12_12_1$
Unit-cell *a, b, c* (Å)	62.78, 83.63, 105.00
Resolution (Å)	29.34- 2.1 (2.18- 2.1)
Unique reflections	31379
Redundancy	4.62 (4.47)
Completeness (%)	96.3 (95.40)
Average $I/\sigma(I)$	12.4 (3.9)
R_{merge} (%)[a]	6.8 (34.2)
Refinement Statistics	

Resolution (Å)	29.34- 2.1
No. of reflections	31280 (4858)
R_{work} (%)	20.2 (24.7)
R_{free} (%)[b]	26.4 (28.3)
R.m.s.d. bonds (Å)	0.007
R.m.s.d. angles (°)	1.7
Dihedral angles	
Most favored (%)	95.76
Allowed (%)	3.71
Average B (Å^2)/atoms	
All atoms	33.5
Protein	32.77
Hemes	30.22
VZHE039	31.26
Water	40.28

[a]$R_{merge} = \Sigma_{hkl}\Sigma_i|I_i(hkl) - <I(hkl)>|/\Sigma_{hkl}\Sigma_iI_i(hkl)$. [b]$R_{free}$ was calculated from 5% randomly selected

reflection for cross-validation. All other measured reflections were used during refinement.
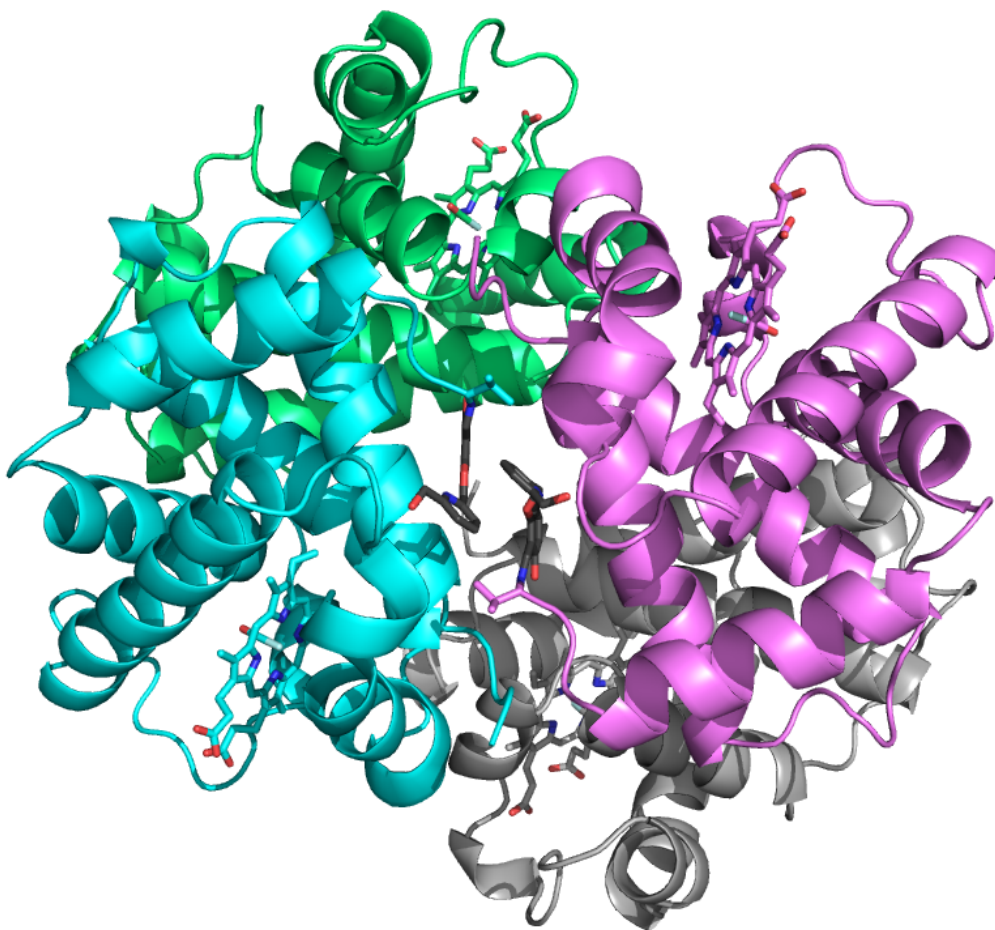
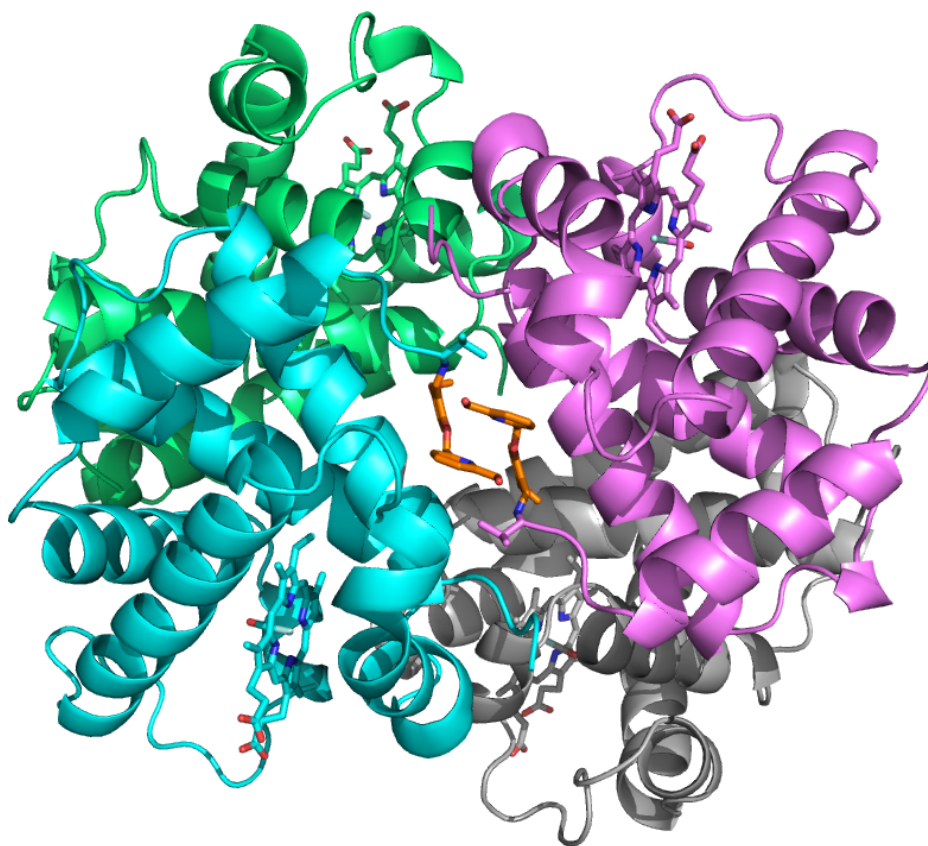**Figure 48.** Crystal structure of Hb in R2 state in complex with pair VZHE039 molecules (dark grey sticks) at the α-cleft of Hb with the α (α$_1$- cyan; α$_2$- magenta) and β (β$_1$- light grey; β$_2$- green) ribbons, heme groups are shown as sticks.

A.

B.
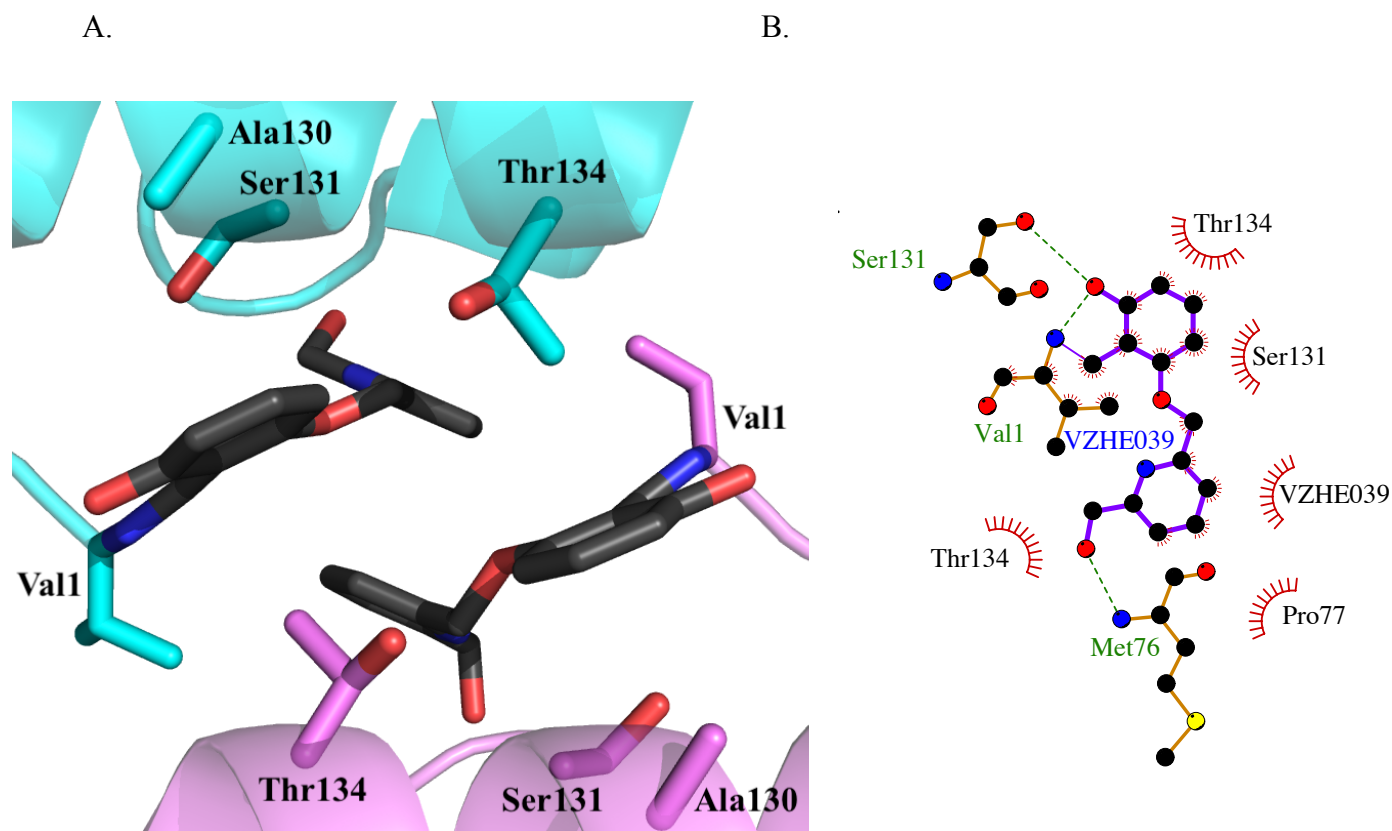
Figure 49. (A) Close up view of the binding pocket of VZHE039 (dark grey sticks) in the central water cavity of Hb shown as ribbons (α_1- cyan; α_2- magenta) (B) Two dimensional contacts between one molecule VZHE039 molecule, protein and the second VZHE039 molecule.

As seen in INN-310 and TD-7, two molecules of VZHE039 also make Schiff-base interactions with the two N-terminal amines of the αVal1 amino acids (Figure **48** and **49**). Since both molecules bound in a symmetry related fashion, detailed interactions between VZHE039 and Hb will be focused on the α2Val1 binding. The Schiff-base interaction leads to sandwiching of the benzaldehyde rings and making intra subunit hydrophobic interactions with α2Ala130, α2Ser131 and α2Thr134. The *ortho* hydroxyl group forms interactions with the nitrogen atom of α2Val1

similar to that seen in PP6 and PP11. The two pyridine rings from the two symmetry-related bound TD-7 molecules also make extensive face-to-face π-π interactions and the pyridinylmethoxy group of VZHE039 that is located *ortho* to the aldehyde group directs out of the central water cavity toward the protein surface.
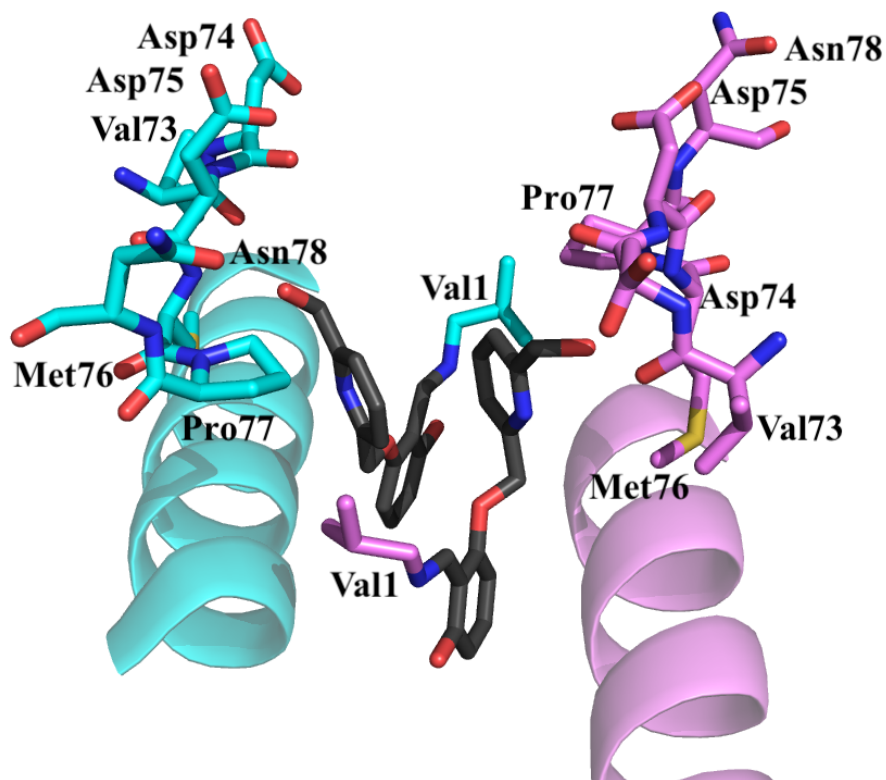
Figure 50. Binding pose of two VZHE039 molecules (dark grey sticks) showing interactions with the αF-helix of Hb with the α (α$_1$- cyan; α$_2$- magenta). Amino acid residues of the protein are shown as sticks.

The pyridine ring in VZHE039 makes similar hydrophobic interactions (3.5-3.7Å) with the α2Pro77 residue of the F-helix similar to that seen in INN-310 and TD-7 (Figure **50**). Interestingly,

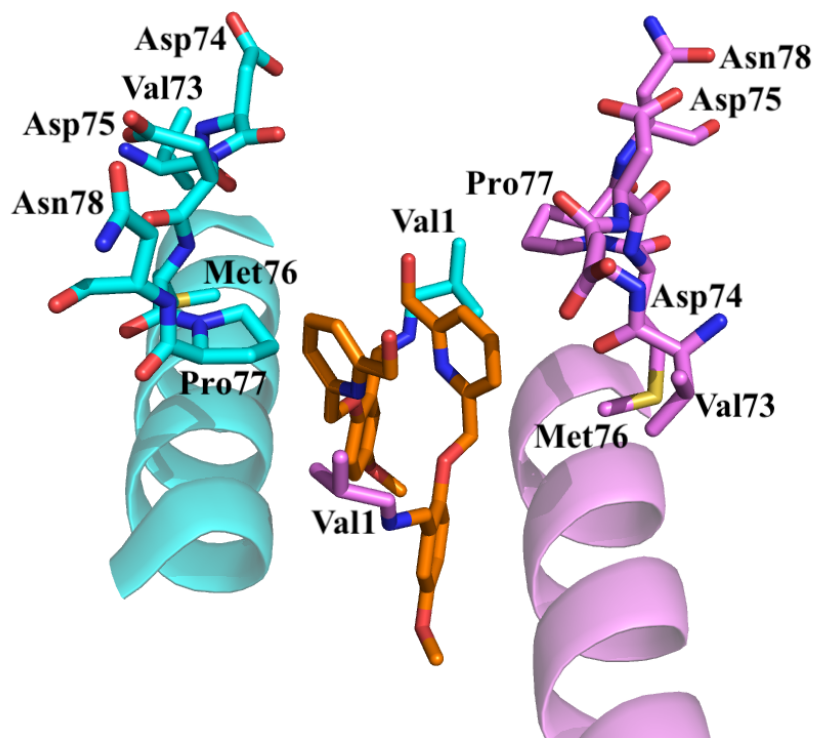although the pyridine hydroxymethyl moiety in TD-7 did not make any hydrogen bonding interactions with the backbone atoms of the F-helix, in case of VZHE039 however, weak hydrogen bonding interactions were observed between its pyridine hydroxymethyl group and the backbone of α2Met76.

5.2.4. Discussion

Modifications on the previously studied aromatic aldehyde, vanillin, led to synthesis of INN compounds by our group. Some of these series of compounds appeared to be significantly more potent than their parent aromatic aldehyde.[187] More interestingly, INN-312 appeared to exhibit dual antisickling activity by not only increasing Hb affinity for O_2 but also destabilizing the Hb S polymer contacts. Structural analysis showed that this was due to the displacement of the pyridine-methoxy moiety directed towards the surface of the protein resulting in interactions with the F-helix.[188] Another compound, INN-310, shows similar pharmacologic profile as that of INN-312. Hence, we carried out crystallization experiments to determine the crystal structure of INN-310/SAJ-310 to help elucidate its mechanism of action. As expected, INN-310/SAJ-310 bound in a similar fashion as INN-312 with its pyridine-methoxy moiety directed towards the surface of the protein and made weak hydrophobic interactions with the amino acid residues of the surface located αF-helix.[200]

Based on the positive outcome of the modification of vanillin to obtain the INN compounds, our group decided to further improve on the allosteric, anti-sickling and pharmacokinetic properties of these compounds. First, hydroxymethyl group was incorporated onto the pyridine ring which would extend the hydroxymethyl-pyridine-methoxy substituent to the surface of the

protein and thus increase its direct polymer destabilization property to give the TD- series of compounds (e.g. TD-7). Second, a hydroxyl group was introduced *ortho*- with respect to the aromatic aldehyde group of TD-7. Like in PP compounds, we hypothesized that the *o*-OH group will help protect the aldehyde group from oxidative metabolism by ALDH by engaging in an intramolecular hydrogen bonding interaction, to give VZHE039.

Although both INN-310 and TD-7 bound as expected with both structures superposing closely with each other, and the *ortho*-positioned pyridinylmethoxy directed toward the F-helix at the surface of the protein, the methylhydroxyl moiety of TD-7 did not make any strong or additional interactions with the F-helix or the protein as anticipated (Figure **51**). Even though this result was unexpected, it explained why both compounds exhibited similar functional and antisickling properties (data not shown). Clearly these structural studies did not lead to improvement in the compound biological activity.

A.
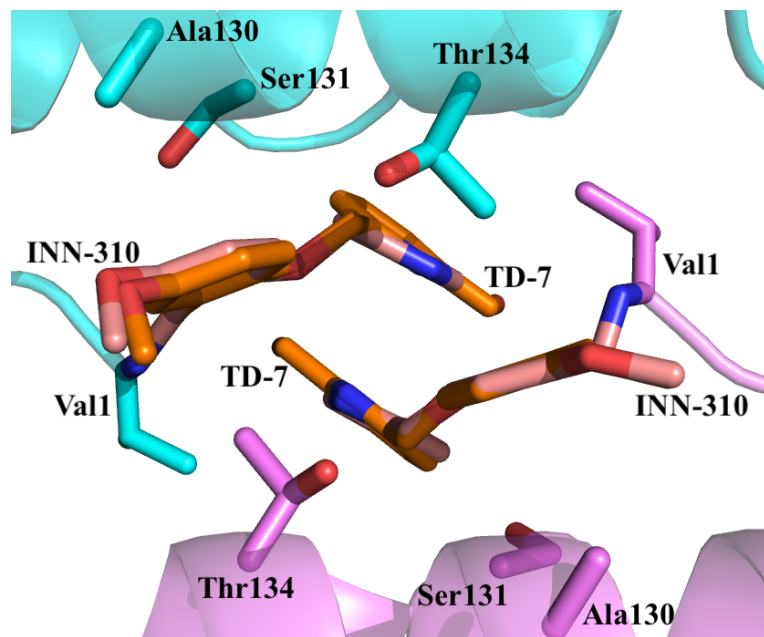
B.
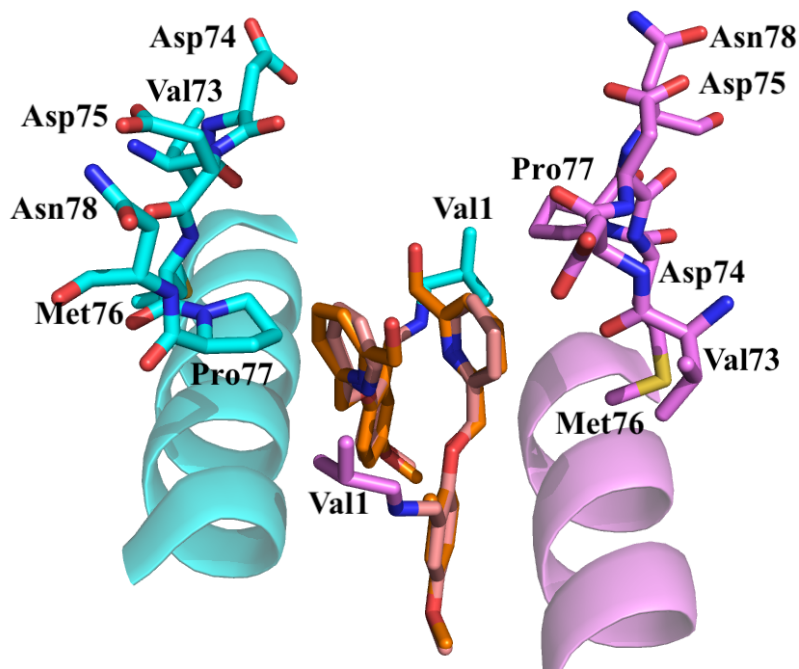
Figure 51. Overlap of INN-310/SAJ-310 (pink sticks) and TD-7 (orange sticks) bound to α-cleft

Hb with the α (α₁- cyan; α₂- magenta) (A) Binding site of the molecules and (B) interactions with

F-helix

Introduction of the *ortho*-hydroxyl group on the benzaldehyde moiety resulted in a sustained

pharmacologic effect seen in VZHE039 vs TD-7 (data not shown). It was observed that although

TD-7 and VZHE039 bound in a similar fashion forming Schiff-base adducts with the N-terminals

of the α- subunits, the resulting conformation of VZHE039 placed the methylhydroxyl group much

closer to the F-helix (Figure **52**). Intra subunit hydrogen bonding interactions with the backbone

atoms of α2Met76 residue were seen which were absent in TD-7. We believe these differences in

their binding would reflect on the antisickling properties of these two compounds and inform us

where to make the next modification to improve the pharmacologic property of the compounds.

A.
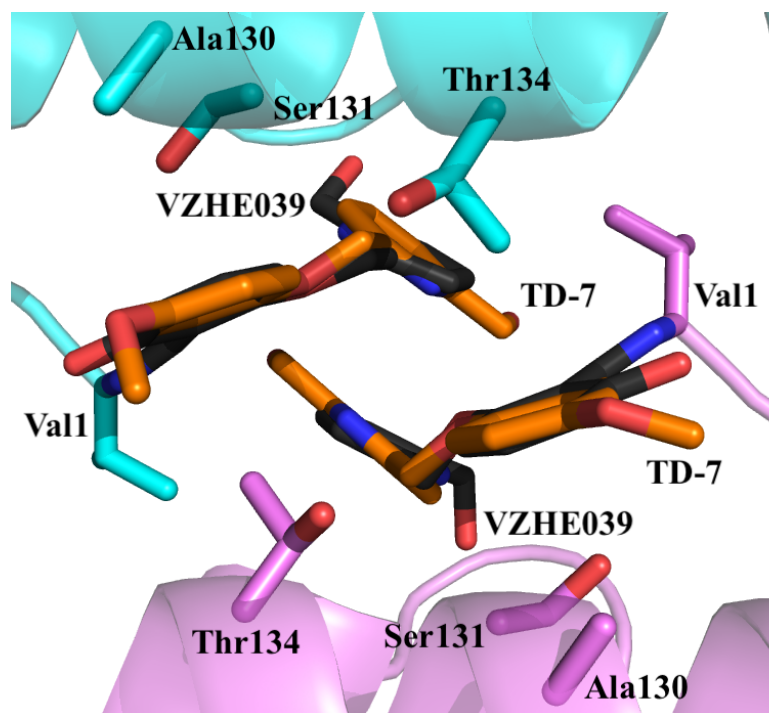
B.
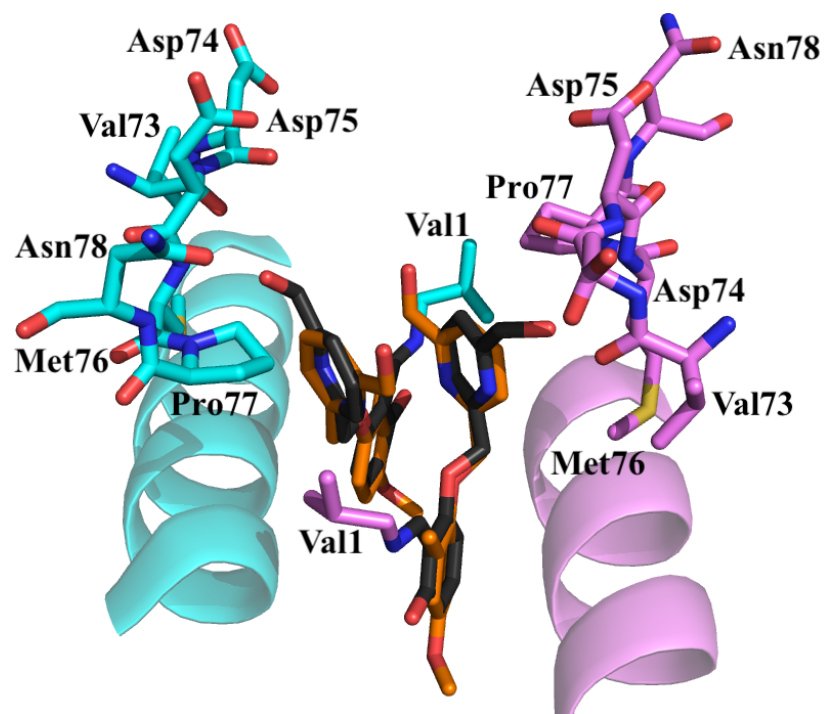
Figure 52. Overlap of TD-7 (orange sticks) and VZHE039 (dark grey sticks) bound to α-cleft Hb with the α (α$_1$- cyan; α$_2$- magenta) (A) Binding site of the molecules and (B) interactions with F-helix

CHAPTER 6

6. CONCLUSIONS

The underlying problem in SCD is that due to the mutation of polar glutamic acid (βGlu6) to hydrophobic valine (βVal6), Hb molecules polymerize under hypoxic conditions. This polymerization leads to deformation of the RBCs into sickle shape making them relatively inflexible. This disease is characterized by symptoms of pain crisis, anemia, vaso-occlusion and organ damage that are unpredictable and differ between individuals.[61,76,77,85] Clinical management of SCD is centered around pain relief, prophylaxis against the infection and periodic transfusion to reduce the concentration of sickle red blood cells in the blood stream. Since most available treatment options currently treat only the symptoms, despite the vast improving care services, the projected life expectancy of adults with SCD remains 20-30 years shorter than the general population.[91] Hydroxyurea, a drug that induces the synthesis of Hb F, remains the only drug widely used clinically to treat SCD. However, it is poorly tolerated in most patients and the side effects prohibit its use in some patients.[93,201]

In an attempt to develop new therapeutics to treat SCD, several aromatic aldehydes including vanillin and its pyridyl derivatives (INN, TD- compounds) have been studied.[187,188,200] These compounds bind to Hb S, stabilize its high O_2 affinity conformation (relaxed or R state) and increase its oxygen affinity with a concomitant prevention of Hb S polymerization. By inhibiting

sickling these compounds not only prevent the primary pathophysiology associated with SCD but also ameliorate several cascading symptoms of this disease. One of the most potent lead compound identified was TD-7. Although it fit most of the criteria of a potential drug candidate in vitro, it lacked good pharmacokinetic properties leading to shorter duration of pharmacologic action and bioavailability. This would necessitate frequent and potentially high doses and therefore TD-7 was an un desirable candidate a chronic disease like SCD.

To overcome this disadvantage, TD-7 was modified by introducing an *o*-OH group on the benzaldehyde ring as well as derivatizing the methyl alcohol into a methyl ester. The presence of a hydroxyl group *ortho* to the aldehyde would result in protecting the aldehyde group via intramolecular hydrogen bonding and thus protect the compounds against metabolism by ALDH and other enzymes in the plasma as well as the RBCs. It was also expected that the presence of an ester group would make additional interactions with the protein further increasing the Hb-O_2 affinity. Overall, 14 compounds (PP-compounds), were synthesized to incorporate these modifications. We hypothesized that these structural modifications would lead to improvement in the compounds bioavailability, as well as extend their pharmacologic activity.

It was observed that, with the exception of PP1 and PP5, most PP compounds modified Hb S and increased its for O_2 in a dose-dependent manner. Compounds with the *o*-OH substitution on the benzaldehyde ring showed extended pharmacologic effect in vitro. Most PP compounds appeared to be very potent antisickling agents with showing almost complete sickling inhibition at 2 mM concentrations. PP2, PP6, PP8, PP9 showed more than 60% sickling inhibition at even 1 mM concentration which was encouraging since it is within the targeted therapeutic window.

121

Previously, the structural basis of the antisickling activity of INN- compounds, especially INN-312, was elucidated using X-ray crystallography.[188] Structure of COHb-INN-312 complex suggests that the mode of binding of INN-312 led to increased polymer destabilization by stereospecifically interacting with the F-helix. X-ray crystal structures of PP2, PP6, PP9 and PP11 in complex with COHb provided structural insights into the binding of these compounds to the protein as well as their potential interaction with the F-helix involved in polymer stabilization. These structural differences helped explain the observed biochemical differences between these compounds and their precursor (TD-7).

Thus, PP compounds exhibit several novel attributes that are lacking in the TD compounds. These compounds show sustained pharmacologic activity in vitro. PP6, PP10 and PP14 also show significantly enhanced as well as sustained activity in vivo, which could be valuable for a regularly administered agent to treat a chronic condition like SCD. Furthermore, these compounds exhibit dual antisickling mechanism of action i.e. they not only increase Hb affinity for O_2 but also show interactions with the F-helix indicating these compounds could directly destabilize polymer contacts between Hb molecules thus translating into enhanced antisickling activities.

CHAPTER 7

7. EXPERIMENTAL SECTION

7.1. Chemical Synthesis

General information: All reagents used in the synthesis and functional assays were purchased from Sigma-Aldrich (St. Louis, MO) and Thermo Fisher Scientific (Waltham, MA) and utilized without additional purification. ^{1}H-NMR and ^{13}C-NMR spectra were obtained on a Bruker 400MHz spectrometer and tetramethylsilane (TMS) was used as an internal standard. Peak positions are given in parts per million (δ). Column chromatography was performed on silica gel (grade 60 mesh; Bodman Industries, Aston, PA). Routine thin-layer chromatography (TLC) was performed on silica gel GHIF plates (250 μm, 2.5 x 10 cm; Analtech Inc., Newark, DE). MS spectra were obtained from a Perkin Elmer Flexar UHPLC with AxION 2 Time of Flight (TOF) Mass Spectrometer, and the molecular weight of the compounds was within 0.005% of calculated values. Infrared spectra were obtained on Thermo Nicolet iS10 FT-IR. Purity of the compounds was determined by HPLC using Varian Microsorb 100-5 C18 column (250 x 4.6 mm), using Prostar 325 UV-Vis (210 nm) as the detector. The HPC parameters used were: injection volume= 15 μL. sample concentration= 3mM, mobile phase= 60MeCN-40H_2O, flow rate= 1 mL/min.

Statistical Analyses: All functional and biological assays evaluating antisickling properties, Hb modification and oxygen affinity changes were conducted in three biological replicates. Results are reported as mean values with standard deviations, from triplicate analyses.

7.1.1. Methyl 6-(bromomethyl)nicotinate

A mixture of methyl 6-methylnicotinate (1eq) and α,α`-Azoisobutyronitrile (AIBN) (10%) was dissolved in carbontetrachloride (CCl4). The solution was heated and N-bromosuccinimide (NBS) (1.1eq) solution in CCl4 was added drop wise and refluxed for 5 hours. The reaction was cooled to room temperature and the solvent evaporated. The mixture was then extracted using dichloromethane and water followed by washing the organic layer with brine. The organic layer was dried over sodium sulfate, filtered, evaporated and the crude product was purified using SiO_2 column chromatography and eluted with the solvent system EtOAc: hexanes = 2:3 to obtain pure product as white powder and the yield was 66%. ^{1}H-NMR (400 MHz, DMSO-d_6): δ 9.16 (d, J = 1.56 Hz, 1H), 8.30 (dd, J = 8.12, 2.2 Hz, 1H), 7.53 (dd, J = 8.12 ,0.48 Hz, 1H), 4.58 (s, 2H), 3.96 (s, 3H). HRMS (ESI) m/z found 229.98 $[M+H]^+$, Calculated 230.0586 $[M]^+$.

7.1.2. Methyl 2-(bromomethyl)nicotinate

A mixture of methyl 2-methylnicotinate (1eq) and α,α`-Azoisobutyronitrile (AIBN) (10%) was dissolved in carbontetrachloride (CCl$_4$). The solution was heated and N-bromosuccinimide (NBS) (1.1eq) solution in CCl$_4$ was added drop wise and refluxed for 5 hours. The reaction was cooled to room temperature and the solvent evaporated. The mixture was then extracted using dichloromethane and water followed by washing the organic layer with brine. The organic layer was dried over sodium sulfate, filtered, evaporated and the crude product was purified using SiO$_2$ column chromatography and eluted with the solvent system EtOAc: hexanes = 2:3 to obtain pure product as orange powder and the yield was 65%. ^{1}H-NMR (400 MHz, DMSO-d$_6$): δ 8.71 (dd, J = 4.8, 1.76 Hz, 1H), 8.28 (dd, J = 7.92, 1.76 Hz, 1H), 7.33 (m, 1H), 5.04 (s, 2H), 3.98 (s, 3H). HRMS (ESI) m/z found 229.98 [M+H]$^+$, Calculated 230.0586 [M]$^+$.

7.1.3. Methyl 6-(bromomethyl)picolinate

A mixture of methyl 6-methylpicolinate (1eq) and α,α`-Azoisobutyronitrile (AIBN) (10%) was dissolved in carbontetrachloride (CCl$_4$). The solution was heated and N-bromosuccinimide (NBS)

(1.1eq) solution in CCl$_4$ was added drop wise and refluxed for 5 hours. The reaction was cooled to room temperature and the solvent evaporated. The mixture was then extracted using dichloromethane and water followed by washing the organic layer with brine. The organic layer was dried over sodium sulfate, filtered, evaporated and the crude product was purified using SiO$_2$ column chromatography and eluted with the solvent system EtOAc: hexanes = 2:3 to obtain pure product as white powder and the yield was 66%. ^{1}H-NMR (400 MHz, DMSO-d$_6$): δ 8.05 (d, J = 7.68 Hz, 1H), 7.99 (t, J = 7.72 Hz, 1H), 7.77 (d, J = 7.68 Hz, 1H), 4.67 (s, 2H), 3.98 (s, 3H). HRMS (ESI) m/z found 229.98 [M+H]$^+$, Calculated 230.0586 [M]$^+$.

7.1.4. Methyl 2-methylisonicotinate
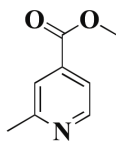
A few drops of concentrated sulphuric aicd was added to a solution of methylisonicotinic acid in methanol. The mixture was refluxed for 48 hours. The resultant reaction mixture was neutralized with saturated sodium bicarbonate solution followed by extraction with ethyl acetate and water. The organic layer was dried over sodium sulfate, filtered and solvent evaporated. The crude product was purified using SiO$_2$ column chromatography and eluted with the solvent system EtOAc: hexanes = 4:1. The pure compound was obtained as colorless oil with 96% yield. ^{1}H-NMR (400 MHz, DMSO-d$_6$): δ 8.66 (d, J = 5.08 Hz, 1H), 7.71 (s, 1H), 7.63 (dd, J = 5.04, 0.32 Hz, 1H), 3.89 (s, 2H), 2.56 (s, 3H) . HRMS (ESI) m/z found 152.07 [M+H]$^+$, Calculated 151.1626 [M]$^+$.
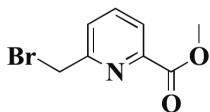
7.1.5. Methyl 2-(bromomethyl)isonicotinate

A mixture of methyl 2-methylisonicotinate (1eq) and α,α`-Azoisobutyronitrile (AIBN) (10%) was dissolved in carbontetrachloride (CCl₄). The solution was heated and N-bromosuccinimide (NBS) (1.1eq) solution in CCl₄ was added drop wise and refluxed for 5 hours. The reaction was cooled to room temperature and the solvent evaporated. The mixture was then extracted using dichloromethane and water followed by washing the organic layer with brine. The organic layer was dried over sodium sulfate, filtered, evaporated and the crude product was purified using SiO_2 column chromatography and eluted with the solvent system EtOAc: hexanes = 2:3 to obtain pure product as dark blue colored powder and the yield was 66%. ^{1}H-NMR (400 MHz, DMSO-d$_6$): δ 8.77 (dd, J = 5, 0.64 Hz, 1H), 8.02 (m, 1H), 7.77 (dd, J = 5, 1.56 Hz, 1H), 4.81 (s, 2H), 3.91 (s, 3H). HRMS (ESI) *m/z* found 229.98 [M+H]$^+$, Calculated 230.0586 [M]$^+$.
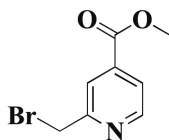
7.1.6. Methyl 5-(bromomethyl)picolinate
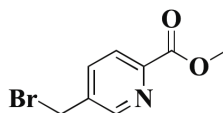
A mixture of methyl 2-methylisonicotinate (1eq) and α,α`-Azoisobutyronitrile (AIBN) (10%) was dissolved in carbontetrachloride (CCl₄). The solution was heated at 48°C and N-

bromosuccinimide (NBS) (1.1eq) solution in CCl$_4$ was added drop wise and stirred for 5 hours. The reaction was cooled to room temperature and the solvent evaporated. The mixture was then extracted using dichloromethane and water followed by washing the organic layer with brine. The organic layer was dried over sodium sulfate, filtered, evaporated and the crude product was purified using SiO$_2$ column chromatography and eluted with the solvent system EtOAc: hexanes = 2:3 to obtain pure product as white powder and the yield was 66%. ^{1}H-NMR (400 MHz, DMSO-d$_6$): δ 8.78 (t, J = 1.48 Hz, 1H), 8.06 (d, J = 1.36 Hz, 2H), 4.82 (s, 2H), 3.89 (s, 3H). HRMS (ESI) m/z found 229.98 [M+H]$^+$, Calculated 230.0586 [M]$^+$.

7.1.7. Methyl 6-((2-formyl-4-methoxyphenoxy)methyl)nicotinate (PP1)

A mixture of 2-hydroxyl-5-methoxybenzaldehyde (1eq) and methyl 6-(bromomethyl)nicotinate (1eq) was dissolved in anhydrous N,N-Dimethylformamide (DMF). Anhydrous potassium carbonate (K$_2$CO$_3$) (1.2eq) was added to this mixture and the reaction was stirred at room temperature for 8-10 hours. The solvent was then evaporated and the reaction mixture extracted with ethyl acetate and water. The organic layer was dried over sodium sulfate, filtered and the solvent evaporated. The crude product was purified using SiO$_2$ column chromatography and eluted with the solvent system EtOAc: hexanes = 3:2 to obtain pure product as white powder with a yield of 82%. IR (Diamond, cm^{-1}): 2922, 2867, 1721, 1669, 1620, 1585,

1499, 1446, 1391, 1370, 1286, 1224, 1174, 1141, 1121; ^{1}H-NMR (400 MHz, DMSO-d$_6$): δ 10.49 (s, 1H), 9.08 (m, 1H), 8.36 (dd, J=8.16,2.16 Hz, 1H), 7.80 (d, J=8.12 Hz, 1H), 7.25 (m, 3H), 5.42 (s, 2H), 3.91 (s, 3H), 3.77(s, 3H); ^{13}C-NMR (100 MHz, DMSO-d$_6$): δ 188.94, 165.00, 161.04, 154.62, 153.62, 149.59, 137.82, 125.03, 124.77, 122.85, 121.31, 115.97, 110.78, 71.02, 55.59, 52.38. HRMS (ESI) *m/z* found 324.07 (M+Na)$^+$, Calculated 301.2940 [M]$^+$. The purity of the compound was checked by HPLC and was found to be 97% pure.

7.1.8. Methyl 2-((2-formyl-4-methoxyphenoxy)methyl)nicotinate (PP2)

A mixture of 2-hydroxyl-5-methoxybenzaldehyde (1eq) and methyl 2-(bromomethyl)nicotinate (1eq) was dissolved in anhydrous N,N-Dimethylformamide (DMF). Anhydrous potassium carbonate (K$_2$CO$_3$) (1.2eq) was added to this mixture and the reaction was stirred at room temperature for 8-10 hours. The solvent was then evaporated and the reaction mixture was extracted with ethyl acetate and water. The organic layer was dried over sodium sulfate, filtered and the solvent evaporated. The crude product was purified using SiO$_2$ column chromatography and eluted with the solvent system EtOAc: hexanes = 3:2 to obtain pure product as pale yellow powder with a yield of 82%. IR (Diamond, cm^{-1}): 2920, 1719, 1684, 1667, 1622, 1583, 1535, 1492, 1445, 1404, 1372, 1276, 1215, 1168, 1142; ^{1}H-NMR (400 MHz, DMSO-d$_6$): δ 10.25 (s, 1H), 8.74 (dd, J = 4.76, 1.48 Hz, 1H), 8.23 (dd, J = 7.8, 1.44 Hz, 1H), 7.55 (m, 1H), 7.2

(m, 3H), 5.56 (s, 2H), 3.78 (s, 3H), 3.75(s, 3H); ^{13}C-NMR (100 MHz, DMSO-d$_6$): δ 188.73, 166.14, 155.39, 155.29, 153.46, 151.55, 138.47, 126.17, 124.86, 123.66, 122.98, 116.13, 110.06, 70.98, 55.61, 52.54. HRMS (ESI) *m/z* found 302.11 (M+H)$^+$, 324.09 (M+Na)$^+$, Calculated 301.2940 [M]$^+$. The purity of the compound was checked by HPLC and was found to be 99% pure.
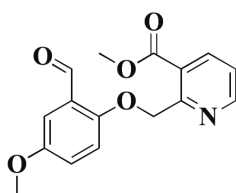
7.1.9. Methyl 6-((2-formyl-4-methoxyphenoxy)methyl)picolinate (PP3)

A mixture of 2-hydroxyl-5-methoxybenzaldehyde (1eq) and methyl 6-(bromomethyl)picolinate (1eq) was dissolved in anhydrous N,N-Dimethylformamide (DMF). Anhydrous potassium carbonate (K$_2$CO$_3$) (1.2eq) was added to this mixture and the reaction was stirred at room temperature for 8-10 hours. The solvent was then evaporated and the reaction mixture extracted with ethyl acetate and water. The organic layer was dried over sodium sulfate, filtered and the solvent evaporated. The crude product was purified using SiO$_2$ column chromatography and eluted with the solvent system EtOAc: hexanes = 3:2 to obtain pure product as white powder with a yield of 82%. IR (Diamond, cm^{-1}): 2953, 2851, 1720, 1682, 1618, 1585, 1494, 1396, 1369, 1296, 1222, 1169, 1141; ^{1}H-NMR (400 MHz, DMSO-d$_6$): δ 10.47 (s, 1H), 8.03 (m, 2H), 7.87 (d, *J* = 7.32 Hz, 1H), 7.26 (m, 3H), 5.38 (s, 2H), 3.90 (s, 3H), 3.76(s, 3H); ^{13}C-NMR (100 MHz, DMSO-d$_6$): δ 189.03, 164.99, 156.95, 154.68, 153.59, 146.99, 138.57, 125.05, 125.01, 123.95, 123.84, 115.99, 110.76, 71.08, 55.59, 52.39. HRMS (ESI) *m/z* found 302.10 (M+H)$^+$,

324.08 (M+Na)$^+$, Calculated 301.2940 [M]$^+$. The purity of the compound was checked by HPLC and was found to be 98% pure.
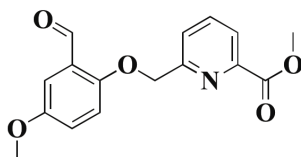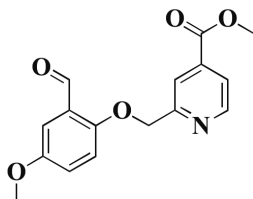
7.1.10. Methyl 2-((2-formyl-4-methoxyphenoxy)methyl)isonicotinate (PP4)

A mixture of 2-hydroxyl-5-methoxybenzaldehyde (1eq) and methyl 2-(bromomethyl)isonicotinate (1eq) was dissolved in anhydrous N,N-Dimethylformamide (DMF). Anhydrous potassium carbonate (K$_2$CO$_3$) (1.2eq) was added to this mixture and the reaction was stirred at room temperature for 8-10 hours. The solvent was then evaporated and the reaction mixture extracted with ethyl acetate and water. The organic layer was dried over sodium sulfate, filtered and the solvent evaporated. The crude product was purified using SiO$_2$ column chromatography and eluted with the solvent system EtOAc: hexanes = 3:2 to obtain pure product as white powder with a yield of 82%. IR (Diamond, cm^{-1}): 2923, 1729, 1686, 1608, 1566, 1450, 1382, 1292, 1276, 1216, 1190, 1171; ^{1}H-NMR (400 MHz, DMSO-d$_6$): δ 10.43 (s, 1H), 8.81 (dd, J = 5, 0.56 Hz, 1H), 8.02 (s, J = 1.44 Hz, 1H), 7.80 (dd, J = 5.04, 1.56 Hz, 1H), 7.24 (m, 3H), 5.41 (s, 2H), 3.91 (s, 3H), 3.76(s, 3H); ^{13}C-NMR (100 MHz, DMSO-d$_6$): δ 188.81, 165.02, 157.80, 154.78, 153.63, 150.44, 137.79, 125.09, 122.92, 121.82, 120.33, 116.25, 110.73, 71.27, 55.58, 52.81. HRMS (ESI) m/z found 302.10 (M+H)$^+$, 324.08 (M+Na)$^+$, Calculated 301.2940 [M]$^+$. The purity of the compound was checked by HPLC and was found to be 98% pure.

7.1.11. Methyl 6-((2-formyl-3-hydroxyphenoxy)methyl)nicotinate (PP5)
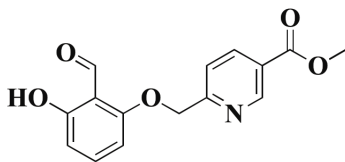
A mixture of 2,6-dihydroxybenzaldehyde (1eq) and methyl 6-(bromomethyl)nicotinate (1eq) was dissolved in anhydrous N,N-Dimethylformamide (DMF). Anhydrous potassium carbonate (K_2CO_3) (1.2eq) was added to this mixture and the reaction was stirred at room temperature for 4 hours. The solvent was then evaporated and the reaction mixture extracted with ethyl acetate and water. The organic layer was dried over sodium sulfate, filtered and the solvent evaporated. The crude product was purified using SiO_2 column chromatography and eluted with the solvent system EtOAc: hexanes = 6:1 to obtain pure product as white powder with a yield of 58%. IR (Diamond, cm^{-1}): 3299, 2959, 1726, 1694, 1620, 1458, 1437, 1382, 1343, 1285, 1233, 1172, 1122; ^{1}H-NMR (400 MHz, DMSO-d$_6$): δ 11.73 (s, 1H), 10.45 (s, 1H), 9.09 (s, 1H), 8.34 (d, J = 8.12, 1H), 7.81 (d, J = 8.28 Hz, 1H), 7.51 (t, J = 8.4 Hz, 1H), 6.67 (d, J = 8.52 Hz, 1H), 6.56 (d, J = 8.36 Hz) 5.41 (s, 2H), 3.90(s, 3H); ^{13}C-NMR (100 MHz, DMSO-d$_6$): δ 193.85, 165.39, 163.86, 160.84, 160.41, 150.66, 138.40, 138.12, 125.47, 120.52, 111.05, 110.86, 102.24, 70.91, 52.47. HRMS (ESI) *m/z* found 288.08 (M+H)$^+$, 310.08 (M+Na)$^+$, Calculated 301.2940 [M]$^+$. The purity of the compound was checked by HPLC and was found to be 100% pure.

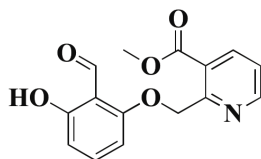### 7.1.12. Methyl 2-((2-formyl-3-hydroxyphenoxy)methyl)nicotinate (PP6)

A mixture of 2,6-dihydroxybenzaldehyde (1eq) and methyl 2-(bromomethyl)nicotinate (1eq) was dissolved in anhydrous N,N-Dimethylformamide (DMF). Anhydrous potassium carbonate (K_2CO_3) (1.2eq) was added to this mixture and the reaction was stirred at room temperature for 4 hours. The solvent was then evaporated and the reaction mixture was extracted with ethyl acetate and water. The organic layer was dried over sodium sulfate, filtered and the solvent evaporated. The crude product was purified using SiO_2 column chromatography and eluted with the solvent system EtOAc: hexanes = 5:2 to obtain pure product as pale yellow powder with a yield of 58%. IR (Diamond, cm^{-1}): 2956, 1713, 1618, 1637, 1571, 1459, 1435, 1396, 1370, 1287, 1238, 1170, 1141; ^{1}H-NMR (400 MHz, DMSO-d$_6$): δ 11.67 (s, 1H), 10.19 (s, 1H), 8.75 (dd, J = 4.8, 1.68 Hz, 1H), 8.25 (dd, J = 7.84, 1.68 Hz, 1H), 7.55 (m, 2H), 6.66 (d, J = 8.2 Hz, 1H), 6.53 (d, J = 8.4 Hz, 1H), 5.58 (s, 2H), 3.79(s, 3H); ^{13}C-NMR (100 MHz, DMSO-d$_6$): δ 193.68, 166.15, 162.26, 161.44, 155.02, 151.73, 138.75, 138.31, 126.02, 123.60, 110.66, 109.49, 103.51, 70.59, 52.50. MS (ESI) *m/z* found 288.09 (M+H)$^+$, 310.07 (M+Na)$^+$, Calculated 301.2940 [M]$^+$. The purity of the compound was checked by HPLC and was found to be 100% pure.

7.1.13. Methyl 2-((2-formyl-3-hydroxyphenoxy)methyl)isonicotinate (PP7)
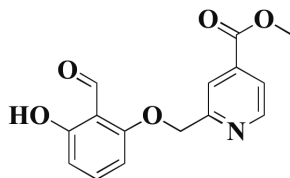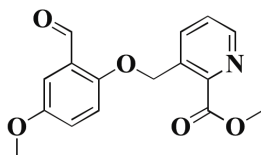

A mixture of 2,6-dihydroxybenzaldehyde (1eq) and methyl 2-(bromomethyl)isonicotinate (1eq) was dissolved in anhydrous N,N-Dimethylformamide (DMF). Anhydrous potassium carbonate (K_2CO_3) (1.2eq) was added to this mixture and the reaction was stirred at room temperature for 4 hours. The solvent was then evaporated and the reaction mixture extracted with ethyl acetate and water. The organic layer was dried over sodium sulfate, filtered and the solvent evaporated. The crude product was purified using SiO_2 column chromatography and eluted with the solvent system EtOAc: hexanes = 5:2 to obtain pure product as pale yellow powder with a yield of 58%. IR (Diamond, cm^{-1}): 2961, 1733, 1716, 1639, 1620, 1577, 1460, 1441, 1373, 1342, 1293, 1235, 1215, 1174; ^{1}H-NMR (400 MHz, DMSO-d$_6$): δ 11.68 (s, 1H), 10.39 (s, 1H), 8.81 (dd, J = 5, 0.6 Hz, 1H), 8.03 (d, J = 0.56 Hz, 1H), 7.81 (dd, J = 5, 1.56 Hz 1H), 7.51 (t, J = 8.4 Hz, 1H), 5.41 (s, 2H), 3.91(s, 3H); ^{13}C-NMR (100 MHz, DMSO-d$_6$): δ 193.51, 165.02, 162.37, 160.80, 157.43, 150.43, 138.66, 137.84, 121.89, 120.38, 110.83, 109.74, 103.56, 70.69, 52.83. MS (ESI) *m/z* found 288.09 (M+H)$^+$, 310.07 (M+Na)$^+$, Calculated 301.2940 [M]$^+$. The purity of the compound was checked by HPLC and was found to be 99% pure.

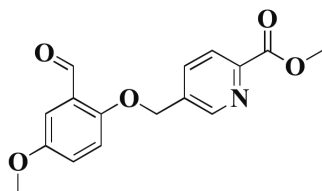### 7.1.14. Methyl 3-((2-formyl-4-methoxyphenoxy)methyl)picolinate (PP8)

A mixture of 2-hydroxyl-5-methoxybenzaldehyde (1eq) and methyl 3-(bromomethyl)picolinate (1eq) was dissolved in anhydrous N,N-Dimethylformamide (DMF). Anhydrous potassium carbonate (K_2CO_3) (1.2eq) was added to this mixture and the reaction was stirred at room temperature for 8-10 hours. The solvent was then evaporated and the reaction mixture extracted with ethyl acetate and water. The organic layer was dried over sodium sulfate, filtered and the solvent evaporated. The crude product was purified using SiO_2 column chromatography and eluted with the solvent system EtOAc: hexanes = 3:2 to obtain pure product as pale yellow powder with a yield of 82%. IR (Diamond, cm^{-1}): 2897, 1712, 1671, 1607, 1567, 1490, 1445, 1398, 1365, 1275, 1232, 1165, 1139, 1106; ^{1}H-NMR (400 MHz, DMSO-d$_6$): δ 10.35 (s, 1H), 8.65 (dd, J = 4.6, 1.28 Hz, 1H), 8.2 (dd, J = 7.84, 0.76 Hz, 1H), 7.66 (dd, J = 7.88, 4.68 Hz, 1H), 7.24 (m, 3H), 5.49 (s, 2H), 3.83 (s, 3H), 3.77(s, 3H); ^{13}C-NMR (100 MHz, DMSO-d$_6$): δ 188.81, 166.12, 154.66, 153.55, 148.49, 146.69, 136.89, 133.04, 126.43, 124.89, 122.96, 115.79, 110.68, 67.44, 55.56, 52.34. MS (ESI) m/z found 324.08 (M+Na)$^+$, Calculated 301.2940 [M]$^+$. The purity of the compound was checked by HPLC and was found to be 98% pure.

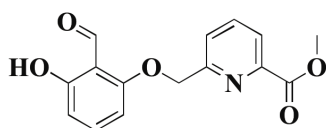## 7.1.15. Methyl 5-((2-formyl-4-methoxyphenoxy)methylpicolinate (PP9)

A mixture of 2-hydroxyl-5-methoxybenzaldehyde (1eq) and methyl 5-(bromomethyl)picolinate (1eq) was dissolved in anhydrous N,N-Dimethylformamide (DMF). Anhydrous potassium carbonate (K_2CO_3) (1.2eq) was added to this mixture and the reaction was stirred at room temperature for 8-10 hours. The solvent was then evaporated and the reaction mixture extracted with ethyl acetate and water. The organic layer was dried over sodium sulfate, filtered and the solvent evaporated. The crude product was purified using SiO_2 column chromatography and eluted with the solvent system EtOAc: hexanes = 3:2 to obtain pure product as white powder with a yield of 82%. IR (Diamond, cm^{-1}): 2962, 2864, 2767, 1719, 1684, 1673, 1588, 1489, 1458, 1395, 1355, 1274, 1218, 1198, 1150, 1127; ^{1}H-NMR (400 MHz, DMSO-d$_6$): δ 10.40 (s, 1H), 8.84 (d, J = 1.36 Hz,1H), 8.10 (m, 2H), 7.28 (m, 2H), 7.2 (d, J = 2.92 Hz, 1H), 5.39 (s, 2H), 3.89 (s, 3H), 3.76(s, 3H); ^{13}C-NMR (100 MHz, DMSO-d$_6$): δ 188.77, 154.89, 154.57, 148.62, 135.93, 135.67, 135.93, 135.67, 125.92, 125.17, 123.28, 114.92, 111.30, 68.52, 55.90, 52.97. MS (ESI) m/z found 302.10 (M+H)$^+$, 324.09 (M+Na)$^+$, Calculated 301.2940 [M]$^+$. The purity of the compound was checked by HPLC and was found to be 98% pure.

7.1.16. Methyl 6-((2-formyl-3-hydroxyphenoxy)methyl)picolinate (PP10)
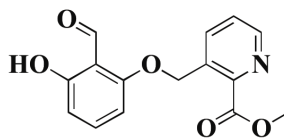

A mixture of 2,6-dihydroxybenzaldehyde (1eq) and methyl 6-(bromomethyl)picolinate (1eq) was dissolved in anhydrous N,N-Dimethylformamide (DMF). Anhydrous potassium carbonate (K_2CO_3) (1.2eq) was added to this mixture and the reaction was stirred at room temperature for 4 hours. The solvent was then evaporated and the reaction mixture extracted with ethyl acetate and water. The organic layer was dried over sodium sulfate, filtered and the solvent evaporated. The crude product was purified using SiO_2 column chromatography and eluted with the solvent system EtOAc: hexanes = 6:1 to obtain pure product as white powder with a yield of 58%. IR (Diamond, cm^{-1}): 3065, 3010, 2956, 2890, 1738, 1697, 1640, 1614, 1583, 1462, 1454, 1400, 1358, 1297, 1242, 1190, 1171, 1150; ^{1}H-NMR (400 MHz, DMSO-d_6): δ 11.74 (s, 1H), 10.44 (s, 1H), 8.04 (m, 2H), 7.91 (dd, J = 7.48, 1.12 Hz, 1H), 7.52 (t, J = 8.4 Hz, 1H), 6.7 (d, J = 8 Hz, 1H), 6.56 (d, J = 8.4 Hz, 1H), 5.39 (s, 2H), 3.90(s, 3H); ^{13}C-NMR (100 MHz, DMSO-d_6): δ 193.79, 164.99, 162.43, 160.69, 160.62, 149.59, 138.65, 137.84, 124.81, 121.26, 110.79, 109.81, 103.42, 70.49, 52.41. MS (ESI) *m/z* found 288.09 (M+H)$^+$, 310.07 (M+Na)$^+$, Calculated 301.2940 [M]$^+$. The purity of the compound was checked by HPLC and was found to be 100% pure.

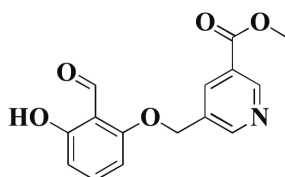### 7.1.17. Methyl 3-((2-formyl-3-hydroxyphenoxy)methyl)picolinate (PP11)

A mixture of 2,6-dihydroxybenzaldehyde (1eq) and methyl 3-(bromomethyl)picolinate (1eq) was dissolved in anhydrous N,N-Dimethylformamide (DMF). Anhydrous potassium carbonate (K_2CO_3) (1.2eq) was added to this mixture and the reaction was stirred at room temperature for 4 hours. The solvent was then evaporated and the reaction mixture extracted with ethyl acetate and water. The organic layer was dried over sodium sulfate, filtered and the solvent evaporated. The crude product was purified using SiO_2 column chromatography and eluted with the solvent system EtOAc: hexanes = 6:1 to obtain pure product as pale yellow powder with a yield of 54%. IR (Diamond, cm^{-1}): 3092, 2923, 2851, 1774, 1712, 1632, 1599, 1566, 1515, 1478, 1366, 1276, 1231, 1180, 1136, 1072; ^{1}H-NMR (400 MHz, DMSO-d$_6$): δ 11.72 (s, 1H), 10.32 (s, 1H), 8.65 (dd, J = 4.64, 1.52 Hz, 1H), 8.22 (m, 1H), 7.66 (dd, J = 7.88, 4.64 Hz, 1H), 7.54 (t, J = 8.4 Hz, 1H), 6.66 (d, J = 8 Hz, 1H), 6.57 (d, J = 8.4 Hz, 1H), 5.51 (s, 2H), 3.84 (s, 3H), ^{13}C-NMR (100 MHz, DMSO-d$_6$): δ 193.59, 166.09, 162.46, 160.68, 148.53, 146.54, 138.72, 136.83, 132.78, 126.44, 110.74, 109.79, 103.26, 67.04, 52.35. MS (ESI) *m/z* found 310.08 (M+Na)$^{+}$, Calculated 301.2940 [M]$^{+}$. The purity of the compound was checked by HPLC and was found to be 100% pure.

### 7.1.18. Methyl 5-((2-formyl-4-methoxyphenoxy)methyl)nicotinate (PP12)
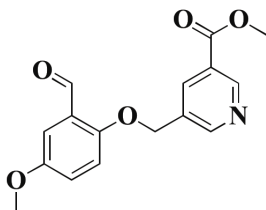
A mixture of 2-hydroxyl-5-methoxybenzaldehyde (1eq) and methyl 5-(bromomethyl)nicotinate (1eq) was dissolved in anhydrous N,N-Dimethylformamide (DMF). Anhydrous potassium carbonate (K$_2$CO$_3$) (1.2eq) was added to this mixture and the reaction was refluxed at room temperature for 8-10 hours. The solvent was then evaporated and the reaction mixture extracted with ethyl acetate and water. The organic layer was dried over sodium sulfate, filtered and the solvent evaporated. The crude product was purified using SiO$_2$ column chromatography and eluted with the solvent system EtOAc: hexanes = 3:2 to obtain pure product as white powder with a yield of 82%. IR (Diamond, cm^{-1}): 2969, 1718, 1670, 1602, 1572, 1498, 1435, 1405, 1382, 1279, 1217, 1185, 1160, 1119; ^{1}H-NMR (400 MHz, DMSO-d$_6$): δ 10.37 (s, 1H), 9.06 (d, J = 2 Hz,1H), 8.97 (d, J = 2.04 Hz, 1H), 8.42 (t, J = 2.04 Hz, 1H), 7.29 (m, 2H), 7.2 (d, J = 3.08 Hz, 1H), 5.38 (s, 2H), 3.9 (s, 3H), 3.77(s, 3H); ^{13}C-NMR (100 MHz, DMSO-d$_6$): δ 188.87, 165.04, 154.64, 153.64, 152.90, 149.49, 135.99, 132.63, 125.44, 125.13, 122.88, 116.21, 110.71, 67.83, 55.58, 52.49. MS (ESI) m/z found 324.08 (M+Na)$^+$, Calculated 301.2940 [M]$^+$. The purity of the compound was checked by HPLC and was found to be 99% pure.

7.1.19. Methyl 5-((2-formyl-3-hydroxyphenoxy)methyl)nicotinate (PP13)

A mixture of 2,6-dihydroxybenzaldehyde (1eq) and methyl 5-(bromomethyl)nicotinate (1eq) was dissolved in anhydrous N,N-Dimethylformamide (DMF). Anhydrous potassium carbonate (K_2CO_3) (1.2eq) was added to this mixture and the reaction was stirred at room temperature for 4 hours. The solvent was then evaporated and the reaction mixture extracted with ethyl acetate and water. The organic layer was dried over sodium sulfate, filtered and the solvent evaporated. The crude product was purified using SiO_2 column chromatography and eluted with the solvent system EtOAc: hexanes = 6:1 to obtain pure product as white powder with a yield of 54%. IR (Diamond, cm^{-1}): 2907, 1719, 1643, 1617, 1584, 1460, 1429, 1397, 1370, 1292, 1246, 1179, 1152, 1121;^{1}H-NMR (400 MHz, DMSO-d_6): δ 11.72 (s, 1H), 10.33 (s, 1H), 9.05 (d, J = 1.8 Hz, 1H), 8.99 (d, J = 1.76 Hz, 1H), 8.43 (t, J = 2 Hz, 1H), 7.55 (t, J = 8.2 Hz, 1H), 6.73 (d, J = 8.2 Hz, 1H), 6.56 (d, J = 8.44 Hz, 1H), 5.39 (s, 2H), 3.91(s, 3H); ^{13}C-NMR (100 MHz, DMSO-d_6): δ 193.74, 176.82, 165.04, 162.40, 160.72, 152.87, 149.53, 138.63, 135.99, 132.32, 110.80, 109.76, 103.42, 67.28, 52.49. MS (ESI) *m/z* found 288.08 (M+H)$^{+}$, Calculated 301.2940 [M]$^{+}$. The purity of the compound was checked by HPLC and was found to be 99% pure.

7.1.20. Methyl 5-((2-formyl-3-hydroxyphenoxy)methyl)picolinate (PP14)
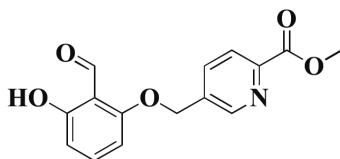
A mixture of 2,6-dihydroxybenzaldehyde (1eq) and methyl 5-(bromomethyl)picolinate (1eq) was dissolved in anhydrous N,N-Dimethylformamide (DMF). Anhydrous potassium carbonate (K_2CO_3) (1.2eq) was added to this mixture and the reaction was stirred at room temperature for 4 hours. The solvent was then evaporated and the reaction mixture extracted with ethyl acetate and water. The organic layer was dried over sodium sulfate, filtered and the solvent evaporated. The crude product was purified using SiO_2 column chromatography and eluted with the solvent system EtOAc: hexanes = 6:1 to obtain pure product as white powder with a yield of 54%. IR (Diamond, cm^{-1}): 2954, 1731, 1679, 1644, 1618, 1574, 1458, 1440, 1392, 1357, 1289, 1249, 1177, 1144, 1122; ^{1}H-NMR (400 MHz, DMSO-d$_6$): δ 11.74 (s, 1H), 10.37 (s, 1H), 8.86 (s, 1H), 8.12 (m, 2H), 7.54 (t, J = 8.4 Hz, 1H), 6.72 (d, J = 8.32 Hz, 1H), 6.56 (d, J = 8.4 Hz, 1H), 5.40 (s, 2H), 3.89 (s, 3H); ^{13}C-NMR (100 MHz, DMSO-d$_6$): δ 193.83, 162.42, 160.69, 148.72, 147.01, 138.64, 136.32, 135.91, 135.78, 124.64, 109.79, 103.37, 67.31, 52.39. MS (ESI) m/z found 310.08 (M+Na)$^+$, Calculated 301.2940 [M]$^+$. The purity of the compound was checked by HPLC and was found to be 99% pure.

7.2. Blood collection and purification of hemoglobin

Human blood samples were obtained from healthy volunteers at Virginia Commonwealth University. Hemoglobin for OEC and crystallographic studies was purified from the same. The use of the biological samples was reviewed and approved by the IRB, in accordance of institutinal regulations. Leftover blood samples from patients with homozygous SS were obtained and utilized, based on an approved IRB protocol at the Children's Hospital of Philadelphia, with informed consent.

Hemoglobin was purified from normal human blood samples according to the literature procedure.[35,202] Human blood was centrifuged at 2500 rpm for 20 min at 4°C. The supernatant solution, plasma, debris and excess serum were then discarded from the centrifuge bottles thus leaving behind the RBCs. The RBCs were washed thrice with an excess volume of 0.9% NaCl and once with 1.0% NaCl, each time centrifuging and discarding the supernatant solution. The RBCs were poled together into a chilled flask and hemolyzed to free Hb by adding 1-2 volume excess of 50 mM Tris buffer, pH 8.6 (containing 0.5 mM EDTA). The mixture was allowed to stand in ice for 30 min with occasional stirring. The Hb solution was centrifuged at 10,000 rpm for 90 min at 4°C. The supernatant Hb solution was pooled into a chilled flask and NaCl (40-60 mg/mL of Hb solution) was slowly added with stirring. Hemoglobin solution was centrifuged at 10,000 rpm for 90 min at 4°C to remove any cell stroma remnants. The clear supernatant Hb solution was then pooled into a chilled flask and he syrupy pellet was discarded. This solution was dialyzed against 50 mM Tris buffer, pH 8.6 (containing EDTA) at 4°C to remove NaCl and other low molecular

weight impurities. Strips of standard cellulose dialysis tubing (12,000-14,000 Da) that had been washed 3-4 times with deionized water were used for dialysis. The pooled fractions were concentrated with an Amicon stirred cell (Amicon, Model 402), to a final Hb A concentration of about 100 mg/mL and this concentrated Hb A was stored at -80°C.

7.3. Oxygen equillibrium studies

OEC study was conducted to determine whether the compounds have any effect on the Hb-O_2 affinity following standard procedure.[187] Whole blood of purified Hb from normal subjects was used for this study. The OEC studies were conducted on whole blood saple with 30% hematocrit, and cell-free purified Hb of 1.56 mM concentration in the absence or presence of compounds solubilized in DMSO. The blood/Hb samples were incubated in IL 237 tonometer (Instrumentation Laboratories, Inc., Lexington, MA) for about 7 min at 37°C against gas mixture containing O_2 concentrations of 0.804%, 2.935% and 5.528% and allowed to equilibrate at O_2 tensions of 6, 20 and 40 mmHg. After equilibration, the sample was removed via syringe and aspirated into a ABL 700 series table top automated blood gas analyzer (Radiometer America, Inc., Westlake, OH) to determine total hemoglobin (tHb), hematocrit (H_{ct}), pH, pCO_2, partial pressure of oxygen (pO_2), and the Hb-O_2 saturation (sO_2) values. The measured values of pO_2 and sO_2 at each oxygen saturation level were then subjected to nonlinear regression analysis using the software Scientist (Micromath, Salt Lake City UT) with the following equation:

$$sO_2\% = 100 \times \frac{pO_2^N \, mmHg}{P_{50}^N(mmHg) + \, pO_2^N(mmHg)}$$

This equation was used to calculate P_{50} and Hill coefficient (N) values. ΔP_{50} (%) was determined as:

$$\Delta P_{50} \, (\%) = 100 \times \frac{P_{50} \text{ in the absence of compound} - P_{50} \text{ in the presence of compound}}{P_{50} \text{ in the absence of compound}}$$

For concentration-dependent OEC studies, 0.5 mM, 1.0 mM and 2 mM concentrations of each compound to be tested were used whereas for time-dependent OEC studies, 2 mM of each compound was used. Aliquots of each sample was tested at 1, 2, 4, 8, 12 and 24 h to obtain the P_{50} and ΔP_{50} values.

7.4. Adduct formation studies using normal whole blood and hemoglobin

Time-dependent and concentration-dependent Hb-compound adduct formation studies were performed using whole blood and Hb. In a 96-well deep well plate (Thermo Scientific), 0.5 mM, 1.0 mM and 2.0 mM concentrations of the compounds were added to 600 µL of whole blood (30% hematocrit) and/or Hb (1.56 mM). These were incubated at 37°C for 24 h with shaking (at 140 rpm). At 0.5, 1, 2, 4, 8, 12 and 24 h time intervals, 50 µL aliquots of this mixture were removed from each well using a multichannel pipette and added to respective tubes containing 50 µL of sodium cyanoborohydride (NaBH$_3$CN) and sodium borohydride (NaBH$_4$) mixture (1:1 v/v 50 mM stock) to terminate the Schiff-base reaction, fix the Schiff-base adducts and reduce the free reactive

aldehyde.[203] After mixing, the tubes were stored immediately at -80ºC until ready for analysis using cation-exchange HPLC (Hitachi D-700 Series, Hitachi Instruments, Inc. San Jose, CA).[171,174] The observed Hb adducts in %Hb modification were plotted as a function of time (h); peak concentration was obtained by visual inspection, and the area under the curve, (AUC 0-24), was obtained by linear trapezoidal rule across the entire 24 h period.

7.5. Hemoglobin modification, oxygen equilibrium and antisickling studies using human sickle blood

Blood suspensions from subjects with homozygous SCD (hematocrit 20%) were incubated under air in the absence or presence of compounds at 37ºC for 1 h to ensure that binding has attained equilibrium. Following this, the suspensions were incubated under hypoxic conditions (4% oxygen/96% nitrogen) at 37ºC for 2 h. Aliquot samples were fixed with 2% glutaraldehyde solution without exposure to air, and then subjected to microscopic morphological analysis of bright field images (at 40x magnification) of single layer cells on an Olympus BX40 microscope fitted with an Infinity Lite B camera (Olympus), and the coupled Image Capture software. The residual samples were washed in phosphate-buffer saline, and hemolyzed in hypotonic lysis buffer for subsequent analyses.[171,174]

For oxygen equilibrium studies, approximately 100 μL aliquot samples from the above clarified lysate were added to 4 mL of 0.1M potassium phosphate buffer, pH 7.0, in cuvettes and subjected to hemoximetry analysis using Hemox^{TM} Analyzer (TCS Scientific Corp.) to assess P_{50}

shifts. Degree of P_{50} shift (ΔP_{50}) was expressed as percentage fractions of control DMSO-treated samples.

$$\Delta P_{50}\ (\%) = 100\ \times \frac{P_{50}\ \text{of lysates from untreated cells} - P_{50}\ \text{of lysates from treated cells}}{P_{50}\ \text{of lysates from unrteated cells}}$$

Finally, for the Hb adduct formation studies, the above clarified lysates were subjected to cation-exchange HPLC (Hitachi D-7000 Series, Hitachi Instruments, Inc., San Jose, CA), using a weak cation-exchange column (Poly CAT A: 30 mm x 4.6 mm, Poly LC, Inc., Columbia, MD). A commercial standard consisting of approximately equal amounts of composite Hb F, Hb A, Hb S and Hb C (Helena Laboratories, Beaumont, TX), was utilized as reference isotypes. The areas of new peaks, representing Hb S adducts were obtained, calculated as percentage fractions of total Hb area, and reported as levels of modified Hb.

For concentration-dependent studies, 0.5 mM, 1.0 mM and 2.0 mM concentrations of the compounds were used.

7.6. Partitioning experiment

Partitioning of PP compounds in the RBCs was indirectly tested using the previously mentioned antisickling assay. PP compounds were incubated in 3x volume of whole blood for 1 h. This was followed by removing 1x volume of aliquot (I) and centrifuging the remaining 2x volume. Centrifugation separated the RBCs and the plasma. The supernatant plasma was removed, and the remaining volume was made up to 2x again using hemox buffer. From this, 1x volume (II)

of blood was removed and the remaining 1x volume was centrifuged. This was followed by removing the plasma and making up the volume back to 1x (III) using hemox buffer. The three 1x volume aliquots thus obtained were subjected to antisickling studies a described in section 7.5 to determine the % sickling inhibition shown by the compounds.

7.7. In Vivo Pharmacologic Effect in Mice

In vivo pharmacologic (pharmacodynamics) effects of select PP compounds were tested in C57BL/6 mice. The animals were treated with a single intraperitoneal (IP) (150mg/kg body weight) dose of PP6, PP10, PP14, and TD-7. Blood samples were obtained prior to treatment (0) and 1, 3 and 6h post-treatment, via submandibular bleeding, and subjected to hemolysis using standard methods. Clarified lysates, free of cell debris and red blood cell ghosts were analyzed by cation-exchange HPLC to determine the levels of drug-modified hemoglobin (adducts); and to conduct oxygen equilibrium studies to determine degrees of shift in P_{50} values using methodologies described earlier for in vitro studies on human blood samples.

7.8. X-ray crystallography

Freshly made solution of compounds in DMSO was added to deoxygenated (deoxy) Hb (30 mg/mL protein) at Hb tetramer-compound ratio of 1:10. Following, the complex mixture was saturated with carbon monoxide and allowed to incubate for 2 h to form COHb-Compound complex. Sodium cyanoborohydride ($NaBH_3CN$) was then added to this mixture to reduce the Schiff-base adduct formed between the protein and compound to the corresponding irreversible

147

alkylamine covalent bond. The resulting solution was crystalized using 10-20% PEG6000, 100 mM HEPES buffer, pH 7.4 using the batch method. Single cherry red needle crystals were formed in 1-3 days and were used to collect x-ray diffraction data at 100 K using Molecular Structure Corporation (MSC) X-Stream Cryogenic System (The Woodlands, TX), an R-Axis IV image plate detector and a Rigaku Micro-Max-007 generator (40kV and 20mA). The crystals were first cryo-protected with 80 μL mother liquor mixed with 62 μL of 50% PEG6000. The dataset was processed with the d*trek software (Rigaku) and the CCP4 suite of programs.[204] Following this, the crystal structures of the COHb-compound complexes were determined by a molecular replacement method with Phenix program,[197,205] using the native R2-state crystal structure (PDB ID 1BBB) as a search model. The structure was refined using both Phenix and CNS while model building and correction was carried out using COOT.[198,199]

REFERENCES

(1) Schechter, A. N. Hemoglobin research and the origins of molecular medicine. *Blood* **2008**, *112*, 3927-3938.

(2) Atlas of molecular structures in biology. Ribonuclease-S - AbeBooks - Frederic M. Richards; Harold Winfield Wyckoff: https://www.abebooks.com/9780198547044/Atlas-molecular-structures-biology-Ribonuclease-S-0198547048/plp (accessed Feb 10, 2018).

(3) Schulz, G. E.; Schirmer, R. H. Hemoglobin: Structure, function, evolution, and pathology. Von R. E. Dickerson Und I. Geis. Benjamin/Cummings Publishing Co., Menlo Park, CA 1983. 176. *Angew. Chem.* **1984**, *96*, 1003-1004.

(4) Hsia, C. C. Respiratory function of hemoglobin. *N. Engl. J. Med.* **1998**, *338*, 239-247.

(5) Dickerson, R. E.; Geis, I. *Hemoglobin: Structure, Function, Evolution & Pathology.*; 1983.

(6) Perutz, M. F. *Science Is Not a Quiet Life: Unravelling the Atomic Mechanism of Haemoglobin*; Singapore : World Scientic ; London : Imperial College Press, 1997.

(7) Safo, M. K.; Abraham, D. J. The X-ray structure determination of bovine carbonmonoxy hemoglobin at 2.1 A resolution and its relationship to the quaternary structures of other hemoglobin crystal forms. *Protein Sci. Publ. Protein Soc.* **2001**, *10*, 1091-1099.

(8) Safo, M. K.; Ahmed, M. H.; Ghatge, M. S.; Boyiri, T. Hemoglobin-ligand binding: Understanding Hb function and allostery on atomic Level. *Biochim. Biophys. Acta* **2011**, *1814*, 797-809.

(9) Bellelli, A.; Brunori, M.; Miele, A. E.; Panetta, G.; Vallone, B. The allosteric properties of hemoglobin: Insights from natural and site directed mutants. *Curr. Protein Pept. Sci.* **2006**, *7*, 17-45.

(10) Perutz, M. F. Nature of haem-haem interaction. *Nature* **1972**, *237*, 495-499.

(11) Perutz, M. F.; Wilkinson, A. J.; Paoli, M.; Dodson, G. G. The stereochemical mechanism of the cooperative effects in hemoglobin revisited. *Annu. Rev. Biophys. Biomol. Struct.* **1998**, *27*, 1-34.

(12) Muirhead, H.; Perutz, M. F. Structure of hæmoglobin: A three-dimensional fourier synthesis of reduced human haemoglobin at 5.5 Å resolution. *Nature* **1963**, *199*, 633-638.

(13) Perutz, M. F.; Muirhead, H.; Cox, J. M.; Goaman, L. C. G. Three-dimensional fourier synthesis of horse oxyhaemoglobin at 2.8 Å resolution: The atomic model. *Nature* **1968**, *219*, 131-139.

(14) Fermi, G.; Perutz, M. F.; Shaanan, B.; Fourme, R. The crystal structure of human deoxyhaemoglobin at 1.74 A resolution. *J. Mol. Biol.* **1984**, *175*, 159-174.

(15) Ladner, R. C.; Heidner, E. J.; Perutz, M. F. The structure of horse methaemoglobin at 2-0 A resolution. *J. Mol. Biol.* **1977**, *114*, 385-414.

(16) Paoli, M.; Liddington, R.; Tame, J.; Wilkinson, A.; Dodson, G. Crystal structure of T state haemoglobin with oxygen bound at all four haems. *J. Mol. Biol.* **1996**, *256*, 775-792.

(17) Paoli, M.; Dodson, G.; Liddington, R. C.; Wilkinson, A. J. Tension in haemoglobin revealed by Fe-His(F8) bond rupture in the fully liganded T-State. *J. Mol. Biol.* **1997**, *271*, 161-167.

(18) Antonini, E. Hemoglobin and myoglobin in their reactions with ligands. *Front. Biol.* **1971**, *21*.

(19) Baldwin, J.; Chothia, C. Haemoglobin: The structural changes related to ligand binding and its allosteric mechanism. *J. Mol. Biol.* **1979**, *129*, 175–220.

(20) Monod, J.; Wyman, J.; Changeux, J. P. On the nature of allosteric transitions: A plausible model. *J. Mol. Biol.* **1965**, *12*, 88-118.

(21) Koshland, D. E.; Némethy, G.; Filmer, D. Comparison of experimental binding data and theoretical models in proteins containing subunits*. *Biochemistry* **1966**, *5*, 365-385.

(22) Ackers, G. K.; Doyle, M. L.; Myers, D.; Daugherty, M. A. Molecular code for cooperativity in hemoglobin. *Science* **1992**, *255*, 54-63.

(23) Bettati, S.; Mozzarelli, A.; Rossi, G. L.; Tsuneshige, A.; Yonetani, T.; Eaton, W. A.; Henry, E. R. Oxygen binding by single crystals of hemoglobin: The problem of cooperativity and inequivalence of alpha and beta subunits. *Proteins Struct. Funct. Bioinforma.* **1996**, *25*, 425-437.

(24) Brunori, M.; Coletta, M.; Di Cera, E. A cooperative model for ligand binding to biological macromolecules as applied to oxygen carriers. *Biophys. Chem.* **1986**, *23*, 215-222.

(25) Szabo, A.; Karplus, M. A mathematical model for structure-function relations in hemoglobin. *J. Mol. Biol.* **1972**, *72*, 163-197.

(26) Lee, A. W.; Karplus, M. Structure-specific model of hemoglobin cooperativity. *Proc. Natl. Acad. Sci.* **1983**, *80*, 7055-7059.

(27) Henry, E. R.; Bettati, S.; Hofrichter, J.; Eaton, W. A. A tertiary two-state allosteric model for hemoglobin. *Biophys. Chem.* **2002**, *98*, 149-164.

(28) Eaton, W. A.; Henry, E. R.; Hofrichter, J.; Bettati, S.; Viappiani, C.; Mozzarelli, A. Evolution of allosteric models for hemoglobin. *IUBMB Life* **2007**, *59*, 586-599.

(29) Minton, A. P.; Imai, K. The Three-State Model: A minimal allosteric description of homotropic and heterotropic effects in the binding of ligands to hemoglobin. *Proc. Natl. Acad. Sci.* **1974**, *71*, 1418-1421.

(30) Sawicki, C. A.; Gibson, Q. H. Quaternary conformational changes in human hemoglobin studied by laser photolysis of carboxyhemoglobin. *J. Biol. Chem.* **1976**, *251*, 1533-1542.

(31) Yonetani, T.; Park, S.; Tsuneshige, A.; Imai, K.; Kanaori, K. Global allostery model of hemoglobin. Modulation Of O(2) affinity, cooperativity, and Bohr effect by heterotropic allosteric effectors. *J. Biol. Chem.* **2002**, *277*, 34508-34520.

(32) Marden, M. C.; Kister, J.; Bohn, B.; Poyart, C. T-State Hemoglobin with four ligands bound. *Biochemistry (Mosc.)* **1988**, *27*, 1659-1664.

(33) Jayaraman, V.; Rodgers, K. R.; Mukerji, I.; Spiro, T. G. Hemoglobin allostery: Resonance Raman spectroscopy of kinetic intermediates. *Science* **1995**, *269*, 1843-1848.

(34) Perrella, M.; Cera, E. D. CO ligation intermediates and the mechanism of hemoglobin cooperativity. *J. Biol. Chem.* **1999**, *274*, 2605-2608.

(35) Safo, M. K.; Abraham, D. J. X-ray crystallography of hemoglobins. In *Hemoglobin Disorders*; Methods in Molecular Biology™; Humana Press, 2003; pp 1–19.

(36) Safo, M. K.; Abdulmalik, O.; Lin, H. R.; Asakura, T.; Abraham, D. J. Structures of R- and T-State hemoglobin bassett: Elucidating the structural basis for the low oxygen affinity of a mutant hemoglobin. *Acta Crystallogr. D Biol. Crystallogr.* **2005**, *61*, 156-162.

(37) Safo, M. K.; Burnett, J. C.; Musayev, F. N.; Nokuri, S.; Abraham, D. J. Structure of human carbonmonoxyhemoglobin at 2.16 A: A snapshot of the allosteric transition. *Acta Crystallogr. D Biol. Crystallogr.* **2002**, *58*, 2031-2037.

(38) Mueser, T. C.; Rogers, P. H.; Arnone, A. Interface sliding as illustrated by the multiple quaternary structures of liganded hemoglobin. *Biochemistry (Mosc.)* **2000**, *39*, 15353-15364.

(39) Jenkins, J. D.; Musayev, F. N.; Danso-Danquah, R.; Abraham, D. J.; Safo, M. K. Structure of relaxed-state human hemoglobin: Insight into ligand uptake, transport and release. *Acta Crystallogr. D Biol. Crystallogr.* **2009**, *65*, 41-48.

(40) Abraham, D. J.; Safo, M. K.; Boyiri, T.; Danso-Danquah, R. E.; Kister, J.; Poyart, C. How allosteric effectors can bind to the same protein residue and produce opposite shifts in the allosteric equilibrium. *Biochemistry (Mosc.)* **1995**, *34*, 15006-15020.

(41) Berg, J. M.; Tymoczko, J. L.; Stryer, L. Hemoglobin transports oxygen efficiently by binding oxygen cooperatively. **2002**.

(42) Pittman, R. N. *Oxygen Transport*; Morgan & Claypool Life Sciences, 2011.

(43) Wiley: Chemistry and Biochemistry of Oxygen Therapeutics: From Transfusion to Artificial Blood - Andrea Mozzarelli, Stefano Bettati http://www.wiley.com/WileyCDA/WileyTitle/productCd-0470686685.html (accessed Oct 26, 2017).

(44) Safo, M. K.; Kato, G. J. Therapeutic strategies to alter the oxygen affinity of sickle hemoglobin. *Hematol. Oncol. Clin. North Am.* **2014**, *28*, 217-231.

(45) Macdonald, R. Red Cell 2,3-Diphosphoglycerate and oxygen affinity. *Anaesthesia* **1977**, *32*, 544-553.

(46) Benesch, R.; Benesch, R. E. Intracellular organic phosphates as regulators of oxygen release by haemoglobin. *Nature* **1969**, *221*, 618-622.

(47) Bunn, H. F.; Jandl, J. H. Control of hemoglobin function within the red cell. *N. Engl. J. Med.* **1970**, *282*, 1414-1421.

(48) Bunn, H. F.; Briehl, R. W. The interaction of 2,3-Diphosphoglycerate with various human hemoglobins. *J. Clin. Invest.* **1970**, *49*, 1088-1095.

(49) Riggs, A. F. The Bohr effect. *Annu. Rev. Physiol.* **1988**, *50*, 181-204.

(50) Hess, D. *Respiratory Care: Principles and Practice*; Jones & Bartlett Learning, 2011.

(51) Collins, J. A.; Rudenski, A.; Gibson, J.; Howard, L.; O'Driscoll, R. Relating oxygen partial pressure, saturation and content: The haemoglobin–oxygen dissociation curve. *Breathe* **2015**, *11*, 194-201.

(52) Reeves, R. B. The effect of temperature on the oxygen equilibrium curve of human blood. *Respir. Physiol.* **1980**, *42*, 317-328.

(53) Manning, L. R.; Russell, J. E.; Padovan, J. C.; Chait, B. T.; Popowicz, A.; Manning, R. S.; Manning, J. M. Human embryonic, fetal, and adult hemoglobins have different subunit interface strengths. Correlation with lifespan in the red cell. *Protein Sci. Publ. Protein Soc.* **2007**, *16*, 1641-1658.

(54) Themes, U. F. O. The present and future global burden of the inherited disorders of hemoglobin. *Oncohema Key*, 2017.

(55) Kohne, E. Hemoglobinopathies. *Dtsch. Ärztebl. Int.* **2011**, *108*, 532-540.

(56) Forget, B. G.; Bunn, H. F. Classification of the Disorders of Hemoglobin. *Cold Spring Harb. Perspect. Med.* **2013**, *3* (2), a011684.

(57) Franklin B. H. *Hemoglobin--molecular, genetic, and clinical aspects*; W.B. Saunders Co.: Philadelphia, 1986.

(58) Herrick, J. B. Peculiar elongated and sickle-shaped red blood corpuscles in a case of severe anemia. 1910. *Yale J. Biol. Med.* **2001**, *74*, 179-184.

(59) Pauling, L.; Itano, H. A. Sickle cell anemia a molecular disease. *Science* **1949**, *110*, 543-548.

(60) Pauling, L. Molecular disease and evolution. *Bull. N. Y. Acad. Med.* **1964**, *40*, 334-342.

(61) Rees, D. C.; Williams, T. N.; Gladwin, M. T. Sickle-cell disease. *Lancet Lond. Engl.* **2010**, *376*, 2018-2031.

(62) Lederberg, J. J. B. S. Haldane (1949) on infectious disease and evolution. *Genetics* **1999**, *153*, 1-3.

(63) Ingram, V. M. Gene mutations in human haemoglobin: The chemical difference between normal and sickle cell haemoglobin. *Nature* **1957**, *180*, 326-328.

(64) Ingram, V. M. Abnormal human haemoglobins. I. The comparison of normal human and sickle-cell haemoglobins by fingerprinting. *Biochim. Biophys. Acta* **1958**, *28*, 539-545.

(65) Ferrone, F. A. Polymerization and sickle cell disease: A molecular view. *Microcirc. N. Y. N 1994* **2004**, *11*, 115-128.

(66) Ghatge, M. S.; Ahmed, M. H.; Omar, A. S. M.; Pagare, P. P.; Rosef, S.; Kellogg, G. E.; Abdulmalik, O.; Safo, M. K. Crystal structure of carbonmonoxy sickle hemoglobin in R-state conformation. *J. Struct. Biol.* **2016**, *194*, 446-450.

(67) Bookchin, R. M.; Nagel, R. L.; Ranney, H. M. The effect of beta 73 Asn on the interactions of sickling hemoglobins. *Biochim. Biophys. Acta* **1970**, *221*, 373-375.

(68) Adachi, K.; Kim, J.; Kinney, T. R.; Asakura, T. Effect of the beta 73 amino acid on the hydrophobicity, solubility, and the kinetics of polymerization of deoxyhemoglobin S. *J. Biol. Chem.* **1987**, *262*, 10470-10474.

(69) Converse, J. L.; Sharma, V.; Reiss-Rosenberg, G.; Ranney, H. M.; Danish, E.; Bowman, L. S.; Harris, J. W. Some properties of hemoglobin mobile (Alpha 2 Beta 2 73 Asp----Val). *Hemoglobin* **1985**, *9*, 33-45.

(70) Nagel, R. L.; Johnson, J.; Bookchin, R. M.; Garel, M. C.; Rosa, J.; Schiliro, G.; Wajcman, H.; Labie, D.; Moo-Penn, W.; Castro, O. Beta-chain contact sites in the haemoglobin S polymer. *Nature* **1980**, *283*, 832-834.

(71) Benesch, R. E.; Kwong, S.; Edalji, R.; Benesch, R. Alpha chain mutations with opposite effects on the gelation of hemoglobin S. *J. Biol. Chem.* **1979**, *254*, 8169-8172.

(72) Rhoda, M. D.; Martin, J.; Blouquit, Y.; Garel, M. C.; Edelstein, S. J.; Rosa, J. Sickle cell hemoglobin fiber formation strongly inhibited by the Stanleyville II Mutation (A78 Asn → Lys). *Biochem. Biophys. Res. Commun.* **1983**, *111*, 8-13.

(73) Thein, M. S.; Igbineweka, N. E.; Thein, S. L. Sickle cell disease in the older adult. *Pathology (Phila.)* **2017**, *49*, 1-9.

(74) Ware, R. E.; de Montalembert, M.; Tshilolo, L.; Abboud, M. R. Sickle cell disease. *The Lancet* **2017**, *390*, 311-323.

(75) Genetics Home Reference. Sickle cell disease https://ghr.nlm.nih.gov/condition/sickle-cell-disease (accessed Mar 11, 2018).

(76) Chaturvedi, S.; DeBaun, M. R. Evolution of sickle cell disease from a life-threatening disease of children to a chronic disease of adults: The last 40 years. *Am. J. Hematol.* **2016**, *91*, 5-14.

(77) Alrayyes, S.; Baghdan, D.; Haddad, R. Y.; Compton, A. A.; Mohama, S.; Goreishi, R.; Kawar, N. Sickle cell disease; An overview of the disease and its systemic effects. *Dis. Mon.* [Online] **2018**. http://www.diseaseamonth.com/article/S0011-5029(17)30204-3/fulltext (accessed Mar 10, 2018).

(78) Piel, F. B.; Patil, A. P.; Howes, R. E.; Nyangiri, O. A.; Gething, P. W.; Dewi, M.; Temperley, W. H.; Williams, T. N.; Weatherall, D. J.; Hay, S. I. Global epidemiology of sickle haemoglobin in neonates: A contemporary geostatistical model-based map and population estimates. *The Lancet* **2013**, *381*, 142-151.

(79) CDC. Data and Statistics | Sickle Cell Disease | NCBDDD | CDC https://www.cdc.gov/ncbddd/sicklecell/data.html (accessed Mar 11, 2018).

(80) Lee, A.; Thomas, P.; Cupidore, L.; Serjeant, B.; Serjeant, G. Improved survival in homozygous sickle cell disease: Lessons from a cohort study. *BMJ* **1995**, *311*, 1600-1602.

(81) Lanzkron, S.; Carroll, C. P.; Carlton Haywood, J. Mortality rates and age at death from sickle cell disease: U.S., 1979–2005. *Public Health Rep.* **2013**, *128*, 110-116.

(82) Charache, S.; Grisolia, S.; Fiedler, A. J.; Hellegers, A. E. Effect of 2,3-Diphosphoglycerate on oxygen affinity of blood in sickle cell anemia. *J. Clin. Invest.* **1970**, *49*, 806-812.

(83) McCurdy, P. R.; Mahmood, L. Intravenous urea treatment of the painful crisis of sickle-cell disease. *N. Engl. J. Med.* **1971**, *285*, 992-994.

(84) Sedrak, A.; Kondamudi, N. P. Sickle cell disease. In *StatPearls*; StatPearls Publishing: Treasure Island (FL), 2018.

(85) Kato, G. J.; Gladwin, M. T.; Steinberg, M. H. Deconstructing sickle cell disease: reappraisal of the role of hemolysis in the development of clinical subphenotypes. *Blood Rev.* **2007**, *21*, 37-47.

(86) Sickle Cell Disease | National Heart, Lung, and Blood Institute (NHLBI) https://www.nhlbi.nih.gov/health-topics/sickle-cell-disease (accessed Mar 10, 2018).

(87) Smiers, F. J.; Krishnamurti, L.; Lucarelli, G. Hematopoietic stem cell transplantation for hemoglobinopathies: Current practice and emerging trends. *Pediatr. Clin. North Am.* **2010**, *57*, 181-205.

(88) Hsieh, M. M.; Kang, E. M.; Fitzhugh, C. D.; Link, M. B.; Bolan, C. D.; Kurlander, R.; Childs, R. W.; Rodgers, G. P.; Powell, J. D.; Tisdale, J. F. Allogeneic hematopoietic stem-cell transplantation for sickle cell disease. *N. Engl. J. Med.* **2009**, *361*, 2309-2317.

(89) Walters, M. C. Stem cell therapy for sickle cell disease: Transplantation and gene therapy. *Hematol. Am. Soc. Hematol. Educ. Program* **2005**, 66–73.

(90) FDA approves hydroxyurea for treatment of pediatric patients with sickle cell anemia https://www.fda.gov/Drugs/InformationOnDrugs/ApprovedDrugs/ucm590096.htm (accessed Mar 10, 2018).

(91) Consumer Updates - The FDA encourages new treatments for sickle cell disease https://www.fda.gov/ForConsumers/ConsumerUpdates/ucm418232.htm (accessed Mar 10, 2018).

(92) Platt, O. S. Hydroxyurea for the treatment of sickle cell anemia. *N. Engl. J. Med.* **2008**, *358*, 1362-1369.

(93) Goldberg, M. A.; Brugnara, C.; Dover, G. J.; Schapira, L.; Lacroix, L.; Bunn, H. F. Hydroxyurea and Erythropoietin therapy in sickle cell anemia. *Semin. Oncol.* **1992**, *19*, 74-81.

(94) Charache, S.; Dover, G. J.; Moore, R. D.; Eckert, S.; Ballas, S. K.; Koshy, M.; Milner, P. F.; Orringer, E. P.; Phillips, G.; Platt, O. S. Hydroxyurea: Effects on hemoglobin F production in patients with sickle cell anemia. *Blood* **1992**, *79*, 2555-2565.

(95) Niihara, Y.; Zerez, C. R.; Akiyama, D. S.; Tanaka, K. R. Oral L-Glutamine therapy for sickle cell anemia: I. Subjective clinical improvement and favorable change in red cell NAD redox potential. *Am. J. Hematol.* **1998**, *58*, 117-121.

(96) Iyamu, E. W.; Turner, E. A.; Asakura, T. In vitro effects of NIPRISAN (Nix-0699): A naturally occurring, potent antisickling agent. *Br. J. Haematol.* **2002**, *118*, 337-343.

(97) Ameh, S. J.; Tarfa, F. D.; Ebeshi, B. U. Traditional herbal management of sickle cell anemia: Lessons from Nigeria. *Anemia* **2012**, *2012*, 1-9.

(98) Akojie, F. O.; Fung, L. W. Antisickling activity of hydroxybenzoic acids in Cajanus Cajan. *Planta Med.* **1992**, *58*, 317-320.

(99) Mehanna, A. S. Sickle cell anemia and antisickling agents then and now. *Curr. Med. Chem.* **2001**, *8*, 79-88.

(100) Sankaran, V. G. Targeted therapeutic strategies for fetal hemoglobin induction. *ASH Educ. Program Book* **2011**, *2011*, 459-465.

(101) Olivieri, N. F.; Weatherall, D. J. The therapeutic reactivation of fetal haemoglobin. *Hum. Mol. Genet.* **1998**, *7*, 1655-1658.

(102) Ley, T. J.; DeSimone, J.; Noguchi, C. T.; Turner, P. H.; Schechter, A. N.; Heller, P.; Nienhuis, A. W. 5-Azacytidine increases gamma-globin synthesis and reduces the proportion of dense cells in patients with sickle cell anemia. *Blood* **1983**, *62*, 370-380.

(103) Charache, S.; Dover, G.; Smith, K.; Talbot, C. C.; Moyer, M.; Boyer, S. Treatment of sickle cell anemia with 5-Azacytidine results in increased fetal hemoglobin production and is associated with nonrandom hypomethylation of DNA around the gamma-delta-beta-globin gene complex. *Proc. Natl. Acad. Sci. U. S. A.* **1983**, *80*, 4842-4846.

(104) Galanello, R.; Stamatoyannopoulos, G.; Papayannopoulou, T. Mechanism of Hb F stimulation by S-stage compounds. In vitro studies with bone marrow cells exposed to 5-Azacytidine, Ara-C, or Hydroxyurea. *J. Clin. Invest.* **1988**, *81*, 1209-1216.

(105) Makis, A. C.; Hatzimichael, E. C.; Stebbing, J. The genomics of new drugs in sickle cell disease. *Pharmacogenomics Lond.* **2006**, *7*, 909-917.

(106) DeSimone, J.; Koshy, M.; Dorn, L.; Lavelle, D.; Bressler, L.; Molokie, R.; Talischy, N. Maintenance of elevated fetal hemoglobin levels by Decitabine during dose interval treatment of sickle cell anemia. *Blood* **2002**, *99*, 3905-3908.

(107) Telen, M. J. Beyond Hydroxyurea: New and old drugs in the pipeline for sickle cell disease. *Blood* **2016**, *127*, 810-819.

(108) Atweh, G. F.; Sutton, M.; Nassif, I.; Boosalis, V.; Dover, G. J.; Wallenstein, S.; Wright, E.; McMahon, L.; Stamatoyannopoulos, G.; Faller, D. V.; et al. Sustained induction of fetal hemoglobin by pulse butyrate therapy in sickle cell disease. *Blood* **1999**, *93*, 1790-1797.

(109) Reid, M. E.; El Beshlawy, A.; Inati, A.; Kutlar, A.; Abboud, M. R.; Haynes, J.; Ward, R.; Sharon, B.; Taher, A. T.; Smith, W.; et al. A double-blind, placebo-controlled Phase II study of the efficacy and safety of 2,2-Dimethylbutyrate (HQK-1001), an oral fetal globin inducer, in sickle cell disease. *Am. J. Hematol.* **2014**, *89*, 709-713.

(110) Meiler, S. E.; Wade, M.; Kutlar, F.; Yerigenahally, S. D.; Xue, Y.; Parseval, L. A. M.; Corral, L. G.; Swerdlow, P. S.; Kutlar, A. Pomalidomide augments fetal hemoglobin production without the myelosuppressive effects of hydroxyurea in transgenic sickle cell mice. *Blood* **2011**, *118*, 1109-1112.

(111) Nagel, R. L.; Vichinsky, E.; Shah, M.; Johnson, R.; Spadacino, E.; Fabry, M. E.; Mangahas, L.; Abel, R.; Stamatoyannopoulos, G. F. Reticulocyte response in sickle cell anemia treated with recombinant human erythropoietin: A double-blind study. *Blood* **1993**, *81*, 9-14.

(112) Letvin, N. L.; Linch, D. C.; Beardsley, G. P.; McIntyre, K. W.; Miller, B. A.; Nathan, D. G. Influence of cell cycle phase-specific agents on Simian fetal hemoglobin synthesis. *J. Clin. Invest.* **1985**, *75*, 1999-2005.

(113) Chou, Y. C.; Chen, R. L.; Lai, Z.-S.; Song, J. S.; Chao, Y. S.; Shen, C. K. J. Pharmacological induction of human fetal globin gene in hydroxyurea-resistant primary adult erythroid cells. *Mol. Cell. Biol.* **2015**, *35*, 2541-2553.

(114) Hoban, M. D.; Orkin, S. H.; Bauer, D. E. Genetic treatment of a molecular disorder: Gene therapy approaches to sickle cell disease. *Blood* **2016**, *127*, 839-848.

(115) Walters, M. C.; Patience, M.; Leisenring, W.; Rogers, Z. R.; Aquino, V. M.; Buchanan, G. R.; Roberts, I. A.; Yeager, A. M.; Hsu, L.; Adamkiewicz, T.; et al. Stable mixed hematopoietic

chimerism after bone marrow transplantation for sickle cell anemia. *Biol. Blood Marrow Transplant* **2001**, *7*, 665-673.

(116) Locatelli, F.; Kabbara, N.; Ruggeri, A.; Ghavamzadeh, A.; Roberts, I.; Li, C. K.; Bernaudin, F.; Vermylen, C.; Dalle, J.-H.; Stein, J.; et al. Outcome of patients with hemoglobinopathies given either cord blood or bone marrow transplantation from an HLA-identical sibling. *Blood* **2013**, *122*, 1072-1078.

(117) Sunshine, H. R.; Hofrichter, J.; Eaton, W. A. Requirements for therapeutic inhibition of sickle haemoglobin gelation. *Nature* **1978**, *275*, 238-240.

(118) Asakura, T.; Ohnishi, S. T.; Adachi, K.; Ozguc, M.; Hashimoto, K.; Singer, M.; Russell, M. O.; Schwartz, E. Effect of Cetiedil on erythrocyte sickling: New type of antisickling agent that may affect erythrocyte membranes. *Proc. Natl. Acad. Sci. U. S. A.* **1980**, *77*, 2955-2959.

(119) Brugnara, C.; Gee, B.; Armsby, C. C.; Kurth, S.; Sakamoto, M.; Rifai, N.; Alper, S. L.; Platt, O. S. Therapy with oral Clotrimazole induces inhibition of the Gardos Channel and reduction of erythrocyte dehydration in patients with sickle cell disease. *J. Clin. Invest.* **1996**, *97*, 1227-1234.

(120) Abu-Salah, K. M.; Gambo, A. H. A. An analysis of the mechanism by which Cetiedil inhibits sickling. *Life Sci.* **2002**, *70*, 1003-1011.

(121) Johnston, M. N.; Ellory, J. C.; Stuart, J. Bepridil protects sickle cells against the adverse rheological effects of cyclical deoxygenation. *Br. J. Haematol.* **1989**, *73*, 522-526.

(122) Johnson, R. M.; Acquaye, C.; Féo, C.; Sarnaik, S. Bepridil as an antisickling agent: membrane internalization and cell rigidity. *Am. J. Hematol.* **1994**, *46*, 310-318.

(123) Steinberg, M. H. Management of sickle cell disease. *N. Engl. J. Med.* **1999**, *340*, 1021-1030.

(124) Ballas, S. K. Sickle cell anaemia: Progress in pathogenesis and treatment. *Drugs* **2002**, *62*, 1143-1172.

(125) Sherer, J. T.; Glover, P. H. Pentoxifylline for sickle-cell disease. *Ann. Pharmacother.* **2000**, *34*, 1070-1074.

(126) Keller, F.; Leonhardt, H. Amelioration of blood viscosity in sickle cell anemia by Pentoxifylline. A case report. *J. Med.* **1979**, *10*, 429-433.

(127) Clark, M. R.; Mohandas, N.; Shohet, S. B. Hydration of sickle cells using the sodium ionophore Monensin. A model for therapy. *J. Clin. Invest.* **1982**, *70*, 1074-1080.

(128) Asakura, T.; Shibutani, Y.; Reilly, M. P.; DeMeio, R. H. Antisickling effect of Tellurite: A potent membrane-acting agent in vitro. *Blood* **1984**, *64*, 305-307.

(129) Özpolat, T.; Chen, J.; Fu, X.; Cate, S. A.; Le, J.; Norby, C.; Konkle, B. A.; Lopez, J. A. Effects of N-acetylcysteine in patients with sickle cell disease. *Blood* **2014**, *124*, 4173-4173.

(130) Shartava, A.; Shah, A. K.; Goodman, S. R. N-Acetylcysteine and Clotrimazole inhibit sickle erythrocyte dehydration induced by 1-Chloro-2,4-Dinitrobenzene. *Am. J. Hematol.* **1999**, *62*, 19-24.

(131) Morris, C. R.; Kuypers, F. A.; Lavrisha, L.; Ansari, M.; Sweeters, N.; Stewart, M.; Gildengorin, G.; Neumayr, L.; Vichinsky, E. P. A randomized, placebo-controlled trial of arginine therapy for the treatment of children with sickle cell disease hospitalized with vaso-occlusive pain episodes. *Haematologica* **2013**, *98*, 1375-1382.

(132) Temiye, E. O.; Duke, E. S.; Owolabi, M. A.; Renner, J. K. Relationship between painful crisis and serum zinc level in children with sickle cell anaemia. *Anemia* **2011**, *2011*, 1-7.

(133) Brewer, G. J.; Oelshlegel, F. J. Antisickling effects of zinc. *Biochem. Biophys. Res. Commun.* **1974**, *58*, 854-861.

(134) Bunn, H. F. Evolution of mammalian hemoglobin function. *Blood* **1981**, *58*, 189-197.

(135) Rose, Z. B. A procedure for decreasing the level of 2,3-Bisphosphoglycerate in red cells in vitro. *Biochem. Biophys. Res. Commun.* **1976**, *73*, 1011-1017.

(136) Rose, Z. B.; Liebowitz, J. 2,3-Diphosphoglycerate phosphatase from human erythrocytes. General properties and activation by anions. *J. Biol. Chem.* **1970**, *245*, 3232-3241.

(137) Patskovska, L. N.; Patskovsky, Y. V.; Almo, S. C.; Hirsch, R. E. COHbC and COHbS crystallize in the R2 quaternary state at neutral pH in the presence of PEG 4000. *Acta Crystallogr. D Biol. Crystallogr.* **2005**, *61*, 566-573.

(138) Safo, M. K.; Boyiri, T.; Burnett, J. C.; Danso-Danquah, R.; Moure, C. M.; Joshi, G. S.; Abraham, D. J. X-ray crystallographic analyses of symmetrical allosteric effectors of hemoglobin: Compounds designed to link primary and secondary binding sites. *Acta Crystallogr. D Biol. Crystallogr.* **2002**, *58*, 634-644.

(139) Benesch, R. E.; Kwong, S.; Benesch, R.; Edalji, R. Location and bond type of intermolecular contacts in the polymerisation of haemoglobin S. *Nature* **1977**, *269*, 772-775.

(140) Pariser, S.; Katz, A. Treatment of sickle cell trait hematuria with oral urea. *J. Urol.* **1994**, *151*, 401-403.

(141) Elbaum, D.; Roth, E. J.; Neumann, G.; Jaffe, E. R.; Bookchin, R. M.; Nagel, R. L. Molecular and cellular effects of antisickling concentrations of alkylureas. *Blood* **1976**, *48*, 273-282.

(142) Schoenborn, B. P. Dichloromethane as an antisickling agent in sickle cell hemoglobin. *Proc. Natl. Acad. Sci. U. S. A.* **1976**, *73*, 4195-4199.

(143) Castro, O.; Reindorf, C. A.; Socha, W. W.; Rowe, A. W. Perfluorocarbon enhancement of heterologous red cell survival: A reticuloendothelial block effect? *Int. Arch. Allergy Appl. Immunol.* **1983**, *70*, 88-91.

(144) Poillon, W. N. Noncovalent inhibitors of sickle hemoglobin gelation: Effects of aryl-substituted alanines. *Biochemistry (Mosc.)* **1982**, *21*, 1400-1406.

(145) Noguchi, C. T.; Schechter, A. N. Inhibition of sickle hemoglobin gelation by amino acids and related compounds. *Biochemistry (Mosc.)* **1978**, *17*, 5455-5459.

(146) Poillon, W. N. Noncovalent inhibitors of sickle hemoglobin gelation: Effects of aliphatic alcohols, amides, and ureas. *Biochemistry (Mosc.)* **1980**, *19*, 3194-3199.

(147) Klotz, I. M.; Haney, D. N.; King, L. C. Rational approaches to chemotherapy: Antisickling agents. *Sci. Wash.* **1981**, *213*, 724-731.

(148) Kumpati, J. Liposome-loaded phenylalanine or tryptophan as sickling inhibitor: A possible therapy for sickle cell disease. *Biochem. Med. Metab. Biol.* **1987**, *38*, 170-181.

(149) Abraham, D. J.; Gazze, D. M.; Kennedy, P. E.; Mokotoff, M. Design, synthesis, and testing of potential antisickling agents. 5. Disubstituted benzoic acids designed for the donor site and proline salicylates designed for the acceptor site. *J. Med. Chem.* **1984**, *27*, 1549-1559.

(150) Patwa, D. C.; Abraham, D. J.; Hung, T. C. Design, synthesis, and testing of potential antisickling agents. 6. Rheologic studies with active phenoxy and benzyloxy acids. *Blood Cells* **1987**, *12*, 589-601.

(151) Fall, A. B. K.; Toppet, M.; Ferster, A.; Fondu, P.; Vanhaelen-Fastré, R.; Vanhaelen, M. In vitro antisickling activity of Cromolyn sodium. *Br. J. Haematol.* **1998**, *103*, 957-959.

(152) Toppet, M.; Fall, A. B.; Ferster, A.; Fondu, P.; Mélot, C.; Vanhaelen-Fastré, R.; Vanhaelen, M. Antisickling activity of sodium cromoglicate in sickle-cell disease. *The Lancet* **2000**, *356*, 309.

(153) Eaton, W. A.; Bunn, H. F. Treating sickle cell disease by targeting HbS polymerization. *Blood* **2017**, *129*, 2719-2726.

(154) Kato, G. J. New insights into sickle cell disease: Mechanisms and investigational therapies. *Curr. Opin. Hematol.* **2016**, *23*, 224-232.

(155) Peterson, C. M. Sodium cyanate induced polyneuropathy in patients with sickle-cell disease. *Ann. Intern. Med.* **1974**, *81*, 152.

(156) Duffel, M. W.; Logan, D. J.; Ziegler, D. M. Cysteamine and Cystamine. In *Methods in Enzymology*; Sulfur and Sulfur Amino Acids; Academic Press, 1987; Vol. 143, pp 149–154.

(157) Hassan, W.; Beuzard, Y.; Rosa, J. Inhibition of erythrocyte sickling by cystamine, a thiol reagent. *Proc. Natl. Acad. Sci. U. S. A.* **1976**, *73*, 3288-3292.

(158) Roth, E. F.; Nagel, R. L.; Bookchin, R. M.; Grayzel, A. I. Nitrogen Mustard: An "in vitro" inhibitor of erythrocyte sickling. *Biochem. Biophys. Res. Commun.* **1972**, *48*, 612-618.

(159) Xu, A. S. L.; Labotka, R. J.; London, R. E. Acetylation of human hemoglobin by methyl acetylphosphate. Evidence of broad region-selectivity revealed by NMR studies. *J. Biol. Chem.* **1999**, *274*, 26629-26632.

(160) Furia, F. G. de; Cerami, A.; Bunn, H. F.; Lu, Y. S.; Peterson, C. M. The effect of Aspirin on sickling and oxygen affinity of erythrocytes. *Proc. Natl. Acad. Sci.* **1973**, *70*, 3707-3710.

(161) Klotz, I. M.; Tam, J. W. O. Acetylation of sickle cell hemoglobin by Aspirin. *Proc. Natl. Acad. Sci. U. S. A.* **1973**, *70*, 1313-1315.

(162) Omar, A. M.; Mahran, M. A.; Ghatge, M. S.; Chowdhury, N.; Bamane, F. H. A.; El-Araby, M. E.; Abdulmalik, O.; Safo, M. K. Identification of a novel class of covalent modifiers of hemoglobin as potential antisickling agents. *Org. Biomol. Chem.* **2015**, *13*, 6353-6370.

(163) Walder, J. A.; Walder, R. Y.; Arnone, A. Development of antisickling compounds that chemically modify hemoglobin S specifically within the 2,3-Diphosphoglycerate binding site. *J. Mol. Biol.* **1980**, *141*, 195-216.

(164) Walder, J. A.; Zaugg, R. H.; Walder, R. Y.; Steele, J. M.; Klotz, I. M. Diaspirins that crosslink beta chains of hemoglobin: Bis(3,5-Dibromosalicyl) succinate and Bis(3,5-Dibromosalicyl) fumarate. *Biochemistry (Mosc.)* **1979**, *18*, 4265-4270.

(165) Mentzer, W. C. Inhibitors of sickling. *Am. J. Pediatr. Hematol. Oncol.* **1982**, *4*, 320-327.

(166) Beddell, C. R.; Goodford, P. J.; Kneen, G.; White, R. D.; Wilkinson, S.; Wootton, R. Substituted benzaldehydes designed to increase the oxygen affinity of human haemoglobin and inhibit the sickling of sickle erythrocytes. *Br. J. Pharmacol.* **1984**, *82*, 397-407.

(167) Merrett, M.; Stammers, D. K.; White, R. D.; Wootton, R.; Kneen, G. Characterization of the binding of the anti-sickling compound, BW12C, to haemoglobin. *Biochem. J.* **1986**, *239*, 387-392.

(168) Arya, R.; Rolan, P. E.; Wootton, R.; Posner, J.; Bellingham, A. J. Tucaresol increases oxygen affinity and reduces haemolysis in subjects with sickle cell anaemia. *Br. J. Haematol.* **1996**, *93*, 817-821.

(169) Zaugg, R. H.; Walder, J. A.; Klotz, I. M. Schiff base adducts of hemoglobin. Modifications that inhibit erythrocyte sickling. *J. Biol. Chem.* **1977**, *252*, 8542-8548.

(170) Abraham, D. J.; Mehanna, A. S.; Wireko, F. C.; Whitney, J.; Thomas, R. P.; Orringer, E. P. Vanillin, a potential agent for the treatment of sickle cell anemia. *Blood* **1991**, *77*, 1334-1341.

(171) Safo, M. K.; Abdulmalik, O.; Danso-Danquah, R.; Burnett, J. C.; Nokuri, S.; Joshi, G. S.; Musayev, F. N.; Asakura, T.; Abraham, D. J. Structural basis for the potent antisickling effect of a novel class of five-membered heterocyclic aldehydic compounds. *J. Med. Chem.* **2004**, *47*, 4665-4676.

(172) Zhang, C.; Li. X.; Lian, L.; Chen, Q.; Abdulmalik, O.; Vassilev, V.; Lai, C. S.; Asakura, T. Anti-sickling effect of MX-1520, a prodrug of vanillin: An in vivo study using rodents. *Br. J. Hematol.* **2004**, *125*, 788-795.

 (173) Xu, G. G.; Pagare, P. P.; Ghatge, M. S.; Safo, R. P.; Gazi, A.; Chen, Q.; David, T.; Alabbas, A. B.; Musayev, F. N.; Venitz, J.; et al. Design, synthesis, and biological evaluation of ester and ether derivatives of antisickling agent 5-HMF for the treatment of sickle cell disease. *Mol. Pharm.* **2017**, *14*, 3499-3511.

(174) Abdulmalik, O.; Safo, M. K.; Chen, Q.; Yang, J.; Brugnara, C.; Ohene-Frempong, K.; Abraham, D. J.; Asakura, T. 5-Hydroxymethyl-2-Furfural modifies intracellular sickle haemoglobin and inhibits sickling of red blood cells. *Br. J. Haematol.* **2005**, *128*, 552-561.

(175) Abdulmalik, O.; Deshpande, T.; Ghatge, M.; Zhang, Y.; Venitz, J.; Parikh, A.; Safo, M. K. Novel structurally-modified allosteric effectors of hemoglobin exhibit superior antisickling properties. *Blood* **2014**, *124*, 218-218.

(176) Oder, E.; Safo, M. K.; Abdulmalik, O.; Kato, G. J. New developments in anti-sickling agents: Can drugs directly prevent the polymerization of sickle haemoglobin in vivo? *Br. J. Haematol.* **2016**, *175*, 24-30.

(177) Holmquist, W. R.; Schroeder, W. A. A new N-terminal blocking group involving a Schiff base in hemoglobin AIc*. *Biochemistry (Mosc.)* **1966**, *5*, 2489-2503.

(178) Bookchin, B.; Bookchin, R. M. Structure of hemoglobin AIc: Nature of the N-terminal beta chain blocking group. *Biochem. Biophys. Res. Commun.* **1968**, *32*, 86-93.

(179) Wireko, F. C.; Abraham, D. J. X-ray diffraction study of the binding of the antisickling agent 12C79 to human hemoglobin. *Proc. Natl. Acad. Sci. U. S. A.* **1991**, *88*, 2209-2211.

(180) Keidan, A. J.; Franklin, I. M.; White, R. D.; Joy, M.; Huehns, E. R.; Stuart, J. Effect of BW12C on oxygen affinity of haemoglobin in sickle-cell disease. *Lancet Lond. Engl.* **1986**, *1*, 831-834.

(181) Fitzharris, P.; McLean, A. E.; Sparks, R. G.; Weatherley, B. C.; White, R. D.; Wootton, R. The effects in volunteers of BW12C, a compound designed to left-shift the blood-oxygen saturation curve. *Br. J. Clin. Pharmacol.* **1985**, *19*, 471-481.

(182) Rolan, P. E.; Mercer, A. J.; Wootton, R.; Posner, J. Pharmacokinetics and pharmacodynamics of Tucaresol, an antisickling agent, in healthy volunteers. *Br. J. Clin. Pharmacol.* **1995**, *39*, 375-380.

(183) Stern, W.; Mathews, D.; McKew, J.; Shen, X.; Kato, G. J. A Phase 1, first-in-man, dose-response study of Aes-103 (5-HMF), an anti-sickling, allosteric modifier of hemoglobin oxygen affinity in healthy normal volunteers. *Blood* **2012**, *120*, 3210-3210.

(184) Godfrey, V. B.; Chen, L. J.; Griffin, R. J.; Lebetkin, E. H.; Burka, L. T. Distribution and metabolism of (5-hydroxymethyl) furfural in male F344 rats and B6C3F1 mice after oral administration. *J. Toxicol. Environ. Health A* **1999**, *57*, 199-210.

(185) Parikh, A. Poster Session II (PII-001–120). *Clin. Pharmacol. Ther.* **2014**, *95*, S83–S84.

(186) Parikh, A. In vitro PK/PD profiling and modeling of the antisickling agents, 5-hydroxylmethyl furfural (5-HMF) and novel synthetic allosteric effectors of hemoglobin (AEH) in human whole blood. *Theses Diss.* **2013**.

(187) Nnamani, I. N.; Joshi, G. S.; Danso-Danquah, R.; Abdulmalik, O.; Asakura, T.; Abraham, D. J.; Safo, M. K. Pyridyl derivatives of benzaldehyde as potential antisickling agents. *Chem. Biodivers.* **2008**, *5*, 1762-1769.

(188) Abdulmalik, O.; Ghatge, M. S.; Musayev, F. N.; Parikh, A.; Chen, Q.; Yang, J.; Nnamani, I.; Danso-Danquah, R.; Eseonu, D. N.; Asakura, T.; et al. Crystallographic analysis of human

hemoglobin elucidates the structural basis of the potent and dual antisickling activity of pyridyl derivatives of vanillin. *Acta Crystallogr. D Biol. Crystallogr.* **2011**, *67*, 920-928.

(189) Ferrone, F. A. GBT440 increases haemoglobin oxygen affinity, reduces sickling and prolongs RBC half-life in a murine model of sickle cell disease. *Br. J. Haematol.* **2016**, *174*, 499-500.

(190) Hutchaleelaha, A.; Patel, M.; Silva, A.; Oksenberg, D.; Metcalf, B. GBT440 demonstrates high specificity for red blood cells in nonclinical species. *Blood* **2015**, *126*, 2172-2172.

(191) Metcalf, B.; Chuang, C.; Dufu, K.; Patel, M. P.; Silva-Garcia, A.; Johnson, C.; Lu, Q.; Partridge, J. R.; Patskovska, L.; Patskovsky, Y.; et al. Discovery of GBT440, an orally bioavailable R-state stabilizer of sickle cell hemoglobin. *ACS Med. Chem. Lett.* **2017**, *8*, 321-326.

(192) Oksenberg, D.; Dufu, K.; Patel, M. P.; Chuang, C.; Li, Z.; Xu, Q.; Silva-Garcia, A.; Zhou, C.; Hutchaleelaha, A.; Patskovska, L.; et al. GBT440 increases haemoglobin oxygen affinity, reduces sickling and prolongs RBC half-life in a murine model of sickle cell disease. *Br. J. Haematol.* **2016**, *175*, 141-153.

(193) Study to evaluate the effect of GBT440 administered orally to patients with sickle cell disease (GBT_HOPE) ClinicalTrials.gov https://clinicaltrials.gov/ct2/show/NCT03036813 (accessed Mar 21, 2018).

(194) Kutney, J. P.; Cretney, W.; Tabata, T.; Frank, M. The reaction of N-bromosuccinimide with some alkyl pyridines. *Can. J. Chem.* **1964**, *42*, 698-702.

(195) Deuticke, B. Properties and structural basis of simple diffusion pathways in the erythrocyte membrane. *Rev. Physiol. Biochem. Pharmacol.* **1977**, *78*, 1-97.

(196) Sha'afi, R. I.; Gary-Bobo, C. M.; Solomon, A. K. Permeability of red cell membranes to small hydrophilic and lipophilic solutes. *J. Gen. Physiol.* **1971**, *58*, 238-258.

(197) Echols, N.; Grosse-Kunstleve, R. W.; Afonine, P. V.; Bunkóczi, G.; Chen, V. B.; Headd, J. J.; McCoy, A. J.; Moriarty, N. W.; Read, R. J.; Richardson, D. C.; et al. Graphical tools for macromolecular crystallography in PHENIX. *J. Appl. Crystallogr.* **2012**, *45*, 581-586.

(198) Emsley, P.; Lohkamp, B.; Scott, W. G.; Cowtan, K. Features and development of Coot. *Acta Crystallogr. D Biol. Crystallogr.* **2010**, *66*, 486-501.

(199) Brünger, A. T.; Adams, P. D.; Clore, G. M.; DeLano, W. L.; Gros, P.; Grosse-Kunstleve, R. W.; Jiang, J. S.; Kuszewski, J.; Nilges, M.; Pannu, N. S.; et al. Crystallography & NMR system:

A new software suite for macromolecular structure determination. *Acta Crystallogr. D Biol. Crystallogr.* **1998**, *54*, 905-921.

(200) Pagare, P. P.; Ghatge, M. S.; Musayev, F. N.; Deshpande, T. M.; Chen, Q.; Braxton, C.; Kim, S.; Venitz, J.; Zhang, Y.; Abdulmalik, O.; Safo, M. K. Rational design of pyridyl derivatives of vanillin for the treatment of sickle cell disease. *Bioorg. Med. Chem.* [Online] **2018** https://www.sciencedirect.com/science/article/pii/S0968089618303699 (accessed April 10, 2018).

(201) Rogers, Z. R. Hydroxyurea therapy for diverse pediatric populations with sickle cell disease. *Semin. Hematol.* **1997**, *34*, 42-47.

(202) Andrade, C. T.; Barros, L. a. M.; Lima, M. C. P.; Azero, E. G. Purification and characterization of human hemoglobin: Effect of the hemolysis conditions. *Int. J. Biol. Macromol.* **2004**, *34*, 233-240.

(203) Davies, R.; Hedebrant, U.; Athanassiadis, I.; Rydberg, P.; Törnqvist, M. Improved method to measure aldehyde adducts to N-terminal valine in hemoglobin using 5-hydroxymethylfurfural and 2,5-furandialdehyde as model compounds. *Food Chem. Toxicol. Int. J. Publ. Br. Ind. Biol. Res. Assoc.* **2009**, *47*, 1950-1957.

(204) Winn, M. D.; Ballard, C. C.; Cowtan, K. D.; Dodson, E. J.; Emsley, P.; Evans, P. R.; Keegan, R. M.; Krissinel, E. B.; Leslie, A. G. W.; McCoy, A.; et al. Overview of the CCP4 Suite and current developments. *Acta Crystallogr. D Biol. Crystallogr.* **2011**, *67*, 235-242.

(205) Adams, P. D.; Afonine, P. V.; Bunkóczi, G.; Chen, V. B.; Echols, N.; Headd, J. J.; Hung, L.-W.; Jain, S.; Kapral, G. J.; Grosse Kunstleve, R. W.; et al. The Phenix software for automated determination of macromolecular structures. *Methods San Diego Calif* **2011**, *55*, 94-106.

APPENDIX

Spectra

Methyl 6-((2-formyl-4-methoxyphenoxy)methyl)nicotinate (**PP1**)

¹HNMR

¹³CNMR

HRMS

IR
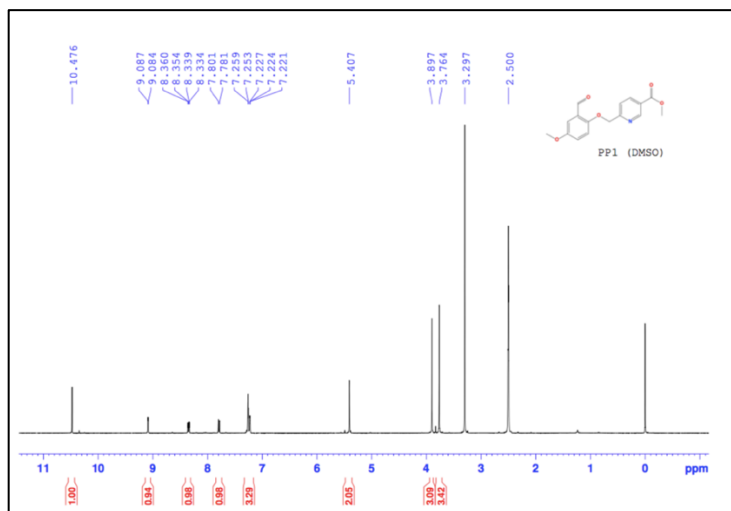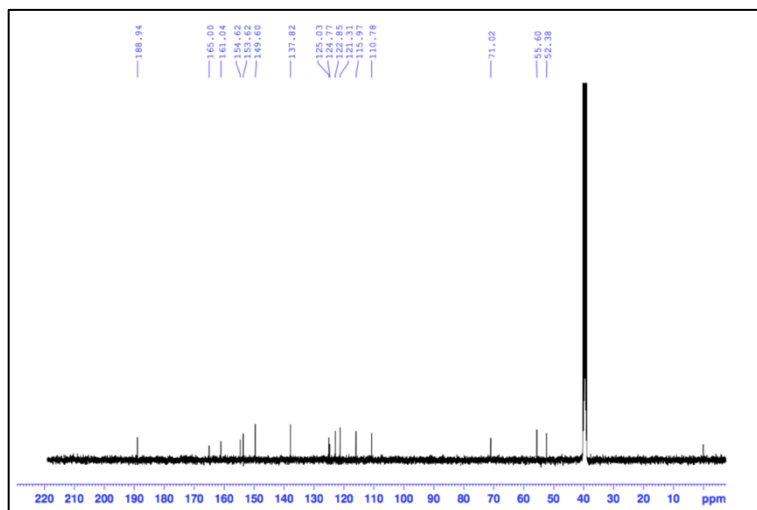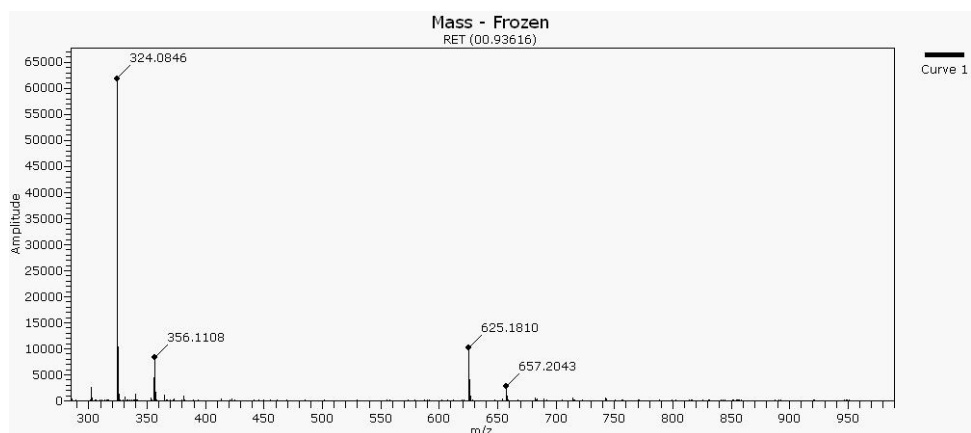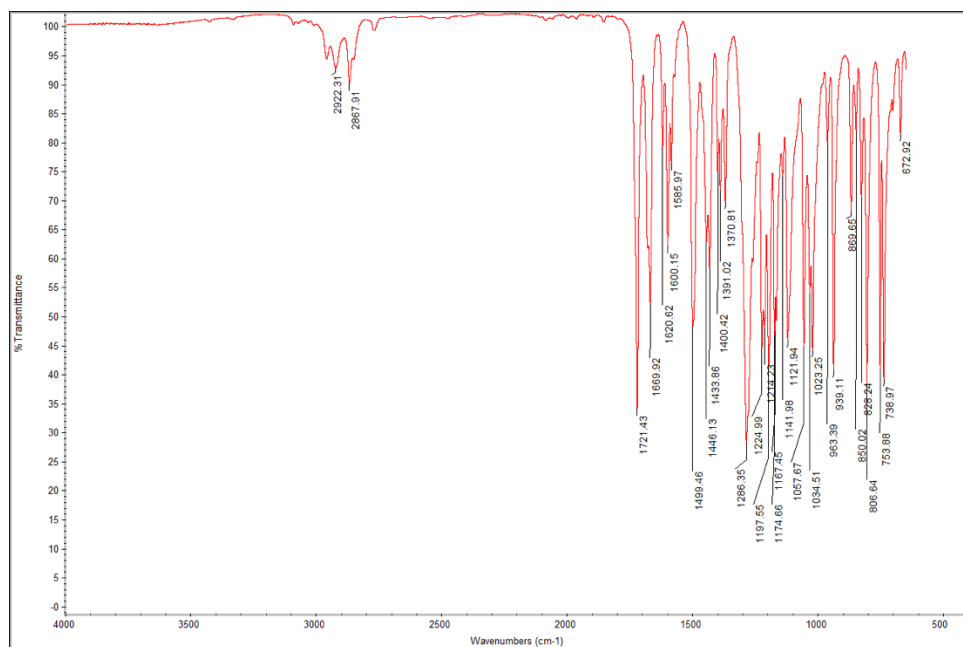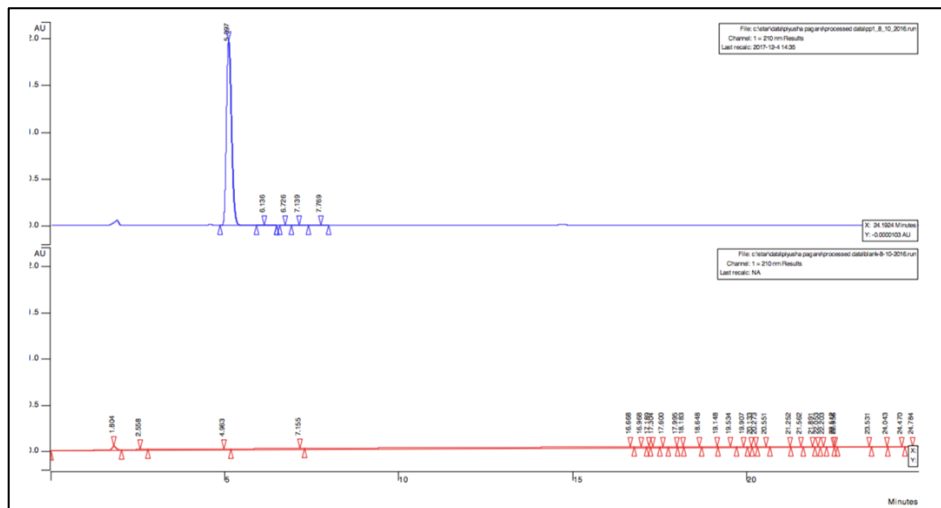
HPLC

Methyl 2-((2-formyl-4-methoxyphenoxy)methyl)nicotinate (**PP2)**

^{1}HNMR

¹³CNMR

HRMS

IR
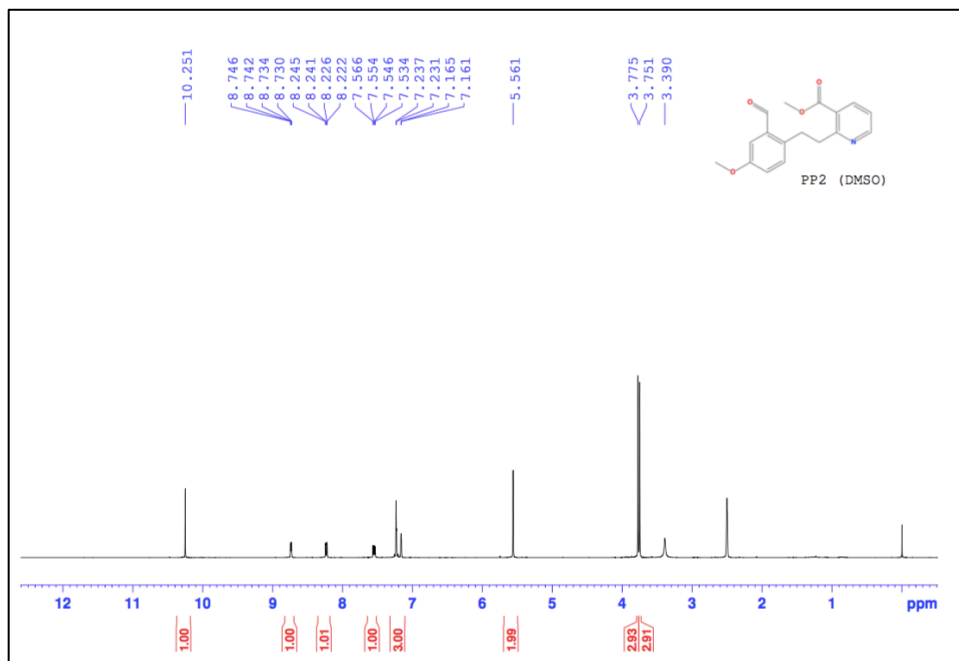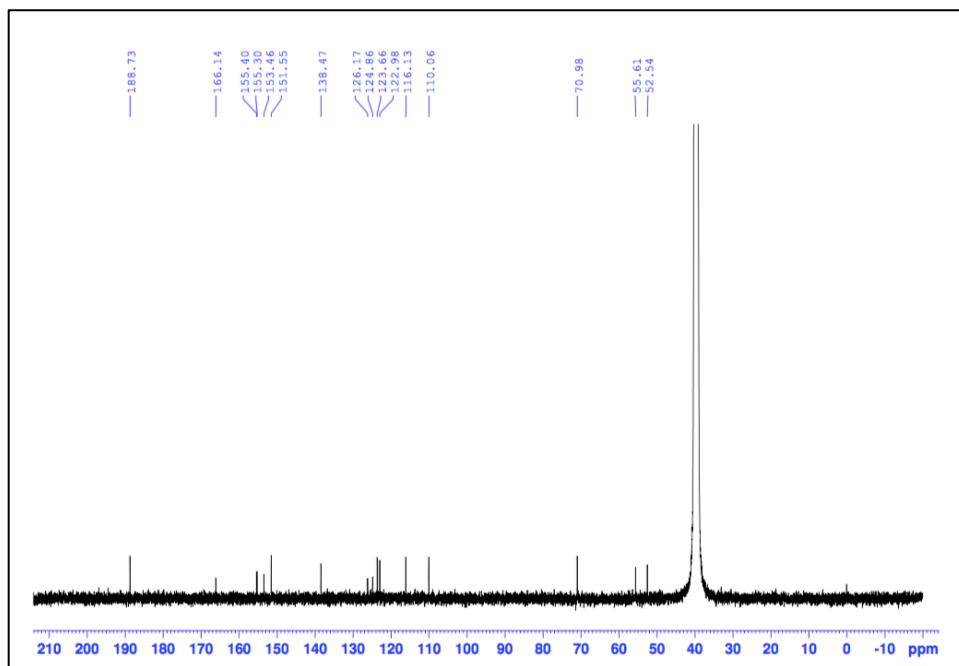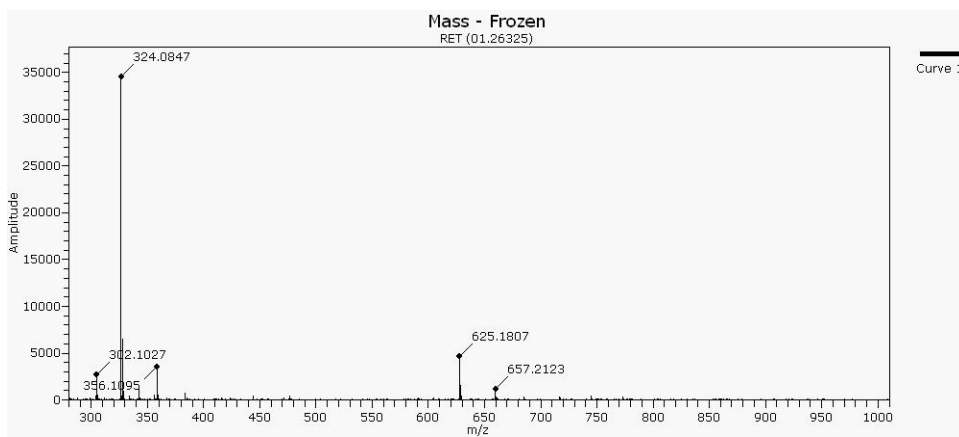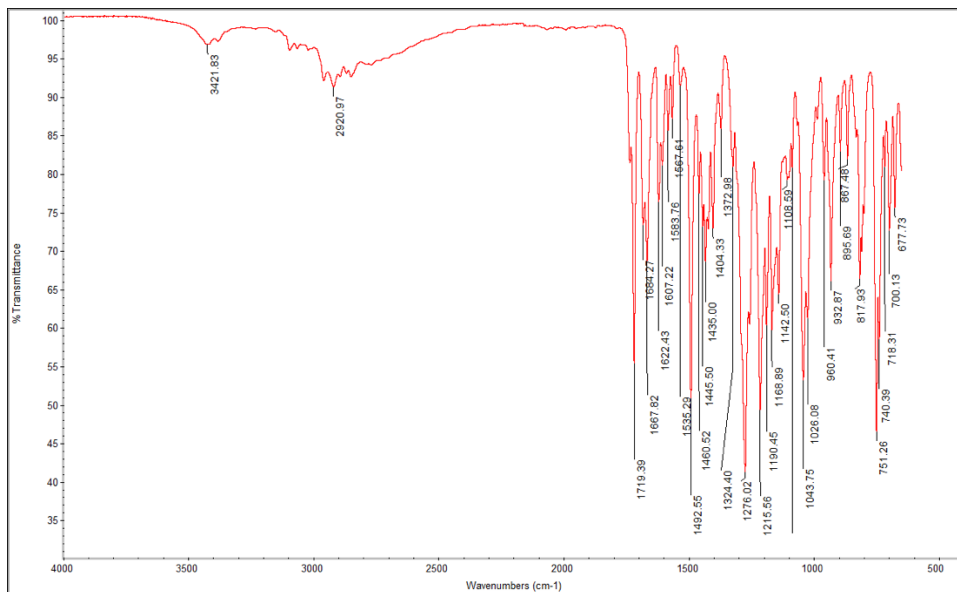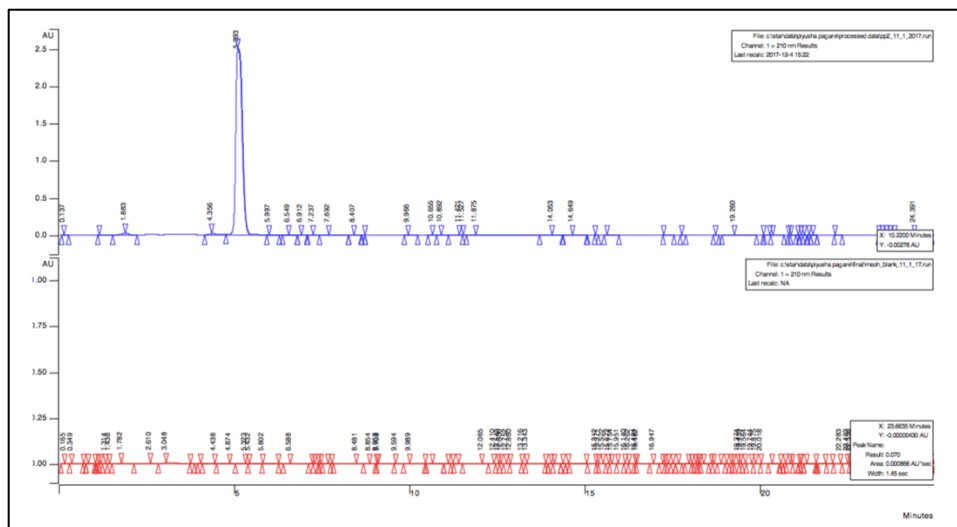
HPLC

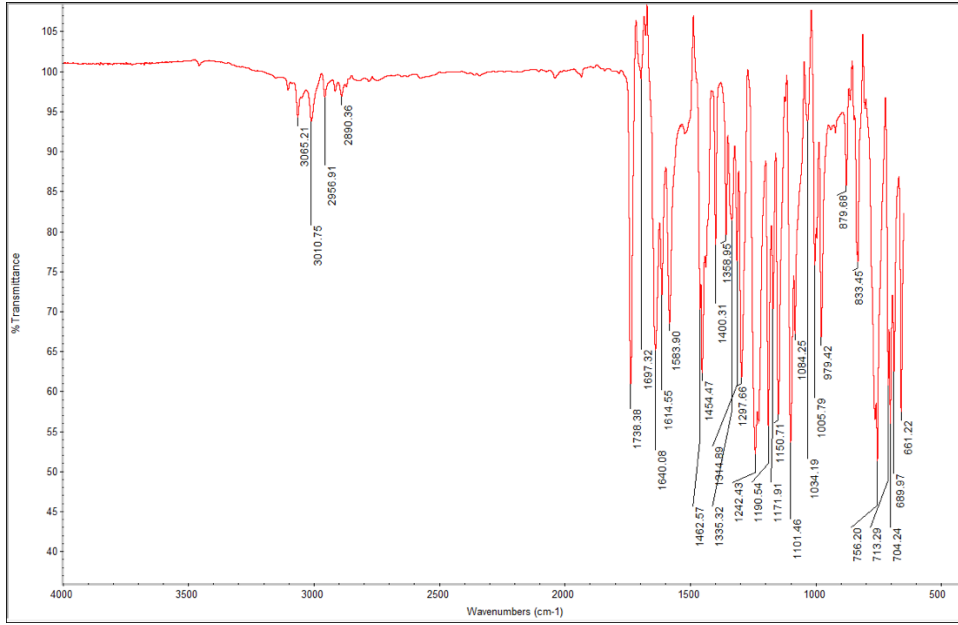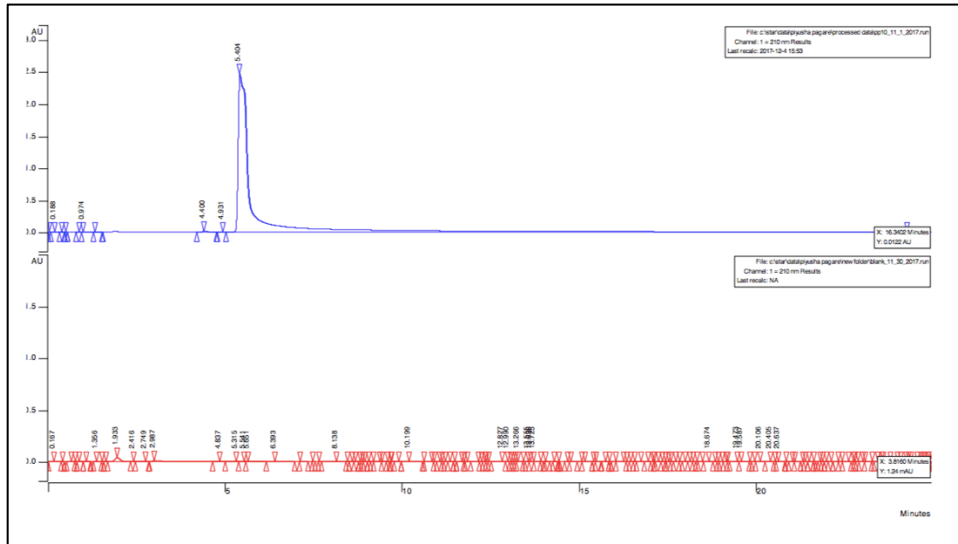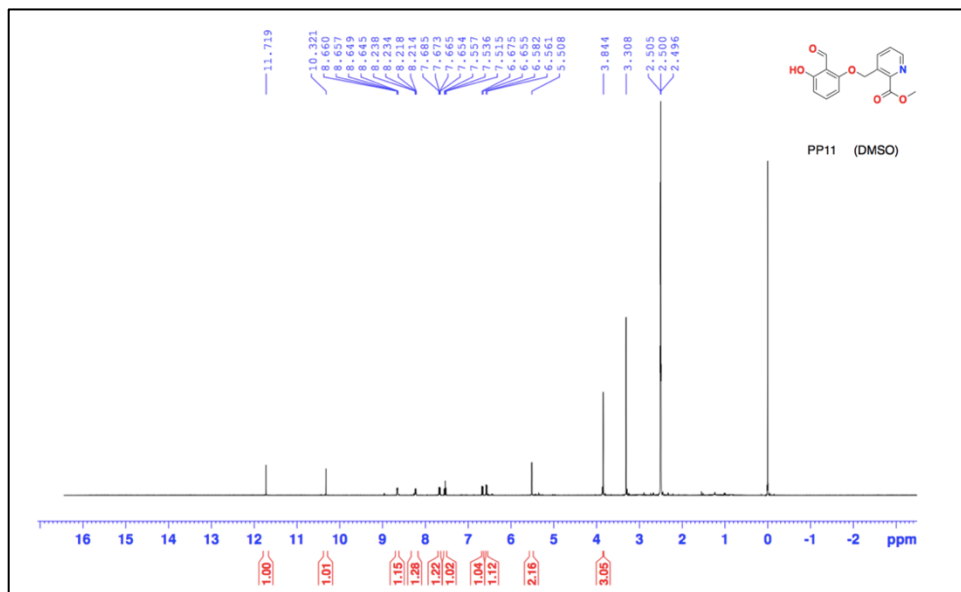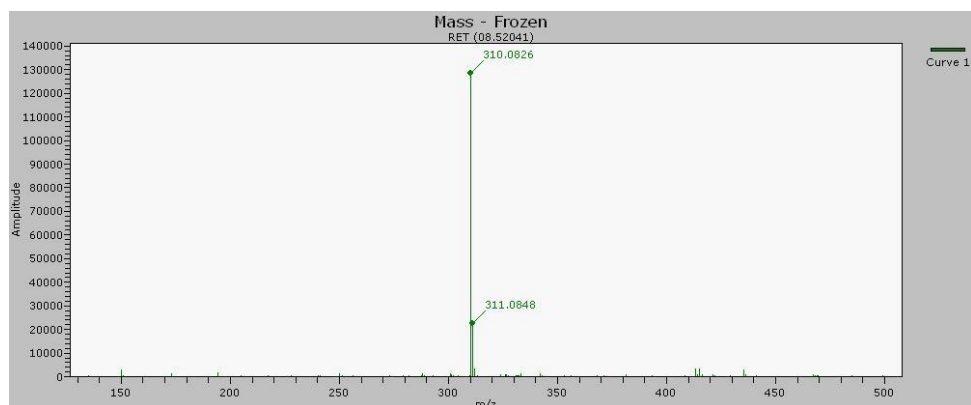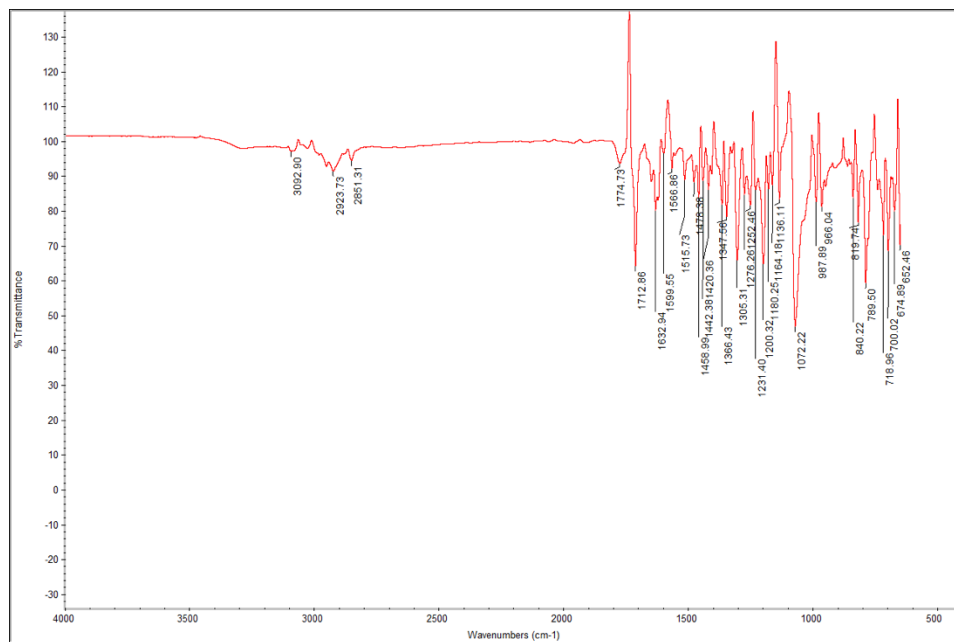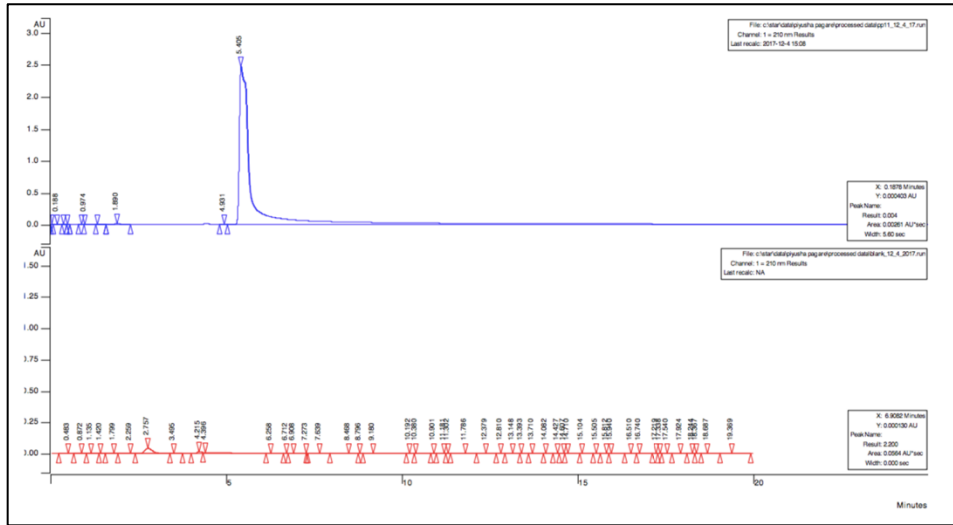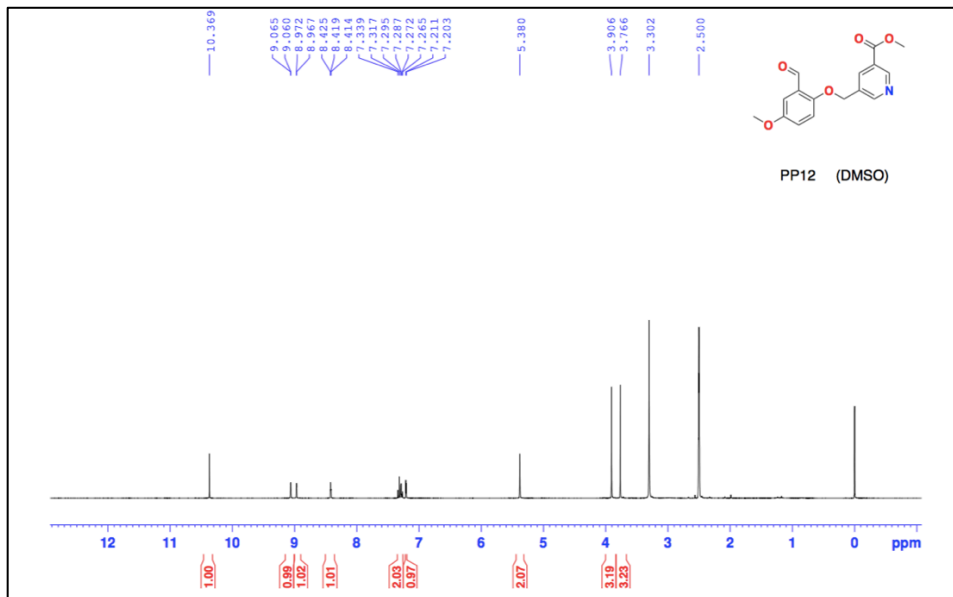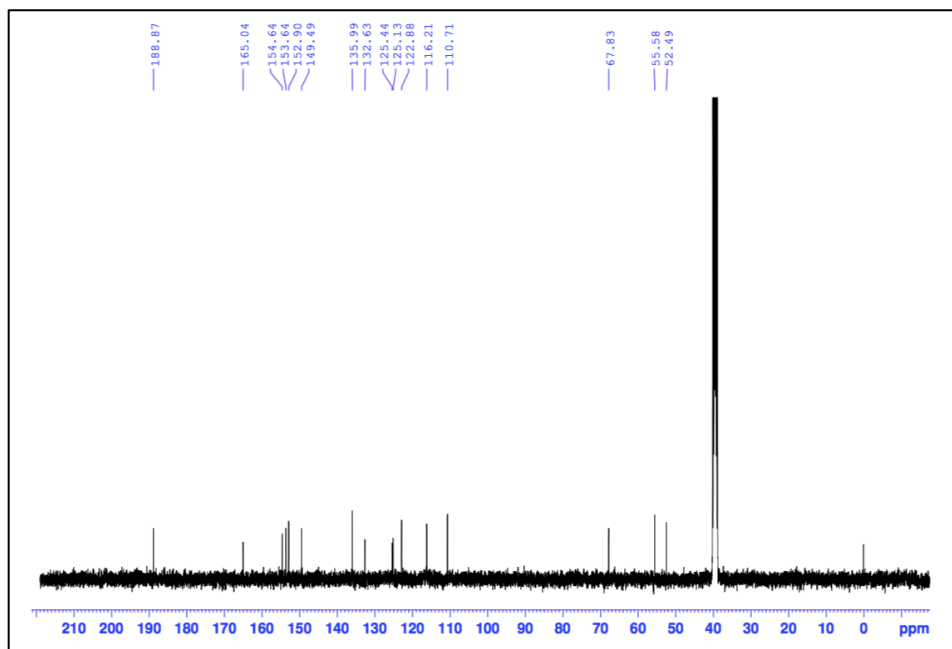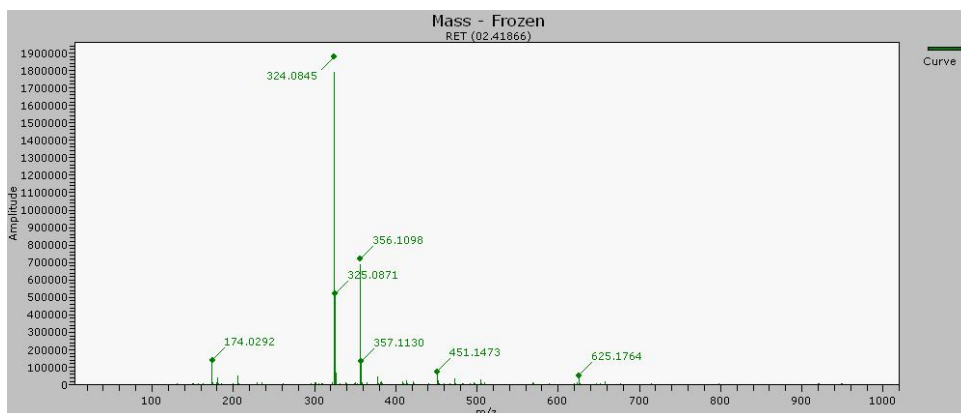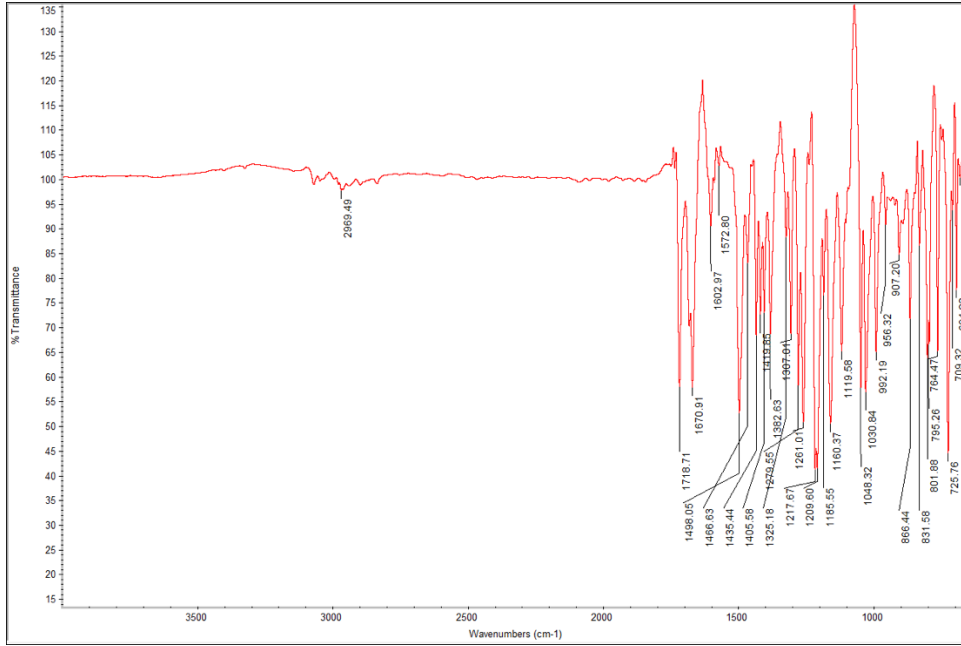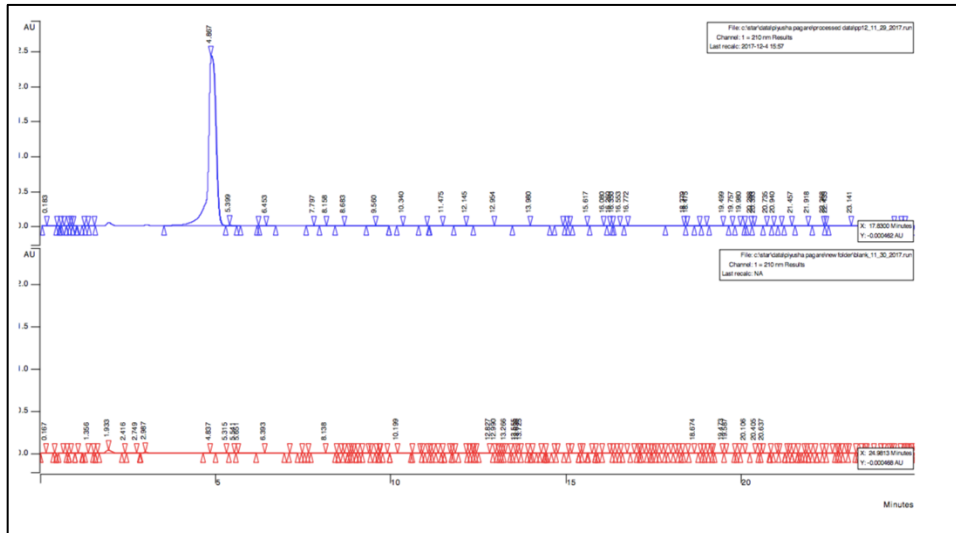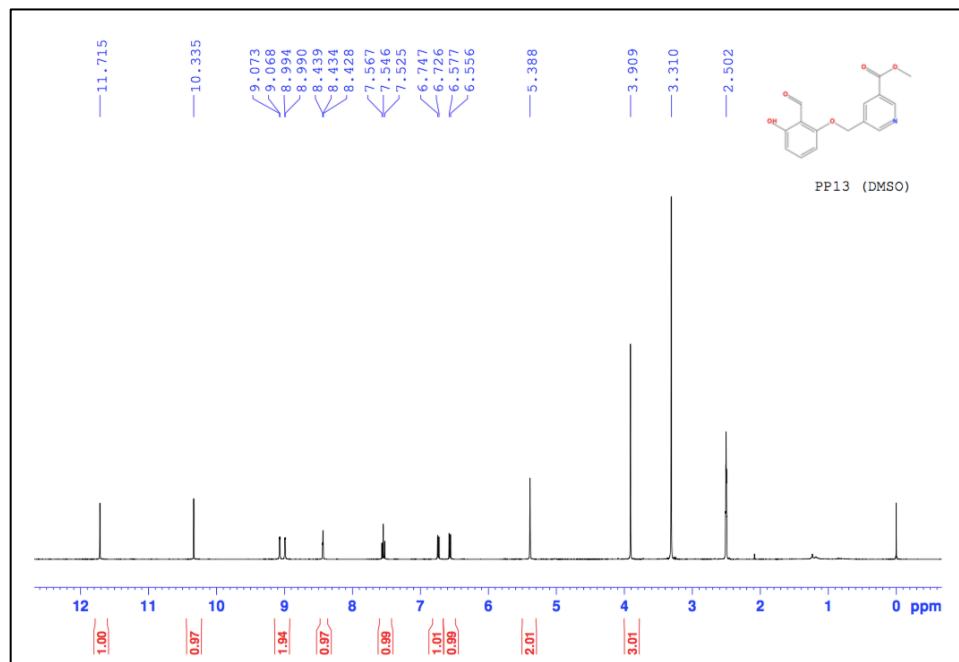# Methyl 6-((2-formyl-4-methoxyphenoxy)methyl)picolinate (**PP3**)

^{1}HNMR

PP3 (DMSO)

^{13}CNMR

HRMS

IR
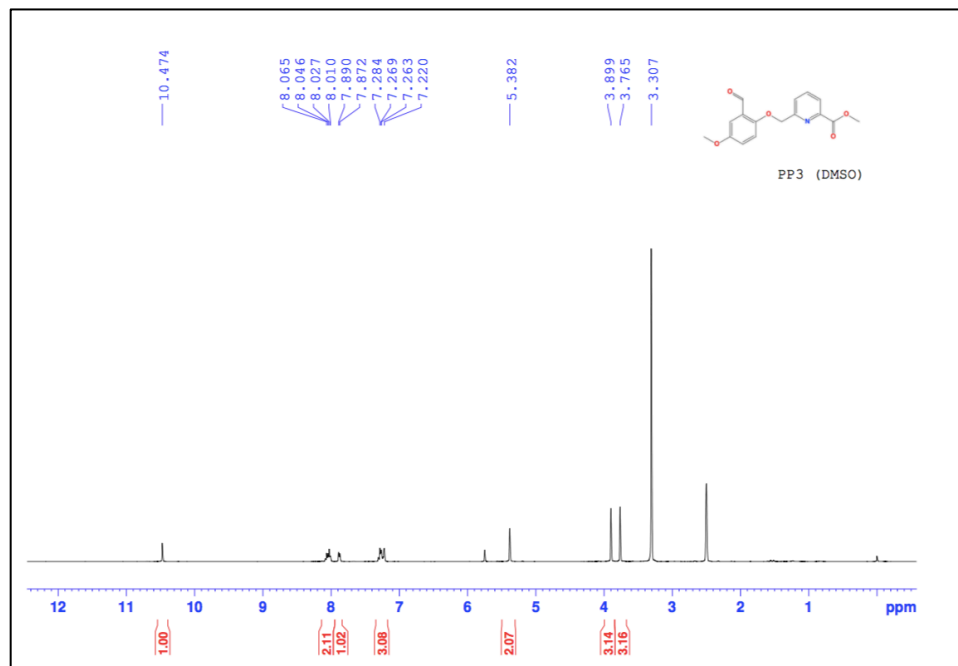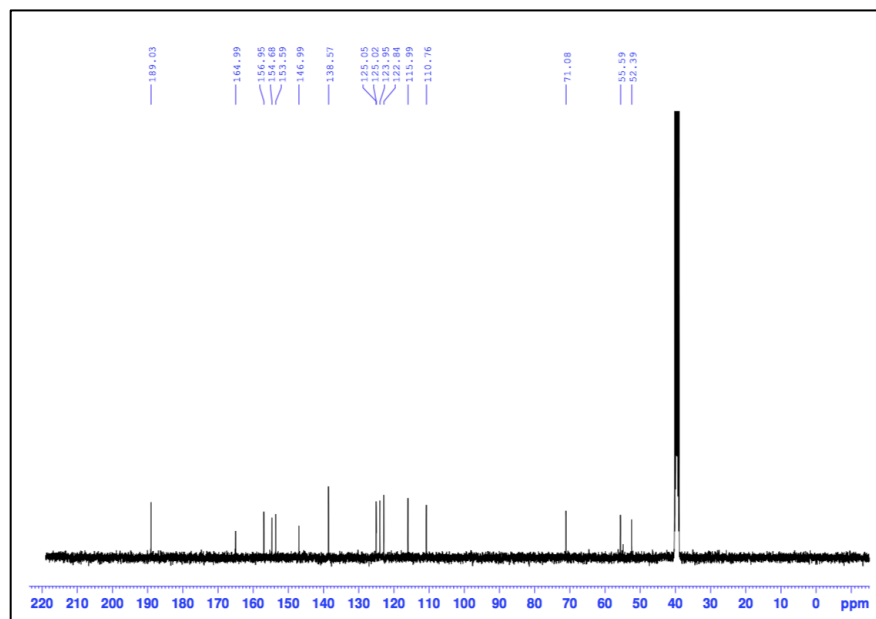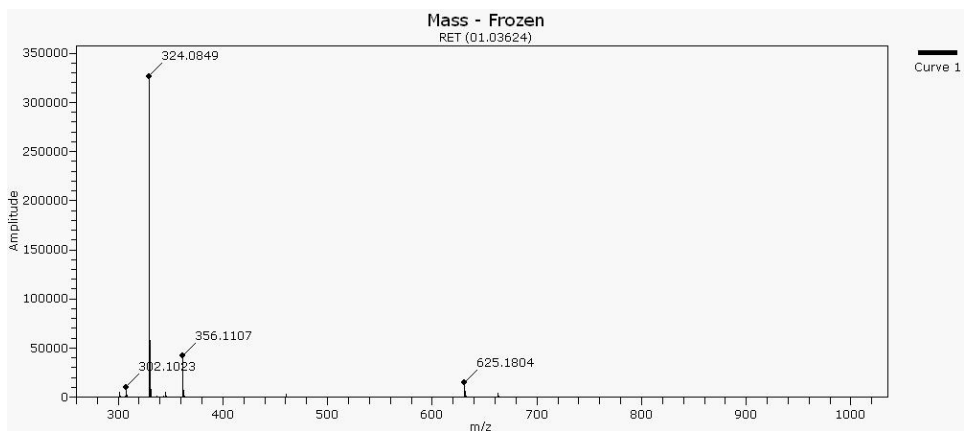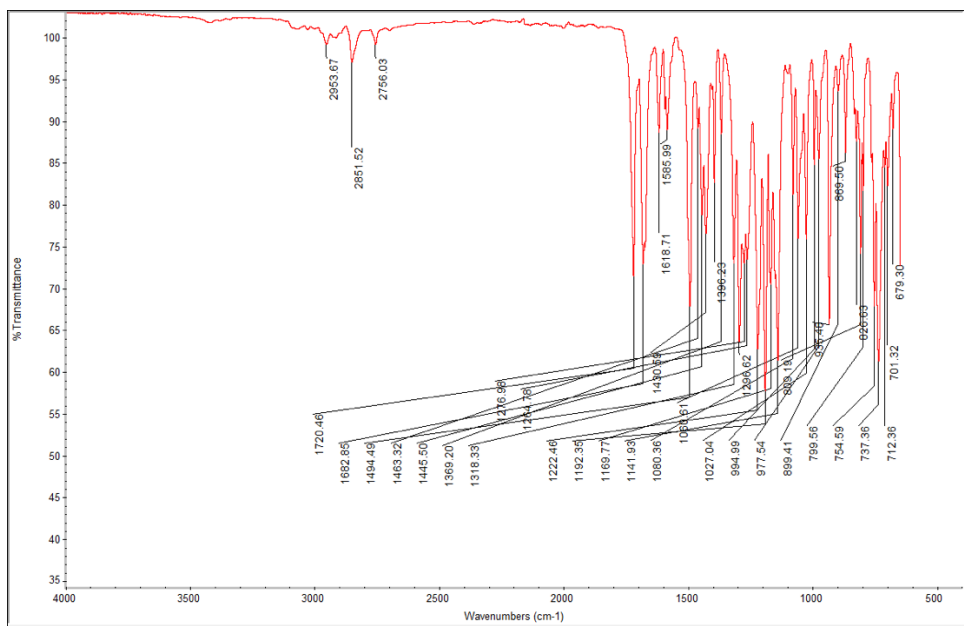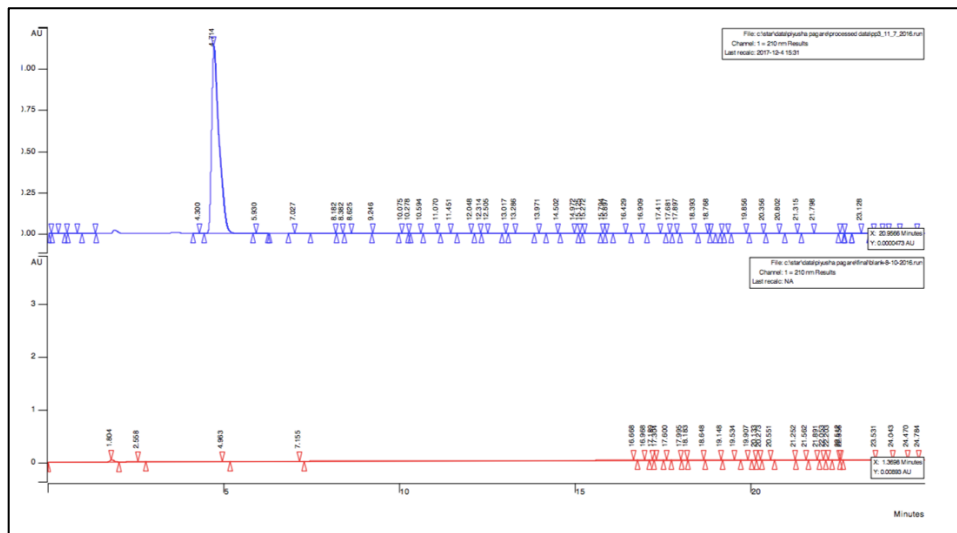
HPLC

Methyl 2-((2-formyl-4-methoxyphenoxy)methyl)isonicotinate (**PP4**)

^{1}HNMR

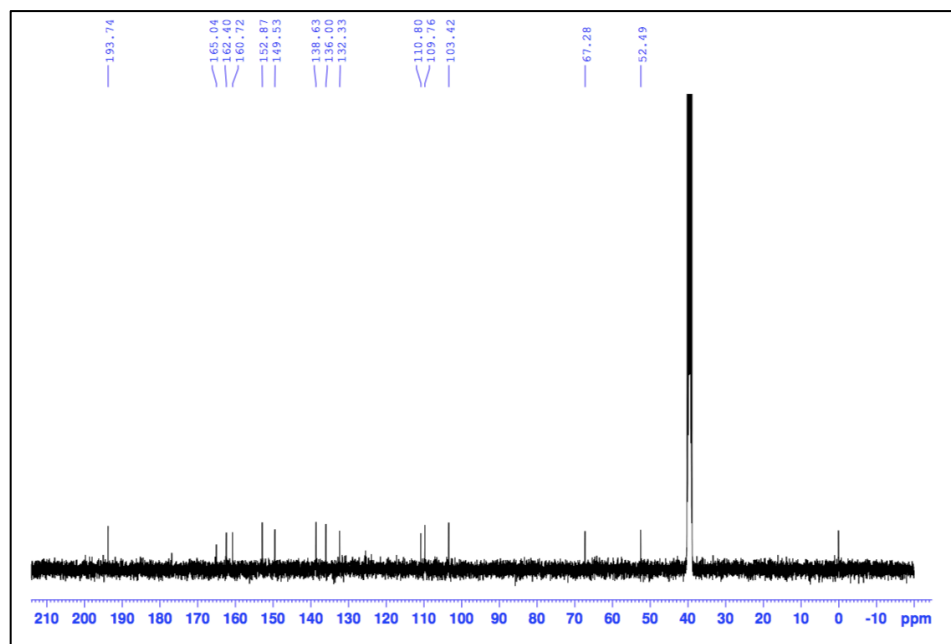¹³CNMR

HRMS

IR
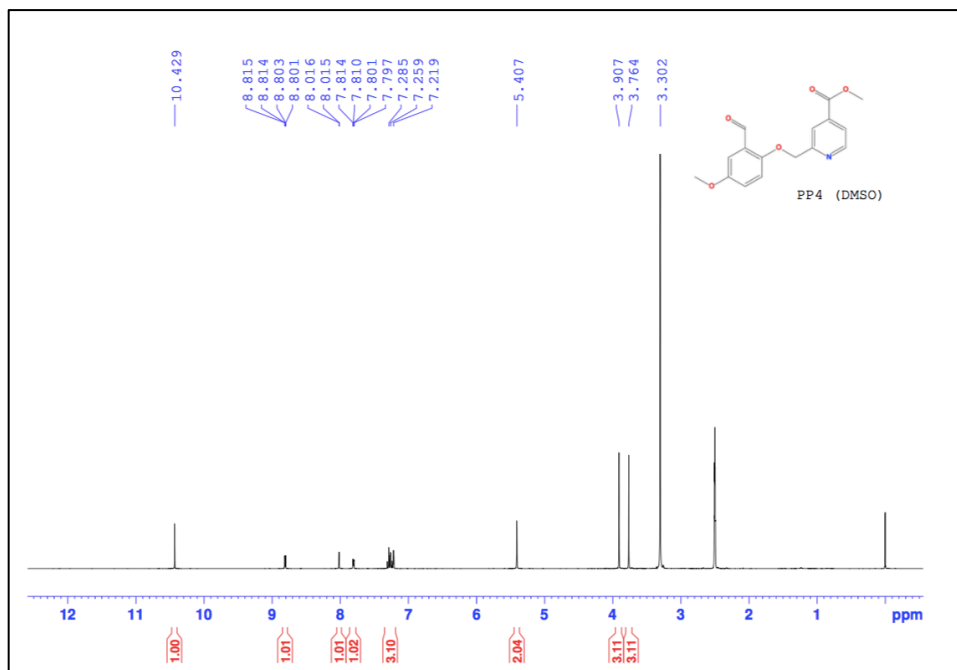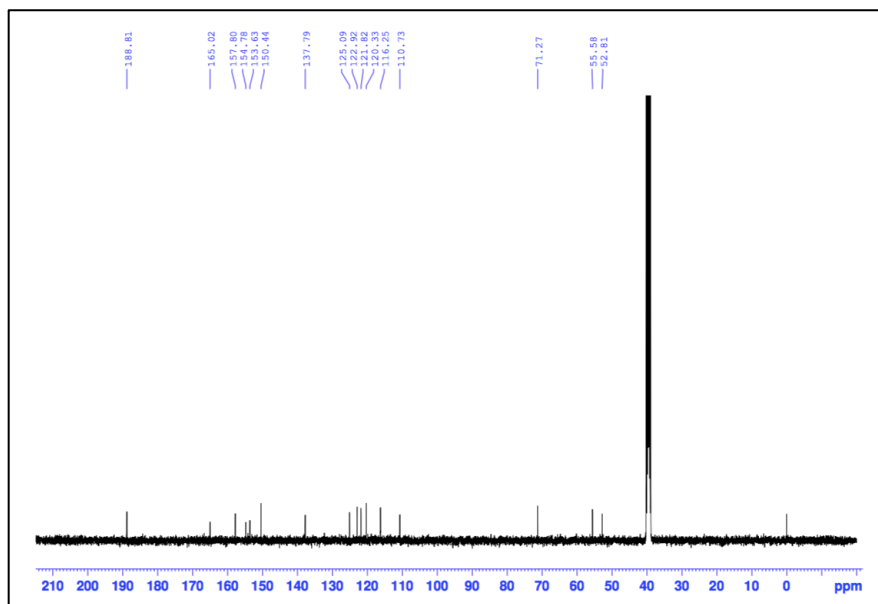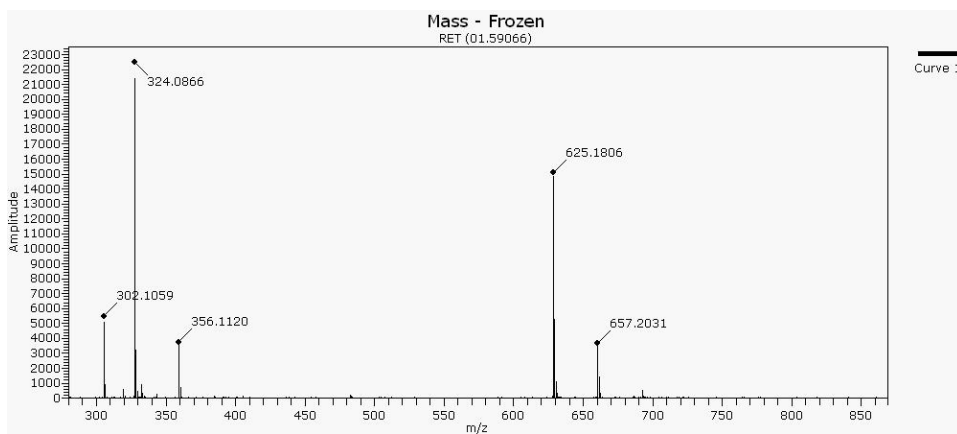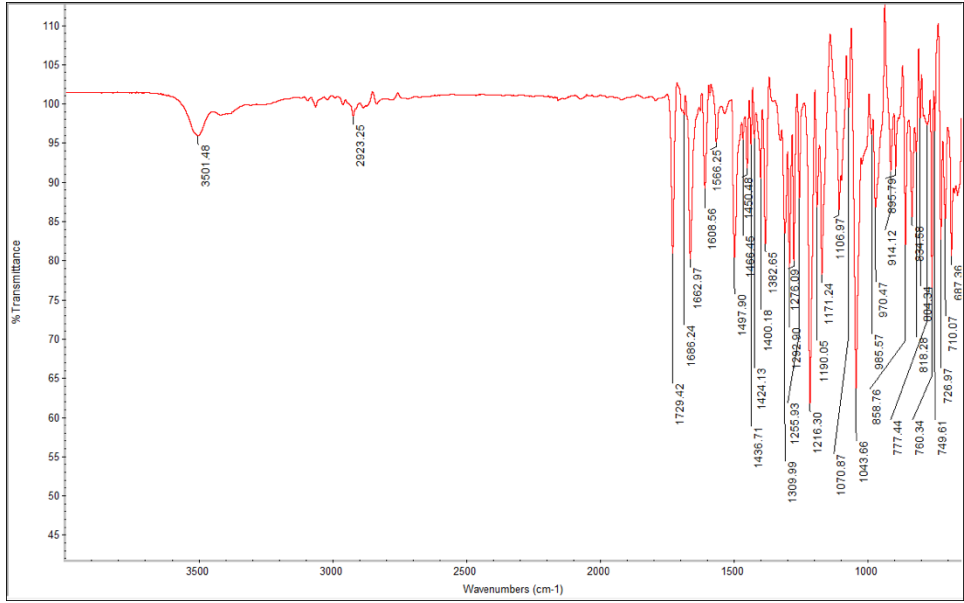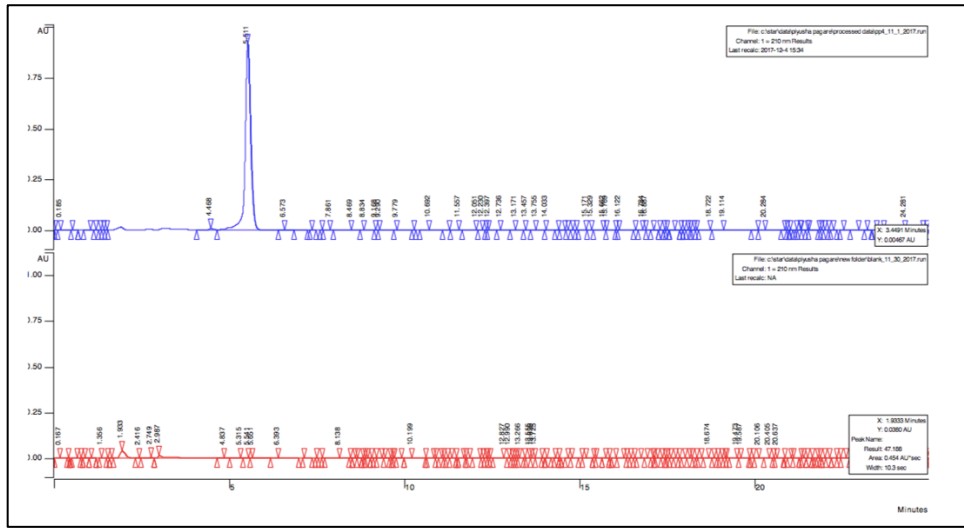
HPLC

Methyl 6-((2-formyl-3-hydroxyphenoxy)methyl)nicotinate (**PP5**)

¹HNMR

¹³CNMR

HRMS

IR
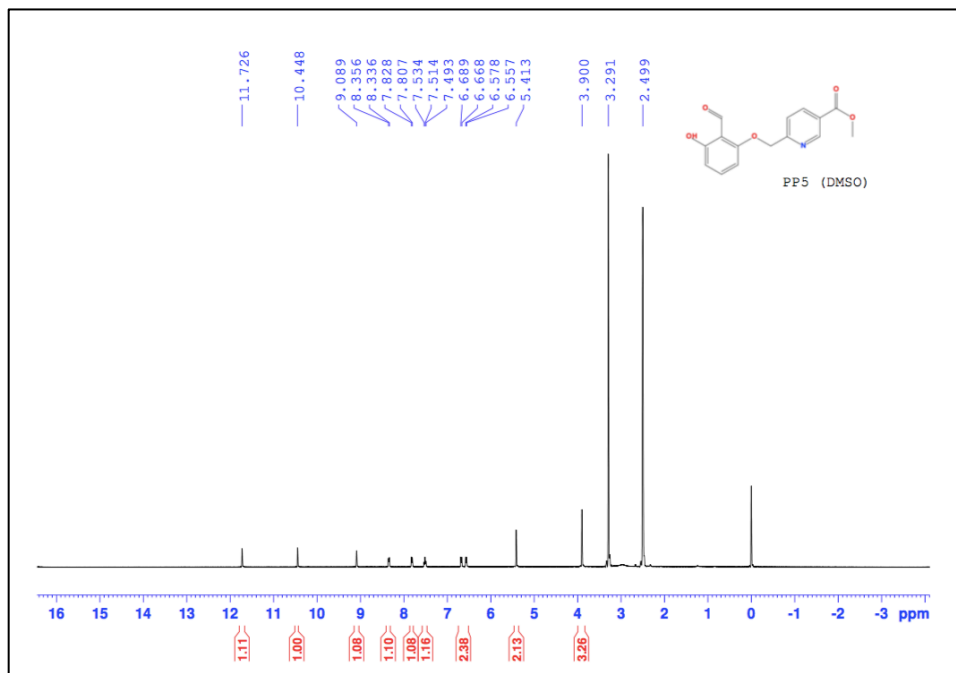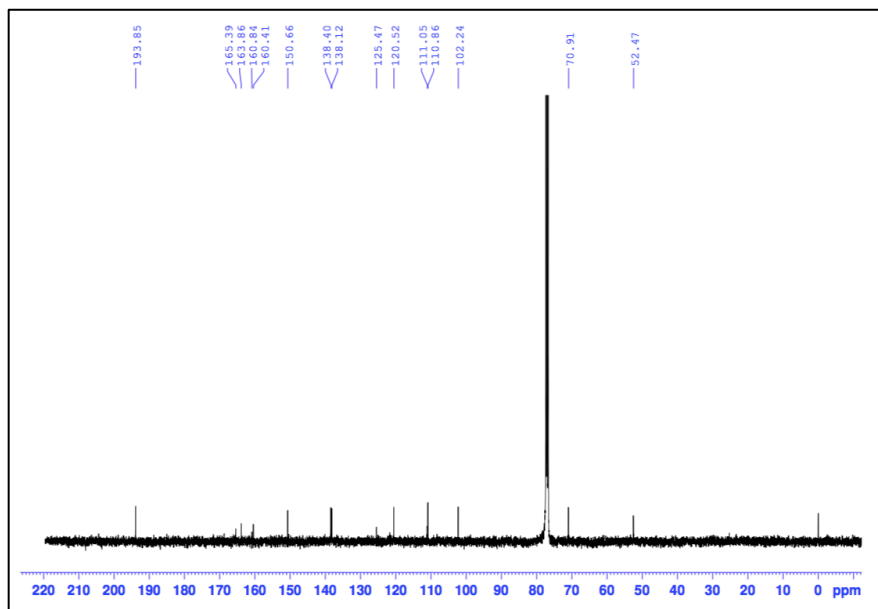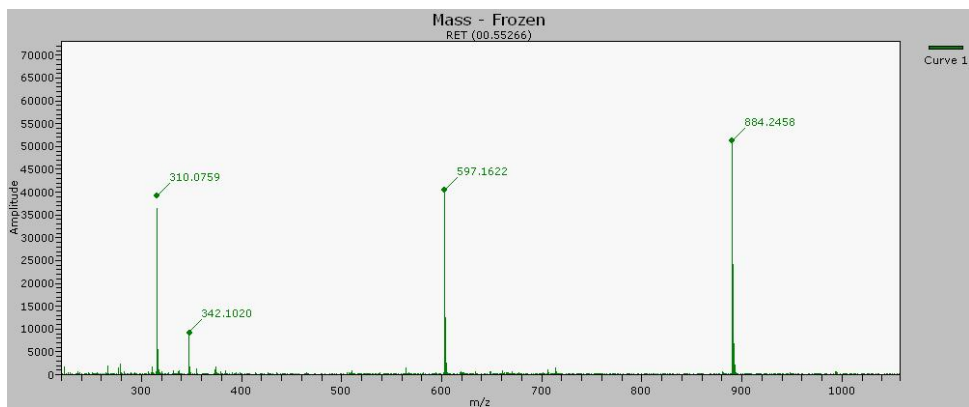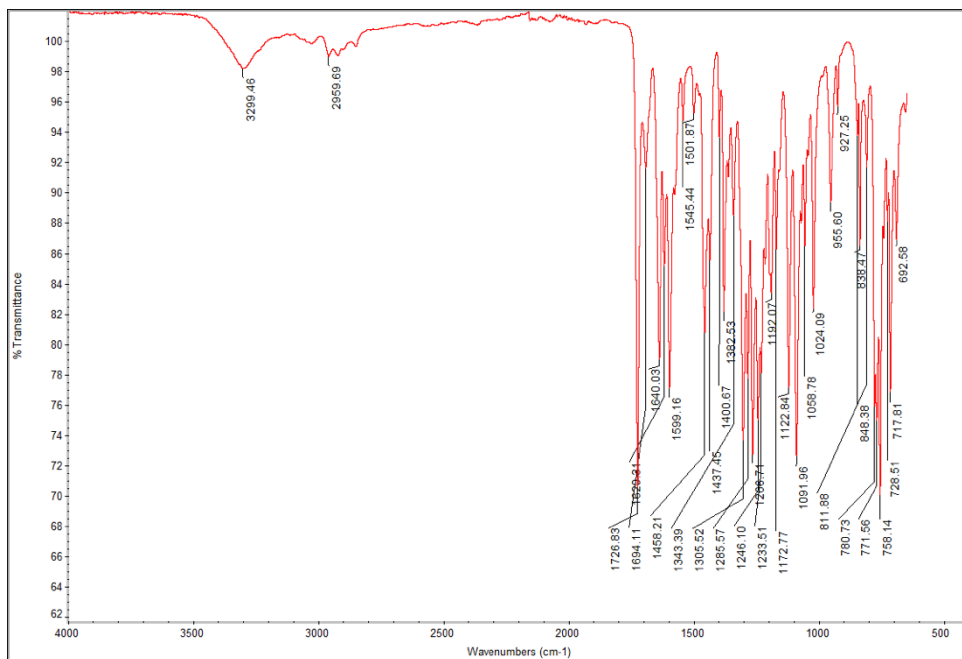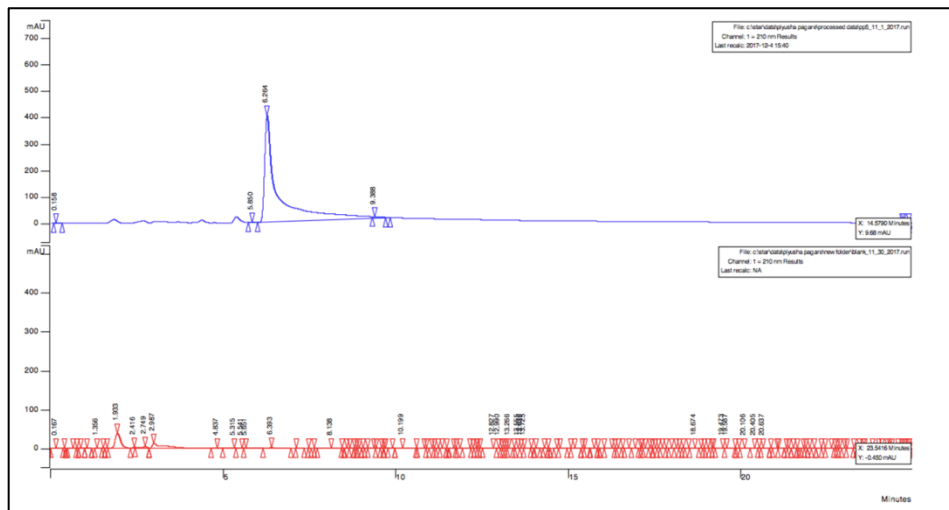
HPLC
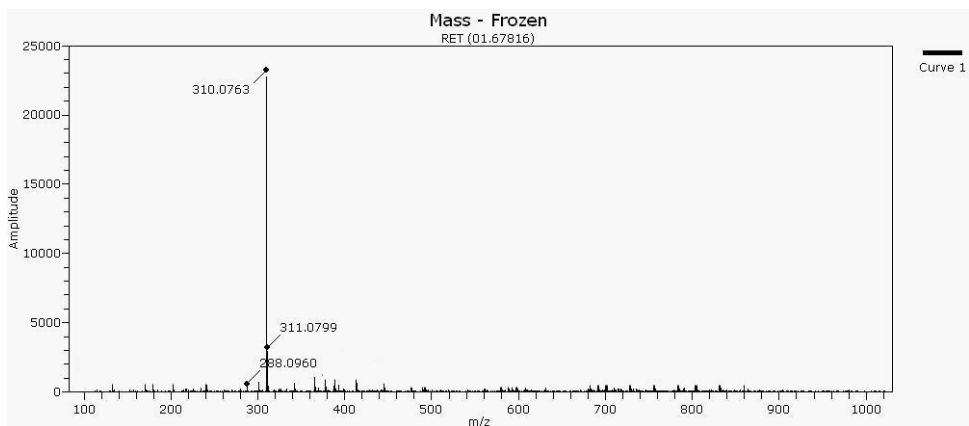

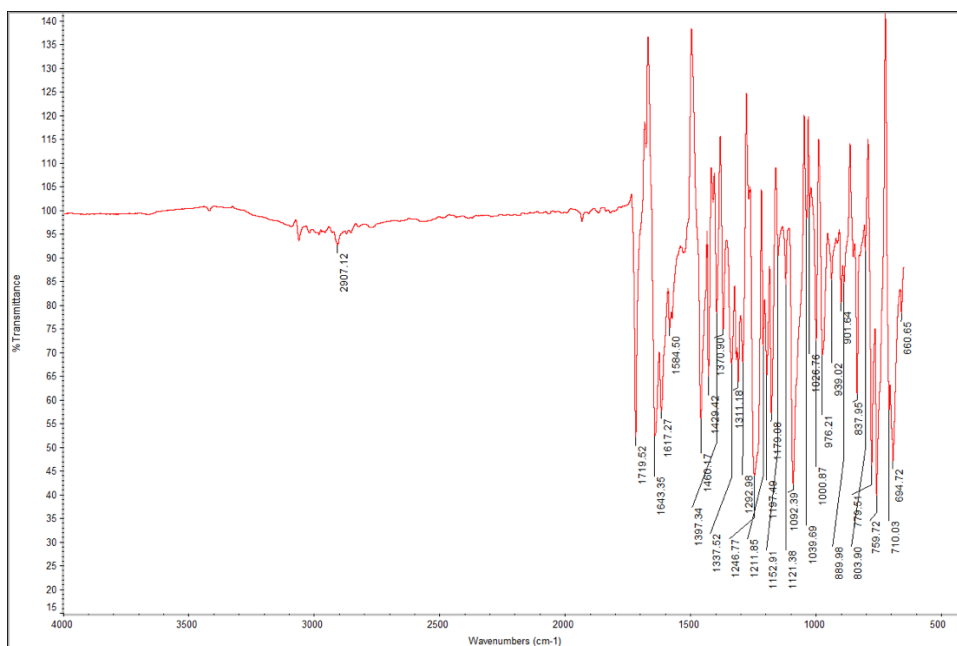Methyl 2-((2-formyl-3-hydroxyphenoxy)methyl)nicotinate (**PP6**)
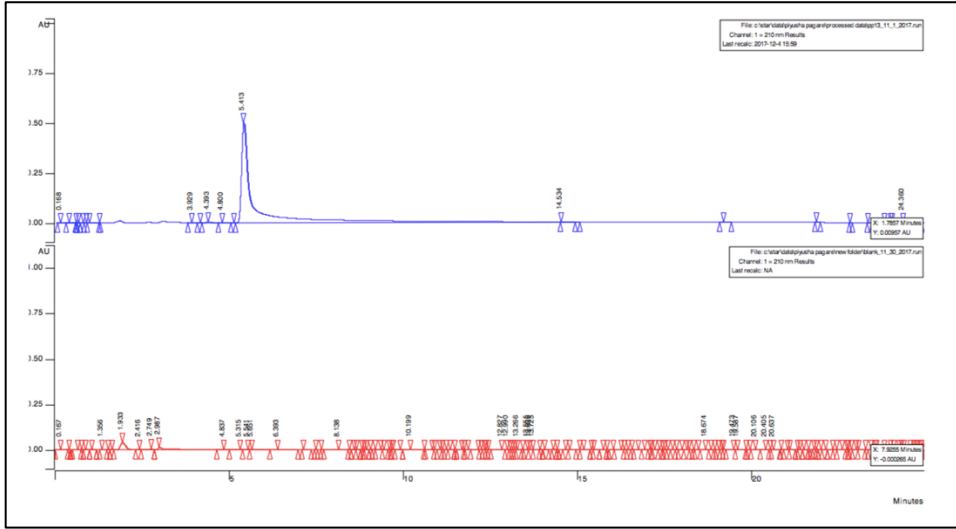
^{1}HNMR

¹³CNMR

HRMS

IR
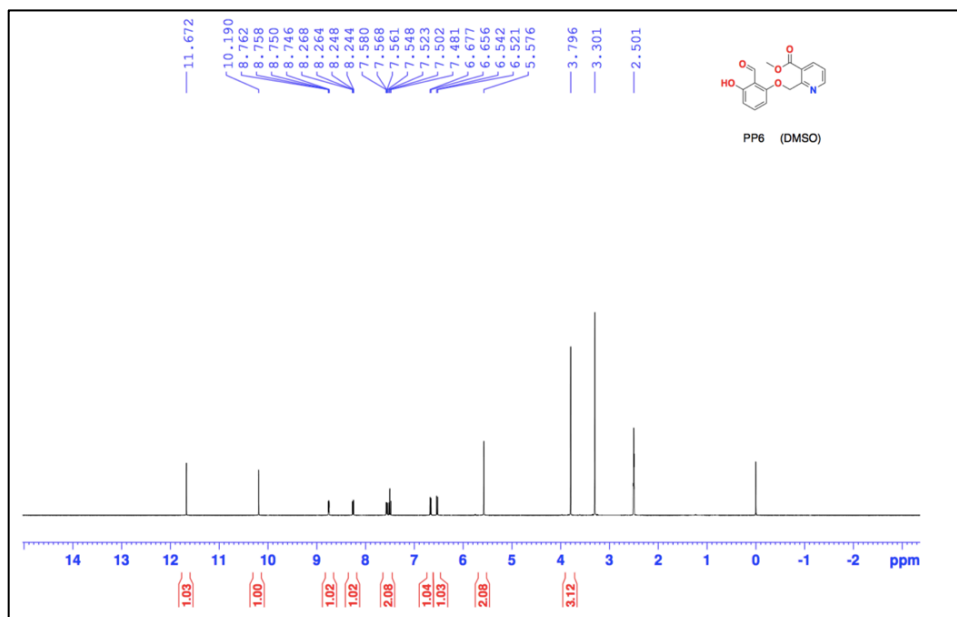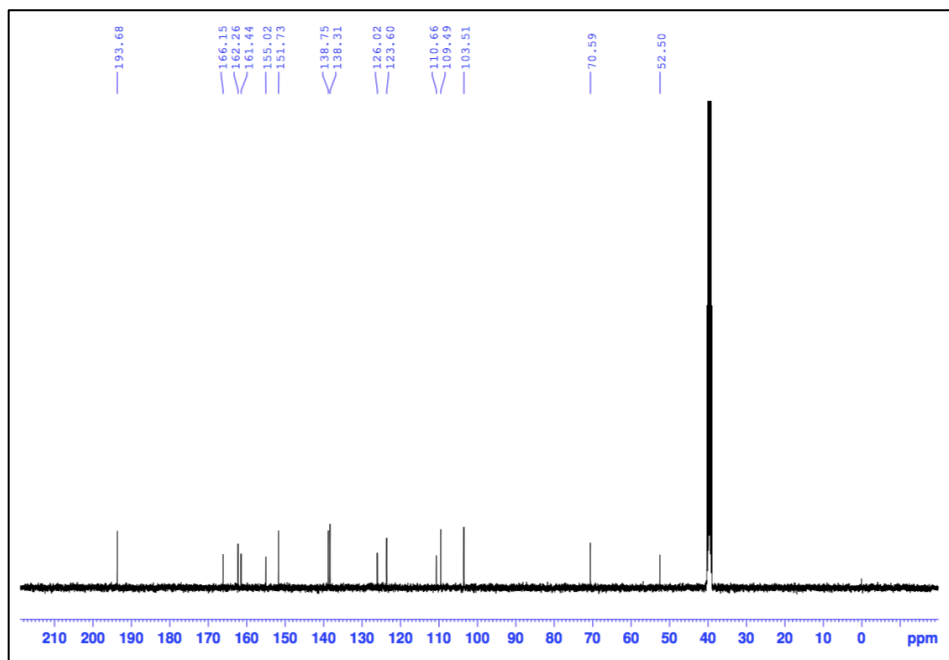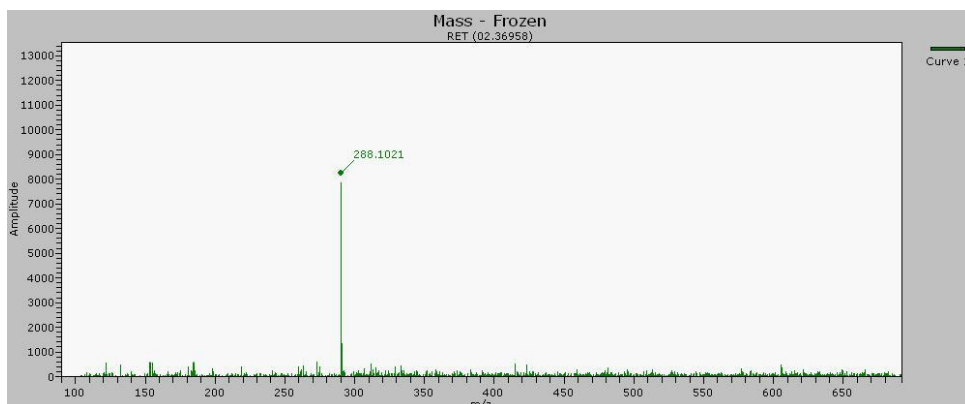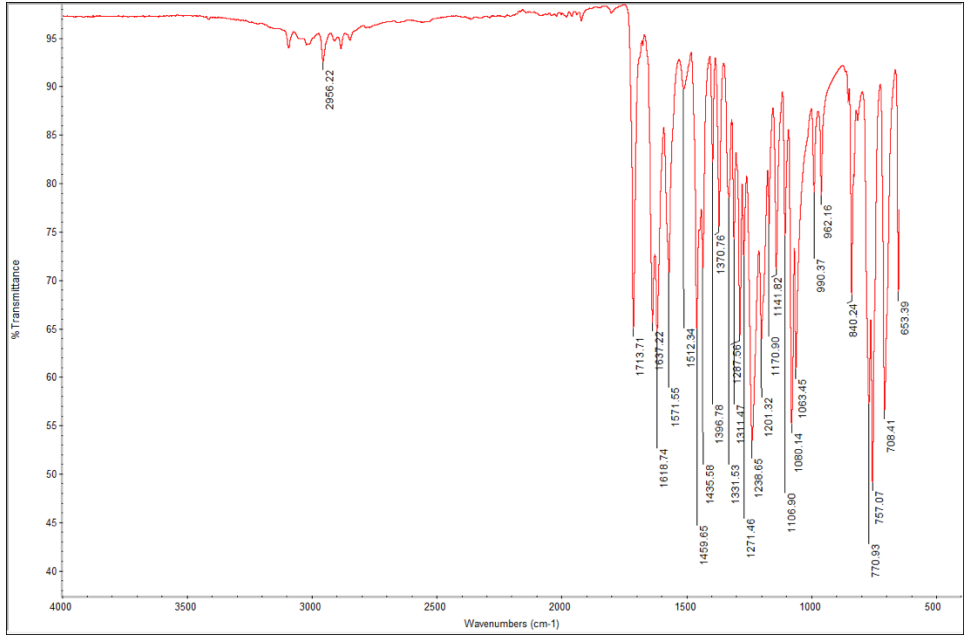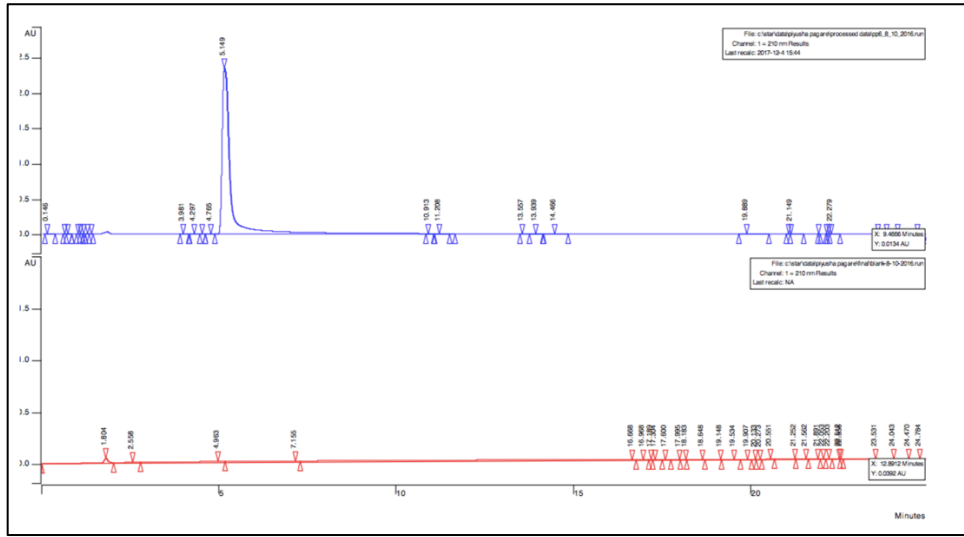
HPLC

Methyl 2-((2-formyl-3-hydroxyphenoxy)methyl)isonicotinate (**PP7**)

¹HNMR

¹³CNMR

HRMS

IR
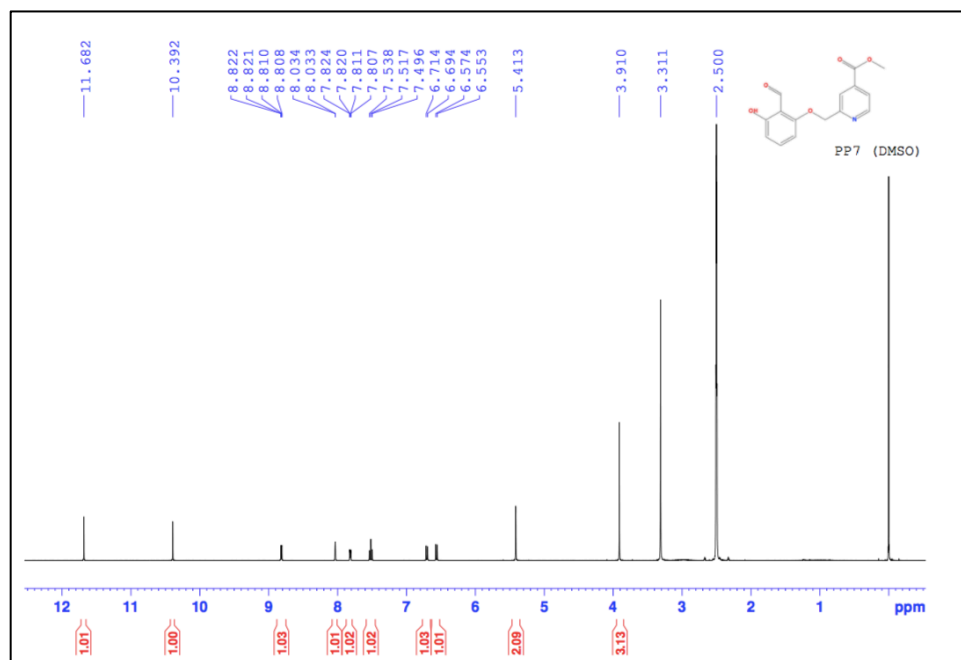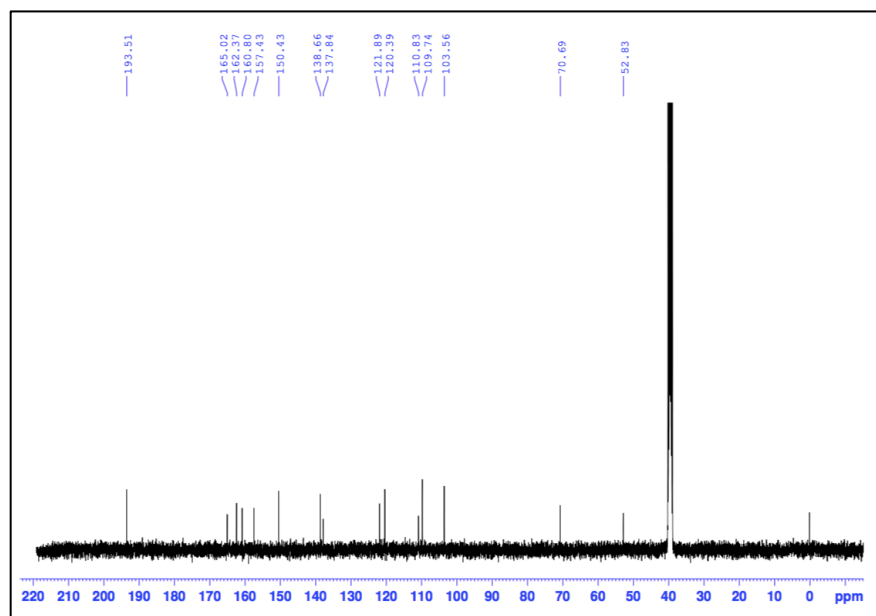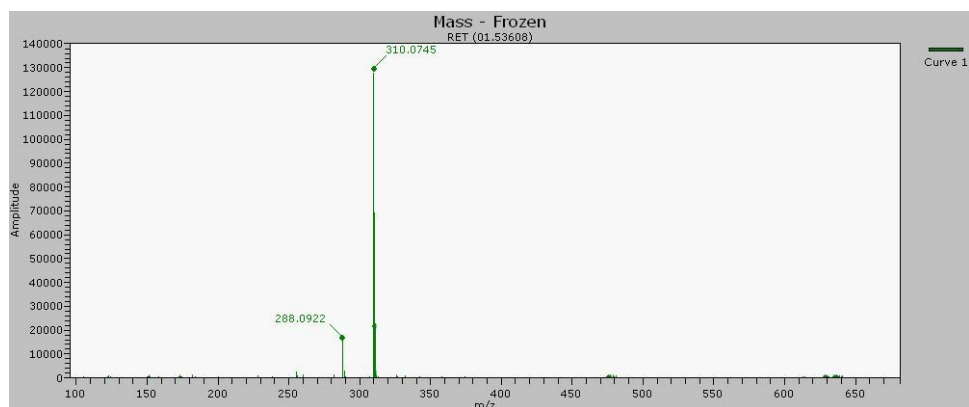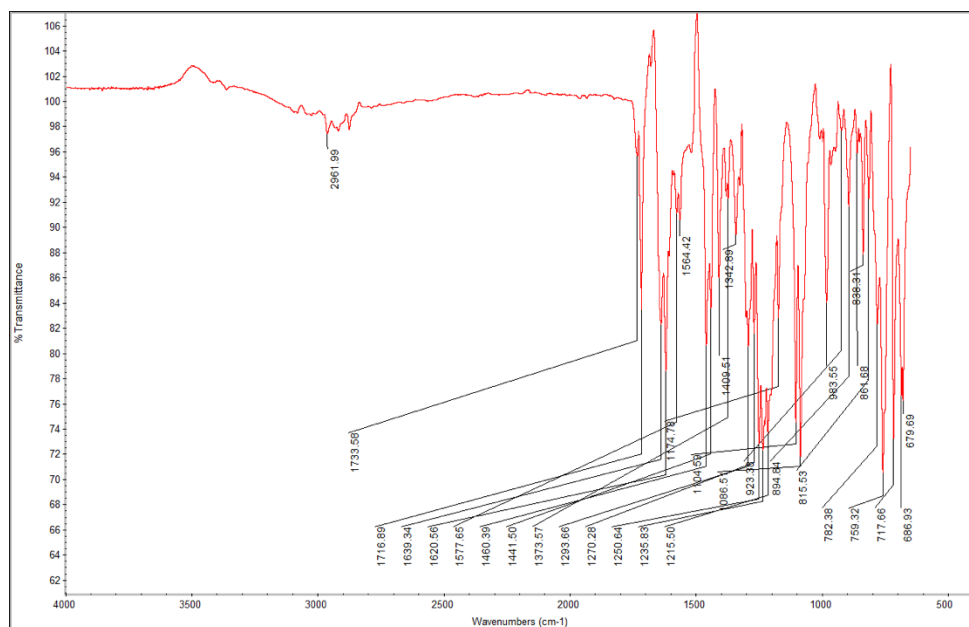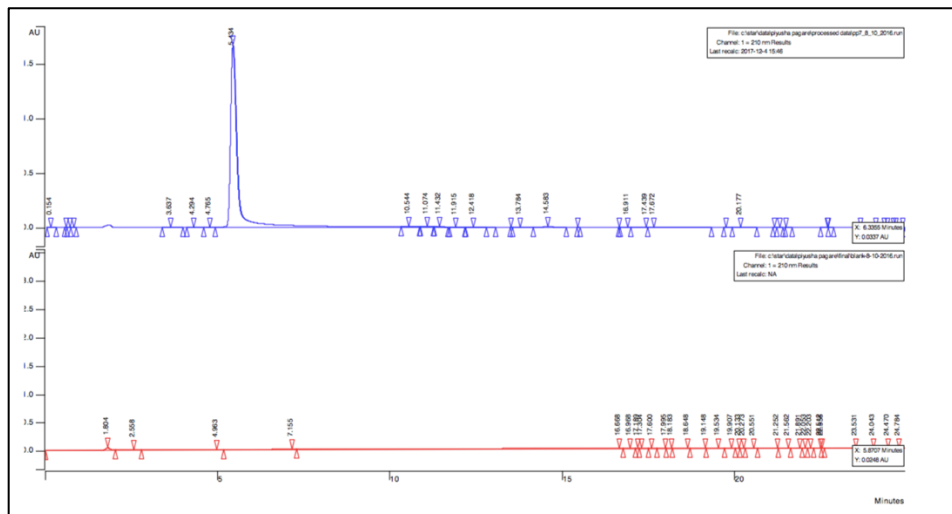
HPLC

Methyl 3-((2-formyl-4-methoxyphenoxy)methyl)picolinate (**PP8**)

^{1}HNMR

<superscript>13</superscript>CNMR

HRMS

IR
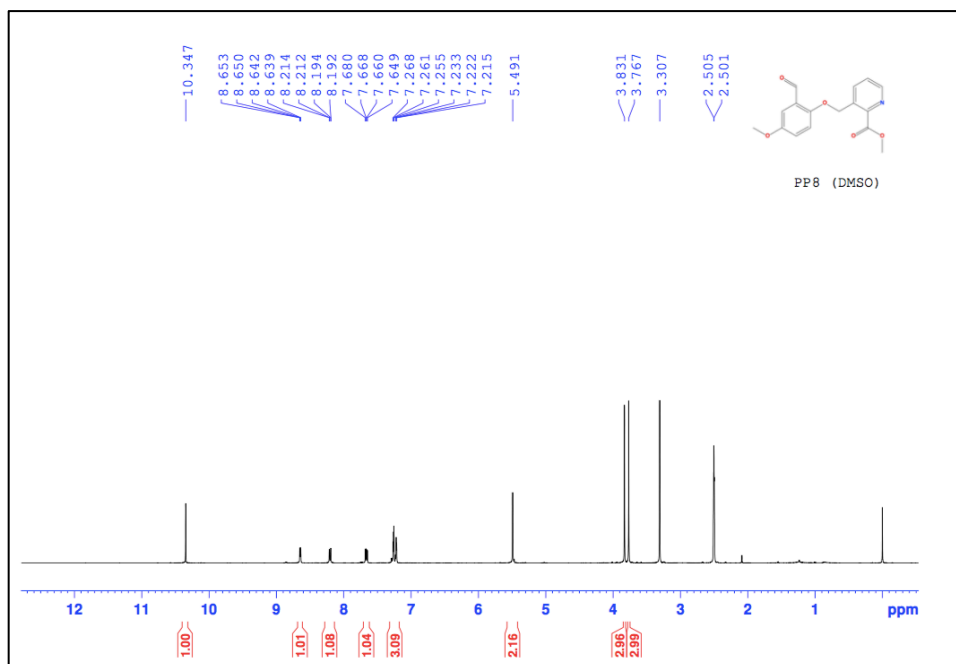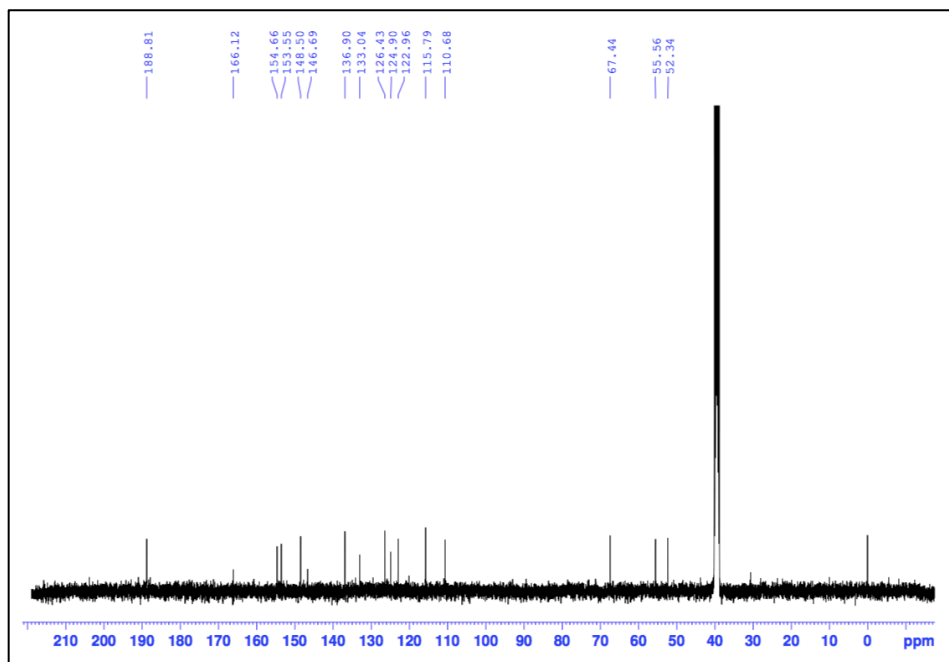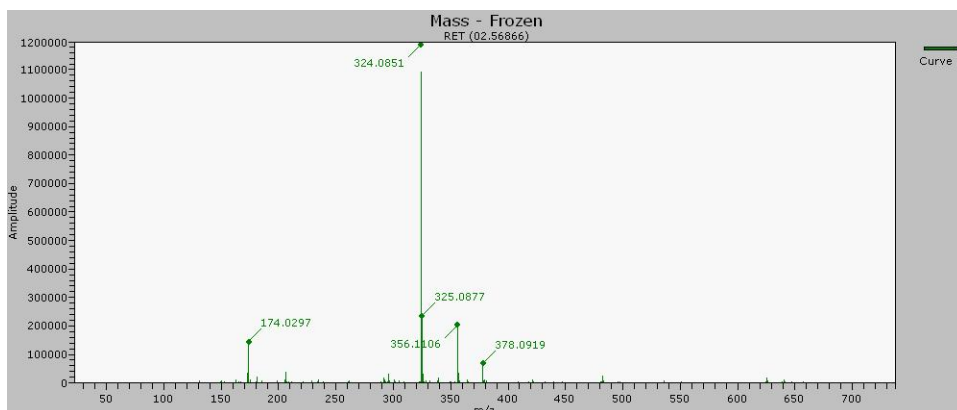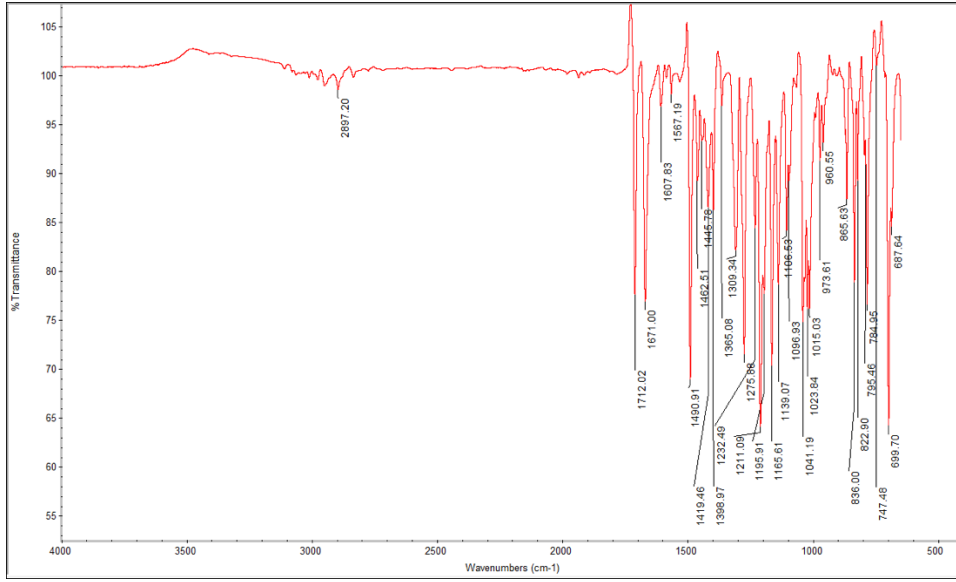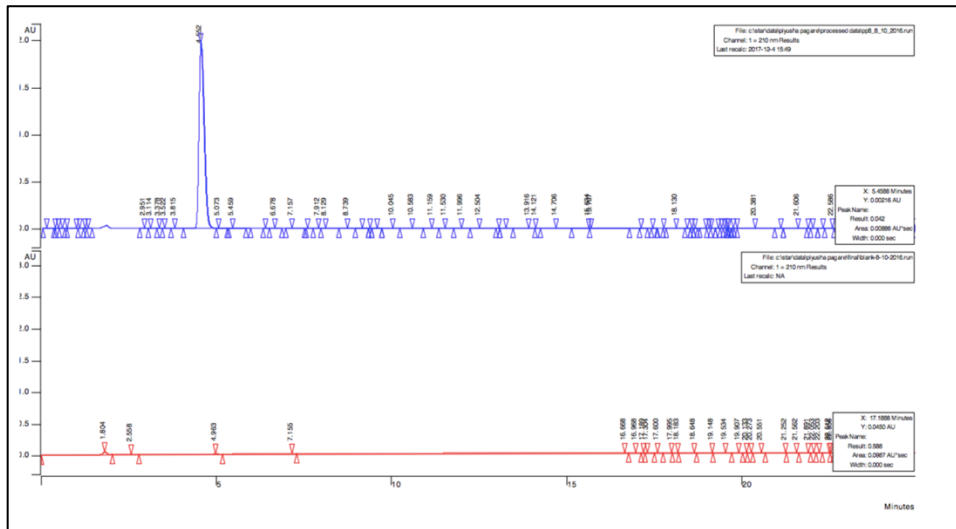
HPLC

Methyl 5-((2-formyl-4-methoxyphenoxy)methylpicolinate (**PP9**)

¹HNMR

¹³CNMR

HRMS

IR
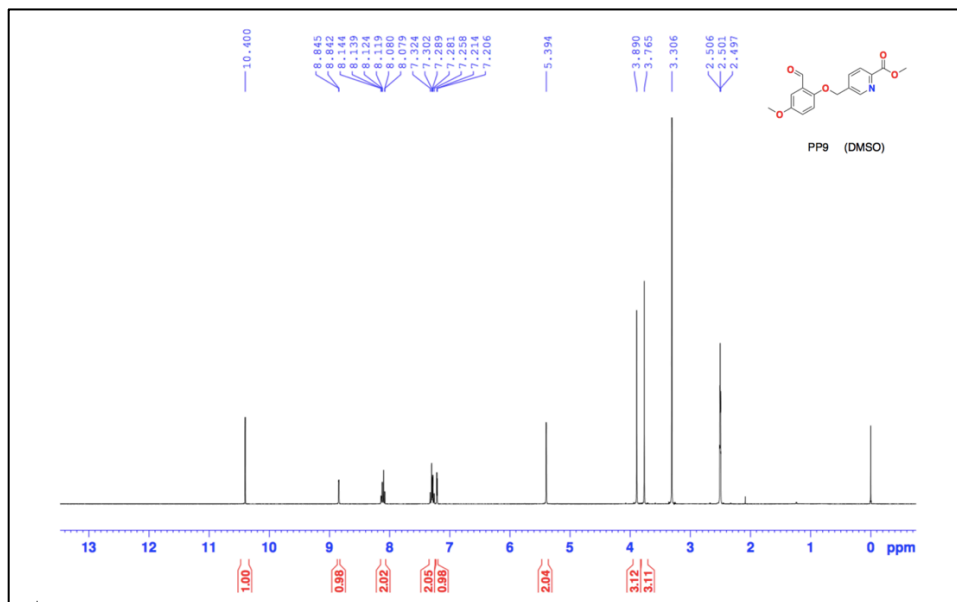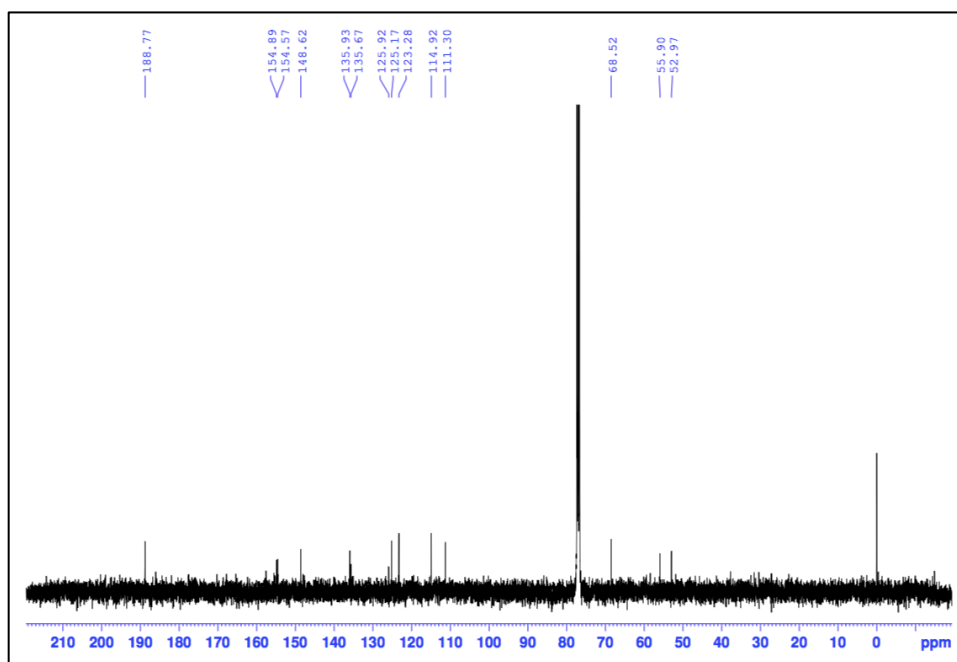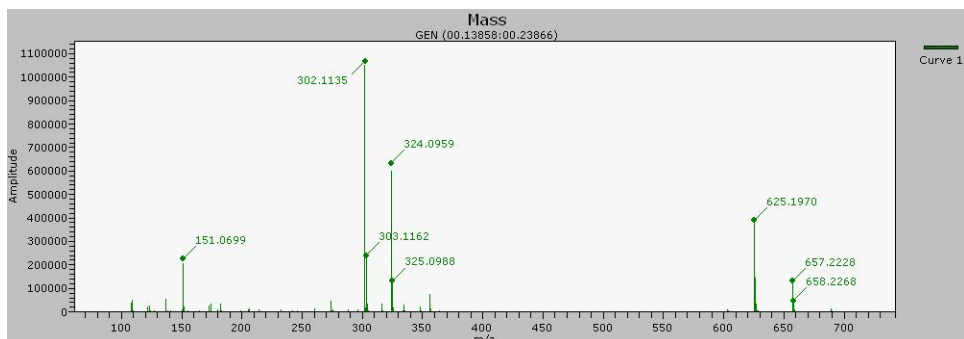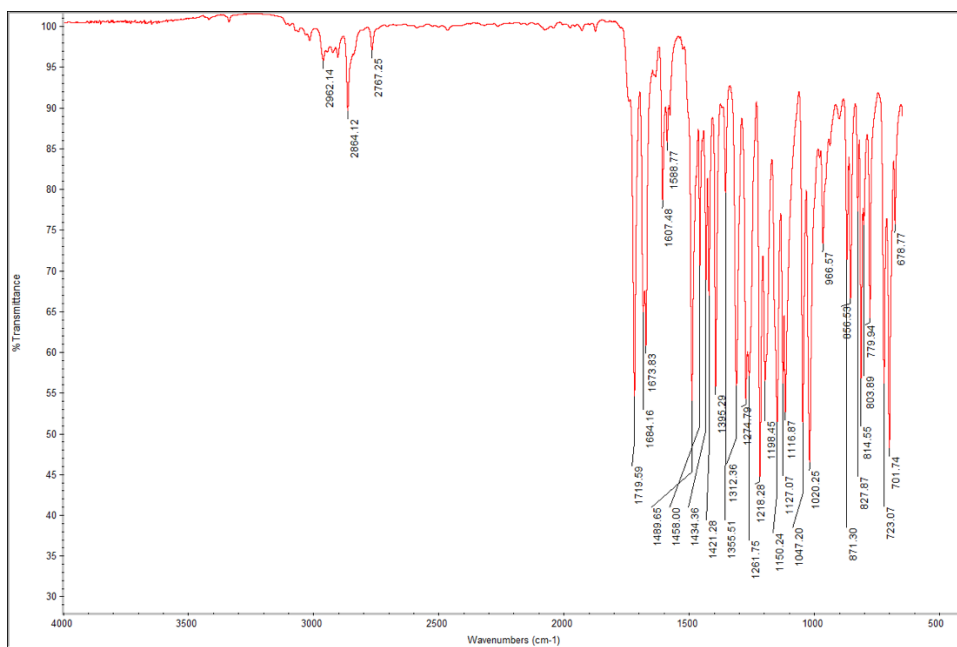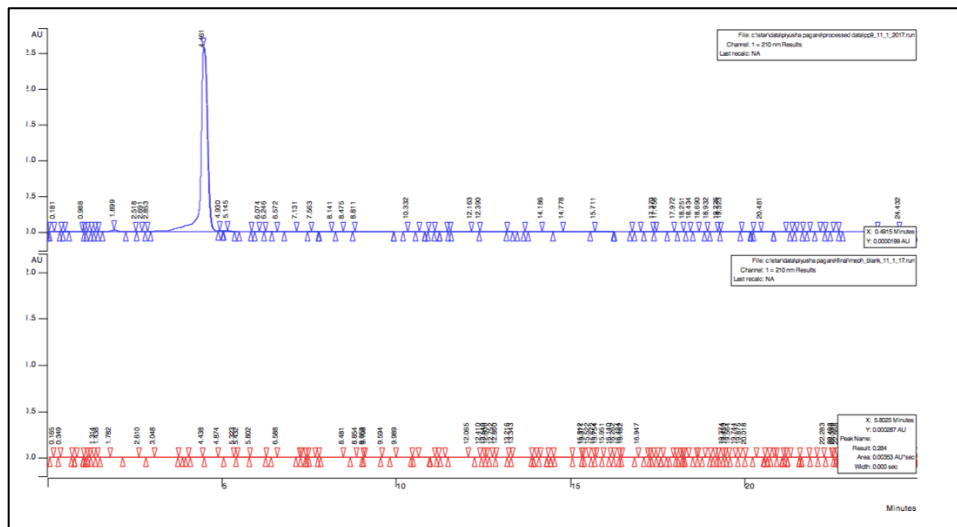
HPLC

Methyl 6-((2-formyl-3-hydroxyphenoxy)methyl)picolinate (**PP10**)

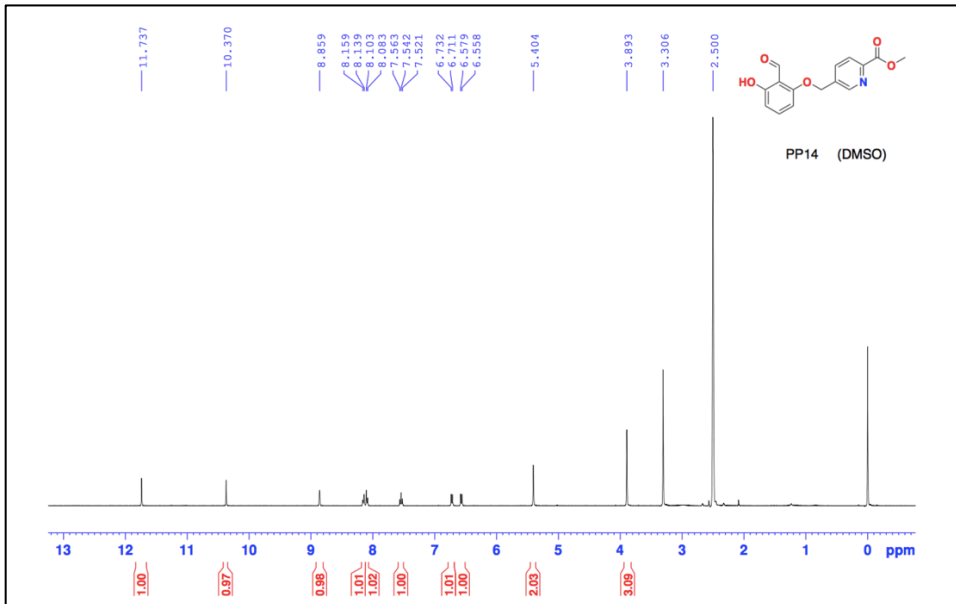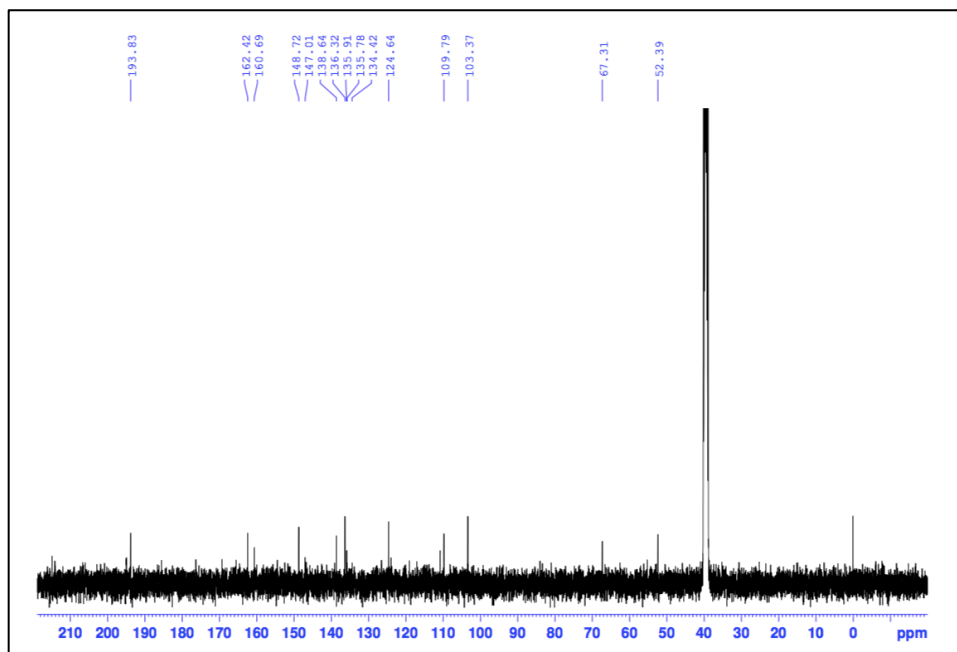¹HNMR

¹³CNMR

HRMS

IR
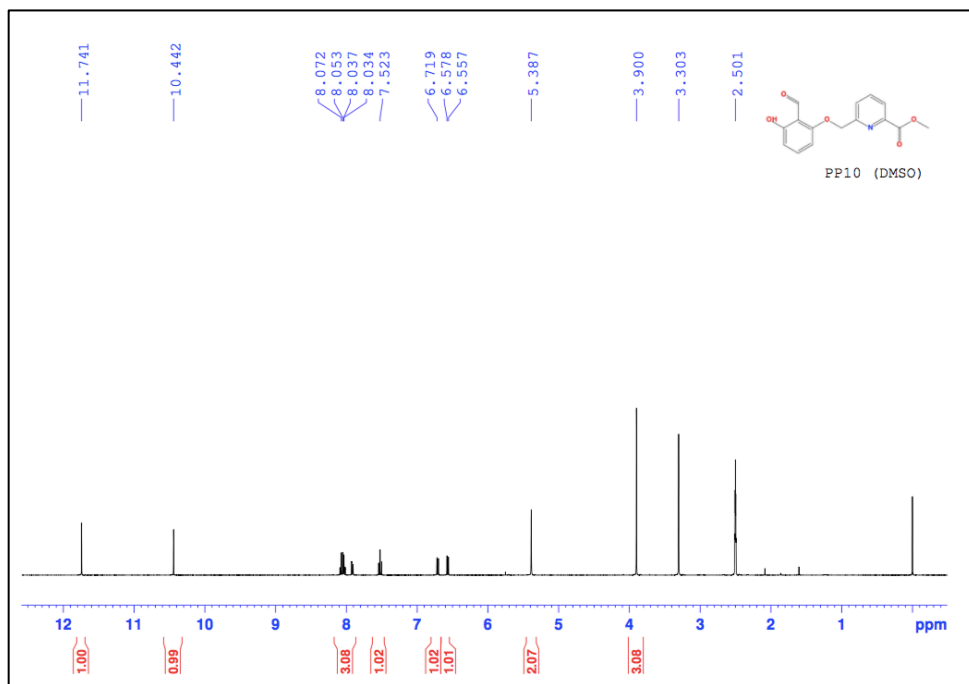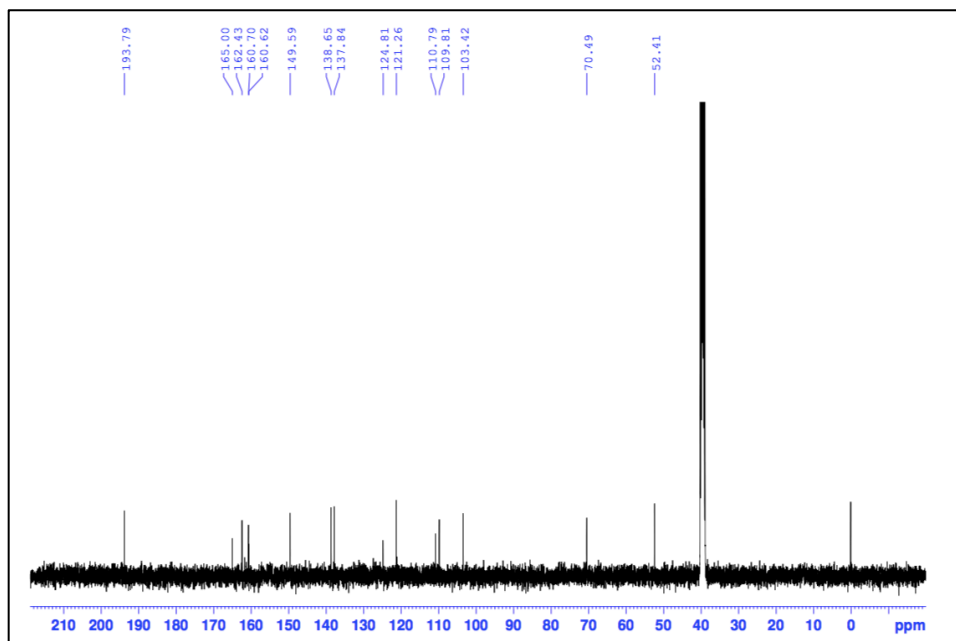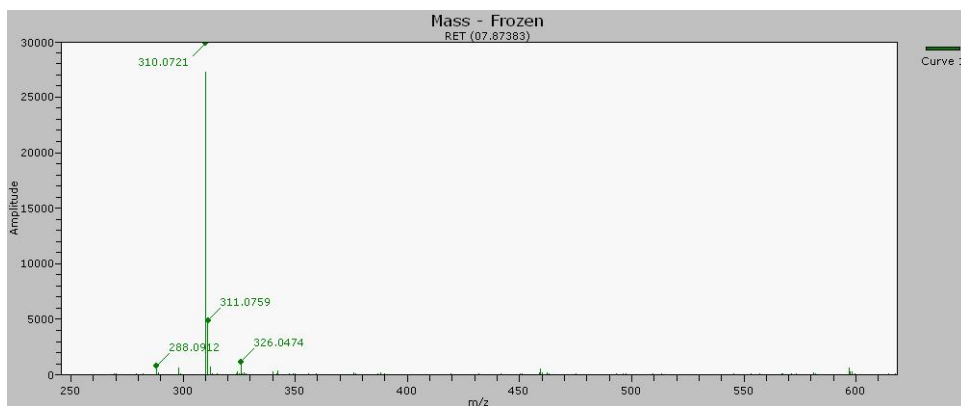
HPLC
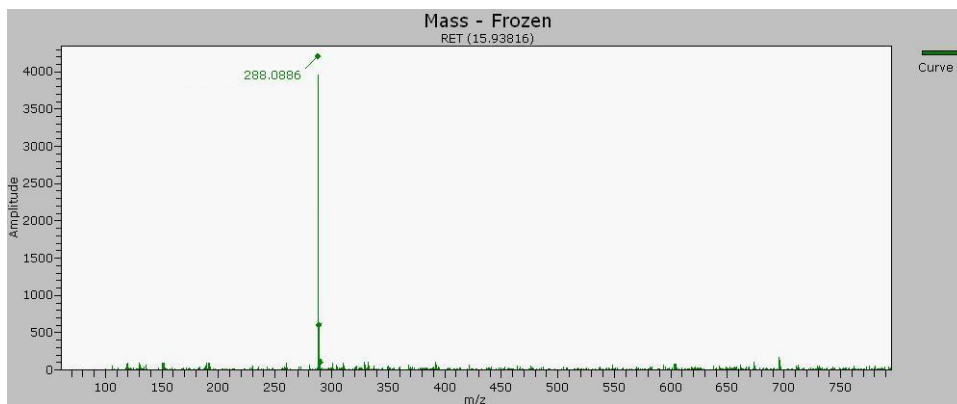
Methyl 3-((2-formyl-3-hydroxyphenoxy)methyl)picolinate (**PP11**)

¹HNMR

¹³CNMR

HRMS

IR
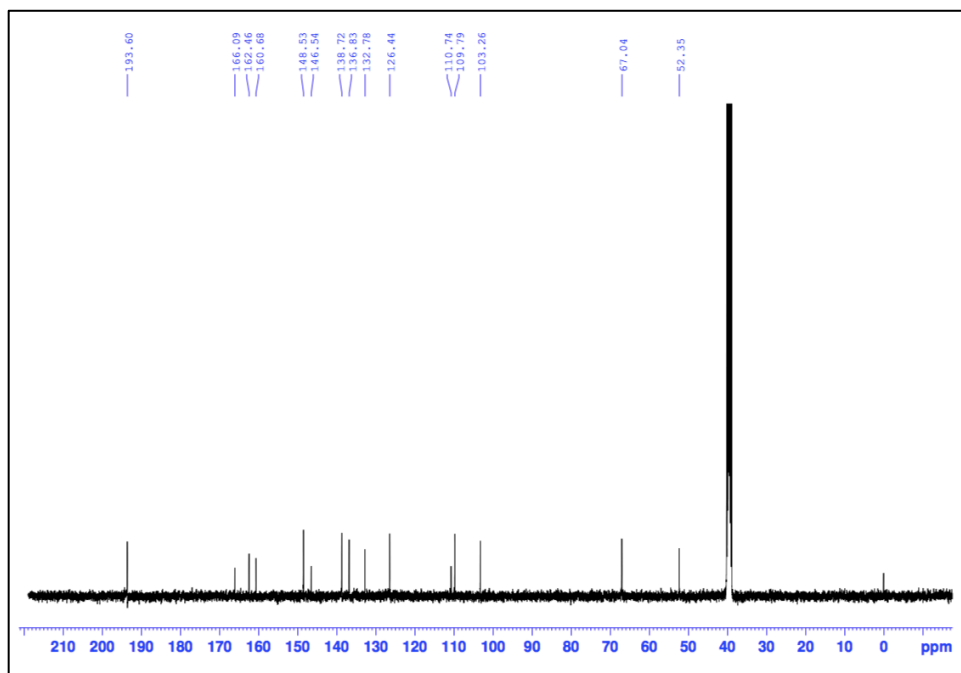
HPLC

Methyl 5-((2-formyl-4-methoxyphenoxy)methyl)nicotinate (**PP12**)

¹HNMR

¹³CNMR

HRMS

IR

HPLC

Methyl 5-((2-formyl-3-hydroxyphenoxy)methyl)nicotinate (**PP13**)

^{1}HNMR

PP13 (DMSO)

^{13}CNMR

HRMS

IR

HPLC

Methyl 5-((2-formyl-3-hydroxyphenoxy)methyl)picolinate (**PP14**)
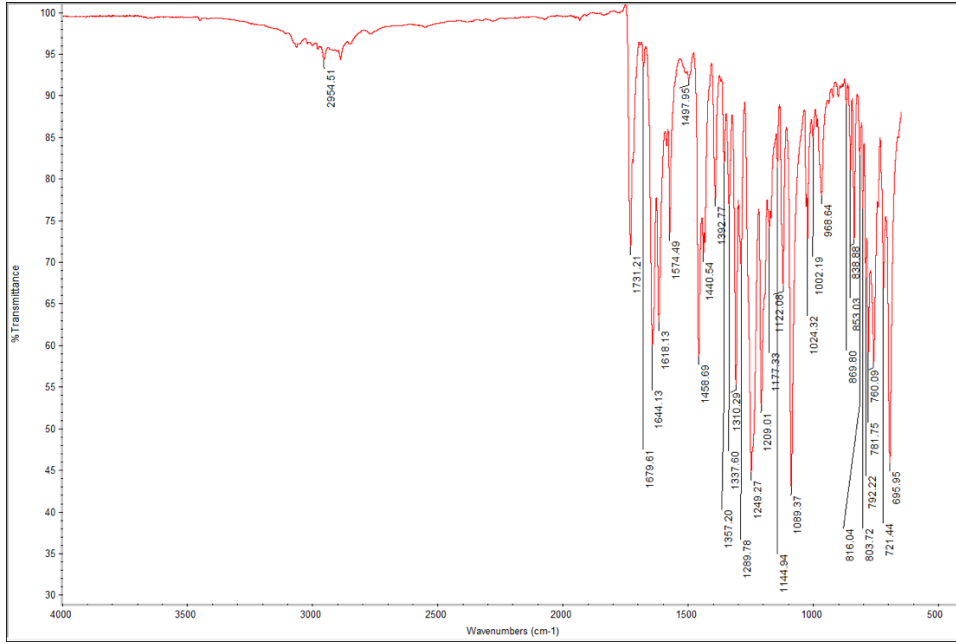
^{1}HNMR
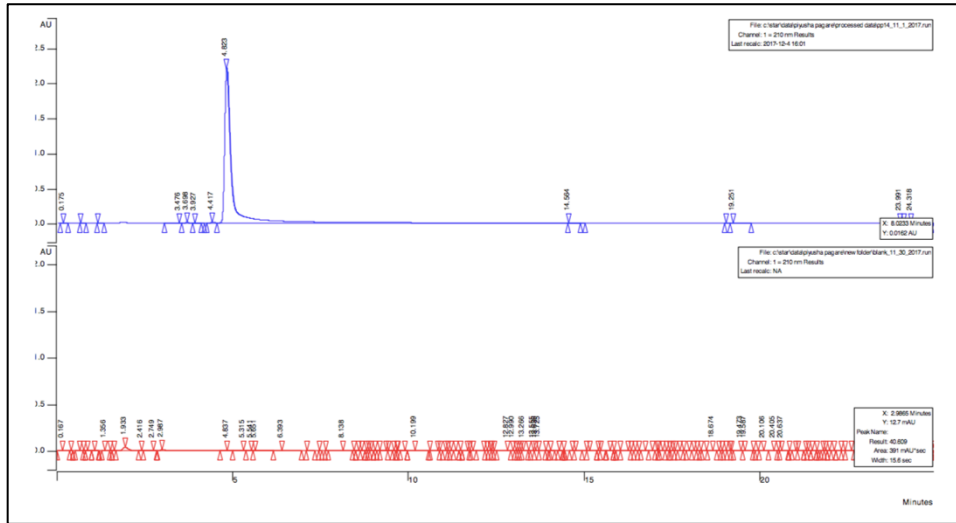
¹³CNMR

HRMS

IR

HPLC

Vita

Piyusha P. Pagare was born on October 30, 1988, in Mumbai, Maharashtra, India. She received her Bachelor of Science (B.Sc.) degree in Chemistry and Master of Science (M.Sc.) degree in Organic Chemistry from Ramnarain Ruia College, University of Mumbai, India in 2009 and 2012, respectively. Subsequently she joined the Medicinal Chemistry department in the School of Pharmacy at Virginia Commonwealth University in August 2013.